In vitro characterisation and modulation of evolving epileptiform activity

Neela Krushna Codadu

Doctor of Philosophy

Institute of Neuroscience
Newcastle University

2017

Abstract

Understanding the role of different neuronal populations in the evolution of epileptic activity remains a major goal for epilepsy research. Physiological neuronal networks may become hyperexcitable if they tip over some apparent threshold level of excitation, or below some threshold level of inhibition, although this process, termed ictogenesis is not understood. This hyperexcitable state of the network underlies the pathological condition of epilepsy. Clinical evidence suggests strongly that different regions in the brain have different epileptic-activity patterns and seizure susceptibility. The reasons for this differential susceptibility, however, are also not known.

In this thesis, two widely used *in vitro* models of epilepsy were used – zero-magnesium, and 4-aminopyridine (4AP) models – to characterise the evolution of epileptiform activity in naïve cortical networks in different regions of brain slices taken from wild-type mice. Various metrics were then used to develop assays for measuring (1) the action of disease-modifying drugs and (2) the effects of genetic mutations on seizure susceptibility. Lastly, the firing properties of neocortical parvalbumin-positive (PV+) interneurons in 4AP were characterised.

Different cortical areas showed notable differences in seizure susceptibility and activity patterns in the two models. In zero-magnesium, development of epileptiform activity in hippocampal regions facilitated transformation of early-stage epileptiform activity to late-stage in the neocortex. Furthermore, activity in the hippocampus entrained neocortical events, and this phenomenon was mediated, at least in part, by non-synaptic mechanisms, providing strong evidence for propagation through non-synaptic pathways.

The effects of diazepam and baclofen were also examined. They showed distinct effects on different cortical areas. Pharmacological suppression of glial functions induced spontaneous activity patterns, and also affected the development of epileptiform activity in the neocortex. Lastly, 4AP was found to alter the firing capability of PV+ interneurons in an input intensity-dependent manner, and induced spontaneous membrane potential oscillations.

Dedicated

to

my family

Acknowledgements

Contents

List of figures

List of tables

Abbreviations

°C	Celcius
μL	Micro-litre
μM	Micro-molar
4AP	4-Aminopyridine
$0Mg^{2+}$	Zero-magnesium ions
ACSF	Artificial cerebrospinal fluid
AED	Anti-epileptic drug
ANOVA	Analysis of variance
Amp.	Amplitude
ATP	Adenosine 5'-triphosphate
D-AP5	D-(-)-2-Amino-5-phosphonopentanoic acid
Bac-IE	Baclofen-induced tonic-clonic like ictal event
Bac	Baclofen
BAPTA	1,2-Bis(2-aminophenoxy)ethane-*N,N,N',N'*-tetraacetic acid
BDZ	Benzodiazepine
CA	Cornu amonis
Ca^{2+}	Calcium ions
$CaCl_2$	Calcium chloride
CO_2	Carbon dioxide
Cst-3	Calsyntenin-3
DZP	Diazepam

EC	Entorhinal cortex
EEG	Electroencephalogram
EFS	Electrode filling solution
FC	Fluorocitrate
GABA	Gamma-aminobutyric acid
$GABA_AR$	$GABA_A$-receptors
$GABA_BR$	$GABA_B$-receptors
GJ	Gap-junctions
HCN	Hyperpolarisation-activated cyclicnucleotide-gated channels
HEPES	4-(2-hydroxyethyl)-1-piperazineethanesulfonic acid
Hz	Hertz
IE	Ictal event
I-inj	Injected current
KA	Kainic acid
KAR	Kainate receptors
KCl	Potassium chloride
kHz	Kilo-hertz
$KMeSO_4$	Potassium-methylsulfate
K_v	Voltage-gated potassium channels
LFP	Local field potentials
LSE	Late stage events
Mg^{2+}	Magnesium ions
Mg-ATP	Adenosine 5'-triphosphate magnesium salt

MgCl$_2$	Magnesium chloride
mM	Millimolar
mm	millimetre
MΩ	Mega-ohms
MP	Membrane potential
MPO	Membrane potential oscillations
ms	milliseconds
MUA	Multiunit activity
mV	millivolts
NBQX	1,2,3,4-Tetrahydro-6-nitro-2,3-dioxo-benzo[f]quinoxaline-7-sulfonamide
Na$_2$-GTP	Guanosine 5'-triphosphate sodium salt
NaCl	Sodium chloride
NaH$_2$PO$_4$	Sodium-dihyrogen-orthophosphate
NaHCO$_3$	Sodium bicarbonate
NaOH	Sodium hydroxide
NCtx	Neocortex
nL	Nano litre
nm	Nano metre
NMDAR	N-methyl-D-aspartate receptor
NP-65	Neuroplastin-65
nRT	Reticular nucleus
O$_2$	Oxygen
pA	Pico-ampere

PDS   Paroxysmal depolarisation shift

PreIE   Pre-ictal event

PSD   Power spectral density

PV   Parvalbumin

RSD   Recurrent short discharges

SWD   Spike-and-wave discharge

s.e.m.   Standard error of means

s   Seconds

SE   Status epilepticus

TC   Thalamo-cortical neurons

TeTx   Tetanus toxin

TLE   Temporal lobe epilepsy

TTX   Tetrodotoxin

VAMP   Vesicle-associated membrane protein

VGSC   Voltage-gated sodium channels

V_{hold} Holding potential

Chapter 1 Introduction

Epilepsy is a chronic condition of the brain, characterized by stereotyped and recurrent alterations in behaviour or conscious state, termed seizures, and by the psychological, and cognitive consequences of these episodes. Seizures are considered to arise from paroxysmal episodes of intense neuronal activity.

Epilepsy affects an estimated 50 million individuals, that is, around 1% of the world population (World Health Organisation, 2017). Epilepsy affects people of both genders and of all ages. Epilepsy patients experience seizures that typically lasts between a few seconds to minutes. 'A seizure is a transient occurrence of signs and/or symptoms due to abnormal excessive or synchronous neuronal activity in the brain' (Fisher *et al.*, 2005). The intervals between seizures are known as interictal periods. When a seizure happens continuously for more than 30 minutes, it is known as status epilepticus (SE). This state is considered a neurological emergency, and is associated with significant mortality, that increases with the duration of the episode (Neligan and Shorvon, 2011).

There are various causes for the development of epilepsy such as traumatic brain injuries, stroke, and abnormal development of the brain, gene mutations, brain tumours, and central nervous system infections (Lancman *et al.*, 1993; Vespa *et al.*, 1999; Singh *et al.*, 2008; Ruda *et al.*, 2010; Poduri and Lowenstein, 2011; Lerche *et al.*, 2013; Aronica and Crino, 2014). Nearly 30 different types of clinical epilepsies have been identified (Berg *et al.*, 2010; Scheffer *et al.*, 2017), and depending on the type, an epilepsy may be associated with other comorbidities such as anxiety (Mazarati *et al.*, 2009; Inostroza *et al.*, 2012), cognitive impairments (Inostroza *et al.*, 2011) or increased mortality (Sillanpaa and Shinnar, 2010). The classification of epilepsies is a necessary tool for clinicians to evaluate a patient with seizures, and also to enable communication between different groups of people namely clinicians, researches, patients, and patient's caretakers. Classification of epilepsies enable clinicians to recognise the type of seizures that the patient is showing, and their likely triggers, and to choose a course for the anti-epileptic therapy. It also gives an idea about the

prognosis of the condition, comorbidities patient may develop such as cognitive impairment, anxiety, and mortality risks. This information is essential for both the clinicians and the caretakers. Classification continues to be a difficult task as it is mainly based on the personal or eye-witness descriptions of the seizures, and electrographic patterns recorded in the clinic. Furthermore, interpretation of the electrographic clinical data is itself extraordinarily difficult for the following reasons: abnormal electric activity in the brain of patients is assessed by using EEG electrodes that are placed on their scalp; firstly, they yield poor quality recordings as the EEG electrodes are not in direct contact with the brain; secondly, since they record the activity occurring over a large area of the brain, one cannot pinpoint the source (location) of the activity; thirdly, clinical recordings are often only of interictal periods and fail to capture seizures; and lastly, we do not know what exactly do recordings reflect? There is a long way for proper classification and AEDs, making it hard for scientific basis of treatment options.

1.1 Current issues in treating epilepsy

A major issue in the treatment of epilepsy is that 30% of the patients are refractory to anti-epileptic drug (AED) treatments (World Health Organisation, 2017). Many patients on AEDs continue to develop seizures, and none of the AEDs can prevent the progression of the disease. Furthermore, AEDs present side effects that may require adjunct medications and worsens patients' quality of life. Currently, there are no anti-epileptogenic drugs available to treat patients at risk of developing epilepsy. Epileptogenesis generally has three stages: (1) the precipitating event, e.g., traumatic brain injury, stroke, (2) the latent period, the time between the brain injury and the onset of seizures, and (3) the final development of epilepsy, defined by the occurrence of spontaneous seizures. In cases of brain injury (precipitating event), during the latent period, the non-epileptic brain undergoes active changes and become epileptic. Administration of AEDs failed to prevent epileptogenesis after the brain injury (Herman, 2002; Loscher, 2002; Walker *et al.*, 2002; Pitkanen, 2010). There are many documented changes in cortical circuits that appear to occur during the latent period (see sections 1.2.1) (Cronin and Dudek, 1988; Schwarzer *et al.*, 1995; Bragin *et al.*, 2000; White *et al.*, 2010; Chauviere *et al.*, 2012), but we continue to have a very poor understanding of the functional relevance of these to the epileptogenic process.

Clinically, the importance of the latent period is that it is a window of opportunity for preventing the development of seizures. Identifying the active processes such as structural, functional changes, gene mutations, will enable us firstly, to identify biomarkers of such processes, secondly, recognise patients with risk of developing epilepsies, and thirdly, to pharmacologically intervene during the latent period to minimise the chances or prevent the development of epilepsy (Walker *et al.*, 2002; Dichter, 2009; Jacobs *et al.*, 2009; Pitkanen, 2010). It is necessary to understand various mechanisms of epilepsies to identify new drug targets that not just alleviates the symptoms, but prevents its development and cure the disease. Understanding the mechanisms of epileptogenesis and refractory epilepsy is the way to go forward for the development of anti-epileptogenic drugs, disease-modifying drugs, treatment strategies that will improve patient's epilepsy condition and associated comorbidities, and for our better understanding of epilepsy. These are some of many reasons for which we need experimental models, both *in vitro* and *in vivo*, that recapitulates various facets of human epilepsies.

1.2 *In vivo* models

Studies on animal models have enhanced our understanding about the various aspects of epilepsy. Different animal models that capture different features of human epilepsy were used extensively to understand the pathophysiology of epilepsy, to screen anti-epileptic drugs, to design new therapies for epilepsies not responding to currently available anti-epileptic drugs and improve comorbidities (Brooks-Kayal *et al.*, 2013). However, there are some limitations in using *in vivo* models such as the experimenters do not have a complete handle on the experiments, they are labour intensive, high animal mortality, animal welfare issues, usually large group sizes are required, and high financial costs.

Chemoconvulsants allow investigations of epileptogenic mechanisms and screening of AEDs. Chemoconvulsants-induced epilepsies in animal models reproduce the phenotypes and symptoms associated with human epilepsies, but they are not entirely clinically validated. Therefore, a model should be chosen based on which specific aspect of epilepsy is the researcher aiming to investigate. Several chemoconvulsants, such as kainate, pilocarpine, tetanus toxin are used for inducing

epileptic activity in animals (rodents are more commonly used as experimental animals). The following are two examples of *in vivo* models with distinctive features that are used for understanding the pathophysiology of one of the most common type of epilepsy – temporal lobe epilepsy (TLE).

1.2.1 **Kainic acid model**

Temporal lobe epilepsy (TLE) in humans is characterised by the presence of seizures, hippocampal sclerosis, mossy fibre sprouting (synaptic reorganisation), dispersion of granule cells in dentate gyrus, and extra-hippocampal pathology (Sutula *et al.*, 1989; Bonilha *et al.*, 2006; Bonilha *et al.*, 2010). Kainic acid-treated rats are used as an animal model for temporal lobe epilepsy. Ben-Ari and Lagowska (1978) developed the kainic acid model of TLE. They showed, in rats, that injecting kainic acid (KA) into amygdala induced lesions and behavioural seizures. KA-induced behavioural seizures and pathological lesions in rats show similarity with those observed in patients with temporal lobe epilepsy (Ben-Ari, 1985; Ben-Ari and Cossart, 2000). Along with amygdala, KA also causes an extensive damage in hippocampus, entorhinal cortex and piriform cortex (Schwob *et al.*, 1980).

Kainic acid is an agonist for kainate receptors (KAR), a subclass of ionotropic glutamate receptors. It enhances the excitatory responses in cortical neurons. KAR are differentially expressed throughout the brain, and their expression patterns play a key role in balancing the excitability of the networks. There are five different types of KAR subunits, namely, KA1, KA2, GluR5, GluR6, and GluR7. The pharmacology, location, and kinetics of KARs are dictated by their subunit composition (Bahn *et al.*, 1994). In the hippocampus, CA3 pyramidal neurons express high levels of KA1 and KA2 subunits, whereas CA1 pyramidal neurons express high levels of KA2 subunits (Werner *et al.*, 1991; Wisden and Seeburg, 1993; Bahn *et al.*, 1994). This differential expression levels of the subunits on the pyramidal neurons make CA3 more susceptible to the damage caused by KA (Ben-Ari and Cossart, 2000). Furthermore, GABAergic interneurons in CA3 and CA1 express high levels of GluR5 subunits (Bloss and Hunter, 2010), while CA3 pyramidal neurons express high levels of GluR6 subunits (Bahn *et al.*, 1994). It has been shown that GluR5 knock-out mice are more susceptible to KA-induced seizures, whereas GluR6 knockout mice are less susceptible to developing seizures (Mulle *et al.*, 1998; Fisahn *et al.*, 2004). Related to

4

these animal findings, there was a downregulation of GluR5 and GluR6 mRNA levels in tissue from patients with TLE (Mathern *et al.*, 1998), suggesting, over time, the expression profile of the subunits could be altered in response to epileptiform activity.

Intracerebral or systemic administration of KA leads to the development of spontaneous recurrent seizures with a latent period of one week to one month after an early episode of status epilepticus (Bragin *et al.*, 1999; Riban *et al.*, 2002; Raedt *et al.*, 2009; Van Nieuwenhuyse *et al.*, 2015). During the latent period, the network undergoes changes both functionally and structurally, and is characterised by interictal events (White *et al.*, 2010; Chauviere *et al.*, 2012). The rate of interictal events is higher and lower in animals that develop and do not develop spontaneous seizures, respectively (White *et al.*, 2010). Chauviere *et al.* reported the occurrence of two different types of interictal events during the latent period. These interictal events showed different development profiles and waveforms: 1) the first type has a spike and wave form and its occurs at a progressively lower rate, and 2) the second type has only the spike component and its occurrence increased during the latent period until the onset of the first spontaneous seizure event (Chauviere *et al.*, 2012). Hippocampal lesions and mossy fibre sprouting are characteristic features of TLE. Hippocampal lesions are characterised by pyramidal cell loss in CA3, CA1, loss of neurons in the hilus, and loss of parvalbumin-positive interneuron in subiculum (Drexel *et al.*, 2012). Best *et al.* reported the existence of two groups of parvalbumin-positive interneuron in CA1: 1) KA-sensitive, soma-targeting PV+ interneurons, and 2) KA-resistant, axon initial segment targeting PV+ interneurons (Best *et al.*, 1994). Damage to dentate gyrus is characterised by mossy fibre sprouting, granule cell layer dispersion and astrogliosis (Bouilleret *et al.*, 2000; Van Nieuwenhuyse *et al.*, 2015).

This model is also used for assessing the effects of AEDs on spontaneous seizures (Riban *et al.*, 2002; Grabenstatter *et al.*, 2005; Grabenstatter *et al.*, 2007; Grabenstatter and Dudek, 2008). KA-induced epileptiform activity is pharmaco-resistant to valproate, phenytoin, and carbamazepine, but are suppressed by diazepam in Swiss male mice (Riban *et al.*, 2002). However, Grabenstatter *et al.* reported strong suppressive actions of carbamazepine on motor seizures induced by KA in male Sprague Dawley rats (Grabenstatter *et al.*, 2007). This highlights one of the

limitations of the model that rodents of different species show different sensitivity to AEDs.

1.2.2 *Tetanus toxin model*

Tetanus toxin (TeTx) has been used as a proconvulsant, inducing chronic epilepsies in rats. Depending on the site of injection in the brain, it has been used for modelling temporal lobe epilepsy when injected into hippocampus or focal neocortical epilepsy when injected into neocortex (Mellanby *et al.*, 1977; Empson and Jefferys, 1993; Jefferys *et al.*, 1995).

TeTx is a zinc protease that cleaves vesicle associated membrane protein (VAMP) in the neuronal terminals and reduces the release of neurotransmitters (Mellanby and Green, 1981; Schiavo *et al.*, 1992). VAMP1 and VAMP2 are two TeTx-sensitive isoforms present in both excitatory and inhibitory neurons. Inhibitory terminals express higher levels of VAMP1 while excitatory neurons express higher levels of VAMP2 (Ferecsko *et al.*, 2015).

Injecting TeTx into the hippocampus produced epileptiform activity with intermittent spontaneous seizures that are sensitive to carbamazepine (Mellanby *et al.*, 1977; Jefferys *et al.*, 1995). Histological studies on tissue from these rats show no detectable cell loss (Mellanby *et al.*, 1977). However, TeTx at higher concentrations induce cell death and high mortality (Bagetta *et al.*, 1990). Early after intra-cortical injections of TeTx, inhibitory and excitatory synaptic transmissions are completely and partially blocked, respectively (Jordan and Jefferys, 1992; Whittington and Jefferys, 1994; Ferecsko *et al.*, 2015). This has a disinhibitory effect on the network, thus making it hyperexcitable and causing epilepsy. A few weeks to months after being injected with TeTx, rats start to show fewer seizures and eventually gain remission, but they continue to show cognitive impairment (Jefferys *et al.*, 1992). Examining tissue taken from these rats, Vreugdenhil *et al.* reported changes in intrinsic properties of neurons, reduced synaptic excitation of interneurons, and the connectivity patterns (Vreugdenhil *et al.*, 2002). Some of these changes may be protective homeostatic responses to epileptic triggers that aid the networks to regain a balance that reduce the rate of development of seizures (Vreugdenhil *et al.*, 2002). An interesting feature of this model is that the epileptiform activity does not develop into status epilepticus (Finnerty and Jefferys, 2002; Barkmeier and Loeb, 2009). Minimal mortality rate at low doses and

the occurrence of spontaneous seizures makes it a good model for *in vivo* screening of antiepileptic drugs (Doheny *et al.*, 2002).

1.3 *In vitro* models

In vitro models have been an important research tool in epilepsy research for many years (see recent review – (Avoli and Jefferys, 2016)). They reliably produce electrographic features of seizure events observed *in vivo*. However, they do not have the long-range anatomical connections or the behavioural component as in *in vivo*. They are suitable for studying network interactions, mechanisms of ictogenesis, and various aspects of it. The most widely used *in vitro* models involve preparing brain slices acutely from wild-type animals, and epileptiform activity from these slices is recorded in a recording chamber after perfusing with a proepileptic medium to induce epileptiform activity.

1.3.1 Zero-magnesium model

In zero magnesium models ($0Mg^{2+}$), acute brain slices are perfused with magnesium-free ACSF. In normal conditions, NMDA channels are blocked by Mg^{2+} ions in a voltage-dependent manner. In $0Mg^{2+}$ models, however, the activity of pyramidal cells is increased as the NMDA channels are free of Mg^{2+} block, thus making the tissue hyperexcitable. Although synaptic inhibition is intact initially, it may eventually fail (Whittington *et al.*, 1995); it enables us to study the activity and interactions of different cellular components during the evolution, progression, and late stage events of ictal discharges.

However, as the pathological activity builds-up, every neuron in the network participates, which is the defining feature of the full ictal, tonic-clonic-like patterns (Mody *et al.*, 1987; Dreier and Heinemann, 1991), which propagate with increasingly high velocities (Trevelyan *et al.*, 2006; Trevelyan *et al.*, 2007). An *in vitro* model of status epilepticus – intractable continuous bursts of relatively short duration ictal events - is studied by bathing the slices for a prolonged period in a solution with low/zero extracellular magnesium ion concentration. It was shown that these late epileptiform events were not suppressed by commonly used anticonvulsant drugs (Anderson *et al.*,

1986; Zhang *et al.*, 1995; Pfeiffer *et al.*, 1996). This model can be used as tool to further investigate the factors influencing refractoriness of late events.

1.3.2 4-Aminopyridine model

In 4-Aminopyridine (4AP) model, acute brain slices are perfused with ACSF supplemented with 4-aminopyridine (Avoli and Jefferys, 2016). 4AP is a voltage-gated potassium channel blocker with high efficacy, particularly for $K_v3.1$ channels. These channels are expressed on all neurons, but they are expressed at a particularly high density on parvalbumin-positive (PV+) fast-spiking basket cells (Du *et al.*, 1996; Martina *et al.*, 1998). Hence, 4AP affects all cells, but primarily PV+ interneurons in the network. This blockade by 4AP causes depolarisation of membrane potential and an increase in input resistance of the cells making them more susceptible to increase their firing rate. Consequently, it changes the activity pattern of the network and makes it hyperexcitable.

In an interface local field potential (LFP) recording setup, 4AP induces different patterns of epileptiform in different regions of the slice. In hippocampal territory, 4AP normally induces recurrent short discharges, and long polyburst events (Watts and Jefferys, 1993). Rate of occurrence of these discharges is lowered by application of baclofen, whereas the polyburst events were enhanced (Watts and Jefferys, 1993). In the parahippocampal structures such as, temporal neocortex, entorhinal cortex, and subiculum it elicits ictal discharges characterised by tonic-clonic like pattern (Avoli *et al.*, 1996). 4AP-induced ictal discharges, but not the recurrent discharges in hippocampal area (CA), are sensitive to standard AEDs (Bruckner and Heinemann, 2000).

1.4 Genetic epilepsies – causes, models, and interpretations

Gene mutations can cause epilepsy as a primary or secondary syndrome. There is a growing list of epileptic gene mutations that affect ion channels and neurotransmitters, and also cortical formation (e.g., microencephaly genes), interneuronopathies (e.g., ARX gene), tubulinopathies (e.g., TUBA1A gene) and many more (Poduri and Lowenstein, 2011; Lerche *et al.*, 2013). Identifying such gene mutations (Epi *et al.*, 2013), and creating genetically-modified animal models (Smart

et al., 1998; Yu *et al.*, 2006), will present opportunities to study the mechanisms of epileptogenesis, their role in brain development, and the physiology of the brain. Such models also provide a better screening platform for assessing clinically used AEDs as they develop spontaneous seizures without any external stimuli such as a chemoconvulsant or electric shock (Hawkins *et al.*, 2017).

Genetic mutations causing loss-of-functions or deletion of ion channels cause many different types of epilepsies. Loss-of-function mutation in scn1a gene, encoding for $Na_v1.1$ channels, underlies the development of severe myoclonic epilepsy in infancy (SMEI) (Yu *et al.*, 2006). Such mutations are expected to lower the network excitability, but it results in increased network excitability due to reduced inhibition. $Na_v1.1$ channels are selectively expressed on GABAergic interneurons and the mutation in scn1a gene causes reduced excitability of inhibitory interneurons, thus causing this epilepsy syndrome (Yu *et al.*, 2006).

Pathogenic gene mutations can be protective or deleterious and this depends on the genomic setting of the organism. Kcna1 gene encodes for a subunit of voltage-gated potassium channel ($K_v1.1$) expressed on the axonal and presynaptic domains of neurons. $K_v1.1$ channel regulates the firing properties and neurotransmitter release from neurons. Deletion of these channels in mice ($kcna1^{-/-}$) cause tonic-clonic seizures (Smart *et al.*, 1998). Cacna1a gene encodes for a subunit of the presynaptic P/Q-calcium channels. These channels mediate neurotransmitter release from nerve terminals. Partial loss-of-function mutation in cacna1a gene (Cacna1a ^{tg}/^{tg}) causes absence seizures in a mouse model (Noebels and Sidman, 1979; Fletcher *et al.*, 1996). Similar mutation in kcna1 and cacna1 were identified in human patients diagnosed for temporal lobe epilepsy and childhood absence epilepsy, respectively (Zuberi *et al.*, 1999; Imbrici *et al.*, 2004). However, mice carrying both the epileptic mutations show improved survival rate, absence of spike-wave seizures and nearly 60% drop in the occurrence of tonic-clonic seizures (Glasscock *et al.*, 2007). In cacna1a ^{tg}/^{tg} mice, the reduced excitability due to loss of function of calcium channels is compensated by increased excitability caused due to $kcna1^{-/-}$ mutation, and vice versa (Glasscock *et al.*, 2007). But in another double mutant mice, carrying a mutation in scan2a gene resulting in enhanced persistent sodium current, and kcnq2 gene resulting in impaired voltage-gated potassium current ($I_{K.M}$), the severity of epilepsy was increased with an

early onset (Kearney *et al.*, 2006). These demonstrate that the severity of epilepsy can be either improved or worsened by the interactions between of two epileptic variants of ion channels. Epilepsy genetics is complicated - it is hard to predict the outcomes of mutations, and the cause of genetic epilepsy based on the EEGs and clinical symptoms.

1.5 Characteristics of epileptiform events: pro-epileptic, epileptic, and anti-epileptic activity

Cortical epilepsy is characterized by propagating neuronal discharges. These are pathological transient high activity events during which neurons show modified firing patterns. There is growing evidence that cortical activity is regulated by inhibitory restraints (Prince and Wilder, 1967; Dichter and Spencer, 1969; Schwartz and Bonhoeffer, 2001; Trevelyan *et al.*, 2006; Trevelyan *et al.*, 2007; Cammarota *et al.*, 2013; Trevelyan and Schevon, 2013). Surges in cortical activity trigger a pattern of intense inhibitory discharges that appears to be a key defence against the initial surge in activity developing into full ictal events. During the spread of ictal activity, PV+ interneurons provide a powerful feedforward inhibition ahead of ictal wavefront, to control or slowdown the spread of the ictal wavefront and recruitment of surrounding territories (Cammarota *et al.*, 2013). These surrounding territories thus experience huge feedforward, synaptic bombardment, a defining feature of what has been termed the ictal penumbra. This phenomenon of restraint observed *in vitro* (Trevelyan *et al.*, 2006; Trevelyan *et al.*, 2007; Cammarota *et al.*, 2013; Trevelyan and Schevon, 2013) and *in vivo* models (Schwartz and Bonhoeffer, 2001; Schevon *et al.*, 2012), further strengthened the concept of protective 'surround inhibition', and arises from the cellular connectivity pattern in cortex.

Prior to the occurrence of paroxysmal depolarising shifts (recruitment into ictal activity), neurons in the penumbra show very low level of firing despite experiencing large rhythmic depolarisations. This may last for a few seconds and is the signature of invading ictal wavefront termed as restrained depolarising shift (pre-ictal inhibitory barrages) (Trevelyan and Schevon, 2013). Sometimes, the activity can return to baseline quiescence, constituting a successful restraint of epileptic discharges

(Schevon *et al.*, 2012). In other cases, after repeated restrained depolarisation shifts, the inhibitory restraint fails, leading to paroxysmal depolarisation shifts bursts.

Ictal discharges propagated in modular fashion by recruiting clusters of pyramidal cells (Trevelyan *et al.*, 2006). This group of pyramidal cells have a common source of inhibition or restraint that opposes and delays their recruitment (Trevelyan *et al.*, 2006). PV+ interneurons in tandem with other classes of interneurons were identified to be the source of this inhibition that plays a pivotal role in providing restraining action against recruitment and propagation. In 4AP model, along with PV+ interneurons , somatostatin-positive interneurons display intense firing activity before recruitment of excitatory cells into ictal activity, but poorly correlated with the inhibitory currents in pyramidal neurons (Cammarota *et al.*, 2013). To summarize, the latency for recruitment into ictal events is directly proportional and propagation speed of ictal events is inversely proportional to the number of pre-ictal inhibitory barrages experienced by neurons in ictal penumbra.

1.6 Aims of this thesis

Understanding the how epileptiform activity develops in different cortical networks remains a major goal for epilepsy research. Clinical evidence suggests strongly that different regions of the brain have different epileptic activity patterns and seizure susceptibility. The reasons for this susceptibility, however, are also not known. Investigating the proneness of cortical networks to develop epileptiform activity and their responsiveness to disease-modifying drugs will enable us to better understand epileptiform activity, to develop new anti-epileptic drugs and novel strategies for epilepsy treatment. Following are the aims of this thesis to provide important insights into understanding various features of epileptiform activity:

- To characterise the evolution of epileptiform activity in different cortical networks induced by using zero-magnesium *in vitro* model of epilepsy, and the interactions between these networks in brain slices.

- To investigate the actions of disease-modifying drugs (diazepam, baclofen, and fluorocitrate), and the effect of genetic mutations on various facets of the development of *in vitro* epileptiform activity in different cortical networks.

- To study the effects of 4-aminopyridine, a chemoconvulsant, on intrinsic properties of neocortical parvalbumin-positive interneuron.

1.7 References

1. Anderson, W.W., Lewis, D.V., Swartzwelder, H.S. and Wilson, W.A. (1986) 'Magnesium-free medium activates seizure-like events in the rat hippocampal slice', *Brain Res*, 398(1), pp. 215-9.

2. Aronica, E. and Crino, P.B. (2014) 'Epilepsy related to developmental tumors and malformations of cortical development', *Neurotherapeutics*, 11(2), pp. 251-68.

3. Avoli, M., Barbarosie, M., Lucke, A., Nagao, T., Lopantsev, V. and Kohling, R. (1996) 'Synchronous GABA-mediated potentials and epileptiform discharges in the rat limbic system *in vitro*', *J Neurosci*, 16(12), pp. 3912-24.

4. Avoli, M. and Jefferys, J.G. (2016) 'Models of drug-induced epileptiform synchronization *in vitro*', *J Neurosci Methods*, 260, pp. 26-32.

5. Bagetta, G., Corasaniti, M.T., Nistico, G. and Bowery, N.G. (1990) 'Behavioural and neuropathological effects produced by tetanus toxin injected into the hippocampus of rats', *Neuropharmacology*, 29(8), pp. 765-70.

6. Bahn, S., Volk, B. and Wisden, W. (1994) 'Kainate receptor gene expression in the developing rat brain', *J Neurosci*, 14(9), pp. 5525-47.

7. Barkmeier, D.T. and Loeb, J.A. (2009) 'An animal model to study the clinical significance of interictal spiking', *Clin EEG Neurosci*, 40(4), pp. 234-8.

8. Ben-Ari, Y. (1985) 'Limbic seizure and brain damage produced by kainic acid: mechanisms and relevance to human temporal lobe epilepsy', *Neuroscience*, 14(2), pp. 375-403.

9. Ben-Ari, Y. and Cossart, R. (2000) 'Kainate, a double agent that generates seizures: two decades of progress', *Trends Neurosci*, 23(11), pp. 580-7.

10. Berg, A.T., Berkovic, S.F., Brodie, M.J., Buchhalter, J., Cross, J.H., van Emde Boas, W., Engel, J., French, J., Glauser, T.A., Mathern, G.W., Moshe, S.L., Nordli, D., Plouin, P. and Scheffer, I.E. (2010) 'Revised terminology and concepts for organization of seizures and epilepsies: report of the ILAE

Commission on Classification and Terminology, 2005-2009', *Epilepsia*, 51(4), pp. 676-85.

11. Best, N., Mitchell, J. and Wheal, H.V. (1994) 'Ultrastructure of parvalbumin-immunoreactive neurons in the CA1 area of the rat hippocampus following a kainic acid injection', *Acta Neuropathol*, 87(2), pp. 187-95.

12. Bloss, E.B. and Hunter, R.G. (2010) 'Hippocampal kainate receptors', *Vitam Horm*, 82, pp. 167-84.

13. Bonilha, L., Elm, J.J., Edwards, J.C., Morgan, P.S., Hicks, C., Lozar, C., Rumboldt, Z., Roberts, D.R., Rorden, C. and Eckert, M.A. (2010) 'How common is brain atrophy in patients with medial temporal lobe epilepsy?', *Epilepsia*, 51(9), pp. 1774-9.

14. Bonilha, L., Rorden, C., Appenzeller, S., Coan, A.C., Cendes, F. and Li, L.M. (2006) 'Gray matter atrophy associated with duration of temporal lobe epilepsy', *Neuroimage*, 32(3), pp. 1070-9.

15. Bouilleret, V., Loup, F., Kiener, T., Marescaux, C. and Fritschy, J.M. (2000) 'Early loss of interneurons and delayed subunit-specific changes in GABA(A)-receptor expression in a mouse model of mesial temporal lobe epilepsy', *Hippocampus*, 10(3), pp. 305-24.

16. Bragin, A., Engel, J., Jr., Wilson, C.L., Vizentin, E. and Mathern, G.W. (1999) 'Electrophysiologic analysis of a chronic seizure model after unilateral hippocampal KA injection', *Epilepsia*, 40(9), pp. 1210-21.

17. Bragin, A., Wilson, C.L. and Engel, J., Jr. (2000) 'Chronic epileptogenesis requires development of a network of pathologically interconnected neuron clusters: a hypothesis', *Epilepsia*, 41 Suppl 6, pp. S144-52.

18. Brooks-Kayal, A.R., Bath, K.G., Berg, A.T., Galanopoulou, A.S., Holmes, G.L., Jensen, F.E., Kanner, A.M., O'Brien, T.J., Whittemore, V.H., Winawer, M.R., Patel, M. and Scharfman, H.E. (2013) 'Issues related to symptomatic and disease-modifying treatments affecting cognitive and neuropsychiatric comorbidities of epilepsy', *Epilepsia*, 54 Suppl 4, pp. 44-60.

19. Bruckner, C. and Heinemann, U. (2000) 'Effects of standard anticonvulsant drugs on different patterns of epileptiform discharges induced by 4-aminopyridine in combined entorhinal cortex-hippocampal slices', *Brain Res*, 859(1), pp. 15-20.

20. Cammarota, M., Losi, G., Chiavegato, A., Zonta, M. and Carmignoto, G. (2013) 'Fast spiking interneuron control of seizure propagation in a cortical slice model of focal epilepsy', *J Physiol*, 591(4), pp. 807-22.

21. Chauviere, L., Doublet, T., Ghestem, A., Siyoucef, S.S., Wendling, F., Huys, R., Jirsa, V., Bartolomei, F. and Bernard, C. (2012) 'Changes in interictal spike features precede the onset of temporal lobe epilepsy', *Ann Neurol*, 71(6), pp. 805-14.

22. Cronin, J. and Dudek, F.E. (1988) 'Chronic seizures and collateral sprouting of dentate mossy fibers after kainic acid treatment in rats', *Brain Res*, 474(1), pp. 181-4.

23. Dichter, M. and Spencer, W.A. (1969) 'Penicillin-induced interictal discharges from the cat hippocampus. II. Mechanisms underlying origin and restriction', *J Neurophysiol*, 32(5), pp. 663-87.

24. Dichter, M.A. (2009) 'Emerging concepts in the pathogenesis of epilepsy and epileptogenesis', *Arch Neurol*, 66(4), pp. 443-7.

25. Doheny, H.C., Whittington, M.A., Jefferys, J.G. and Patsalos, P.N. (2002) 'A comparison of the efficacy of carbamazepine and the novel anti-epileptic drug levetiracetam in the tetanus toxin model of focal complex partial epilepsy', *Br J Pharmacol*, 135(6), pp. 1425-34.

26. Dreier, J.P. and Heinemann, U. (1991) 'Regional and time dependent variations of low Mg2+ induced epileptiform activity in rat temporal cortex slices', *Exp Brain Res*, 87(3), pp. 581-96.

27. Drexel, M., Preidt, A.P. and Sperk, G. (2012) 'Sequel of spontaneous seizures after kainic acid-induced status epilepticus and associated neuropathological

changes in the subiculum and entorhinal cortex', *Neuropharmacology*, 63(5), pp. 806-17.

28. Du, J., Zhang, L., Weiser, M., Rudy, B. and McBain, C.J. (1996) 'Developmental expression and functional characterization of the potassium-channel subunit Kv3.1b in parvalbumin-containing interneurons of the rat hippocampus', *J Neurosci*, 16(2), pp. 506-18.

29. Empson, R.M. and Jefferys, J.G. (1993) 'Synaptic inhibition in primary and secondary chronic epileptic foci induced by intrahippocampal tetanus toxin in the rat', *J Physiol*, 465, pp. 595-614.

30. Epi, K.C., Epilepsy Phenome/Genome, P., Allen, A.S., Berkovic, S.F., Cossette, P., Delanty, N., Dlugos, D., Eichler, E.E., Epstein, M.P., Glauser, T., Goldstein, D.B., Han, Y., Heinzen, E.L., Hitomi, Y., Howell, K.B., Johnson, M.R., Kuzniecky, R., Lowenstein, D.H., Lu, Y.F., Madou, M.R., Marson, A.G., Mefford, H.C., Esmaeeli Nieh, S., O'Brien, T.J., Ottman, R., Petrovski, S., Poduri, A., Ruzzo, E.K., Scheffer, I.E., Sherr, E.H., Yuskaitis, C.J., Abou-Khalil, B., Alldredge, B.K., Bautista, J.F., Berkovic, S.F., Boro, A., Cascino, G.D., Consalvo, D., Crumrine, P., Devinsky, O., Dlugos, D., Epstein, M.P., Fiol, M., Fountain, N.B., French, J., Friedman, D., Geller, E.B., Glauser, T., Glynn, S., Haut, S.R., Hayward, J., Helmers, S.L., Joshi, S., Kanner, A., Kirsch, H.E., Knowlton, R.C., Kossoff, E.H., Kuperman, R., Kuzniecky, R., Lowenstein, D.H., McGuire, S.M., Motika, P.V., Novotny, E.J., Ottman, R., Paolicchi, J.M., Parent, J.M., Park, K., Poduri, A., Scheffer, I.E., Shellhaas, R.A., Sherr, E.H., Shih, J.J., Singh, R., Sirven, J., Smith, M.C., Sullivan, J., Lin Thio, L., Venkat, A., Vining, E.P., Von Allmen, G.K., Weisenberg, J.L., Widdess-Walsh, P. and Winawer, M.R. (2013) 'De novo mutations in epileptic encephalopathies', *Nature*, 501(7466), pp. 217-21.

31. Ferecsko, A.S., Jiruska, P., Foss, L., Powell, A.D., Chang, W.C., Sik, A. and Jefferys, J.G. (2015) 'Structural and functional substrates of tetanus toxin in an animal model of temporal lobe epilepsy', *Brain Struct Funct*, 220(2), pp. 1013-29.

32. Finnerty, G.T. and Jefferys, J.G. (2002) 'Investigation of the neuronal aggregate generating seizures in the rat tetanus toxin model of epilepsy', *J Neurophysiol*, 88(6), pp. 2919-27.

33. Fisahn, A., Contractor, A., Traub, R.D., Buhl, E.H., Heinemann, S.F. and McBain, C.J. (2004) 'Distinct roles for the kainate receptor subunits GluR5 and GluR6 in kainate-induced hippocampal gamma oscillations', *J Neurosci*, 24(43), pp. 9658-68.

34. Fisher, R.S., van Emde Boas, W., Blume, W., Elger, C., Genton, P., Lee, P. and Engel, J., Jr. (2005) 'Epileptic seizures and epilepsy: definitions proposed by the International League Against Epilepsy (ILAE) and the International Bureau for Epilepsy (IBE)', *Epilepsia*, 46(4), pp. 470-2.

35. Fletcher, C.F., Lutz, C.M., O'Sullivan, T.N., Shaughnessy, J.D., Jr., Hawkes, R., Frankel, W.N., Copeland, N.G. and Jenkins, N.A. (1996) 'Absence epilepsy in tottering mutant mice is associated with calcium channel defects', *Cell*, 87(4), pp. 607-17.

36. Glasscock, E., Qian, J., Yoo, J.W. and Noebels, J.L. (2007) 'Masking epilepsy by combining two epilepsy genes', *Nat Neurosci*, 10(12), pp. 1554-8.

37. Grabenstatter, H.L., Clark, S. and Dudek, F.E. (2007) 'Anticonvulsant effects of carbamazepine on spontaneous seizures in rats with kainate-induced epilepsy: comparison of intraperitoneal injections with drug-in-food protocols', *Epilepsia*, 48(12), pp. 2287-95.

38. Grabenstatter, H.L. and Dudek, F.E. (2008) 'A new potential AED, carisbamate, substantially reduces spontaneous motor seizures in rats with kainate-induced epilepsy', *Epilepsia*, 49(10), pp. 1787-94.

39. Grabenstatter, H.L., Ferraro, D.J., Williams, P.A., Chapman, P.L. and Dudek, F.E. (2005) 'Use of chronic epilepsy models in antiepileptic drug discovery: the effect of topiramate on spontaneous motor seizures in rats with kainate-induced epilepsy', *Epilepsia*, 46(1), pp. 8-14.

40. Hawkins, N.A., Anderson, L.L., Gertler, T.S., Laux, L., George, A.L., Jr. and Kearney, J.A. (2017) 'Screening of conventional anticonvulsants in a genetic mouse model of epilepsy', *Ann Clin Transl Neurol*, 4(5), pp. 326-339.

41. Herman, S.T. (2002) 'Epilepsy after brain insult: targeting epileptogenesis', *Neurology*, 59(9 Suppl 5), pp. S21-6.

42. Imbrici, P., Jaffe, S.L., Eunson, L.H., Davies, N.P., Herd, C., Robertson, R., Kullmann, D.M. and Hanna, M.G. (2004) 'Dysfunction of the brain calcium channel CaV2.1 in absence epilepsy and episodic ataxia', *Brain*, 127(Pt 12), pp. 2682-92.

43. Inostroza, M., Cid, E., Brotons-Mas, J., Gal, B., Aivar, P., Uzcategui, Y.G., Sandi, C. and Menendez de la Prida, L. (2011) 'Hippocampal-dependent spatial memory in the water maze is preserved in an experimental model of temporal lobe epilepsy in rats', *PLoS One*, 6(7), p. e22372.

44. Inostroza, M., Cid, E., Menendez de la Prida, L. and Sandi, C. (2012) 'Different emotional disturbances in two experimental models of temporal lobe epilepsy in rats', *PLoS One*, 7(6), p. e38959.

45. Jacobs, M.P., Leblanc, G.G., Brooks-Kayal, A., Jensen, F.E., Lowenstein, D.H., Noebels, J.L., Spencer, D.D. and Swann, J.W. (2009) 'Curing epilepsy: progress and future directions', *Epilepsy Behav*, 14(3), pp. 438-45.

46. Jefferys, J.G., Borck, C. and Mellanby, J. (1995) 'Chronic focal epilepsy induced by intracerebral tetanus toxin', *Ital J Neurol Sci*, 16(1-2), pp. 27-32.

47. Jefferys, J.G., Evans, B.J., Hughes, S.A. and Williams, S.F. (1992) 'Neuropathology of the chronic epileptic syndrome induced by intrahippocampal tetanus toxin in rat: preservation of pyramidal cells and incidence of dark cells', *Neuropathol Appl Neurobiol*, 18(1), pp. 53-70.

48. Jordan, S.J. and Jefferys, J.G. (1992) 'Sustained and selective block of IPSPs in brain slices from rats made epileptic by intrahippocampal tetanus toxin', *Epilepsy Res*, 11(2), pp. 119-29.

49. Kearney, J.A., Yang, Y., Beyer, B., Bergren, S.K., Claes, L., Dejonghe, P. and Frankel, W.N. (2006) 'Severe epilepsy resulting from genetic interaction between Scn2a and Kcnq2', *Hum Mol Genet*, 15(6), pp. 1043-8.

50. Lancman, M.E., Golimstok, A., Norscini, J. and Granillo, R. (1993) 'Risk factors for developing seizures after a stroke', *Epilepsia*, 34(1), pp. 141-3.

51. Lerche, H., Shah, M., Beck, H., Noebels, J., Johnston, D. and Vincent, A. (2013) 'Ion channels in genetic and acquired forms of epilepsy', *J Physiol*, 591(4), pp. 753-64.

52. Loscher, W. (2002) 'Current status and future directions in the pharmacotherapy of epilepsy', *Trends Pharmacol Sci*, 23(3), pp. 113-8.

53. Martina, M., Schultz, J.H., Ehmke, H., Monyer, H. and Jonas, P. (1998) 'Functional and molecular differences between voltage-gated K+ channels of fast-spiking interneurons and pyramidal neurons of rat hippocampus', *J Neurosci*, 18(20), pp. 8111-25.

54. Mathern, G.W., Pretorius, J.K., Kornblum, H.I., Mendoza, D., Lozada, A., Leite, J.P., Chimelli, L., Born, D.E., Fried, I., Sakamoto, A.C., Assirati, J.A., Peacock, W.J., Ojemann, G.A. and Adelson, P.D. (1998) 'Altered hippocampal kainate-receptor mRNA levels in temporal lobe epilepsy patients', *Neurobiol Dis*, 5(3), pp. 151-76.

55. Mazarati, A.M., Shin, D., Kwon, Y.S., Bragin, A., Pineda, E., Tio, D., Taylor, A.N. and Sankar, R. (2009) 'Elevated plasma corticosterone level and depressive behavior in experimental temporal lobe epilepsy', *Neurobiol Dis*, 34(3), pp. 457-61.

56. Mellanby, J., George, G., Robinson, A. and Thompson, P. (1977) 'Epileptiform syndrome in rats produced by injecting tetanus toxin into the hippocampus', *J Neurol Neurosurg Psychiatry*, 40(4), pp. 404-14.

57. Mellanby, J. and Green, J. (1981) 'How does tetanus toxin act?', *Neuroscience*, 6(3), pp. 281-300.

58. Mody, I., Lambert, J.D. and Heinemann, U. (1987) 'Low extracellular magnesium induces epileptiform activity and spreading depression in rat hippocampal slices', *J Neurophysiol*, 57(3), pp. 869-88.

59. Mulle, C., Sailer, A., Perez-Otano, I., Dickinson-Anson, H., Castillo, P.E., Bureau, I., Maron, C., Gage, F.H., Mann, J.R., Bettler, B. and Heinemann, S.F. (1998) 'Altered synaptic physiology and reduced susceptibility to kainate-induced seizures in GluR6-deficient mice', *Nature*, 392(6676), pp. 601-5.

60. Neligan, A. and Shorvon, S.D. (2011) 'Prognostic factors, morbidity and mortality in tonic-clonic status epilepticus: a review', *Epilepsy Res*, 93(1), pp. 1-10.

61. Noebels, J.L. and Sidman, R.L. (1979) 'Inherited epilepsy: spike-wave and focal motor seizures in the mutant mouse tottering', *Science*, 204(4399), pp. 1334-6.

62. Pfeiffer, M., Draguhn, A., Meierkord, H. and Heinemann, U. (1996) 'Effects of gamma-aminobutyric acid (GABA) agonists and GABA uptake inhibitors on pharmacosensitive and pharmacoresistant epileptiform activity *in vitro*', *Br J Pharmacol*, 119(3), pp. 569-77.

63. Pitkanen, A. (2010) 'Therapeutic approaches to epileptogenesis--hope on the horizon', *Epilepsia*, 51 Suppl 3, pp. 2-17.

64. Poduri, A. and Lowenstein, D. (2011) 'Epilepsy genetics--past, present, and future', *Curr Opin Genet Dev*, 21(3), pp. 325-32.

65. Prince, D.A. and Wilder, B.J. (1967) 'Control mechanisms in cortical epileptogenic foci. "Surround" inhibition', *Arch Neurol*, 16(2), pp. 194-202.

66. Raedt, R., Van Dycke, A., Van Melkebeke, D., De Smedt, T., Claeys, P., Wyckhuys, T., Vonck, K., Wadman, W. and Boon, P. (2009) 'Seizures in the intrahippocampal kainic acid epilepsy model: characterization using long-term video-EEG monitoring in the rat', *Acta Neurol Scand*, 119(5), pp. 293-303.

67. Riban, V., Bouilleret, V., Pham-Le, B.T., Fritschy, J.M., Marescaux, C. and Depaulis, A. (2002) 'Evolution of hippocampal epileptic activity during the

development of hippocampal sclerosis in a mouse model of temporal lobe epilepsy', *Neuroscience*, 112(1), pp. 101-11.

68. Ruda, R., Trevisan, E. and Soffietti, R. (2010) 'Epilepsy and brain tumors', *Curr Opin Oncol*, 22(6), pp. 611-20.

69. Scheffer, I.E., Berkovic, S., Capovilla, G., Connolly, M.B., French, J., Guilhoto, L., Hirsch, E., Jain, S., Mathern, G.W., Moshe, S.L., Nordli, D.R., Perucca, E., Tomson, T., Wiebe, S., Zhang, Y.H. and Zuberi, S.M. (2017) 'ILAE classification of the epilepsies: Position paper of the ILAE Commission for Classification and Terminology', *Epilepsia*, 58(4), pp. 512-521.

70. Schevon, C.A., Weiss, S.A., McKhann, G., Jr., Goodman, R.R., Yuste, R., Emerson, R.G. and Trevelyan, A.J. (2012) 'Evidence of an inhibitory restraint of seizure activity in humans', *Nat Commun*, 3, p. 1060.

71. Schiavo, G., Benfenati, F., Poulain, B., Rossetto, O., Polverino de Laureto, P., DasGupta, B.R. and Montecucco, C. (1992) 'Tetanus and botulinum-B neurotoxins block neurotransmitter release by proteolytic cleavage of synaptobrevin', *Nature*, 359(6398), pp. 832-5.

72. Schwartz, T.H. and Bonhoeffer, T. (2001) '*In vivo* optical mapping of epileptic foci and surround inhibition in ferret cerebral cortex', *Nat Med*, 7(9), pp. 1063-7.

73. Schwarzer, C., Williamson, J.M., Lothman, E.W., Vezzani, A. and Sperk, G. (1995) 'Somatostatin, neuropeptide Y, neurokinin B and cholecystokinin immunoreactivity in two chronic models of temporal lobe epilepsy', *Neuroscience*, 69(3), pp. 831-45.

74. Schwob, J.E., Fuller, T., Price, J.L. and Olney, J.W. (1980) 'Widespread patterns of neuronal damage following systemic or intracerebral injections of kainic acid: a histological study', *Neuroscience*, 5(6), pp. 991-1014.

75. Sillanpaa, M. and Shinnar, S. (2010) 'Long-term mortality in childhood-onset epilepsy', *N Engl J Med*, 363(26), pp. 2522-9.

76. Singh, G., Prabhakar, S. and Modi, M. (2008) 'Central nervous system infections and epilepsy', *Epilepsia*, 49 Suppl 6, p. 1.

77. Smart, S.L., Lopantsev, V., Zhang, C.L., Robbins, C.A., Wang, H., Chiu, S.Y., Schwartzkroin, P.A., Messing, A. and Tempel, B.L. (1998) 'Deletion of the K(V)1.1 potassium channel causes epilepsy in mice', *Neuron*, 20(4), pp. 809-19.

78. Sutula, T., Cascino, G., Cavazos, J., Parada, I. and Ramirez, L. (1989) 'Mossy fiber synaptic reorganization in the epileptic human temporal lobe', *Ann Neurol*, 26(3), pp. 321-30.

79. Trevelyan, A.J. and Schevon, C.A. (2013) 'How inhibition influences seizure propagation', *Neuropharmacology*, 69, pp. 45-54.

80. Trevelyan, A.J., Sussillo, D., Watson, B.O. and Yuste, R. (2006) 'Modular propagation of epileptiform activity: evidence for an inhibitory veto in neocortex', *J Neurosci*, 26(48), pp. 12447-55.

81. Trevelyan, A.J., Sussillo, D. and Yuste, R. (2007) 'Feedforward inhibition contributes to the control of epileptiform propagation speed', *J Neurosci*, 27(13), pp. 3383-7.

82. Van Nieuwenhuyse, B., Raedt, R., Sprengers, M., Dauwe, I., Gadeyne, S., Carrette, E., Delbeke, J., Wadman, W.J., Boon, P. and Vonck, K. (2015) 'The systemic kainic acid rat model of temporal lobe epilepsy: Long-term EEG monitoring', *Brain Res*, 1627, pp. 1-11.

83. Vespa, P.M., Nuwer, M.R., Nenov, V., Ronne-Engstrom, E., Hovda, D.A., Bergsneider, M., Kelly, D.F., Martin, N.A. and Becker, D.P. (1999) 'Increased incidence and impact of nonconvulsive and convulsive seizures after traumatic brain injury as detected by continuous electroencephalographic monitoring', *J Neurosurg*, 91(5), pp. 750-60.

84. Vreugdenhil, M., Hack, S.P., Draguhn, A. and Jefferys, J.G. (2002) 'Tetanus toxin induces long-term changes in excitation and inhibition in the rat hippocampal CA1 area', *Neuroscience*, 114(4), pp. 983-94.

85. Walker, M.C., White, H.S. and Sander, J.W. (2002) 'Disease modification in partial epilepsy', *Brain*, 125(Pt 9), pp. 1937-50.

86. Watts, A.E. and Jefferys, J.G. (1993) 'Effects of carbamazepine and baclofen on 4-aminopyridine-induced epileptic activity in rat hippocampal slices', *Br J Pharmacol*, 108(3), pp. 819-23.

87. Werner, P., Voigt, M., Keinanen, K., Wisden, W. and Seeburg, P.H. (1991) 'Cloning of a putative high-affinity kainate receptor expressed predominantly in hippocampal CA3 cells', *Nature*, 351(6329), pp. 742-4.

88. White, A., Williams, P.A., Hellier, J.L., Clark, S., Dudek, F.E. and Staley, K.J. (2010) 'EEG spike activity precedes epilepsy after kainate-induced status epilepticus', *Epilepsia*, 51(3), pp. 371-83.

89. Whittington, M.A. and Jefferys, J.G. (1994) 'Epileptic activity outlasts disinhibition after intrahippocampal tetanus toxin in the rat', *J Physiol*, 481 (Pt 3), pp. 593-604.

90. Whittington, M.A., Traub, R.D. and Jefferys, J.G. (1995) 'Erosion of inhibition contributes to the progression of low magnesium bursts in rat hippocampal slices', *J Physiol*, 486 (Pt 3), pp. 723-34.

91. Wisden, W. and Seeburg, P.H. (1993) 'A complex mosaic of high-affinity kainate receptors in rat brain', *J Neurosci*, 13(8), pp. 3582-98.

92. World Health Organisation (2017) *Epilepsy*. Available at: http://www.who.int/mediacentre/factsheets/fs999/en/.

93. Yu, F.H., Mantegazza, M., Westenbroek, R.E., Robbins, C.A., Kalume, F., Burton, K.A., Spain, W.J., McKnight, G.S., Scheuer, T. and Catterall, W.A. (2006) 'Reduced sodium current in GABAergic interneurons in a mouse model of severe myoclonic epilepsy in infancy', *Nat Neurosci*, 9(9), pp. 1142-9.

94. Zhang, C.L., Dreier, J.P. and Heinemann, U. (1995) 'Paroxysmal epileptiform discharges in temporal lobe slices after prolonged exposure to low magnesium are resistant to clinically used anticonvulsants', *Epilepsy Res*, 20(2), pp. 105-11.

95. Zuberi, S.M., Eunson, L.H., Spauschus, A., De Silva, R., Tolmie, J., Wood, N.W., McWilliam, R.C., Stephenson, J.B., Kullmann, D.M. and Hanna, M.G.

(1999) 'A novel mutation in the human voltage-gated potassium channel gene (Kv1.1) associates with episodic ataxia type 1 and sometimes with partial epilepsy', *Brain*, 122 (Pt 5), pp. 817-25.

Chapter 2 Materials and Methods

In this chapter I provide information about materials and methods that apply across the whole thesis. Subsequent chapters will include short additional methodology sections to provide further detail that are specific to those studies.

2.1 Animal husbandry

All animal handling and experiments were done according to the guidelines laid by the UK Home Office, Animals (Scientific Procedures) Act 1986, and Animal Welfare Ethical Review Board at Newcastle University. All mice used in this study were housed in individually ventilated cages in a 12 hours light (7 a.m. to 7 p.m.), 12 hours dark (7 p.m. to 7 a.m.) lightning regime. All cages were cleaned weekly and provided with ASPEN wood chip bedding (sizes: 2HK and 4HK) and sizzle-nest. All mice were provided with food and water *ad libitum*.

2.2 Mouse lines

Following mouse lines were used for different experiments mentioned in this thesis: C57BL/6J mice (Stock # 000664, The Jackson Laboratory, USA), PV-Cre mice, (Stock # 008069, The Jackson Laboratory, USA), Calsyntenin-3 transgenic mice (MRC Harwell, U.K.), and Neuroplastin-65 transgenic mice (MRC Harwell, U.K.).

2.3 Viral injections

Parvalbumin (PV)-positive interneurons were labelled in PV-Cre mice (heterozygous or homozygous) by injecting AAV9.hEF1a.lox.mCherry.lox.mTFP1 virus, purchased from the UPENN Vector Core (PA, USA). Following procedures were conducted in aseptic conditions. Viral injections were done in post-natal day 0-1 pups. First, EMLA, a local anaesthetic cream containing lidocaine and prilocaine, was applied on the left-dorsal side of their head. They were later anaesthetised for the duration of the procedure using volatile isoflurane. Hamilton syringe (10 µl) fitted with a bevelled 36-gauge needle (World Precision Instruments) was used for doing injections.

Injections were made at four different depths at a single site (50 nL per depth) in the left hemisphere, approximately 1 mm anterior to lambda and 1mm lateral to the midline. The first injection was the deepest at 1.7 mm from the pia and the subsequent injections were made at 0.3 mm dorsal to the previous. In total, approximately 200 nL of virus was injected in a single pup. The body temperature of the pups was maintained throughout the procedure and immediate recovery period by heating pads. Post injections, pups were returned to home cages and maintained in the incubator overnight.

2.4 Brain slices preparation

Young adult mice (2-3 months; male and female) were sacrificed either by schedule-1 method of cervical dislocation or nonschedule-1 method (transcardial perfusion, see below). Slices were prepared in three different methods for different experiments. All the solutions used were being bubbled continuously to saturate with carboxygen (95% O_2 and 5% CO_2). Brain tissue was obtained from C57BL/J6 (wild-type) mice, unless otherwise mentioned. At different stages of the thesis work, I used different methods for preparing brain slices. In following sections, I will describe different slice preparation methods used and the rationale for each method.

2.4.1 *Slice preparation method 1*

Slice preparation method 1 was used to preserve the health of slices during their transportation from *slicing area* to *experimentation area* that were in separate rooms. In this method, following cervical dislocation, the brains were removed and immersed in ice-cold artificial cerebrospinal fluid containing (mM): 126, NaCl; 26, $NaHCO_3$; 3, $MgCl_2$; 3.5 KCl; 1.26 NaH_2PO_4; 10, glucose; 1, Kynurenic acid sodium salt; 0.3, ascorbate sodium. Using Leica vibratome (Nussloch, Germany), horizontal slices, each of 400μm thickness, were cut in above mentioned artificial cerebrospinal fluid. Slices were immediately transferred to an interface tissue holding chamber and incubated for 1-1.5 hours at room temperature in artificial cerebrospinal fluid containing (mM): 126 NaCl; 26 $NaHCO_3$; 2, $CaCl_2$; 1 $MgCl_2$; 3.5 KCl; 1.26 NaH_2PO_4; 10 glucose; 1 Kynurenic acid sodium salt; 0.3, ascorbate sodium. Slices were then washed two times, 10 minutes each, with artificial cerebrospinal fluid (ACSF) containing (mM): 126,

NaCl; 26, NaHCO$_3$; 2, CaCl$_2$; 1, MgCl$_2$; 3.5, KCl; 1.26, NaH$_2$PO$_4$; 10, glucose, and transferred to and stored in an interface tissue holding chamber containing ACSF at room temperature (Note on ACSF terminology: throughout this thesis, I used slight variants of this ACSF, and will make this clear when I do so; but wherever I refer simply to "ACSF", it is this formulation that I describe).

2.4.2 *Slice preparation method 2*

Slice preparation method 2 was used when both the *slicing* and *experimentation areas* are in the same room. In this method, following cervical dislocation, the brains were removed and immersed in ice-cold artificial cerebrospinal fluid containing (mM): 126, NaCl; 26, NaHCO$_3$; 3, MgCl$_2$; 3.5 KCl; 1.26 NaH$_2$PO$_4$; 10 glucose. Using Leica vibratome (Nussloch, Germany), for different experiments, coronal or horizontal slices, each of 400µm thickness, were cut in the aforementioned artificial cerebrospinal fluid. Slices were immediately transferred to an interface tissue holding chamber containing ACSF and incubated for 1-1.5 hours at room temperature.

2.4.3 *Slice preparation method 3*

Slice preparation method 3 was used for experiments involving targeted-patch of PV+ interneurons. In slices prepared by this method, fluorescently labelled PV+ interneurons appeared to be easier to patch compared to slices prepared by other methods. In this method, young adult mice were sacrificed through a nonschedule-1 method. Mice were anaesthetised by intraperitoneal injection of ketamine/meditomidate and the unconscious state was maintained by using isoflurane. After loss of consciousness, transcardial perfusion was then performed using ice-cold sucrose-based artificial cerebrospinal fluid (sucrose-ACSF) containing (mM): 227.87 sucrose; 24 NaHCO$_3$; 1.26 NaH$_2$PO$_4$; 3 KCl; 4 MgCl$_2$; 10 glucose. Animals were decapitated, the brains were removed and immersed in ice-cold in sucrose-aCSF. Using Leica vibratome (Nussloch, Germany), coronal slices, each of 350µm thickness, were cut in above mentioned sucrose-ACSF. Slices were immediately transferred to a submerged tissue holding chamber containing ACSF and incubated for 1-1.5 hours at room temperature.

2.5 Electrophysiology

2.5.1 *Local field potential recordings*

Local field potential (LFP) recordings were performed in interface recording chambers. Slices were placed in the recording chamber perfused with aCSF. Recordings were obtained using 1-3 MΩ borosilicate glass microelectrodes (GC120TF-10; Harvard apparatus, Kent) filled with ACSF. In other experiments, the microelectrodes were placed in deep layers of neocortex, layer 2/3 of entorhinal cortex (EC), and CA3/CA1 of the hippocampus. Microelectrodes were pulled using Narishige electrode puller (Narishige Scientific Instruments, Tokyo, Japan). The temperature of the chamber, perfusate, and slices were maintained at 33-36 °C using a closed circulating heater Grant FH16D (Grant instruments, Cambridge, UK). The solutions were perfused at the rate of 2-3 ml/min by a peristaltic pump Watson Marlow 501U (Watson-Marlow Pumps Limited, Cornwall UK). Waveform signals were acquired using in-house built headstages (gain: 10x) that were connected to BMA-931 biopotential amplifier (Dataq instruments, Akron, USA). Signals from the amplifier were fed into Micro 1401-3 data acquisition unit (Cambridge Electronic Design, UK), that was in turn connected to a computer. Data was acquired using Spike2 software ver. 7.10 (Cambridge Electronic Design, UK). Signals were sampled at 10 kHz, amplified (gain: 200 - 500) and bandpass filtered (1-3000 Hz). A CED4001-16 Mains Pulser (Cambridge Electronic Design, UK) was connected to the events input of CED micro 1401-3 unit and was used for removing 50Hz hum offline using an in-built tool in Spike2 software.

2.5.2 *Patch clamp recordings*

Patch clamp recordings were made in a recording chamber mounted with a heater plate (Warner Instruments, Hamden, CT), with temperatures set to 33-34 °C, and micromanipulators (Scientifica, UK) on a movable top plate (Scientifica, UK) fitted to an upright spinning disc-confocal microscope (Olympus, UK). Slices were bathed in the incoming carboxygenated solution perfused at 3-5 mls/min by a peristaltic pump (501U, Watson-Marlow Pumps Limited, Cornwall, UK) and heated to 33-34 °C by a sleeve heater element (Warner Instruments, Hamden, CT). Patch clamp data was acquired using pClamp software v10.3, Multiclamp 700B, and Digidata acquisition board (Molecular Devices, CA, USA). Signals were recorded with a sampling

frequency of 10 kHz. These recordings were made using 4-7 MΩ microelectrodes (GC150F-10, Harvard apparatus, Kent) pulled using micropipette puller (Model-P87, Sutter Instruments, CA, USA).

Two types of electrode filling solutions were used to fill the microelectrodes used for patching: (1) $KMeSO_4$-based electrode filling solution containing (mM): 125 $KMeSO_4$, 6 NaCl, 10 HEPES, 2.5 Mg-ATP, 0.3 Na_2-GTP, 0.5% (W/V) biocytin; (2) $KMeSO_4$/BAPTA-based electrode filling solution containing (mM): 115 $KMeSO_4$, 10 BAPTA, 6 NaCl, 10 HEPES, 2.5 Mg-ATP, 0.3 Na_2-GTP. pH and osmolarity of the electrode filling solutions used were adjusted to 7.4 and 284 mOsms, respectively. All patch experiments were performed using $KMeSO_4$-based electrode filling solution, unless otherwise mentioned.

Neocortical parvalbumin-positive (PV+) fast-spiking interneurons expressing mCherry or YFP fluorescent tags were targeted for whole-cell recordings. Fluorescent neurons were visualised using x40 water-immersion objective, and either rhodamine (535-585 nm) filter that was fitted to the microscope. SimplePCI software (Hamamatsu Corporation, USA) was used for visualising fluorescent-positive neurons. Selected fluorescent PVINs were then identified in differential interference contrast, and recorded by patch-clamp techniques.

2.6 *In vitro* models

2.6.1 *0 Mg^{2+} model*

Slices were placed in an interface chamber for extracellular field recordings and perfused with ACSF. After placing the electrodes in the tissue, perfusate was changed to $0Mg^{2+}$-ACSF containing: (in mM): 2, $CaCl_2$; 126, NaCl; 26, $NaHCO_3$; 3.5, KCl; 1.26, NaH_2PO_4; 10, glucose to induce ictal events.

2.6.2 *4AP model*

Slices were placed in an interface chamber for extracellular field recordings and perfused with ACSF. After placing the electrodes in the tissue, 4-aminopyridine (100 µM) was added to the perfusate.

2.7 Data analysis

2.7.1 *Band-pass filtering*

Data were analysed offline using Clampfit (Molecular Devices, CA, USA), Igor (WaveMetrics, Lake Oswego, OR), Spike2 (CED, UK) and custom-written scripts in Matlab R2015b (MathWorks, USA). To isolate multiunit activity, raw data (sampling frequency of 10 kHz) were band-pass filtered for frequencies greater than 300 Hz and lower than 3000 Hz (Schevon *et al.*, 2012; Weiss *et al.*, 2013). Band-pass filtering was performed in Matlab software using 'fir1' and 'filtfilt' in-built functions (Matlab code: fd = fir1(1000, [low_pass high_pass]); signal = filtfilt(fd, 1, raw_signal);). In Figure 2.1, I show an example using an epileptiform event recorded in CA3 (Figure 2.1, black trace) that was processed for 300-3000 Hz frequencies (Figure 2.1, red trace). Signatures of multiunit activity involved in the event can clearly be seen in the raw trace as well as in the band-pass filtered trace (Figure 2.1, right), thus demonstrating that these signals are not filtering artefacts, but genuine signals reflecting multiunit activity. This analysis of band-pass filtered data enables us to identify and isolate epileptiform events involving local neuronal firing from false-positives.
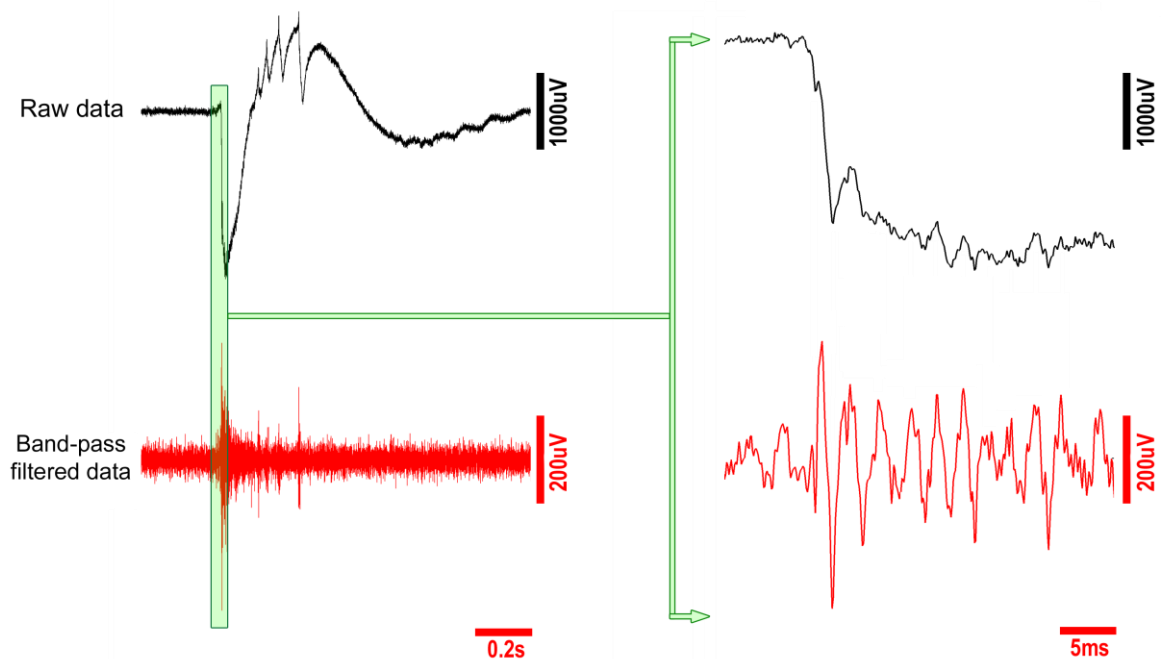
Figure 2.1 Identification of multiunit activity involved in an event by band-pass filtering for frequencies between 300Hz to 3000Hz. Raw data, black trace; band-pass filtered data, red trace. Green highlight is shown expanded in right column.

2.7.2 *Boxplots*

Boxplots were plotted using a web-tool: BoxPlotsR (http://boxplot.tyerslab.com/), or Matlab 2015b (Figure 2.2). In boxplots, the top and bottom edges of the box indicate 75th and 25th percentiles, respectively. Median is indicated by central mark, mean is represented by either filled square or '+' sign and individual data points as filled circles. Whiskers are plotted by Tukey's method; whiskers extend to data points that are 1.5 times the inter-quartile range (difference between 75th and 25th percentile) away from 25th and 75th percentile.
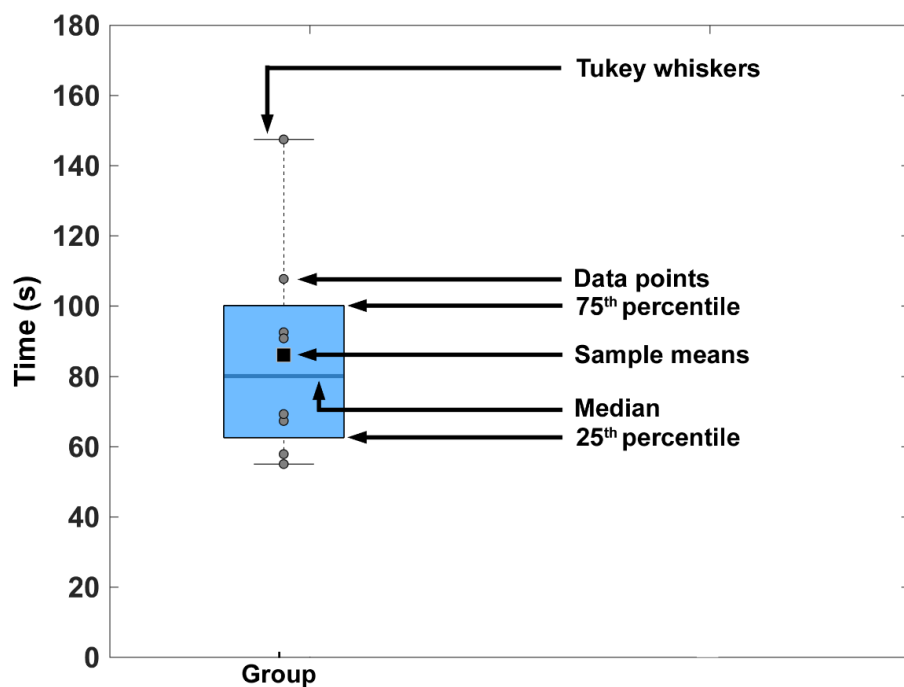
Figure 2.2 Boxplot description; labels explaining the notations in boxplot.

Data in this thesis is represented as mean ± s.e.m., and 'n' value is the number of brain slices, unless otherwise stated. Any additional data analysis performed are mentioned under 'data analysis' section in respective chapters.

2.8 Statistics

Statistical tests were performed using Matlab 2015b or Graphpad Prism Software (CA, USA). For data sets which showed normal distributions, statistical tests were made using 2-tailed paired or unpaired Student's t-tests for pairs of experimental groups, or using one-way ANOVA and Tukey's multiple comparisons test for group sizes three or more (specified for each case in the text). Differences between groups were considered significant if $p \leq 0.05$. Bonferroni correction was conducted for multiple pairwise comparisons. Bonferroni corrected critical value was calculated using the formula (α/n), where 'α' is the critical value (0.05) and 'n' is the number of comparisons. To determine if any of the multiple pairwise comparisons are statistically significant, Bonferroni corrected p-value should be: $p \leq (\alpha/n)$. To calculate normalised percentage changes, measures taken for treatment group were normalised to pre-treatment (controls). A power analysis of the 2-tailed t-test was made, where mentioned, to compute required sample size to see a significant effect ($\alpha = 0.05$). It was calculated using G*power v3.1.9.2 software (Germany).

2.7 Terminology

In this thesis, I reserve specific nomenclature for particular types of epileptiform events in these recordings. The term 'ictal event' is used to describe tonic-clonic like events associated with intense local neuronal firing (Figure 3.2 A, green highlight; Figure 3.3 A). When the activity showed a second transition, from intermittent ictal events to sustained recurrent discharges, then the latter events are termed "late-stage events" (LSEs) (Figure 3.2A, yellow highlight; Figure 3.4A). The recurrent discharges recorded in CA3 with a typical waveform of single large fast-spike followed by a slow-wave are referred to as spike-wave discharges (SWDs) (Figure 3.2 C, yellow highlight; Figure 3.4 C). The term 'epileptiform' activity is used as an umbrella term, to refer to all types of pathological activity – ictal events, late-stage events, and spike-wave discharges, field events – that are induced by epileptogenic media with or without any additional drug treatments.

2.8 References

1   Schevon, C.A., Weiss, S.A., McKhann, G., Jr., Goodman, R.R., Yuste, R., Emerson, R.G. and Trevelyan, A.J. (2012) 'Evidence of an inhibitory restraint of seizure activity in humans', *Nat Commun*, 3, p. 1060.

2   Weiss, S.A., Banks, G.P., McKhann, G.M., Jr., Goodman, R.R., Emerson, R.G., Trevelyan, A.J. and Schevon, C.A. (2013) 'Ictal high frequency oscillations distinguish two types of seizure territories in humans', *Brain*, 136(Pt 12), pp. 3796-808.

Chapter 3 Non-synaptic interactions between hippocampal and neocortical networks in brain slices

3.1 Introduction

The intrinsic excitability of cortical networks is of fundamental importance for our understanding of epilepsy (Traub and Wong, 1982; Miles and Wong, 1983; Prince and Connors, 1984; Dichter and Ayala, 1987; Timofeev and Steriade, 2004; Trevelyan and Schevon, 2013). Most epileptic seizures are thought to arise from pathology located either in hippocampal or neocortical circuits, but identifying exactly where and what is the underlying pathology in particular cases remains a major challenge, both for research and clinical practice.   The chief difficulty lies in the sheer complexity of the systems involved and the multifaceted nature of the condition. Brain slice preparations have been a mainstay of our experimental armoury, providing many insights into a wide range of topics from cellular excitability and synaptic interactions, up to network dynamics. This preparation has proved particularly helpful for studying epilepsy, for instance, by providing a framework to understand human recordings where the potential for invasive investigation is greatly limited (Schevon *et al.*, 2012; Smith *et al.*, 2016). An important series of studies using rat brain slices (Anderson *et al.*, 1986; Mody *et al.*, 1987; Dreier and Heinemann, 1990; Dreier and Heinemann, 1991; Zhang *et al.*, 1995; Dreier *et al.*, 1998), characterised a notable transition, from early tonic-clonic patterns of epileptiform discharges that were suppressed by many different pharmacological agents, into a different, recurrent pattern of discharge which was refractory to most pharmacological intervention. The authors likened this late stage activity to pharmaco-resistant status epilepticus (Heinemann *et al.*, 1994; Zhang *et al.*, 1995), but the nature of this critical transition remained elusive.

I now show that the same evolution of activity is also seen in mouse brain slices. I further identify an important correlate of the transition, which is the surprisingly late involvement of hippocampal activation in this model, and which subsequently acts as a pacemaker, entraining activity in other cortical networks.   Interestingly, the entrainment of overlying neocortex does not require intact synaptic pathways, but instead can arise from field effects secondary to focal discharges (Jefferys, 1995; Frohlich and McCormick, 2010; Anastassiou *et al.*, 2011). These results show that the

transition, from pharmaco-sensitive to pharmaco-resistant activity in this model, reflects a change in which cortical territories are involved and how the activity spreads to other networks. These models can provide a wealth of metrics for comparing drug or genetic effects on network excitability in different cortical territories.

3.2 Materials and methods

3.2.1 *Slice preparation and electrophysiology*

For all the experiments described below, combined neocortical-hippocampal horizontal slices were used, that were prepared and stored as described in *slice preparation method 2* (chapter 2, sub-heading 2.4.2). Local field potentials (LFPs) were recorded simultaneously from both the pyramidal cell layer of CA subfield (CA1 or CA3) of hippocampus and infragranular layers of neocortex (temporal association areas; Figure 3.1). The recording setup and the equipment used were as described in chapter 2 (sub-heading 2.5.1).
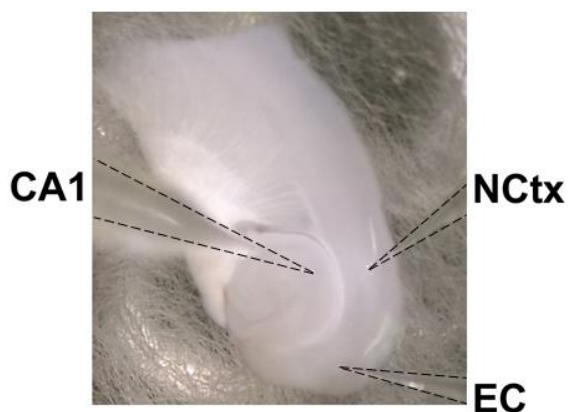
Figure 3.1 Recording setup showing an intact hippocampal-entorhinal cortex-neocortical horizontal slice in the interface recording chamber with electrodes placed in the pyramidal cell layer of CA1 (left), and infragranular layers of neocortex (NCtx, top-right), and entorhinal cortex (EC, bottom-right).

3.2.2 *Protocols*

Brain slices were placed in the interface recording chamber, which were perfused initially with ACSF. Electrodes were placed in the regions of interest and the baseline activity was recorded in ACSF. After 10-15 minutes, the perfusate was switched from ACSF to epileptogenic medium ($0Mg^{2+}$-ACSF). Experiments were performed in three types of brain slice preparations: 1) intact horizontal brain slices with hippocampal (CA), entorhinal, and neocortical regions (NCtx) (intact slice), 2) horizontal brain slices with only the hippocampal and neocortical regions (disconnected slices); entorhinal cortex (EC) was dissected out to remove any polysynaptic connectivity between neocortical and hippocampal regions, and 3) cortical subfields, NCtx, EC, and CA, were all physically separated, so that there are

no anatomical connections between all the three regions. From here on, slices prepared by this method will be referred to as 'isolated slices'. Dissections in the slices were made using a scalpel blade of size 10 (Fine Scientific Tools, U.K).

First, in intact slices, the evolution of 0 Mg^{2+}-ACSF induced epileptiform activity was characterised simultaneously in neocortex, EC, and CA territories. EC was dissected out after the development of spike-and-wave discharges (SWDs) in CA and late-stage recurrent discharges in the neocortex. In the next set of experiments, the evolution and entrainment of epileptiform activity was investigated in disconnected slices. A second cut was made along the axis of the white matter and the two regions were physically separated (≥ 3 mm apart) after the development of SWDs in CA and late-stage recurrent discharges in the neocortex. I then examined the effect of making only a cut along the white matter without physically moving the regions apart on the entrainment and activity patterns in neocortex and CA of the hippocampus. In the final set of experiments, epileptiform activity was induced by 0Mg^{2+}-ACSF in isolated entorhinal cortex, CA, and neocortex.

3.2.3 *Data analysis*

Data was analysed as describes in chapter 2 (sub-heading 2.7). Additionally, the analysis of entrainment of epileptiform events was performed on "template-filtered" traces (Figure 3.7Bii) of the recordings from different brain locations. This was done to remove the confounding effects of higher frequency components of these discharges which can lead to aliasing issues in analyses using cross-correlations. I first created a template of an average discharge (6-10 events), aligned by the time point at which they exceeded a threshold set at between 25-40% of the peak deflection. The templates were then used as a normalising filter on their respective raw traces, by deriving peak cross-correlation coefficients for the time-shifted template relative to the trace. This "template-filtered" trace (Figure 3.7Bii) removed most of the fine structure of the individual discharges, but preserved their timing. Since the individual events in the late-stage activity are extremely reproducible, the peaks in this filtered trace tend towards 1. I used the cross-correlation between these template-filtered recordings as a measure of the entrainment of the two recording locations.

3.3 Results

3.3.1 *Characteristics of evolving epileptiform activity in neocortical, entorhinal, and hippocampal networks in brain slices*

Following wash-out of Mg^{2+} ions, there was a gradual build-up of epileptiform discharges, evolving in a highly characteristic way (Figure 3.2). The earliest large field deflections in the raw traces were seen at all recording sites, although the events appeared far larger in the neocortex and entorhinal cortex. This early activity involved episodes of sustained rhythmic bursts suggestive of the temporal dynamics of clinical tonic-clonic discharges (Figure 3.3Ai, Bi). The mean number of tonic-clonic like events in the neocortical was 9.35 ± 0.73 per slice (n = 17; range 4-17), before a second transition to regular epileptiform bursts ("late-stage activity pattern"), with individual bursts lasting a few hundred milliseconds, and occurring every 3.32 ± 0.38 s (n = 10; Figure 3.4Ai, Bi). This pattern of evolution has been described previously in rat brain slices (Mody *et al.*, 1987; Dreier and Heinemann, 1990; Dreier and Heinemann, 1991), noting also an important pharmacological difference between the early and late epileptiform discharges: several different anti-epileptic drugs can suppress the early discharges, whereas the late regular bursts are resistant to these drugs (Dreier and Heinemann, 1990; Dreier *et al.*, 1998). This transition therefore represents a potentially valuable tool for investigating pharmaco-resistant epilepsy (Heinemann *et al.*, 1994).
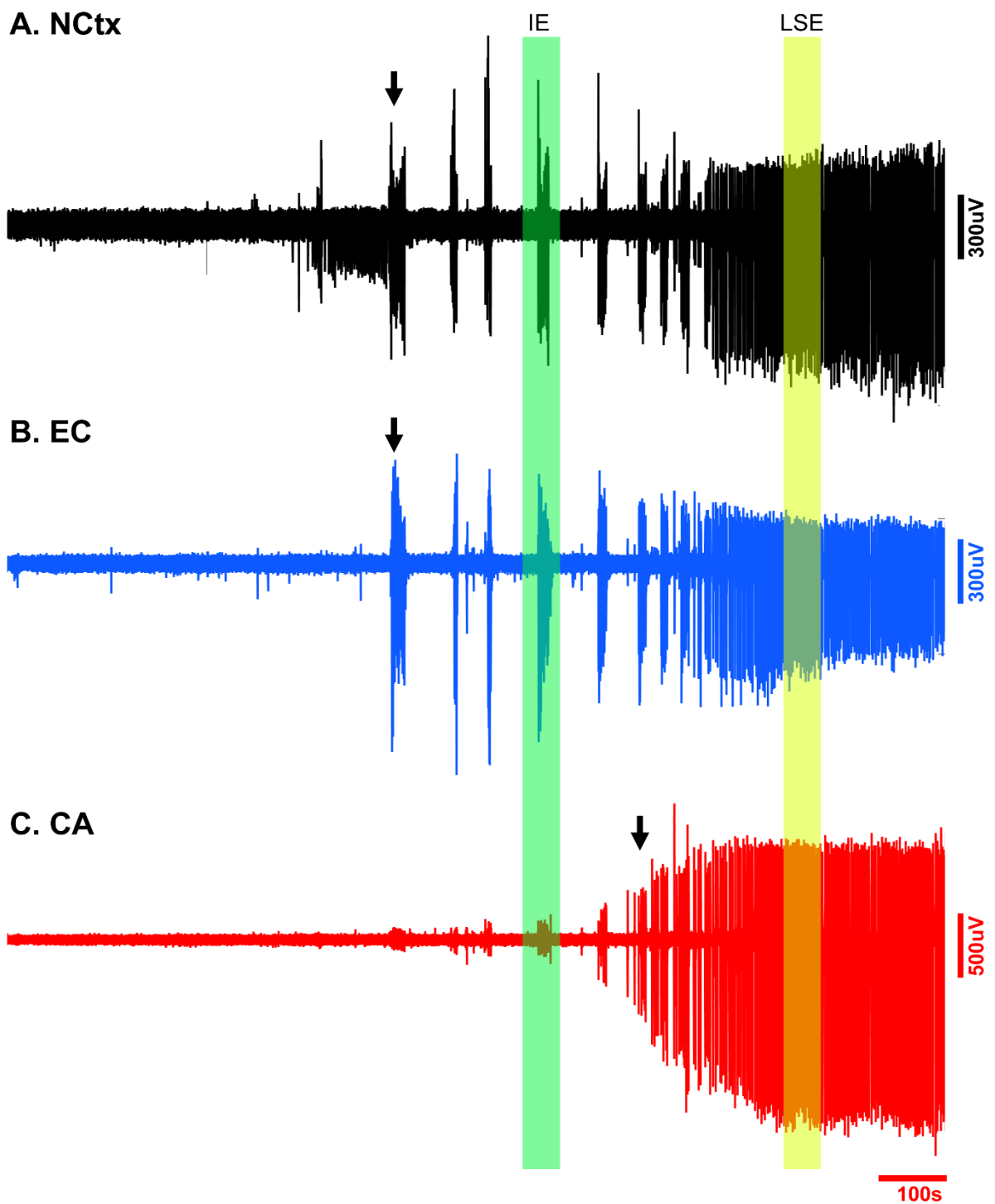
Figure 3.2 Typical pattern of evolving epileptiform activity following wash-out of Mg^{2+} ions from the bathing media (0 Mg^{2+} model), showing delayed recruitment of hippocampal circuits relative to neocortex. Extracellular recordings (broad band) from neocortex (A, black; NCtx), entorhinal cortex (B, blue; EC), and hippocampus (C, red; CA) showing typical pattern of evolving epileptiform activity following washing out of Mg^{2+}. The arrows indicate the first full ictal events, as indicated by intense multiunit (high frequency) activity, in all three recordings. Areas shaded in green and yellow are shown expanded in Figure 3.3 and 3.4, respectively. Note, the time scale at the bottom of the figure applies to all the traces in the figure.
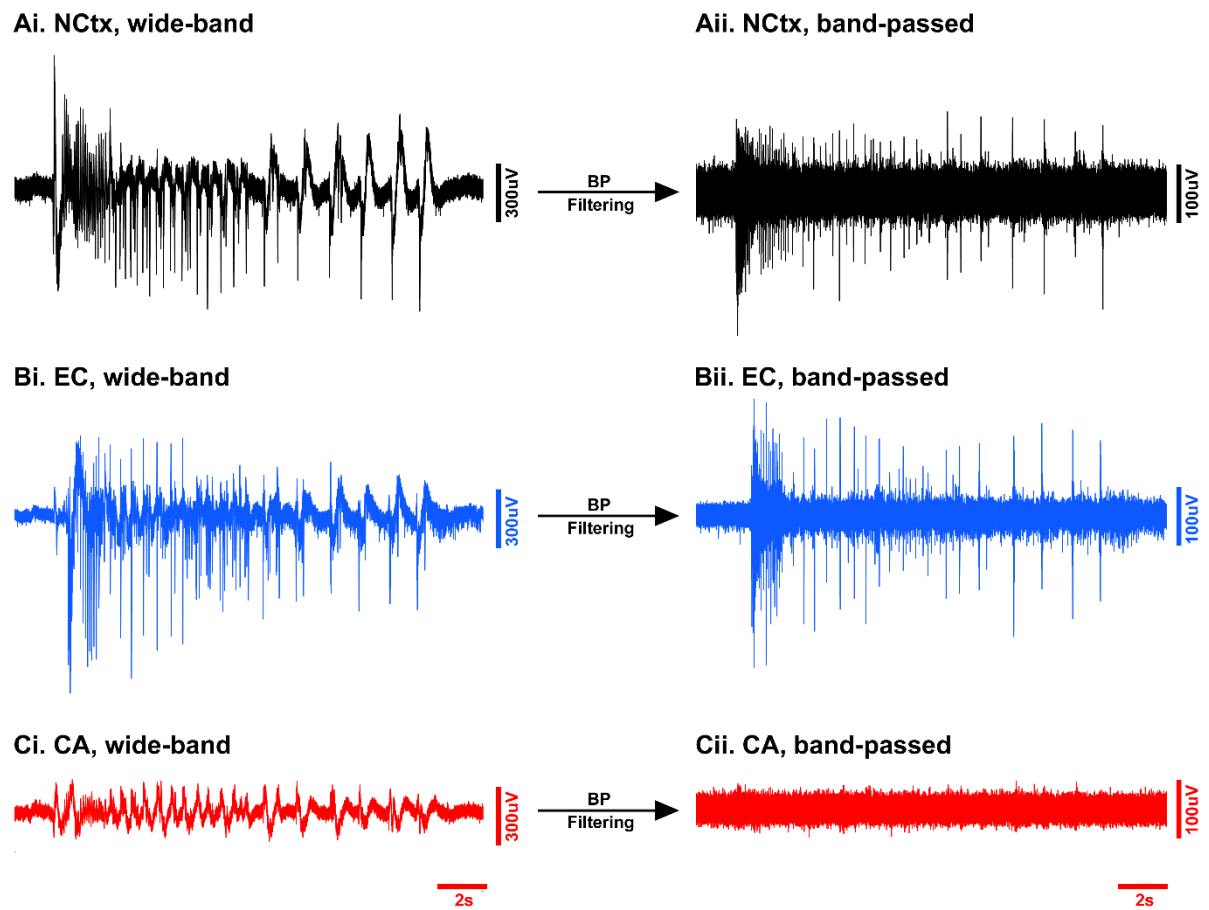
Figure 3.3 Absence of multiunit activity in CA. Broad band signals show small deflections in the hippocampal field (Ci) at the time of large neocortical (Ai) and entorhinal discharges (Bi), but high pass filtering shows that, unlike neocortical (Aii) and entorhinal (Bii) signals, these hippocampal signals (Cii) are not associated with any significant unit activity. Expanded from Figure 3.2, green shaded area. Time scale at the bottom of the figure applies to all the traces in the figure.
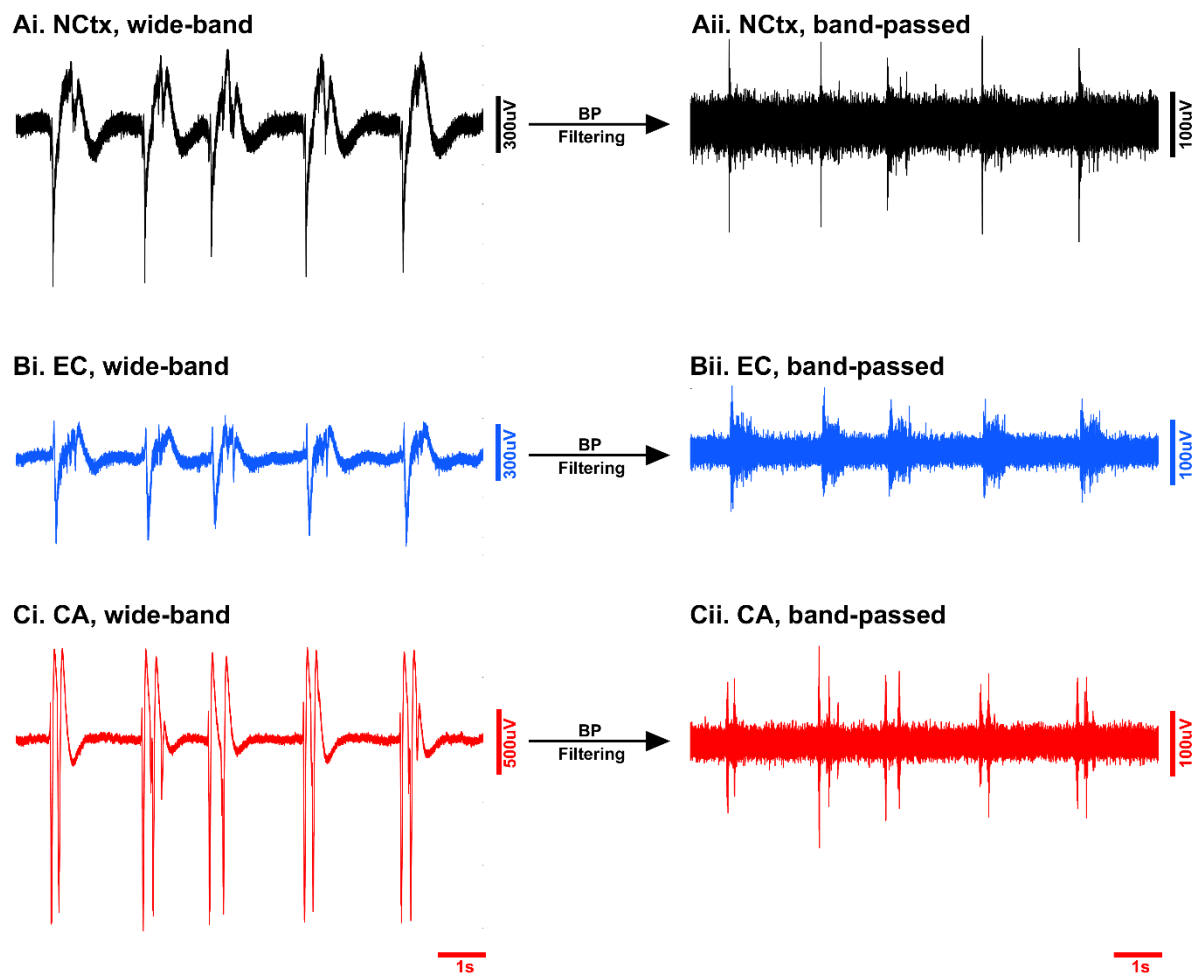
Figure 3.4 Late-stage events in neocortex (Ai) and entorhinal cortex (Bi), and the later hippocampal events characterised by large field deflections (ci) all show multiunit activity upon band pass filtering the broad band signal (NCtx, Aii; EC, Bii; CA, Cii). Expanded from Figure 3.2, yellow shaded area. Time scale at the bottom of the figure applies to all the traces in the figure.

Recent studies of human extracellular recordings of epileptic discharges in humans have highlighted the importance of examining the high frequency component of epileptiform discharges to determine whether an event involves locally active neurons (Schevon *et al.*, 2012; Weiss *et al.*, 2013). In this regard, there appeared a striking difference between activity recorded in the hippocampus and the neocortical signals: the early events, including the tonic-clonic ictal events, were associated with only small field events in the hippocampus, and notably, with no measurable high frequency component, indicating there is little local neuronal firing (Figure 3.2C, 3.3Ci, Cii, red trace). It is therefore considered that these early events did not invade the local hippocampal networks. Using this high frequency component as the critical

marker of ictal involvement, the first hippocampal ictal discharges occurred significantly later than the first neocortical discharges (Figure 3.2 arrows; Figure 3.5; Neocortex latency, 671 ± 41 s; Entorhinal cortex, 699 ± 69s: Hippocampus, 2238 ± 284 s; post-hoc Tukey test, $p < 0.01$). Epileptiform discharges in entorhinal cortex evolved in tandem with the neocortical discharges (Neocortex v Entorhinal, not significant; Entorhinal v Hippocampal, $p < 0.01$).
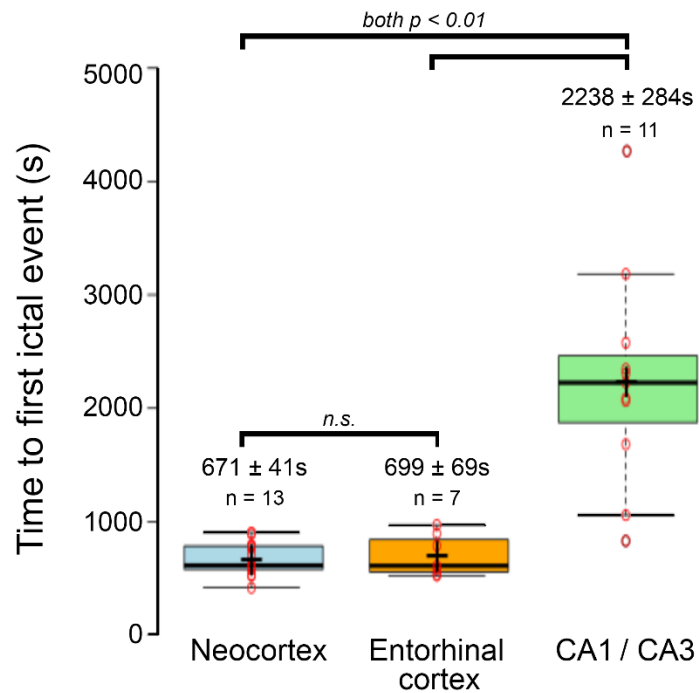
Figure 3.5 Ictal discharges are induced earlier in neocortical and entorhinal cortical networks than in hippocampus. Boxplot illustrating a significant delay of the earliest hippocampal epileptiform discharges relative to the first neocortical or entorhinal discharges (ANOVA $F_{[2,28]} = 25.76$, $p < 0.001$). The results of individual comparisons (post-hoc Tukey tests) are shown above the data distributions.

When finally, the hippocampal epileptiform discharges began, they showed a fundamentally different pattern, generally being a single large spike and wave discharge lasting up to 1.26 ± 0.11 s (n = 10), or a short burst of discharges, and the protracted tonic-clonic patterns, as seen in neocortex or entorhinal cortex, occur only extremely rarely (1 in 13 slices). In a further contrast to the prior neocortical activity, the inter-event intervals were very short (2.98 ± 0.78 s, n = 10), compared with the intervals between neocortical tonic-clonic ictal events ($1^{st} - 2^{nd}$ event interval = 126.2

42

± 17.2 s; 2nd – 3rd interval = 117.1 ± 15.1 s; 3rd – 4th interval = 68.9 ± 10.6 s).   Notably, once the hippocampal discharges started, the pattern of neocortical discharges also changed to the same pattern of transient, but regular, spike and wave discharges. Discharges in the two structures, from this time forward, were tightly coordinated (Figure 3.4Ai, Aii, Ci, Cii), but with the hippocampal discharges occurring fractionally earlier than the neocortical unit activity. Latency of onset of neocortical activity after hippocampal activity = 87.1 ± 25.5 ms (n = 8).

3.3.2 *Hippocampal entrainment of neocortical activity is independent of synaptic connectivity*

I hypothesized that events propagated to the neocortex through a polysynaptic pathway involving the entorhinal cortex. To test this, I dissected out the caudal pole of the brain slice, thereby entirely removing any potential synaptic pathway. Surprisingly, following the removal of the entorhinal pole, the hippocampal entrainment of neocortical discharges persisted unchanged (Figure 3.6; Neocortex, pre-cut rate = 0.47 ± 0.08 Hz, post-cut = 0.47 ± 0.09 Hz, n = 5, paired t-test, p = 0.96; Hippocampus, pre-cut rate = 0.48 ± 0.09 Hz, post-cut = 0.49 ± 0.11 Hz, n = 5, paired t-test, p = 0.83), and latency of onset of neocortical activity after hippocampal activity also remained unaltered (pre-cut = 71.1 ± 7.7 ms, post-cut = 62.4 ±3.6 ms, n = 5, paired t-test, p = 0.13).
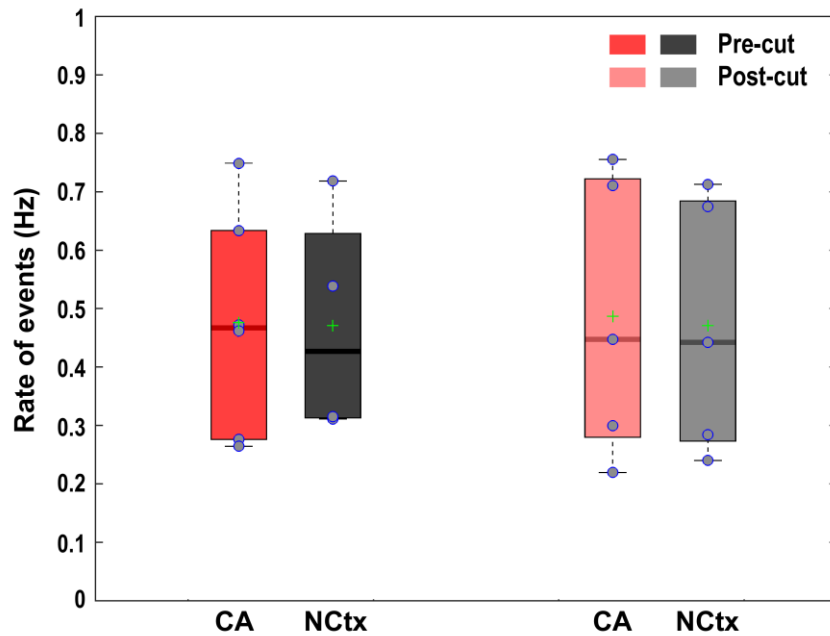
Figure 3.6 Hippocampal entrainment of neocortical LSEs persisted after dissecting out the entorhinal cortex. The rate of events in both the regions were unaltered following removal of EC.

I then investigated the evolution and entrainment of epileptiform activity in horizontal brain slices in which I dissected out the entorhinal cortex to remove any polysynaptic connectivity between hippocampal and neocortical regions (Figure 3.7A). Hereafter, I will refer to this preparation to as disconnected slices. Following wash-out of Mg^{2+} ions, epileptiform discharges, in both neocortex and hippocampal territories, developed in a similar pattern as observed in intact slices except in that the latency to first tonic-clonic discharges in neocortex is longer in disconnected slices (Neocortex latency, 1035.7 ± 77.8 s, n = 14; intact v disconnected, unpaired t-test, p = 0.0006). In contrast to tonic-clonic discharges in neocortex, as observed in intact slices, the early small field events of tonic-clonic discharges in hippocampus show no measurable high frequency component (Figure 3.7A, inset). The first hippocampal ictal discharge occurred significantly later than the first neocortical discharge (hippocampus latency, 2356.10 ± 189.10 s, n = 14; latency: hippocampus v neocortex, paired t-test, p = 0.0004; hippocampus latency, intact v disconnected, unpaired t-test, p = 0.79). Once the activity began in hippocampus, the neocortical activity pattern changed from tonic-clonic to late-stage events. Despite lacking polysynaptic connectivity between the two regions, hippocampal activity entrained (Figure 3.7A, B) and preceded neocortical

activity (Figure 3.7Ci, Cii; Figure 3.8; latency, 57.8 ± 9.1 ms; intact v dissected, unpaired t-test, p = 0.27).
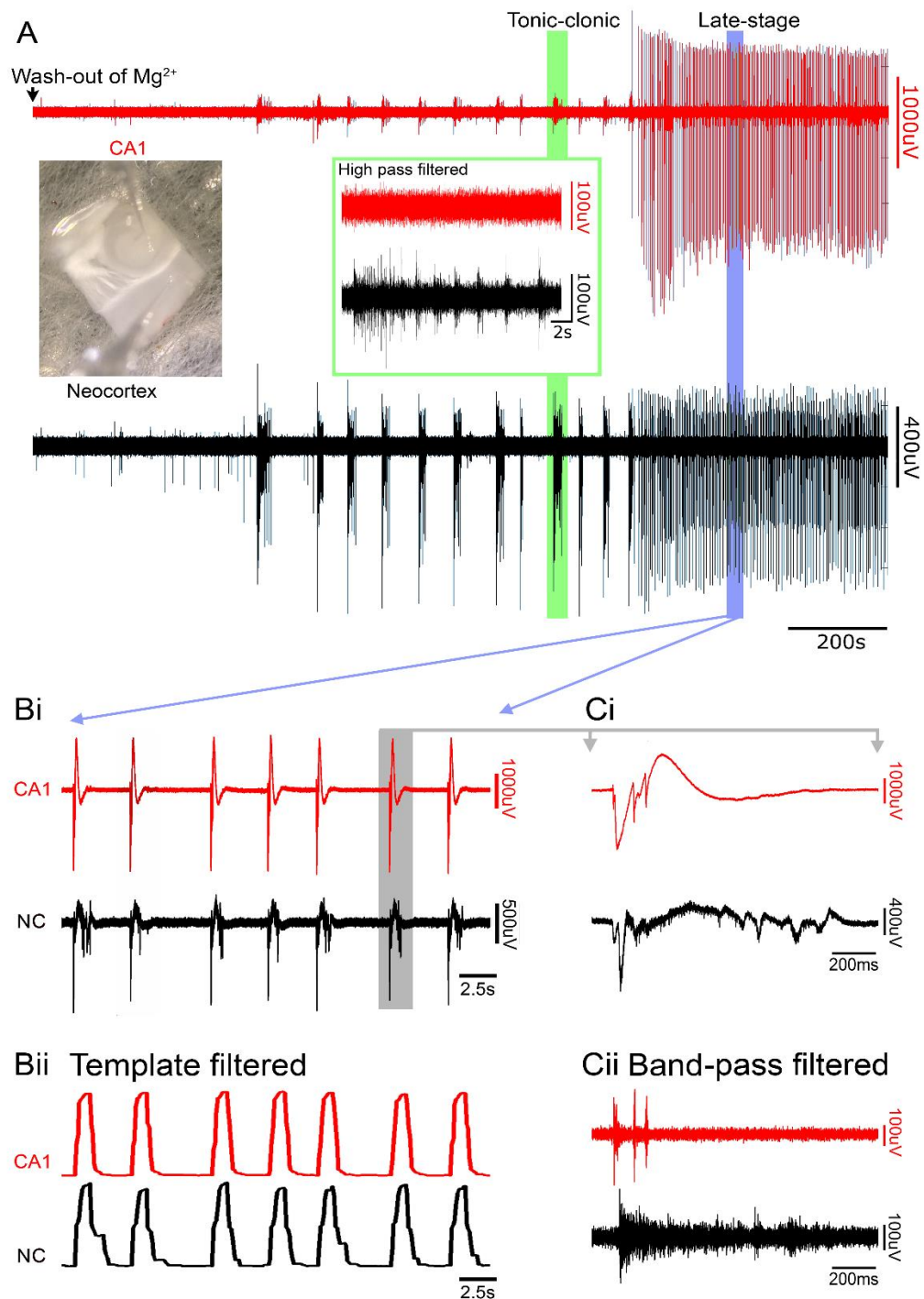
Figure 3.7 The late-stage epileptiform discharges are coordinated in hippocampal and neocortical networks through a non-synaptic pathway. (A) Extended recording of extracellular field potentials in CA1 (red) and neocortex (black, NC), following wash-out of Mg^{2+}, in a disconnected slice i.e., with entorhinal cortex removed, thereby

disconnecting the two regions via any conventional multi-synaptic path. As in intact slices, the early discharges showed pronounced unit activity in neocortex, but not in the CA1 pyramidal layer (inset, green box). (Bi) Expanded view of late stage activity in the same slice, and (Bii) the same traces filtered by a moving template of an average discharge. Note the synchronous occurrence of discharges in the two, synaptically-disconnected territories. (Ci) Further expansion of a single discharge, and (Cii) a high-pass filtered view of the same event, showing prominent levels of unit activity in both territories.
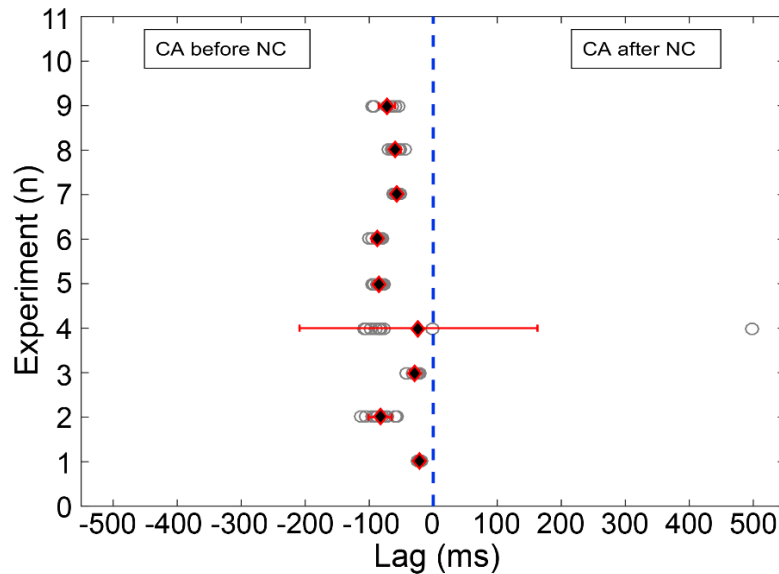
Figure 3.8 Hippocampal discharges precedes neocortical discharges during late-stage events. In synaptically-disconnected, hippocampal-neocortical slices, late-stage discharges in neocortex (NC) follow hippocampal (CA) discharges with a mean lag of 57.8 ± 9.1 ms (One-sample t-test: $p < 0.05$, $n = 9$).

I next made a second cut along the axis of the white matter bundle deep to the neocortical layer 6, and physically separated the neocortical and hippocampal networks, after which, the earlier observed entrainment phenomenon in these slices was lost (Figures 3.9 and 3.10) and the hippocampal discharge rate increased significantly (pre-cut, 0.35 ± 0.07 Hz; post-cut, 0.49 ± 0.13 Hz; $n = 9$, $p = 0.0451$; Figures 3.9Ci, Cii, 3.10A), whereas the neocortical discharge rate dropped significantly (pre-cut, 0.31 ± 0.05 Hz; post-cut, 0.12 ± 0.02 Hz; $n = 9$, $p = 0.0099$; Figures 3.9Ci, Cii, 3.10A). In tandem with the reduced rate of discharges in the neocortical networks, the duration of events showed a significant increase (pre-cut = 1.78 ± 0.22 s, post-cut = 6.86 ± 2.30 s, $n = 9$, $p = 0.048$; Figure 3.10A). This result suggests that the interactions

between hippocampal and neocortical networks are in both directions in this late stage activity pattern: the hippocampal-to-neocortical influence is reflected in the pacing of neocortex by hippocampus; whereas the opposite influence is manifest as a mild brake on the hippocampal pacing. Consistent with these opposite changes in rates, there was a highly significant drop in the correlation of events in the two networks (Figure 3.10B, C; $p = 4.1 \times 10^{-7}$). I concluded from these experiments that the late stage epileptiform discharges arise in hippocampus, and these act as a pacemaker, driving discharges also in juxtaposed neocortical territories, but that this entrainment was mediated, at least in part, by a non-synaptic path.
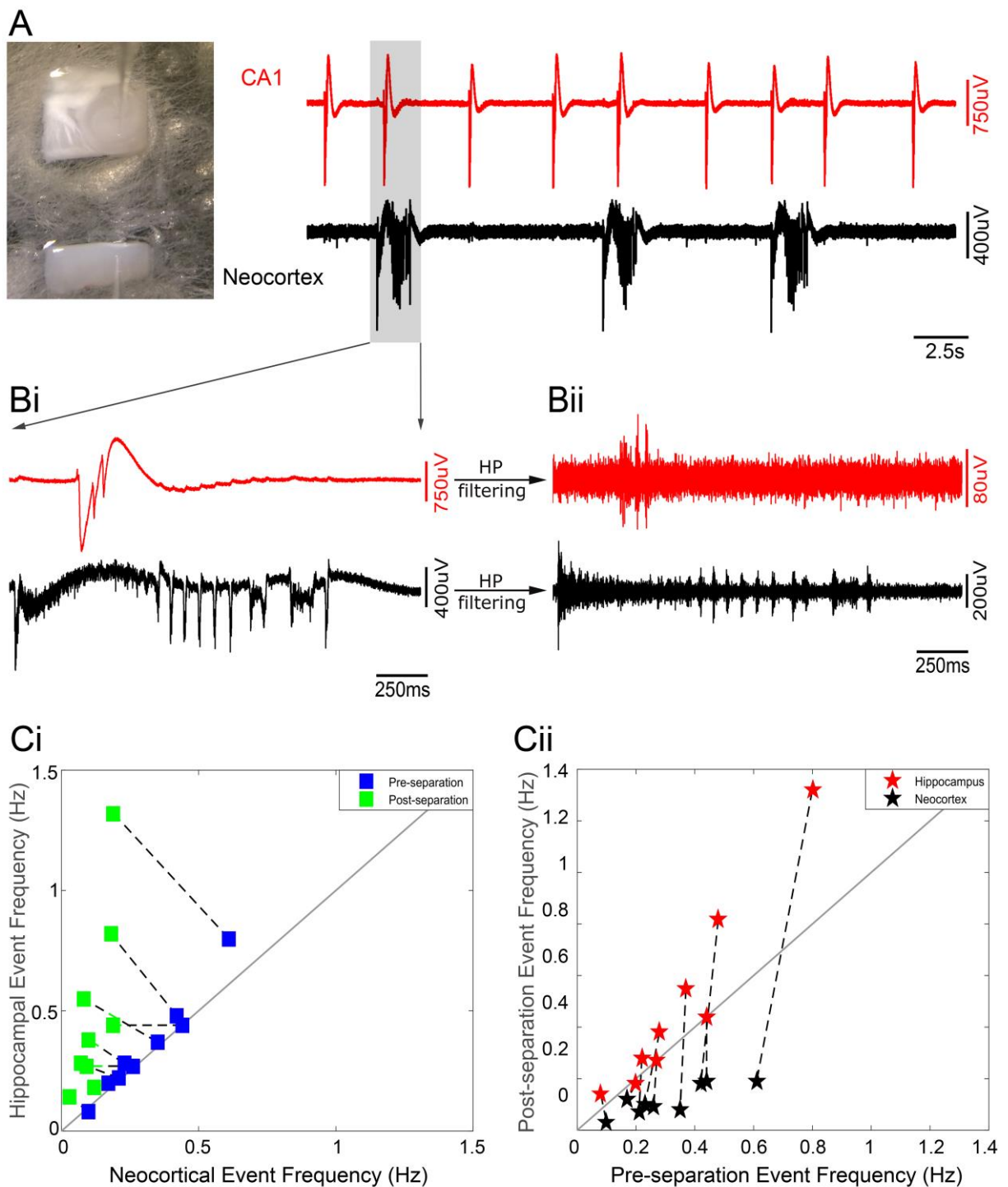
Figure 3.9 Entrainment of discharges is lost following physical separation of hippocampal and neocortical networks (A) Photomicrograph showing the electrode placements in physically separated CA1 and neocortical areas, derived from a single horizontal brain slice, together with a period of late stage epileptiform discharges. Note the desynchronised discharges in the two territories, with a far slower rate of discharges in the neocortical tissue. (Bi) Further expansions show the broadband signal of the de-synchronised hippocampal and neocortical discharges. (Bii) Prominent unit activity is seen in both territories. (Ci) The relative rates of epileptiform discharges in the two territories before (blue) and after (green) physically separated. In

disconnected slices ("pre-separation"), the rates were equivalent ("pre-separation", red squares; CA: 0.35 ± 0.07 Hz, NCtx: 0.31 ± 0.05 Hz; n.s., n=9), but following physical separation of the tissues, the rates are significantly different ("post-separation", black squares; CA: 0.49 ± 0.13 Hz, NCtx: 0.12 ± 0.02 Hz; p < 0.05, n=9). (Cii) Comparisons of discharge rates before and after physical separation of the hippocampal and neocortical tissues. Note how the neocortical data all fall below the line of unity, indicating a consistent slowing of the rate of discharges there (black stars; pre-separation: 0.31 ± 0.05 Hz, post-separation: 0.12 ± 0.02 Hz, p < 0.05, n = 9). In contrast, the hippocampal data tend to lie above the line, indicative of an increase in hippocampal rate after the separation (red stars; pre-separation: 0.35 ± 0.07 Hz, post-separation: 0.49 ± 0.13 Hz, p < 0.05, n = 9).
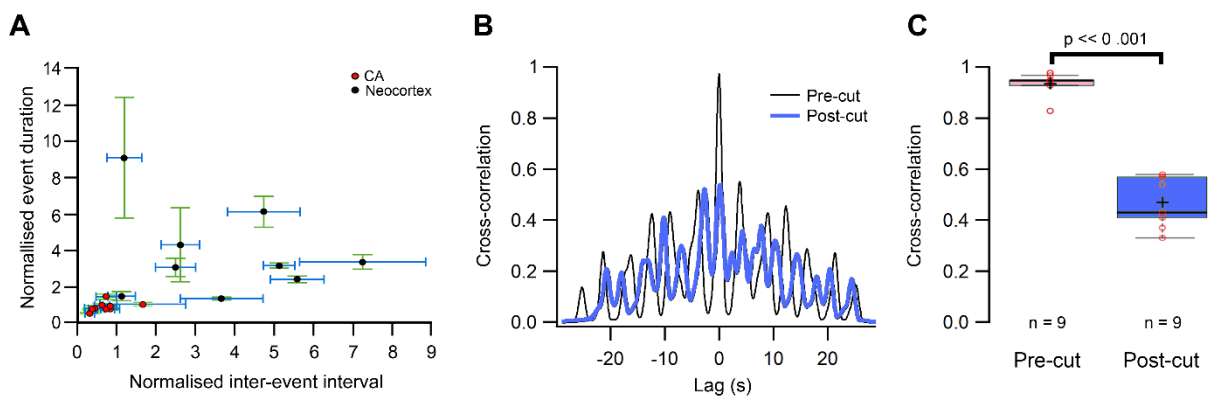
Figure 3.10 Separation of hippocampal and neocortical territories alters the timing and structure of the activity patterns in the two territories. (A) The duration and inter-event intervals in the physically separated hippocampal and neocortical tissues, normalised to the values in the pre-cut brain slice. (B) An example of the change in cross-correlogram between hippocampal and neocortical activity from the disconnected slice ("pre-cut", black) to the physically separated tissues ("post-cut", blue). (C) Pooled data showing a highly significant difference in the degree of correlated activity in these two regions in disconnected versus the physically separated slices.

3.3.3 *Hippocampal entrainment of neocortical activity requires anatomical contiguity*

I next examined whether observed entrainment phenomenon persists after making only an incision along the white matter without physically separating the two regions. In disconnected slices, hippocampal entrainment of neocortical activity that developed in 0 Mg^{2+}-ACSF was lost after making only an incision along the white

matter (Figure 3.11 A, B). Furthermore, prior to making the cut, the discharge rates were equivalent in both the regions, but after the cut, the neocortical discharge rate significantly dropped (pre-cut: 0.18 ± 0.03 Hz, post-cut: 0.06 ± 0.01 Hz; n = 6; p < 0.01), whereas the hippocampal discharge rate increased significantly (pre-cut: 0.2 ± 0.03 Hz, post-cut: 0.27 ± 0.04 Hz; n = 6; p = 0.02) (Figure 3.11C).
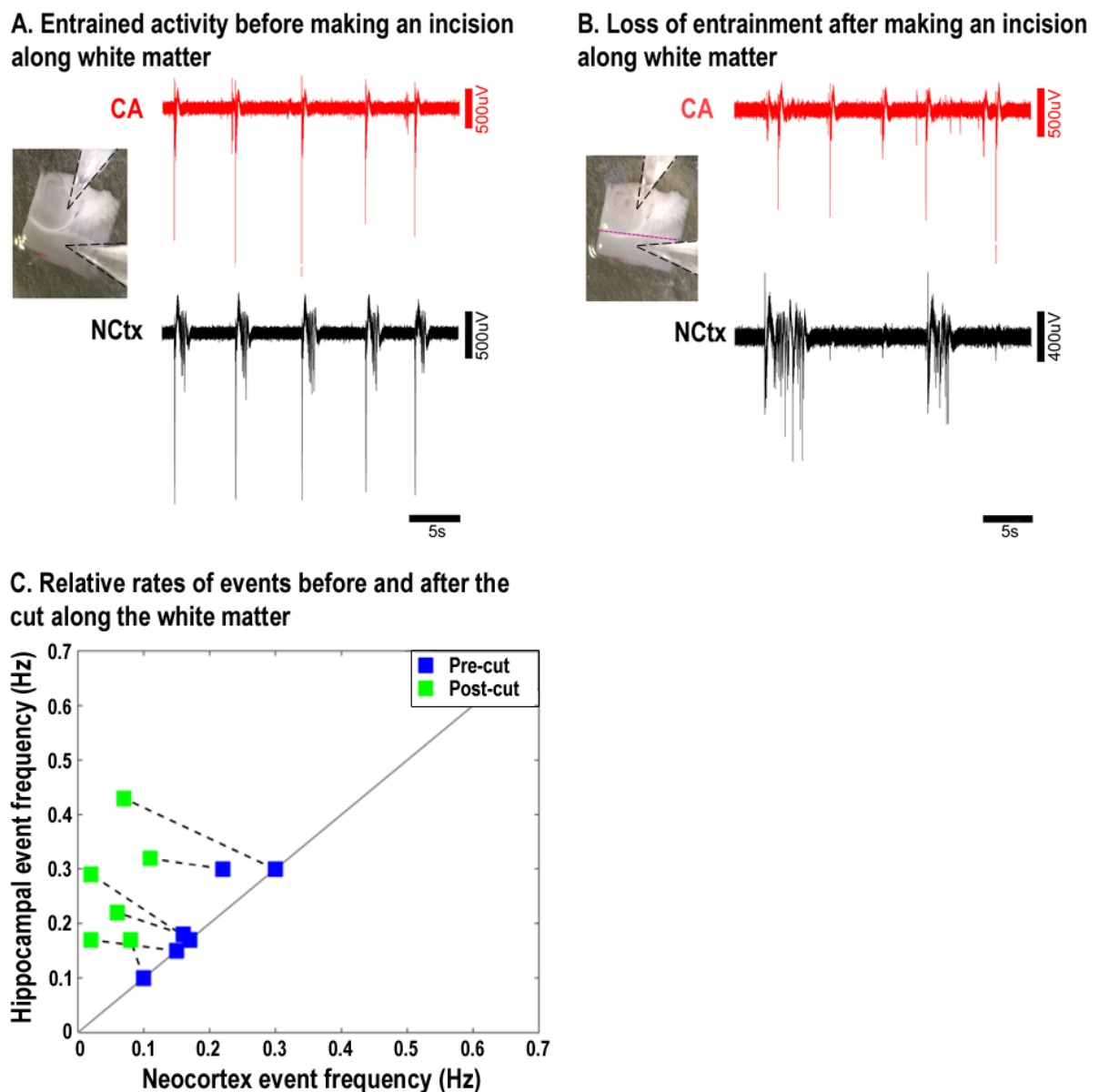
Figure 3.11 Hippocampal entrainment of neocortical activity in a disconnected slice (A) is lost after making a cut along the white matter (B; pink dotted line indicates the line of cut). (C) Relative rates of discharges before (blue squares) and after (green squares) making the cut along the white matter.

3.3.4 *Epileptiform activity evolve with similar latencies in the same regions in intact and isolated slices*

Finally, I examined whether the latency to the first ictal events in the different cortical subfields was altered if these networks were kept separate from the first exposure to 0 Mg^{2+} ACSF. I measured the time to first ictal events in slices that were dissected to isolate the neocortex, entorhinal cortex and hippocampal subfields. In all three territories was unaltered, relative to recordings from intact slices (isolated neocortex, 607.3 ± 107.3 s, n = 6, unpaired t-test; vs intact: p = 0.5; Entorhinal cortex, 1057.2 ± 200.1, n = 5, unpaired t-test; vs intact: p = 0.08; Hippocampus, 1595.4 ± 186.3, n = 6, unpaired t-test; vs intact: p = 0.14; Figure 3.12).
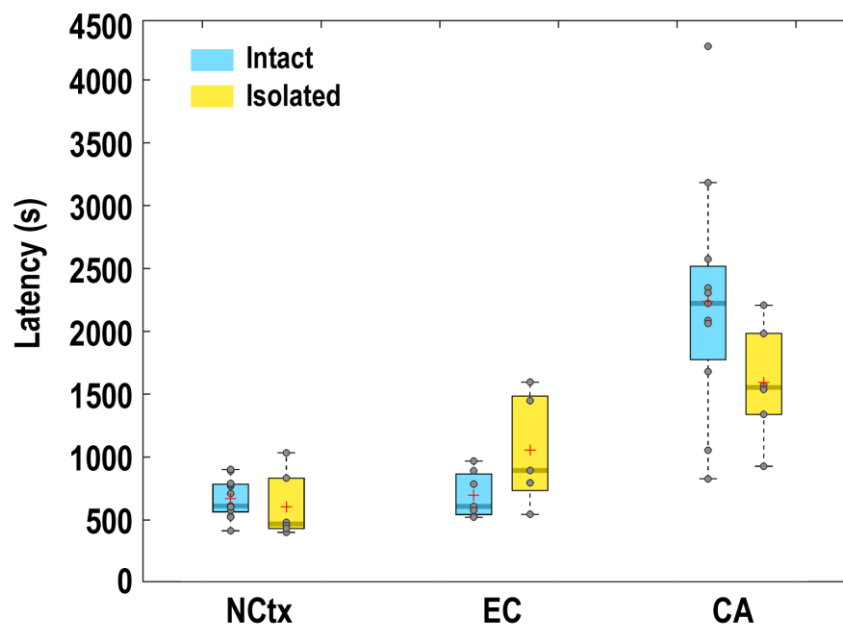
Figure 3.12 Latencies to the first ictal events in isolated NCtx and EC, and SWDs in isolated CA were similar to that measured in intact slices.

3.4 Discussion

These results illustrate several important features of the 0 Mg^{2+} model. First, I found that the earliest ictal activity in the 0 Mg^{2+} model is in the neocortex. Hippocampal ictal activity, in contrast, develops late, but then acts as a pacemaker for rapidly generalised spike and wave events that are coordinated in all cortical areas. There is thus a characteristic shift from neocortical to hippocampal epileptic activation, which is also mirrored in the transition from tonic-clonic ictal events to more transient spike and wave discharges, reflecting that the two territories also differ with respect to the dominant forms of ictal discharge in each. Although ictal activity only arises later in hippocampal networks, once this happens, this quickly becomes the dominant network, entraining activity elsewhere from that time. Of added interest is that this transition had previously been associated with a change in sensitivity of the discharges to anti-epileptic drugs (Mody *et al.*, 1987; Dreier and Heinemann, 1990; Dreier and Heinemann, 1991; Zhang *et al.*, 1995; Dreier *et al.*, 1998).

I further present a demonstration of epileptiform discharges propagating through a non-synaptic mechanism in mouse brain slices. I thereby provide a proof of principle that very large discharges of neuronal populations can show non-conventional neuronal entrainment at a distance. Note however, that this does not downgrade the clear importance of conventional, synaptically mediated spread. An important feature of this pattern of spread is that we only see it in a very particular situation, spreading into tissue that is already hyperexcitable, with a history of repeated epileptiform discharges. Thus, the specific instances of non-synaptic spread occur only in what I have termed "late-stage" epileptiform activity in the 0 Mg^{2+} model. The earliest discharges, which occur in neocortex, cause a field potential deflection at recording sites in the hippocampus, but fail to elicit local firing there. In contrast, the late stage hippocampal discharges appear to entrain the neocortical discharges. The fact that separating the neocortex and hippocampus influences this late stage activity in both directions (the neocortex shows a significant slowing of the rate of discharges, whereas the hippocampal rate increases significantly) indicates that the interactions are indeed bilateral in hyperexcitable networks. This suggests first, that the neocortical discharges, which tend to last longer than the hippocampal ones, may impose additional refractoriness, and second, that the critical determinant of spread is that the follower network is "primed" for activation.

There are several puzzles still to be resolved. Firstly, the precise mechanism by which any of the discharges in any region are actually initiated remains mysterious. These need not even be the same (e.g. a postulated, pro-epileptic role for excessive interneuronal activation in the 4-aminopyridine model (Avoli and de Curtis, 2011) versus glial involvement in a mixed low Mg^{2+} / 4-aminopyridine model (Gomez-Gonzalo *et al.*, 2010). Consequently, it is also unclear what changes in the hippocampus to initiate discharges there, thereby causing the transition from the early to the late pattern of epileptiform activity. One possible mechanism is that repeated synaptic bombardment can gradually cause a shift in the balance of power between inhibition and excitation. For instance, previous work has shown that continual perforant pathway stimulation can, over time, give rise to spontaneous epileptiform discharges occurring in hippocampal networks (Scharfman and Schwartzkroin, 1990a; Scharfman and Schwartzkroin, 1990b), and associated with changes in excitability occurring preferentially in cell classes lacking Ca^{2+} buffering properties (Scharfman and Schwartzkroin, 1989).

The precise mechanism of hippocampal entrainment of neocortex also remains unclear. I follow Jefferys' nomenclature (Jefferys, 1995) in not referring to this as "ephaptic spread"; he reserves this term for activation of juxtaposing cells (it derives from the Greek word "to touch"), whereas the effect I describe clearly occurs at a distance, either through direct field effects or by transiently raised K^+. There is, however, an important precedent of this result, whereby epileptiform discharges can be entrained by minimal activation in an already hyperexcitable network: this is the demonstration that bursts of action potentials of a single pyramidal cell can entrain these discharges in disinhibited hippocampal networks (Miles and Wong, 1983). Future work involves examination of the involvement of extracellular potassium ions levels on the entrainment phenomenon. It can be examined by (a) measuring their extracellular potassium ion levels simultaneously in both hippocampal and neocortical regions, and (b) examining the effect of having different concentrations of potassium ions in ACSF on the entrained activity pattern.

Finally, our results obtained using zero-magnesium *in vitro* model run rather counter to the prevailing view that hippocampal circuits are inherently more "pro-epileptic" than neocortical networks. This notion has its origin, perhaps, from clinical

observations, where temporal lobe epilepsy (TLE) is recognised as a leading cause of medically refractory epilepsy.   In this particular *in vitro* model, hippocampal networks are surprisingly refractory to the change in bathing medium, but notably, once the hippocampal territories start to show epileptiform discharges, these become the dominant, pacemaker activity pattern. It is important to note that this refractoriness of hippocampal networks is also dependent on the *in vitro* model used in the studies (see Chapter 4, Figure 4.12). Previous work has shown that the late stage activity pattern is resistant to commonly used anti-epileptic drugs. This last observation is perhaps the most relevant to the clinical feature, pharmaco-resistance, of TLE. Here, I predict that the pharmaco-sensitivity of the cortical networks may have been altered following the de-entrainment and change in activity patterns observed post-separation of regions in brain slices. This can be examined in future studies, using the *in vitro* model and experimental procedures described in chapter, by assessing the effects of anti-epileptic drugs on the post-separated activity pattern. The highly characteristic pattern of evolution of activity, with key transitions representative of shifts in interactions between the various networks, offers a wealth of metrics for analysing drug actions and the effects of genetic mutations in transgenic mouse models, suggesting that these simple acute *in vitro* models still offer great utility for epilepsy research.

3.5 References

1. Anastassiou, C.A., Perin, R., Markram, H. and Koch, C. (2011) 'Ephaptic coupling of cortical neurons', *Nat Neurosci*, 14(2), pp. 217-23.

2. Anderson, W.W., Lewis, D.V., Swartzwelder, H.S. and Wilson, W.A. (1986) 'Magnesium-free medium activates seizure-like events in the rat hippocampal slice', *Brain Res*, 398(1), pp. 215-9.

3. Avoli, M. and de Curtis, M. (2011) 'GABAergic synchronization in the limbic system and its role in the generation of epileptiform activity', *Prog Neurobiol*, 95(2), pp. 104-32.

4. Dichter, M.A. and Ayala, G.F. (1987) 'Cellular mechanisms of epilepsy: a status report', *Science*, 237(4811), pp. 157-64.

5. Dreier, J.P. and Heinemann, U. (1990) 'Late low magnesium-induced epileptiform activity in rat entorhinal cortex slices becomes insensitive to the anticonvulsant valproic acid', *Neurosci Lett*, 119(1), pp. 68-70.

6. Dreier, J.P. and Heinemann, U. (1991) 'Regional and time dependent variations of low Mg2+ induced epileptiform activity in rat temporal cortex slices', *Exp Brain Res*, 87(3), pp. 581-96.

7. Dreier, J.P., Zhang, C.L. and Heinemann, U. (1998) 'Phenytoin, phenobarbital, and midazolam fail to stop status epilepticus-like activity induced by low magnesium in rat entorhinal slices, but can prevent its development', *Acta Neurol Scand*, 98(3), pp. 154-60.

8. Frohlich, F. and McCormick, D.A. (2010) 'Endogenous electric fields may guide neocortical network activity', *Neuron*, 67(1), pp. 129-43.

9. Gomez-Gonzalo, M., Losi, G., Chiavegato, A., Zonta, M., Cammarota, M., Brondi, M., Vetri, F., Uva, L., Pozzan, T., de Curtis, M., Ratto, G.M. and Carmignoto, G. (2010) 'An excitatory loop with astrocytes contributes to drive neurons to seizure threshold', *PLoS Biol*, 8(4), p. e1000352.

10. Heinemann, U., Draguhn, A., Ficker, E., Stabel, J. and Zhang, C.L. (1994) 'Strategies for the development of drugs for pharmacoresistant epilepsies', *Epilepsia*, 35 Suppl 5, pp. S10-21.

11. Jefferys, J.G. (1995) 'Nonsynaptic modulation of neuronal activity in the brain: electric currents and extracellular ions', *Physiol Rev*, 75(4), pp. 689-723.

12. Miles, R. and Wong, R.K. (1983) 'Single neurones can initiate synchronized population discharge in the hippocampus', *Nature*, 306(5941), pp. 371-3.

13. Mody, I., Lambert, J.D. and Heinemann, U. (1987) 'Low extracellular magnesium induces epileptiform activity and spreading depression in rat hippocampal slices', *J Neurophysiol*, 57(3), pp. 869-88.

14. Prince, D.A. and Connors, B.W. (1984) 'Mechanisms of epileptogenesis in cortical structures', *Ann Neurol*, 16 Suppl, pp. S59-64.

15. Scharfman, H.E. and Schwartzkroin, P.A. (1989) 'Protection of dentate hilar cells from prolonged stimulation by intracellular calcium chelation', *Science*, 246(4927), pp. 257-60.

16. Scharfman, H.E. and Schwartzkroin, P.A. (1990a) 'Consequences of prolonged afferent stimulation of the rat fascia dentata: epileptiform activity in area CA3 of hippocampus', *Neuroscience*, 35(3), pp. 505-17.

17. Scharfman, H.E. and Schwartzkroin, P.A. (1990b) 'Responses of cells of the rat fascia dentata to prolonged stimulation of the perforant path: sensitivity of hilar cells and changes in granule cell excitability', *Neuroscience*, 35(3), pp. 491-504.

18. Schevon, C.A., Weiss, S.A., McKhann, G., Jr., Goodman, R.R., Yuste, R., Emerson, R.G. and Trevelyan, A.J. (2012) 'Evidence of an inhibitory restraint of seizure activity in humans', *Nat Commun*, 3, p. 1060.

19. Smith, E.H., Liou, J.Y., Davis, T.S., Merricks, E.M., Kellis, S.S., Weiss, S.A., Greger, B., House, P.A., McKhann, G.M., 2nd, Goodman, R.R., Emerson, R.G., Bateman, L.M., Trevelyan, A.J. and Schevon, C.A. (2016) 'The ictal wavefront is the spatiotemporal source of discharges during spontaneous human seizures', *Nat Commun*, 7, p. 11098.

20. Timofeev, I. and Steriade, M. (2004) 'Neocortical seizures: initiation, development and cessation', *Neuroscience*, 123(2), pp. 299-336.

21. Traub, R.D. and Wong, R.K. (1982) 'Cellular mechanism of neuronal synchronization in epilepsy', *Science*, 216(4547), pp. 745-7.

22. Trevelyan, A.J. and Schevon, C.A. (2013) 'How inhibition influences seizure propagation', *Neuropharmacology*, 69, pp. 45-54.

23. Weiss, S.A., Banks, G.P., McKhann, G.M., Jr., Goodman, R.R., Emerson, R.G., Trevelyan, A.J. and Schevon, C.A. (2013) 'Ictal high frequency oscillations distinguish two types of seizure territories in humans', *Brain*, 136(Pt 12), pp. 3796-808.

24. Zhang, C.L., Dreier, J.P. and Heinemann, U. (1995) 'Paroxysmal epileptiform discharges in temporal lobe slices after prolonged exposure to low magnesium are resistant to clinically used anticonvulsants', *Epilepsy Res*, 20(2), pp. 105-11.

Chapter 4 The effect of diazepam on evolving epileptiform activity in the cortical networks

4.1 Introduction

Status epilepticus (SE) is a neurological emergency that is characterised by self-sustaining generalised-convulsive or non-convulsive seizures that could alter the structure and functions of the cellular (neuronal and glial) networks, and which clinically is associated with high rates of morbidity and mortality (Shorvon *et al.*, 2008). Since the time of discovery of benzodiazepines (e.g., diazepam, lorazepam, etc.), clinicians have been using them as the first-line treatment for controlling status epilepticus. Benzodiazepines have the advantages of rapid onset of action, low toxicity, and high efficacy (Kapur, 2002).

Benzodiazepines are positive allosteric modulators at $GABA_A$ receptors ($GABA_AR$). $GABA_ARs$ are ligand-gated pentameric channels, which are permeable to chloride and bicarbonate ions (Kaila *et al.*, 1997). There are 19 different types of subunits of $GABA_ARs$, and the pharmacology, localisation, and kinetics of $GABA_ARs$ are dictated by their subunit composition. $GABA_ARs$ containing a γ-subunit, but not a δ-subunit, are sensitive to benzodiazepines. The binding site for benzodiazepines is on the extracellular site of the receptors, at the interface between a γ2 and α1-3 subunits or γ2 and α5 subunits. Benzodiazepine-sensitive $GABA_ARs$ composed of α1-3, and α5 subunits are localised at synaptic- and extra/perisynaptic-regions, respectively, and their expression varies, both, in different cell populations and regions of the brain (Bai *et al.*, 2001; Hamann *et al.*, 2002; Nusser and Mody, 2002). This subunit dependent localisation of $GABA_ARs$ renders benzodiazepines with the ability to differentially modulate phasic and tonic inhibition in different regions of the brain. Benzodiazepines enhances the GABAergic synaptic currents by increasing the frequency of $GABA_AR$ channel opening, while not by altering the mean channel open times (Study and Barker, 1981; Otis and Mody, 1992; Rogers *et al.*, 1994). Use of benzodiazepines for controlling status epilepticus have limitations. Benzodiazepines can become ineffective in patients with increasing duration of status epilepticus, and the status epilepticus in such patients can eventually become refractory to any line of drug treatment (Treiman *et al.*, 1998).

The antiepileptic property and reduced potency of benzodiazepines when administered at an early stage (discrete electrographic seizures) and late stage (SE; recurrent epileptiform discharges), respectively, were studied *in vivo* in rats that were injected with pilocarpine and lithium to induce seizures (Walton and Treiman, 1988; Kapur and Macdonald, 1997). These effects of benzodiazepines on early (tonic-clonic like ictal events) and late (status epilepticus like events) stages of epileptiform activity were also demonstrated *in vitro* in brain slices using low-magnesium model (Dreier and Heinemann, 1990; Zhang *et al.*, 1995; Dreier *et al.*, 1998). These *in vitro* studies assessed benzodiazepines on their ability to affect only the tonic-clonic like discharges and late-stage recurrent discharges.

I show here that having diazepam, a commonly used clinical benzodiazepine, in the proepileptic media do not block the development of neither early-stage nor late-stage epileptiform activity in neocortex in two *in vitro* models examined, zero-magnesium and 4-aminopyridine models. Interestingly, in zero-magnesium model, diazepam delayed the development of early tonic-clonic like activity in neocortex but had no effect on its latency in 4-aminopyridine model. These results show that the same drug can have different effects on the epileptiform activity induced by different mechanisms in the same type of neuronal tissue, and highlights the need for understanding the underlying mechanisms of epileptiform activity for better treatment.

4.2 Materials and Methods

4.2.1 *Slice preparation and electrophysiology*

For all the experiments described below, combined neocortical-hippocampal horizontal slices were used, that were prepared and stored as described in *slice preparation method 2* (chapter 2, sub-heading 2.4.2). For experiments in zero-magnesium model, local field potentials (LFPs) were recorded only from infragranular layers of neocortex. For experiments in 4-aminopyridine model, LFPs were recorded simultaneously from the pyramidal cell layer of CA3 subfield of hippocampus and infragranular layers of neocortex (Figure 4.1). The recording setup and the equipment used were as described in chapter 2 (sub-heading 2.5.1).
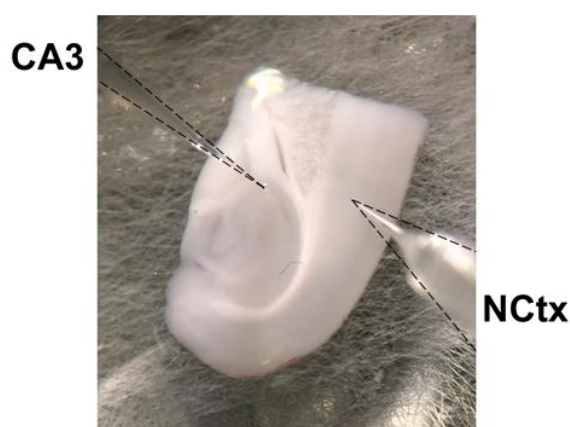
Figure 4.1 Recording setup showing a slice in the interface recording chamber with electrodes placed in the pyramidal cell layer of CA3 (top-left) and infragranular layers of neocortex (NCtx, right).

4.2.2 *Protocols and drugs*

The acute effects of diazepam (DZP), a benzodiazepine, on the evolution of epileptiform activity were studied in two different *in vitro* models of epilepsy: zero-magnesium (0 Mg^{2+}-ACSF) and 4AP (4AP-ACSF). The protocol was as follows: brain slices were placed in the interface recording chamber, which was perfused initially with ACSF. Electrodes were placed in the regions of interest and the baseline activity was recorded in ACSF. After 10-15 minutes, the perfusate was switched from ACSF to epileptogenic medium (0 Mg^{2+}-ACSF or 4AP-ACSF). Measures taken from this set of experiments were considered as controls for comparisons with similarly treated brain slices that were additionally exposed to diazepam. For the treatment group, after

baseline recordings, the solutions were switched to 0 Mg^{2+}-ACSF containing diazepam (0Mg^{2+}/DZP-ACSF) and 4AP-ACSF containing diazepam (4AP/DZP-ACSF), in respective experiments. To study the effects of DZP on late-stage events, slices were superfused with epileptogenic solution until the development of late-stage recurrent discharges, and only at this stage were the epileptogenic solutions supplemented with diazepam.

Diazepam was purchased from Sigma-Aldrich (USA). DZP stock solution (10mM) was prepared and stored in -20 °C. Diazepam was added to the perfusate just before the start of the experiment. 1-3 µM DZP was shown to be effective in maximally increasing GABAergic currents that were measured in neurons of naïve animals (Kapur and Macdonald, 1997). Hence, I chose to use 3 µM of diazepam as final concentration, unless otherwise mentioned. 100 µM 4AP (Sigma-Aldrich) was added to ACSF for experiments in 4AP model.

4.2.3 *Terminology*

'Pre-ictal period' is defined as the period starting from the occurrence of the first pre-ictal discharge (individual pre-ictal event; Figure 4.4Bi) until the precipitation of the ictal event (Figure 4.2, green bars; Figure 4.4A).

4.2.4 *Data analysis*

Data was analysed as described in chapter 2 (sub-heading 2.7). Additionally, estimates of power-spectral density (PSD) for different frequency bandwidths was analysed on hum-removed traces each of 25 seconds length. It was calculated using 'pwelch', a built-in function in Matlab 2015b, with window length of 1638 ms, 25% overlap, and for frequency ranges of 1-10 Hz, 10-40 Hz, and 60-100 Hz (>> [p, f] = pwelch(trace, b, b/4, b, Fs);   where p is the power spectrum for the frequency range, f; b is the epoch length and Fs is the sampling frequency (https://uk.mathworks.com/help/signal/ref/pwelch.html)). PSD ratios were calculated for each frequency bandwidth separately, by measuring PSDs for events in diazepam (post-DZP) and dividing it by PSD measured for events in control (pre-DZP).

4.3 Results

4.3.1 *Positive allosteric modulation of GABA$_A$Rs delays epileptiform evolution in 0 Mg^{2+} in vitro model*

Enhancing GABA$_A$R activity by diazepam from start of washing out Mg^{2+} ions slowed the development of early epileptiform activity, but did not alter the pattern of its evolution nor the latency for its progression to late-stage events (Figure 4.2A). Diazepam increased the latency to the first tonic-clonic like ictal event (IE) (Figure 4.3A, Table 4.1), and the duration of ictal events (Figure 4.3B, Table 4.2).

A. NCtx, 0Mg^{2+}/DZP
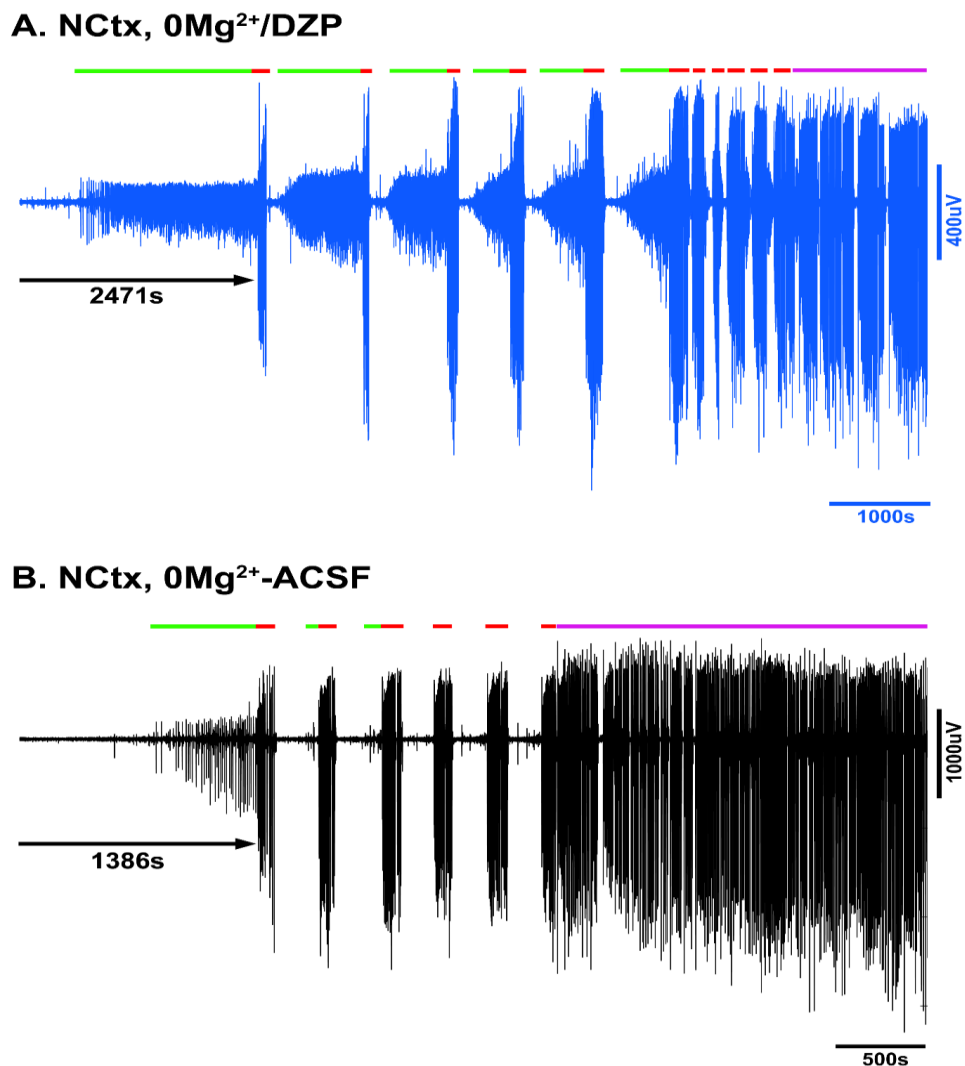
B. NCtx, 0Mg^{2+}-ACSF

Figure 4.2 0 Mg^{2+}-ACSF induced evolution of epileptiform activity in neocortex (NCtx) (A) with diazepam (blue trace) and (B) without diazepam. Latency to first tonic-clonic like ictal events in 0 Mg^{2+}/DZP and 0Mg^{2+}-ACSF was 2471 s and 1386 s, respectively, after washing out Mg^{2+} ions. Note: traces in panels A and B were plotted on different time scales. Green bars, pre-ictal discharges; red bars, tonic-clonic like discharges; purple bars, late-stage recurrent discharges.
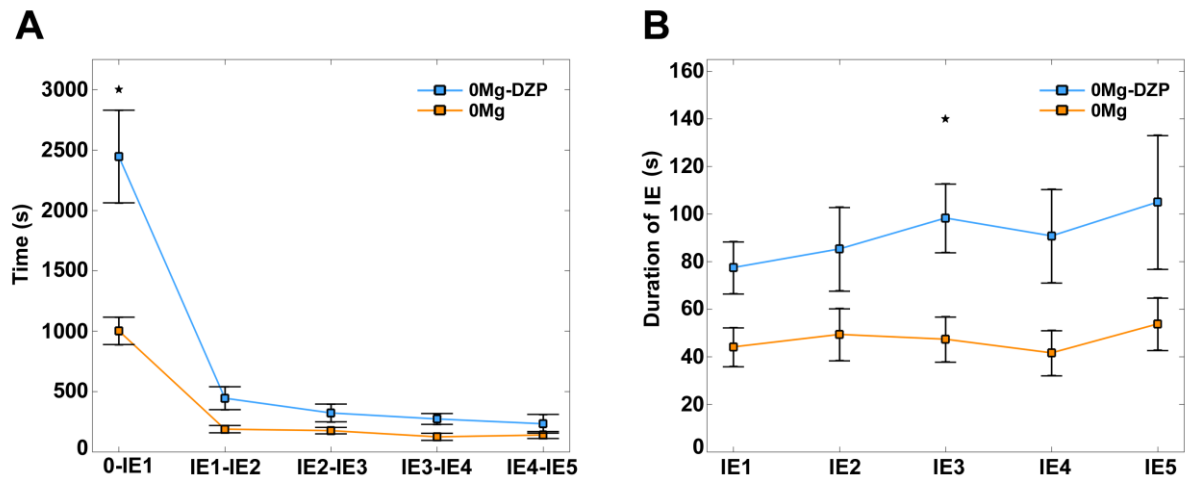
Figure 4.3 A. In 0 Mg^{2+}/DZP treated slices, latency for the development of first IE was longer and the subsequent IEs precipitated at a faster rate (see Table 4.1). B. Tonic-clonic like ictal events lasted longer in slices treated with DZP (see Table 4.2). *p-values less than or equal to Bonferroni corrected critical value (α = 0.01).

Ictal event intervals (s)	0 Mg^{2+}-ACSF (n)	0 Mg^{2+}/DZP-ACSF (n)	p-values ^(α = 0.01)
0-IE1*	1001.77 ± 113.34 (8)	2445.5 ± 383.54 (8)	*0.003
IE1-IE2*	187.83 ± 30.4 (8)	444.25 ± 94.9 (8)	0.02
IE2-IE3	175.65 ± 26.8 (8)	322.22 ± 73.4 (8)	0.08
IE3-IE4*	124.35 ± 29.39 (7)	272.37 ± 44.94 (7)	0.02
IE4-IE5	139.42 ± 28.78 (7)	232.45 ± 77.73 (7)	0.28

Table 4.1 Times to first ictal event and inter-event intervals. Latency (in secs) for the development of the first tonic-clonic like ictal event (IE), and the interval between subsequent IEs were longer in slices treated with DZP compared to the controls (0 Mg^{2+}/DZP-ACSF). **p-values less than or equal to ^Bonferroni corrected critical value (α).

Duration (s) of ictal events	0 Mg^{2+} ACSF (n)	0 Mg^{2+}/DZP-ACSF (n)	p-values ^(α = 0.01)
IE1*	44.14 ± 8.17 (8)	77.49 ± 10.94 (8)	0.02
IE2	49.39 ± 10.93 (8)	85.32 ± 17.58 (8)	0.10
IE3*	47.37 ± 9.48 (8)	98.32 ± 14.44 (8)	*0.01
IE4	41.63 ± 9.47 (7)	90.8 ± 19.65 (7)	0.05
IE5	53.79 ± 11.01 (7)	105.03 ± 28.11 (7)	0.11

Table 4.2 Duration of tonic-clonic like ictal events in 0 Mg^{2+}-ACSF and 0 Mg^{2+}/DZP-ACSF. *p-values less than or equal to ^Bonferroni corrected critical value (α).

A notable feature in the evolution of epileptiform events is the occurrence pre-ictal events (PreIEs) (Trevelyan *et al.*, 2006; Trevelyan *et al.*, 2007; Cammarota *et al.*, 2013). In all the experiments with diazepam, there was a substantial enhancement of the pre-ictal activity. PreIEs in a pre-ictal period started off at a lower rate with few events, and their rate and number of events progressively increased until the precipitation of tonic-clonic like ictal event (Figure 4.4A, Bi, Bii). Diazepam increased the rate and number of PreIEs, and the duration of pre-ictal periods (Figure 4.5, Table 4.3). Latency to the first IE increased in parallel with an increase in the duration of the pre-ictal period (Figure 4.6; times to first IE: 0 Mg^{2+}, 986.9 ± 129.7 s, n = 7; 0 Mg^{2+}/DZP, 2428.3 ± 442.4s, n = 7; duration of first pre-ictal periods: 0 Mg^{2+}, 471.5 ± 64.5 s, n = 7 0 Mg^{2+}/DZP, 1460.7 ± 210.5 s).
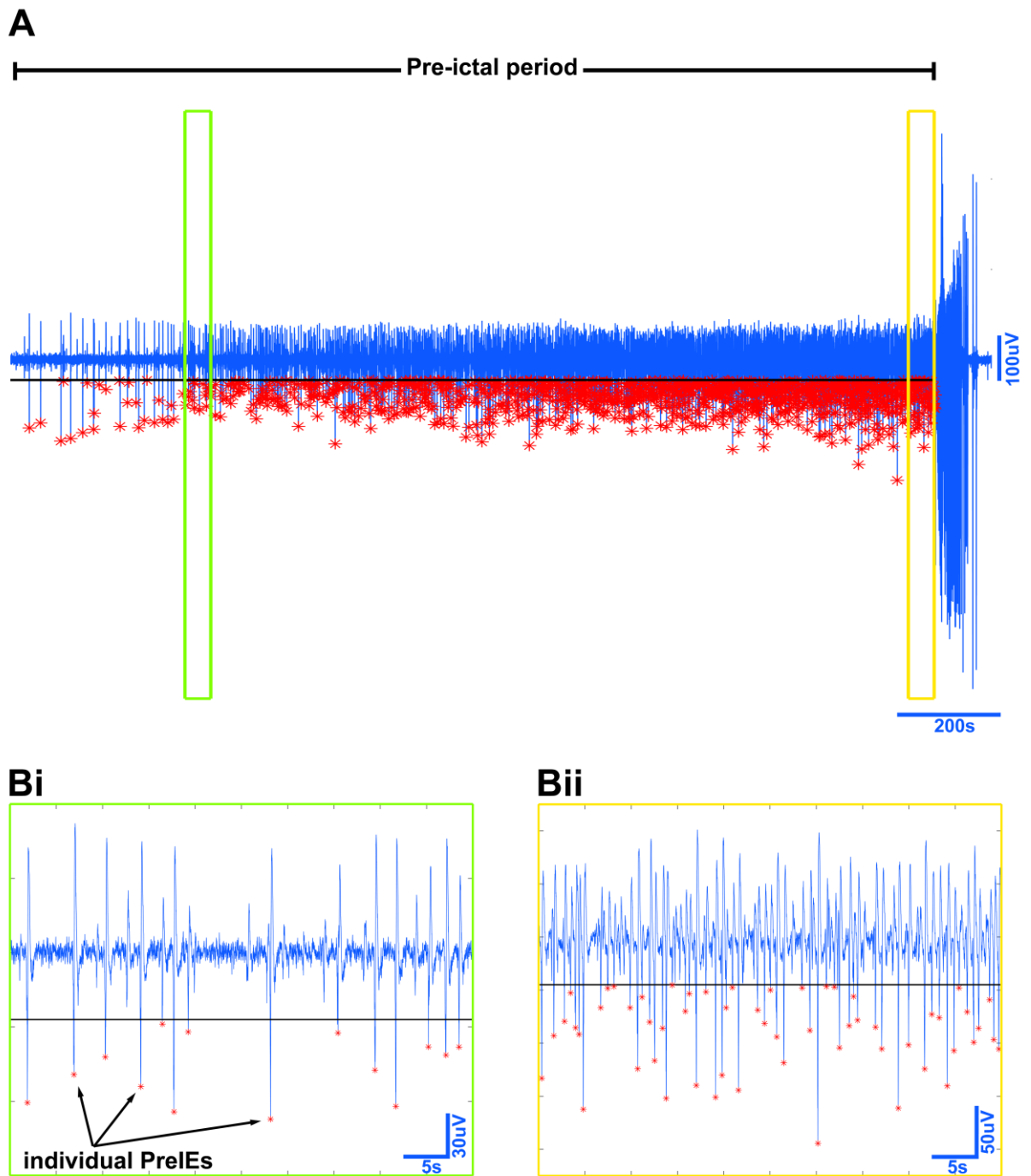
Figure 4.4 A. An example trace recorded in 0 Mg^{2+}/DZP ACSF, displaying pre-ictal events developed prior to the first tonic-clonic like ictal event. Bi and Bii are expanded views of the green yellow boxed areas, respectively, in panel A. Individual pre-ictal events (PreIEs) initially occurred at a lower rate (Bi) that progressively increased until the precipitation of the ictal event (Bii). In A, Bi, and Bii, black horizontal line indicates the threshold level used to identify the PreIEs (red asterisk).

Metrics of the pre-ictal events that occurred prior to the fisrt ictal event
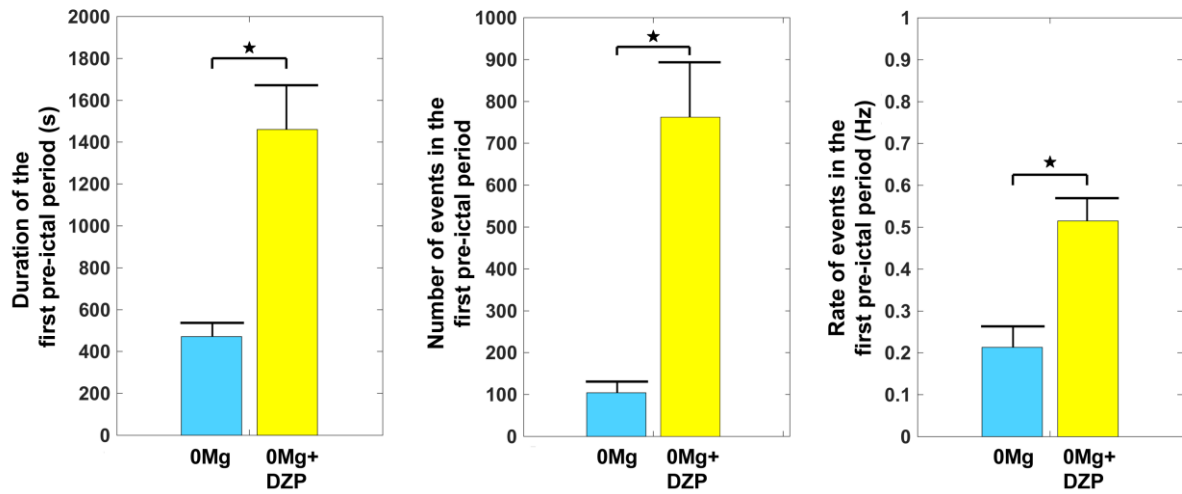
Figure 4.5 Diazepam enhanced the rate and number of pre-ictal events and the duration of pre-ictal period in 0 Mg^{2+}-ACSF. Filled stars in the figure are represented in the text as '*'. *p-values less than the Bonferroni corrected critical value (α): 0.01; See table 4.3 for mean ± s.e.m and p-values.

Pre-ictal period – 1 (prior to the first IE)	0 Mg^{2+}	0 Mg^{2+}/DZP	p-values (α = 0.01)
Duration (s)	471.5 ± 64.5	1460.7 ± 210.5	*< 0.001
Rate of PreIE (Hz)	0.21 ± 0.05	0.52 ± 0.05	*0.001
Number of PreIEs	104.0 ± 26.5	762.3 ± 130.9	*< 0.001

Table 4.3 Measures of the pre-ictal events that developed prior to the first ictal event (IE). For all measures, n = 7. *p-values less than the ^Bonferroni corrected critical value (α).
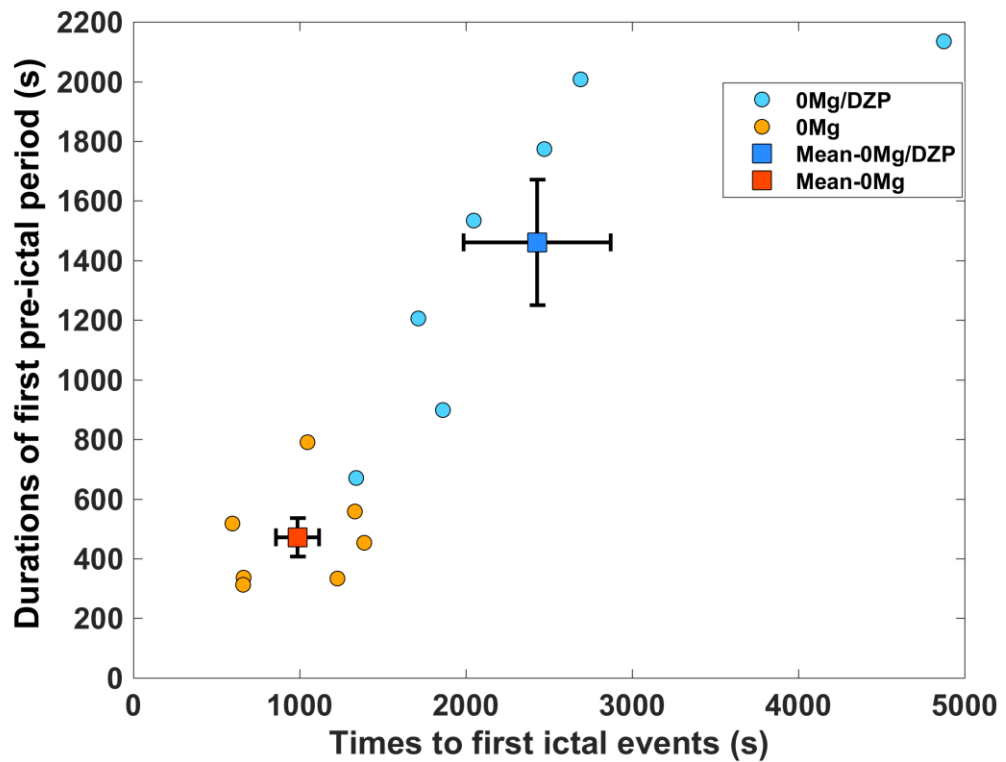
Figure 4.6 Time taken for the development of first tonic-clonic like ictal event is increased in parallel with an increase in the duration of pre-ictal periods.

Although DZP had a clear effect on various facets of early epileptiform discharges, it did not affect the latency for the development of late-stage activity (Figure 4.7A; 0 Mg^{2+}, 3018.1 ± 397.8 s; 0 Mg^{2+}/DZP, 3945.6 ± 492.9; unpaired t-test, p > 0.05). To examine whether in DZP-treated slices there was a delay in transition of activity from early IE to late-stage, the latency to LSEs was measured from the start of the first IE. DZP did not delay the activity transition from early to late stage (Figure 4.7B; 0 Mg^{2+}, 2016.4 ± 318.4 s; 0 Mg^{2+}/DZP, 2015.4 ± 321.8 s; unpaired t-test, p > 0.05). The rate of late-stage events was also not affected by diazepam (Figure 4.7C 0 Mg^{2+}, 0.18 ± 0.03 Hz; 0 Mg^{2+}/DZP, 0.18 ± 0.02 Hz; unpaired t-test, p > 0.05).
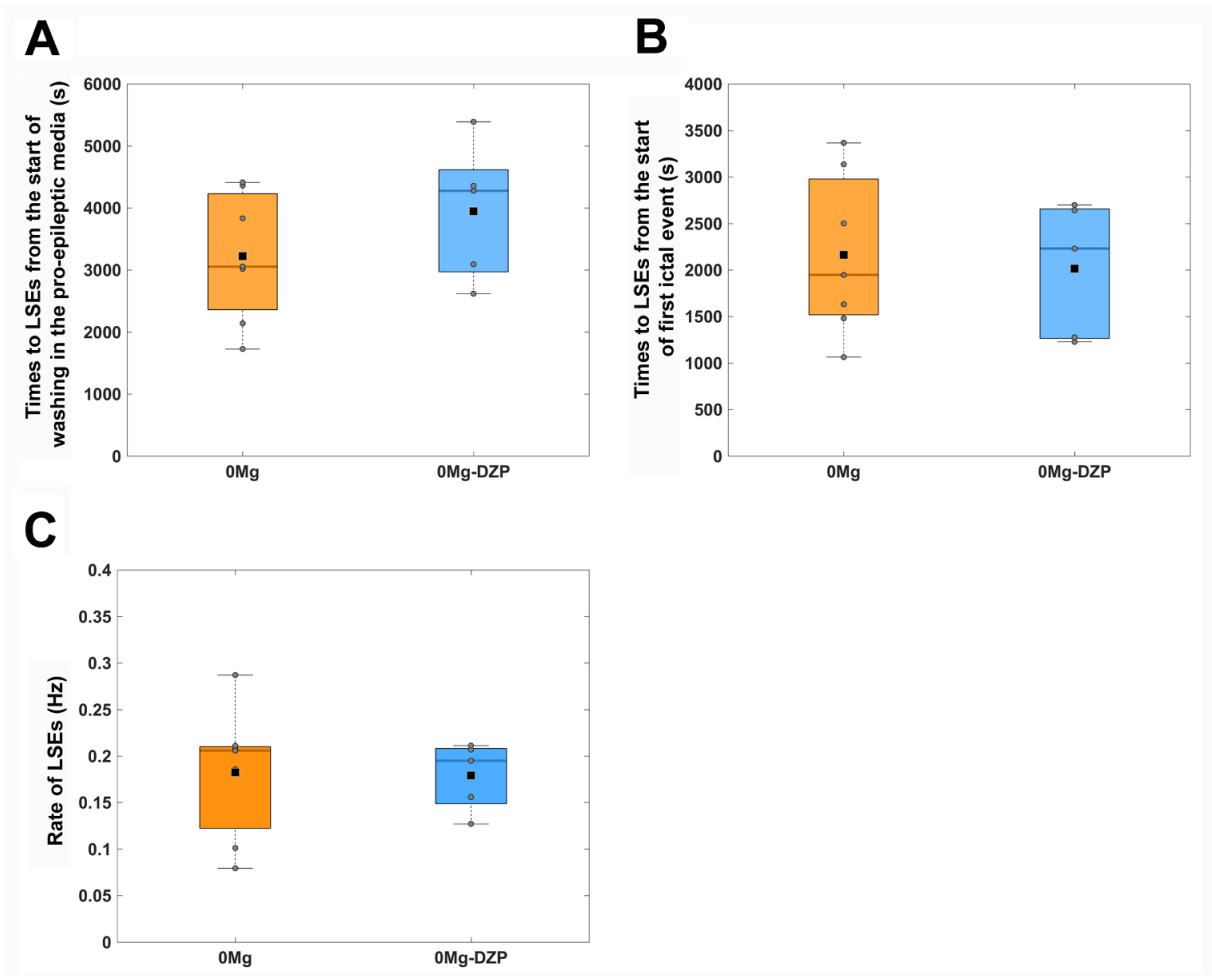
Figure 4.7 Diazepam neither influenced the latency for the development of late-stage events (LSEs) nor the rate of occurrence of LSEs. A. Latency to LSEs measured from the start of washing in the epileptogenic media. B. Latency to LSEs measured from the start of first IE. C. Rate of LSEs was similar in both the groups.

4.3.2 *Zero-Mg^{2+} induced IEs and LSEs in neocortex were not suppressed by diazepam*

Previous studies have shown that midazolam and carbamazepine, benzodiazepine, suppressed 0 Mg^{2+}-ACSF induced early tonic-clonic like ictal events, but not LSEs in entorhinal cortical networks in slices prepared from Wistar rats (Zhang *et al.*, 1995; Dreier *et al.*, 1998). I tested whether diazepam shows similar anti-epileptic properties, in neocortical networks in slices prepared from wild-type mice (C57BL6). In all three recordings, diazepam failed to suppress the on-going 0 Mg^{2+}-ACSF induced tonic-clonic like ictal events even after increasing the concentration of DZP to 30µM (Figure 4.8).
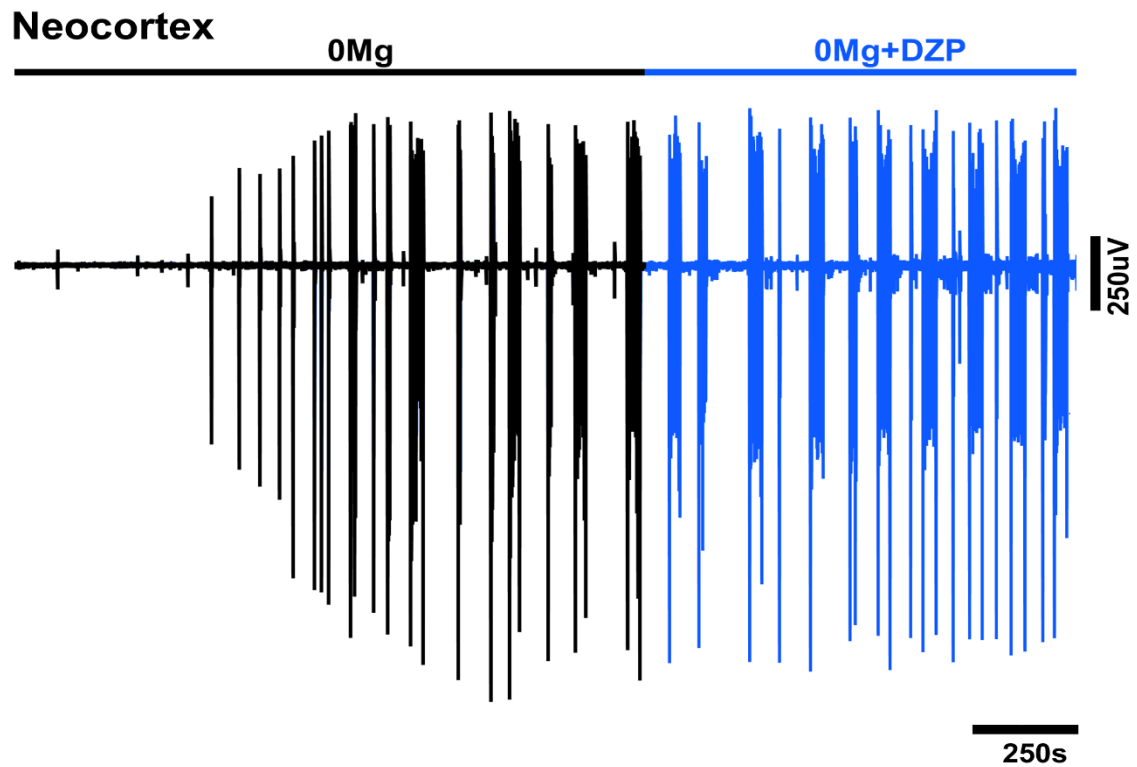
Figure 4.8 In neocortex, diazepam did not suppress the on-going 0 Mg^{2+}-ACSF induced tonic-clonic like ictal events. Black, 0 Mg^{2+}-ACSF; blue, 0 Mg^{2+}/DZP-ACSF.

However, similar to the results of previous studies that used different benzodiazepines (Zhang *et al.*, 1995), diazepam did not suppress the on-going 0 Mg^{2+}-ACSF induced LSEs (Figure 4.9; n = 7). The effect of diazepam on the rate, maximal amplitude, and duration of LSEs was inconsistent in different experiments; that is, in a few experiments DZP increased these parameters and decreased in other experiments (Figure 4.10; Table 4.4).

A. LSE, 0Mg^{2+}

B. LSE, 0Mg^{2+}/DZP
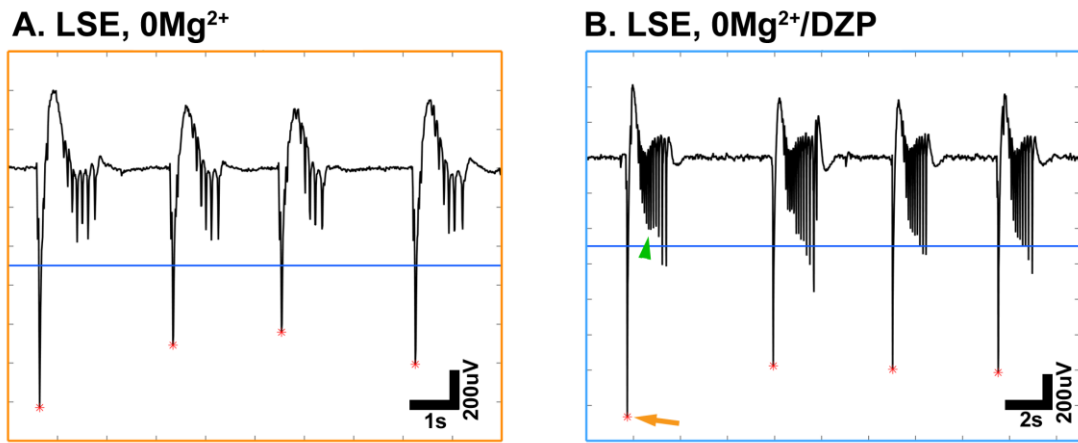
Figure 4.9 Diazepam failed to suppress the on-going 0 Mg^{2+}-ACSF induced LSEs in neocortical networks. A. Pre-DZP: 0Mg^{2+}-ACSF induced LSEs. B. Post-DZP: LSEs in 0 Mg^{2+}+DZP-ACSF. Although diazepam did not suppress the LSEs, it mediated an increase in the amplitude of the first spike (large downward deflection; orange arrow) and following spikelets (green arrow head) of an event. In A and B, horizontal blue line indicates the threshold level used event detection (red asterisks).
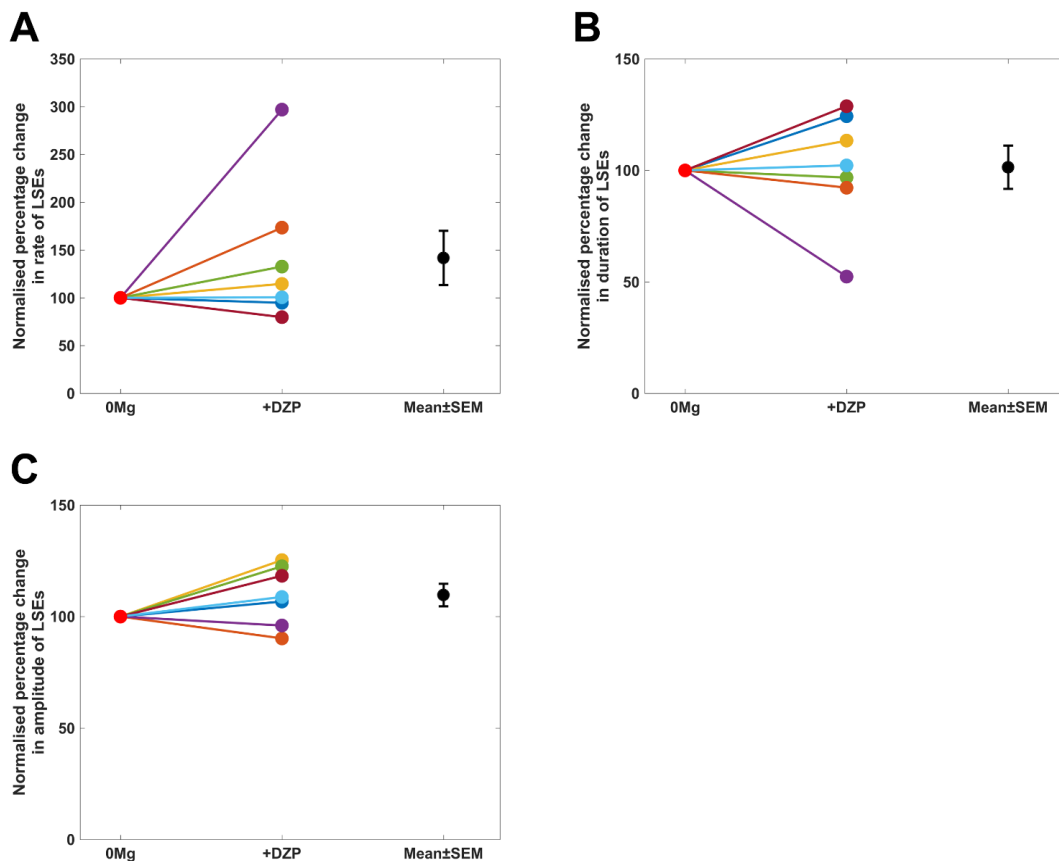
Figure 4.10 Effects of diazepam on LSEs were varying in different experiments. Data represented for rates (A), duration (B), and maximal amplitudes (C), is normalised to controls. For mean ± s.e.m and p-values, see table 4.4.

0 Mg^{2+} model	Neocortical LSE			
	Pre-DZP	Post-DZP	Norm. % change	p =
Rate (Hz)	0.18 ± 0.03	0.23 ± 0.03	141.8 ± 28.3	0.19
Duration (s)	2.49 ± 0.35	2.37 ± 0.23	101.4 ± 9.6	0.88
Max. Amp. (µV)	933.6 ± 116.9	1017.9 ± 129.8	109.7 ± 5.0	0.10

Table 4.4 Rate, duration, and maximal amplitude (Max. Amp.) measures of LSEs taken before (pre-DZP) and after adding DZP (post-DZP) to 0 Mg^{2+}-ACSF. For all measures, n = 7. p-values were calculated using paired Student's t-test.

Power-spectral density (PSD) analysis was carried out to test whether diazepam influenced the frequency components of 0 Mg^{2+}-ACSF induced late-stage events (Figure 4.11Ai, Aii). Diazepam did not affect frequency components in 1-10 Hz nor 60-100 Hz bandwidths, but increased PSDs for frequencies in 10-40 Hz bandwidth (Figure 4.11 Aiii, B; post-DZP/pre-DZP PSD ratios (n = 7; Bonferroni corrected critical value (α) is 0.016): 1-10 Hz: 1.21 ± 0.09, p = 0.069; 10-40 Hz: 2.36 ± 0.39, p = 0.01; 60-100 Hz: 1.58 ± 0.22, p = 0.03)
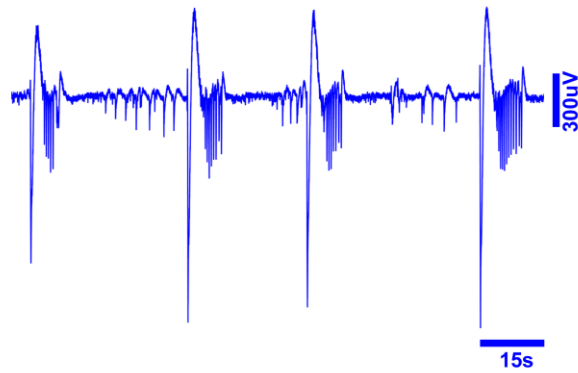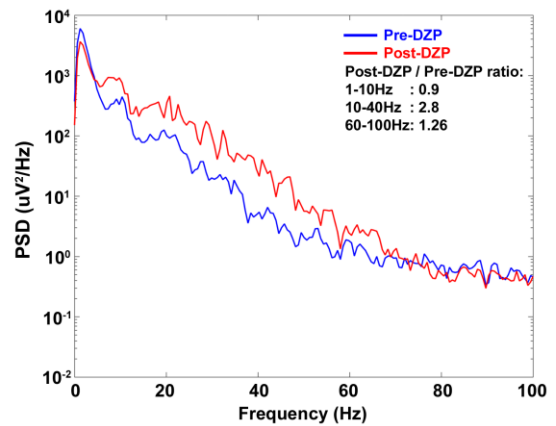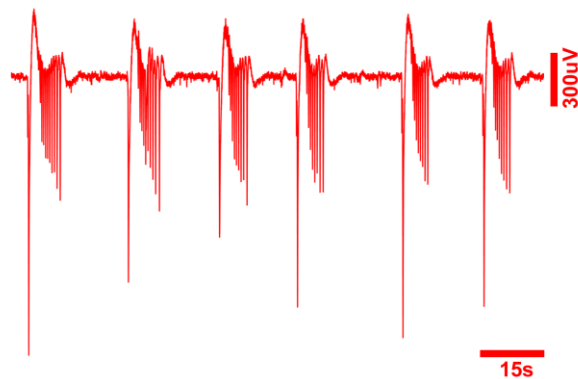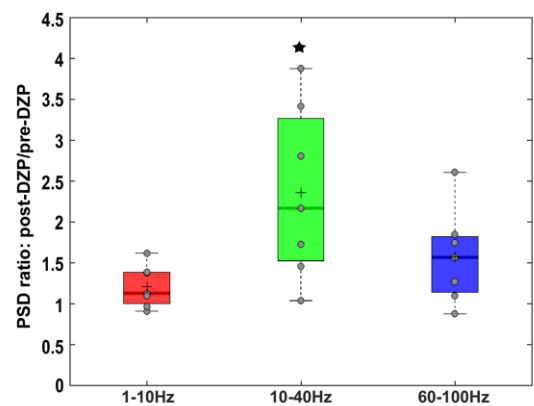
Figure 4.11 Diazepam increased the power-spectral densities (PSD) of frequency components of 0 Mg^{2+}-ACSF induced neocortical LSEs in10-40 Hz bandwidth. Example traces displaying $0Mg^{2+}$-ACSF induced LSEs (pre-DZP; Ai) and LSEs after diazepam treatment (post-DZP; Aii) in the same slice. Aiii. Power-spectral density (PSD) analysis of the data shown in Ai and Aii. B. Bar graphs of PSD ratios (post-DZP/pre-DZP) for different frequency bandwidths. *p = 0.01; Bonferroni corrected critical value (α) = 0.016.

4.3.3 *Positive allosteric modulation of GABAARs delayed the onset of epileptiform activity in CA3, but not in neocortex in 4-aminopyridine in vitro model*

In the next series of *in vitro* experiments, I studied the effect of diazepam on the evolution of epileptiform activity simultaneously in neocortex (NCtx) and hippocampal CA3 subfield (CA3) using 4-aminopyridine (4AP) *in vitro* model. Control group consists of experiments carried out only in 4AP-ACSF. In the control group, following wash-in of 4AP-ACSF, there was a gradual build-up of epileptiform activity in the neocortex,

pre-ictal events were followed by tonic-clonic like ictal events (IE) and a second transition into late-stage recurrent discharges (LSEs) (Figure 4.12A, black trace). In CA3, on the other hand, epileptiform discharges were of different pattern having recurrent large spike-and-wave discharges (SWDs) (Figure 4.12A, red trace) and, furthermore, these events began with similar latency as the development of the first IE in neocortex as can be seen with multiunit activity associated with the events in both the regions (Figure 4.12A inset; Table 4.5).

In the presence of diazepam, epileptiform activity appeared to evolve simultaneously, in both the neocortex and CA3 (Figure 4.12B). Diazepam appeared to delay the development of epileptiform activity in CA3, but not in neocortex (Figure 4.13; Table 4.5). Furthermore, unlike in $0Mg^{2+}$, diazepam did not mediate any long-lasting pre-ictal discharges in the neocortex.
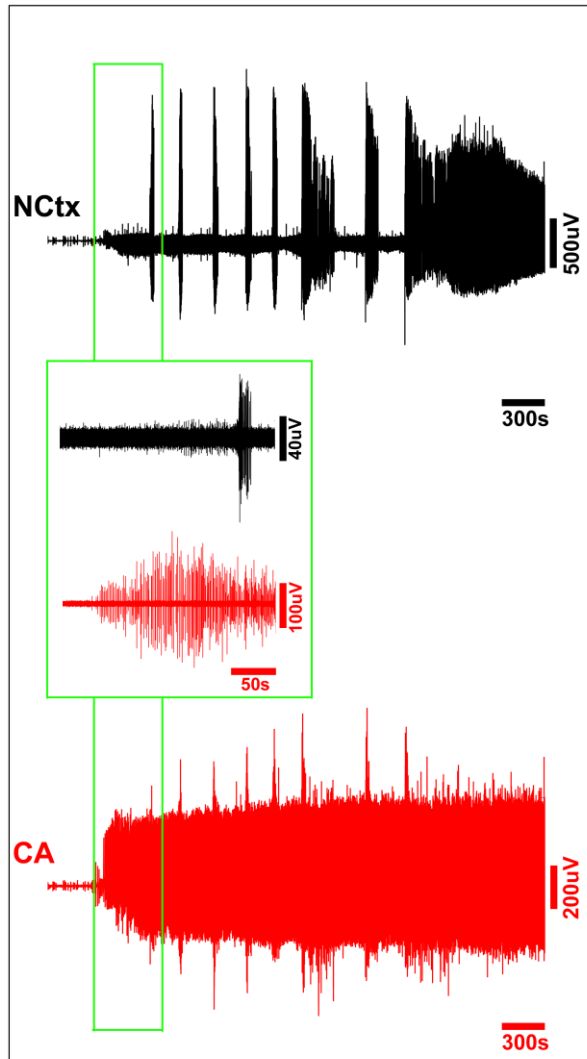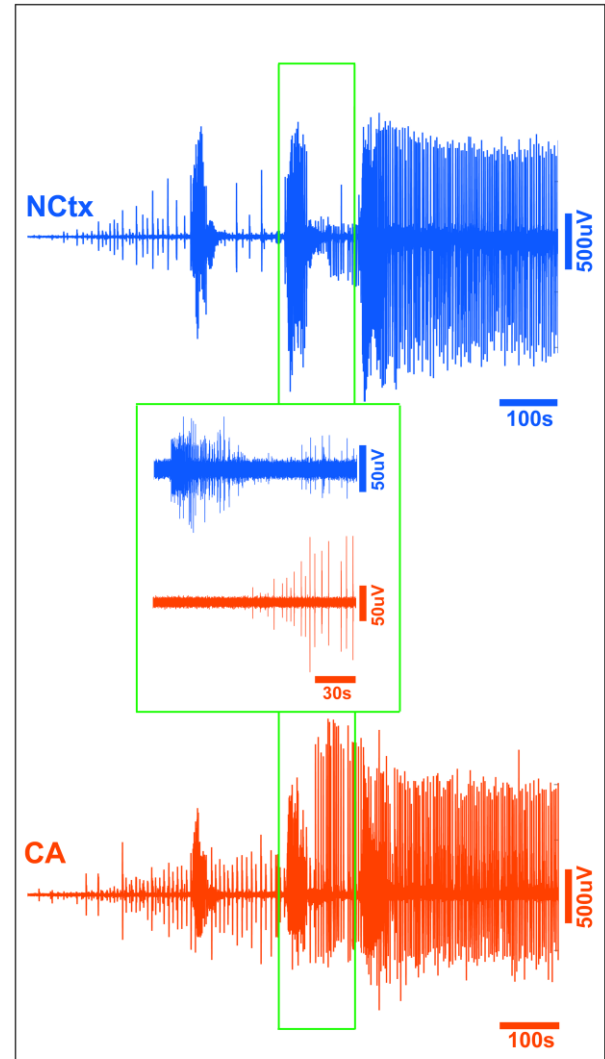
Figure 4.12 A. 4AP induced different pattern of evolution of epileptiform activity in neocortex (NCtx; black trace) and CA3 (red trace). Epileptiform discharges developed earlier in CA3 than in the neocortex. These were the simultaneous recordings from neocortex and CA3 in the slice. Insets: multiunit activity (300 – 3000 Hz) of the boxed areas. B. Diazepam in 4AP-ACSF delayed the development of epileptiform activity in CA3 (orange trace), but did not affect neocortex (blue trace). Insets: multiunit activity (300 – 3000 Hz) of the boxed areas.
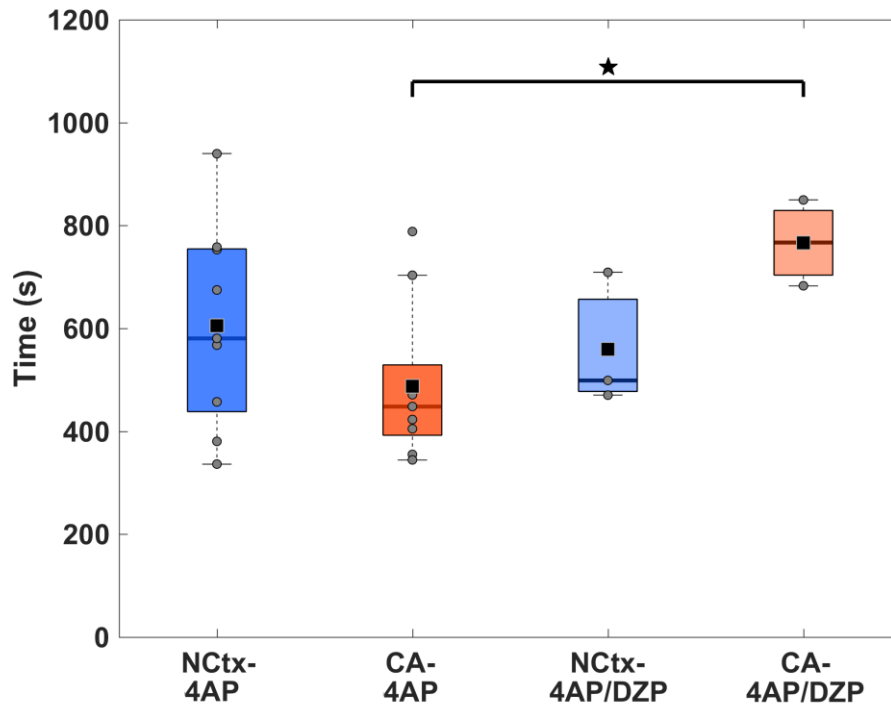
Figure 4.13 In control group (4AP-ACSF), epileptiform activity associated with local neuronal firing developed earlier in CA3 than in the neocortex, whereas, in diazepam treated group, the first IE in neocortex occurred earlier than the first SWD in CA3. *Unpaired Student's t-test with p-values less than or equal to the Bonferroni corrected critical value (α): 0.01. For mean ± s.e.m, see Table 4.5.

Latency (s)	Neocortex (n)	CA3 (n)	Paired t-test, p-values (^α = 0.01)
4AP	605 ± 21.8 (9)	487.4 ± 17.1 (9)	0.04
4AP/DZP	559.6 ± 75.4 (3)	766.6 ± 48.3 (3)	0.13
Unpaired t-test, p-values (^α = 0.01)	0.71	*0.01	

Table 4.5 Times to the first IE in neocortex and SWD in CA3 in 4AP- and 4AP/DZP-ACSF. *p-values less than or equal to the ^Bonferroni corrected critical value (α).

4.3.4 *4AP-induced neocortical LSEs, and SWDs in CA3 were not suppressed by diazepam*

I next examined whether diazepam has any effect on 4AP-ACSF induced late-stage events and SWDs in neocortex and CA3, respectively. Diazepam had minimal influence on the rates, durations, and maximal amplitudes of SWDs in CA3 (Figure 4.14, Table 4.6), and neocortical LSEs (Figure 4.15, Table 4.7). There was a small trend towards an increase in maximal amplitude of LSEs in neocortex after diazepam-treatment (post-DZP) compared to 4AP-ACSF (pre-DZP) in the same slices.

Power-spectral density (PSD) analysis was carried out to test whether diazepam influenced the frequency components of the LSEs (Figure 4.16 A) and SWDs (Figure 4.17 A). Diazepam did not greatly influence the PSDs of frequencies in any of the three frequency bandwidths tested, neither in the neocortex (Figure 4.16B; Table 4.8) nor in CA3 (Figure 4.17 B; Table 4.8). However, in CA3 SWDs, there is a small trend towards a higher PSD ratio for the frequencies in 10-40 Hz bandwidth. Since, the sample size was small, power analysis was performed to validate the statistical test, and to yield an approximate sample size that will be required to see a significant difference ($p < 0.05$) in the reported results. Our ability to find significant difference in 10-40 Hz bandwidth, but not in 1-10 Hz or 60-100 Hz bandwidths, was limited by the sample size (Table 4.9).
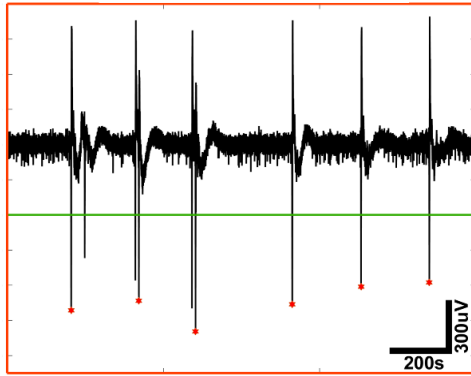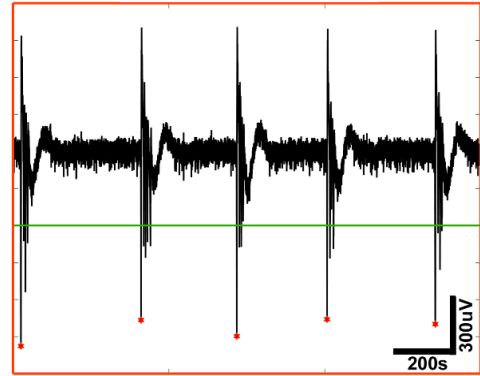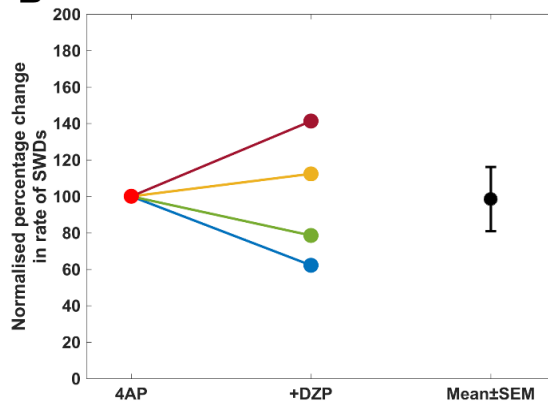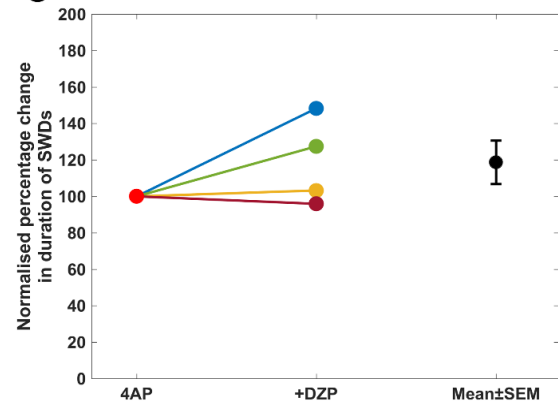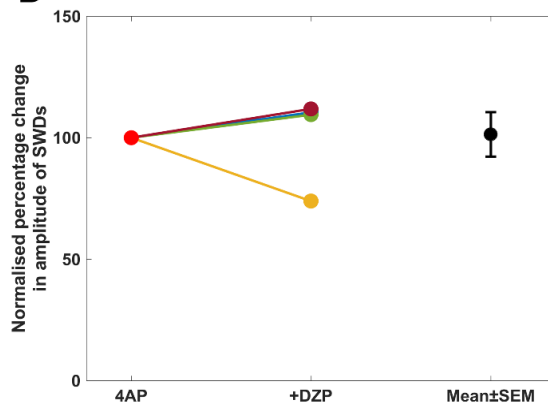
Figure 4.14 Diazepam had variable effect on the rate (B), duration (C), and maximal amplitude (D) of the on-going 4AP-ACSF induced SWDs in CA3 hippocampal networks. Data represented in B, C, and D is normalised to controls. Ai. Pre-DZP: 4AP-ACSF induced SWDs. Aii. Post-DZP: SWDs in 4AP+DZP-ACSF. For mean ± s.e.m., see Table 4.6.

4-AP model	CA3 SWDs			
	Pre-DZP (n)	Post-DZP (n)	Norm. % change	p =
Rate (Hz)	0.63 ± 0.08 (4)	0.62 ± 0.12 (4)	98.6 ± 17.6	0.94
Duration (s)	0.92 ± 0.05 (4)	1.09 ± 0.14 (4)	118.7 ± 11.9	0.22
Max. Amp. (µV)	1429.8 ± 261.3 (4)	1468.2 ± 336.3 (4)	101.4 ± 9.2	0.77

Table 4.6 Rate, duration, and maximal amplitude (Max. Amp.) measures of SWDs in CA3 taken before (pre-DZP) and after (post-DZP) adding DZP to 4AP-ACSF. p-values were calculated using paired Student's t-test.

Ai. NCtx, pre-DZP

Aii. NCtx, post-DZP

200uV

2.5s

200uV

2.5s

B

Normalised percentage change in rate of LSEs

4AP   +DZP   Mean±SEM

C

Normalised percentage change in duration of LSEs

4AP   +DZP   Mean±SEM

D

Normalised percentage change in amplitude of LSEs

4AP   +DZP   Mean±SEM
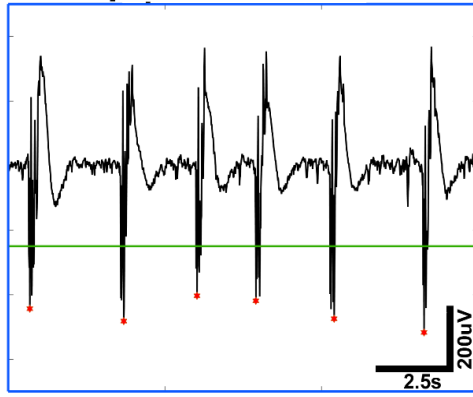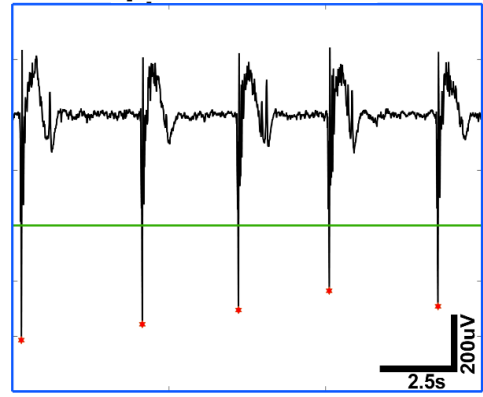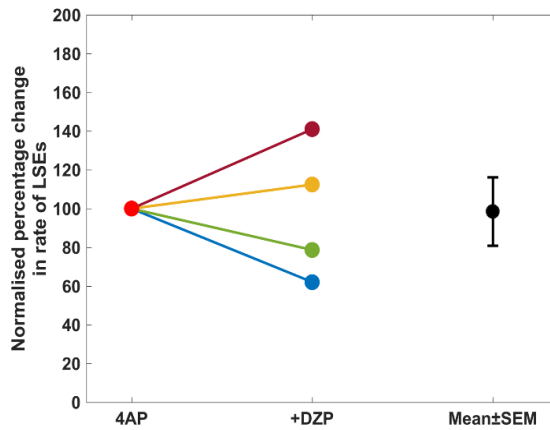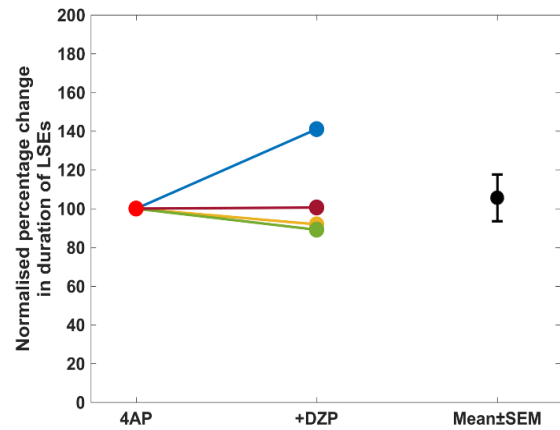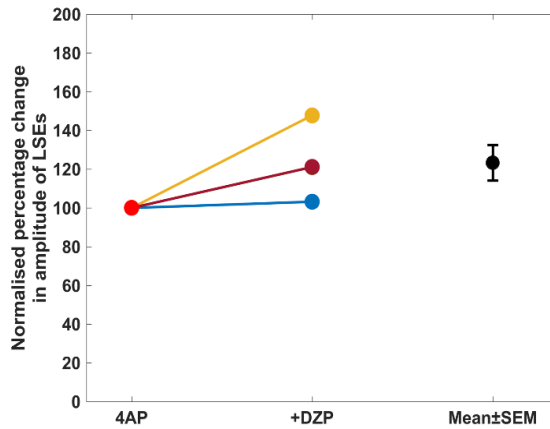
Figure 4.15 Diazepam had variable effect on the rate (B), duration (C), and a small trend towards an increase in maximal amplitude (D) of the on-going 4AP-ACSF induced LSEs in neocortex. Data represented in B, C, and D is normalised to controls. Ai. Pre-DZP: 4AP-ACSF induced LSEs. Aii. Post-DZP: LSEs in 4AP+DZP-ACSF. For mean ± s.e.m., see Table 4.7.

4-AP model	Neocortical LSE			
	Pre-DZP (n)	Post-DZP (n)	Norm. % change	p =
Rate (Hz)	0.63 ± 0.08 (4)	0.62 ± 0.12 (4)	98.6 ± 17.6	0.94
Duration (s)	1.12 ± 0.02 (4)	1.19 ± 0.16 (4)	105.6 ± 12.1	0.67
Max. Amp. (μV)	757.9 ± 201 (4)	972.6 ± 332.8 (4)	123.3 ± 9.2	0.08

Table 4.7 Rate, duration, and maximal amplitude (Max. Amp.) measures of neocortical LSEs taken before (pre-DZP) and after (post-DZP) adding DZP to 4AP-ACSF. p-values were calculated using paired Student's t-test.

Figure 4.16 Diazepam did not affect the frequency components of 4AP-induced neocortical LSEs. Example traces displaying 4AP-ACSF induced LSEs (pre-DZP; Ai) and LSEs after diazepam treatment (post-DZP; Aii) in the same slice. Aiii. Power-spectral density (PSD) analysis of the data shown in Ai and Aii. B. Bar graphs of PSD ratios (post-DZP/pre-DZP) for different frequency bandwidths examined (1-10 Hz, 10-40 Hz, and 60-100 Hz). For mean ± s.e.m., see Table 4.8

Ai. CA3, 4AP, pre-DZP

300uV

4s

Aii. CA3, 4AP, post-DZP

300uV

4s

Aiii

Pre-DZP
Post-DZP
Post-DZP/Pre-DZP ratio:
1-10Hz   : 1.53
10-40Hz : 1.17
60-100Hz: 0.96

PSD (uV²/Hz)

Frequency (Hz)

B

PSD ratio: post-DZP/pre-DZP

1-10Hz   10-40Hz   60-100Hz
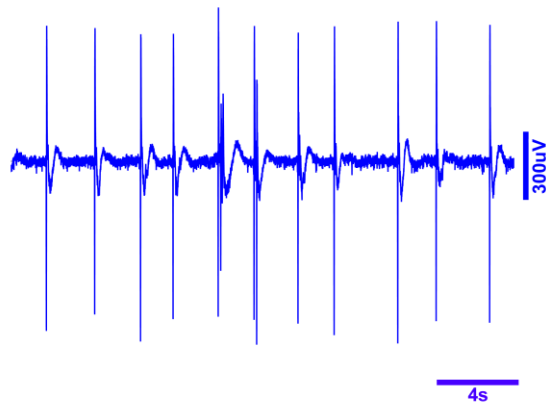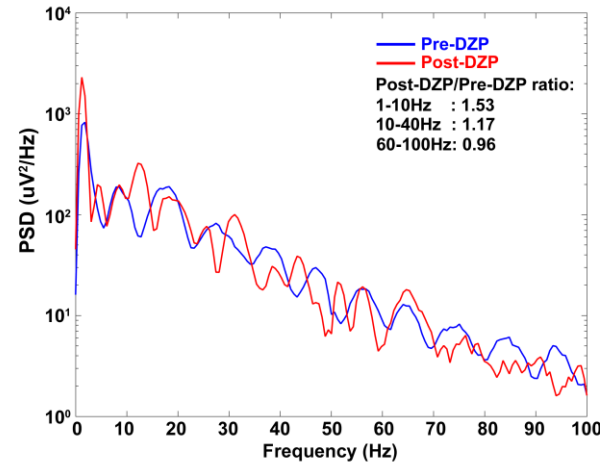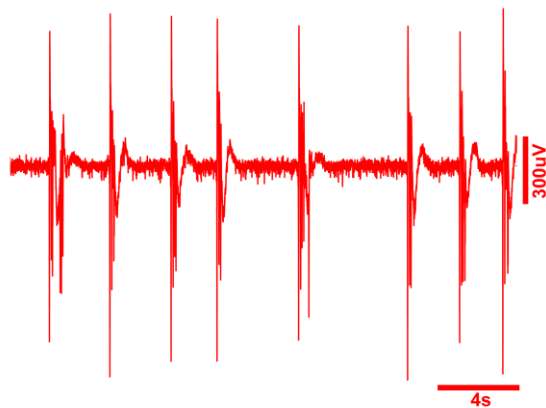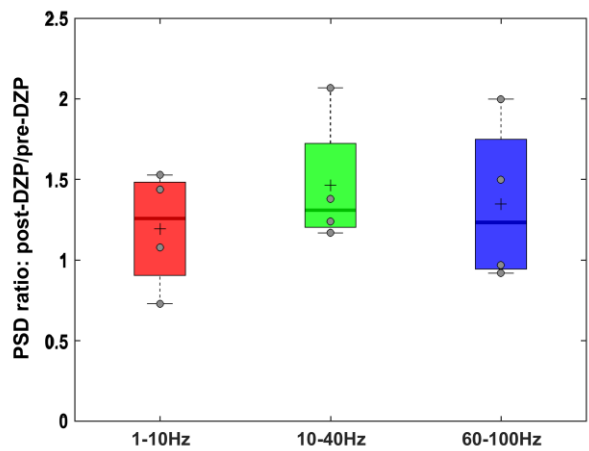
Figure 4.17 Diazepam did not affect the frequency components of 4AP-induced hippocampal SWDs. Example traces displaying 4AP-ACSF induced SWDs (pre-DZP; Ai) and SWDs after diazepam treatment (post-DZP; Aii) in the same slice. Aiii. Power-spectral density (PSD) analysis of the data shown in Ai and Aii. B. Bar graphs of PSD ratios (post-DZP/pre-DZP) for different frequency bandwidths examined (1-10 Hz, 10-40 Hz, and 60-100 Hz. For mean ± s.e.m., see Table 4.8

82

PSD ratio: Post-DZP / Pre-DZP in 4AP model				
Frequency bandwidths	**Neocortical LSEs (n)**	**p-value** **^(α = 0.016)**	**CA3 SWDs (n)**	**p-value** **^(α = 0.016)**
1-10 Hz	1.19 ± 0.41 (4)	0.65	1.19 ± 0.18 (4)	0.36
10-40 Hz	1.13 ± 0.21 (4)	0.57	1.46 ± 0.21 (4)	0.11
60-100 Hz	1.12 ± 0.23 (4)	0.65	1.34 ± 0.25 (4)	0.2

Table 4.8 Power-spectral density ratios of frequency components of events measured before and after adding diazepam in 4AP model. **^**Bonferroni corrected critical value (α).

Frequency Bandwidths	**Neocortical LSEs**		**CA3 SWDs**	
	Effect size	**Required total Sample size**	**Effect size**	**Required total Sample size**
1-10 Hz	0.232	149	0.528	31
10-40 Hz	0.309	85	1.095	9
60-100 Hz	0.261	118	0.680	19

Table 4.9 Required total sample sizes to achieve a significant difference (p<0.05) in the effect of diazepam on PSD ratios of the frequency components of neocortical LSEs, and SWDs in CA3.

4.4 Discussion

Benzodiazepines are used as a first-line therapy for status epilepticus. However, they have a variable effect on the management of status epilepticus (Chin *et al.*, 2008). It is not known why few patients respond to benzodiazepines and others do not. One of the factors is the time of treatment; that is, treatment early-on after the onset of status epilepticus was reported to have better treatment outcomes (Chin *et al.*, 2008). To understand this variable effect of benzodiazepines better, it is important to explore which facets of the evolving epileptiform activity pattern is influenced by a clinically used modulator of $GABA_AR$ activity, namely, diazepam.

Results of this chapter illustrate several distinct effects of diazepam on the evolution of epileptiform activity in different cortical networks in brain slices, using different *in vitro* models of epilepsy. Firstly, in 0 Mg^{2+}-model, diazepam enhanced pre-ictal discharges and delayed the development of tonic-clonic like ictal events (ictal events) in neocortex. Pre-ictal and inter-ictal events are transient events that occur prior to and in between ictal events, respectively, and the relationship between these transient events and ictal events remains unclear (Avoli *et al.*, 2002; Dzhala and Staley, 2003; Khalilov *et al.*, 2003; Staley *et al.*, 2005; Avoli *et al.*, 2006; White *et al.*, 2010; Chauviere *et al.*, 2012). These events were demonstrated to be anti-epileptic as well as pro-epileptic in nature (Swartzwelder *et al.*, 1987; Bragdon *et al.*, 1992; de Curtis *et al.*, 1998; de Curtis and Avanzini, 2001; Avoli *et al.*, 2002; Librizzi and de Curtis, 2003; Staley *et al.*, 2005; Avoli *et al.*, 2006; Trevelyan *et al.*, 2006; Trevelyan *et al.*, 2007; White *et al.*, 2010; Huberfeld *et al.*, 2011; Chauviere *et al.*, 2012; Cammarota *et al.*, 2013). Previous studies identified and confirmed two types of interictal events (Voskuyl and Albus, 1985; Michelson and Wong, 1991; Perreault and Avoli, 1992; Watts and Jefferys, 1993; Huberfeld *et al.*, 2011). Type one events were sensitive to glutamatergic antagonism resembling events in disinhibited tissues. Type two events were not sensitive to glutamatergic antagonism, but are sensitive to $GABA_A$-receptors antagonism. An *in vivo* study also demonstrated the presence of two types of inter-ictal events, of which the rate of one type reduced and the other increased as the activity developed into a seizure event. This increase is not observed in animals that did not develop spontaneous seizures (Chauviere *et al.*, 2012).

Other sets of studies suggested that pre-ictal events are protective (anti-epileptic) in nature and are dominated by GABA mediated inhibitory currents (Trevelyan *et al.*, 2006; Trevelyan *et al.*, 2007; Cammarota *et al.*, 2013). The inhibitory signalling during pre-ictal events was provided largely by parvalbumin-positive interneurons (Cammarota *et al.*, 2013), and when this functional inhibition collapses, activity shows a transition from pre-ictal to ictal events (Trevelyan *et al.*, 2006; Trevelyan *et al.*, 2007; Cammarota *et al.*, 2013). Based on the results presented in this chapter and literature, I hypothesise that pre-ictal events developed in presence of diazepam are protective in nature as their enhancement by diazepam appeared to delay the onset of ictal events. If they were pro-epileptic, ictal events would have developed much earlier. The nature of synaptic currents underlying diazepam-induced pre-ictal events needs to be investigated at a cellular level to identify whether they are protective events involving functional inhibitory currents or causative events involving compromised inhibitory currents (absence and/or depolarising GABA mediated currents).

In 0 Mg^{2+} model, as diazepam delayed the development of ictal events, I hypothesised that it would increase the latency for the development of late-stage events in neocortex. But, surprisingly, diazepam did not affect the time taken for the early activity to evolve into late-stage activity. This suggests that increasing the frequency of channel opening do not play a direct role in the transition of activity from ictal to late-stage, but may work together with other mechanisms such as altered surface expression and turnover of $GABA_ARs$ and their subunits (Brooks-Kayal *et al.*, 1998; Peng *et al.*, 2004; Terunuma *et al.*, 2008), deficits in the activity of potassium-chloride cotransporters (KCC2) (Silayeva *et al.,* 2015), cellular fatigue, reduced availability of synaptically released GABA, (Schousboe *et al.*, 1983; Pfeiffer *et al.*, 1996). It has been shown that, after intense activation of GABAergic interneurons, particularly the parvalbumin-positive fast-spiking basket cells, the reversal potential of $GABA_A$ currents (E_{GABA}) is shifted from hyperpolarising to depolarising potentials and thus, diminishing the effective inhibitory currents (Isomura *et al.*, 2003), and the E_{GABA} in pyramidal neurons were at depolarising levels in pilocarpine induced-status epilepticus (Barmashenko *et al.*, 2011). However, it is not known whether the transition into late-stage activity is due to this shift in E_{GABA}, and what role do positive modulators of $GABA_A$-receptors play, if any, during this activity transition. This could

be one of the mechanisms that work at GABA$_A$Rs that underlie the second transition to late-stage activity. This can be examined by performing perforated-patch recording from pyramidal neurons and periodically assessing E$_{GABA}$ as the epileptiform activity evolves from early to late-stage activity.

Late-stage events developed in slices exposed to zero-magnesium ACSF were shown to be not suppressed by midazolam (a benzodiazepine) (Zhang *et al.*, 1995). In agreement with these previous studies, diazepam neither suppressed neocortical late-stage events nor had any substantial effect on duration, amplitude, or the rates of these events. Previous studies reported a decrease in the surface expression of γ2 and β2/3 subunits of GABA$_A$Rs in epileptic rats, suggesting the reduced availability of benzodiazepine-sensitive GABA$_A$Rs (Naylor *et al.*, 2005; Goodkin *et al.*, 2008). This downregulation of benzodiazepine-sensitive GABA$_A$R subunits could be one of the explanations for the insensitivity of epileptiform activity to diazepam.

Earlier studies have researched the sensitivity of different types of 4-aminopyridine (4AP)-induced epileptiform activity to the standard anti-epileptic drugs, but not the evolution of activity (Watts and Jefferys, 1993; Yonekawa *et al.*, 1995; Bruckner *et al.*, 1999; Bruckner and Heinemann, 2000). Current results reveal the contrasting effects of diazepam on evolving epileptiform activity in 4AP- and 0 Mg^{2+}-models. In 4AP model, diazepam did not affect the latency for the development of early-stage epileptiform activity in the neocortex, but in CA3. In the neocortex, unlike in 0Mg^{2+}-model, diazepam failed, both, to produce long-lasting pre-ictal events, and to increase the latency to the first tonic-clonic like ictal event. Early activity evolved into late-stage in two of three slices and the latency for this transition is similar to control group. In CA3, the onset of spike-wave discharges was delayed by diazepam compared to controls.

4AP-induced neocortical late-stage events and spike-wave discharges in CA3 are resistant to standard anti-epileptic drugs (Yonekawa *et al.*, 1995; Bruckner *et al.*, 1999; Bruckner and Heinemann, 2000). In accordance with these findings, diazepam neither suppressed nor altered any characteristics of the neocortical late-stage events and spike-wave discharges in CA3. However, there was a trend towards an increase in the PSDs of frequencies in 10-40 Hz bandwidth of diazepam modulated

SWDs. Power analyses suggest that the ability to see a significant increase was limited by the small sample size.

Future studies examining the effects of diazepam on epileptiform activity induced by different *in vitro* models, how E_{GABA} changes during the progression of epileptiform activity, and how might diazepam affect these changes will further strengthen our understanding about the effects of anti-epileptic drugs on different stages and types of epileptiform activity and provide a scope for developing new multidrug therapies for controlling epilepsy.

4.5 References

1. Avoli, M., Biagini, G. and de Curtis, M. (2006) 'Do interictal spikes sustain seizures and epileptogenesis?', *Epilepsy Curr*, 6(6), pp. 203-7.

2. Avoli, M., D'Antuono, M., Louvel, J., Kohling, R., Biagini, G., Pumain, R., D'Arcangelo, G. and Tancredi, V. (2002) 'Network and pharmacological mechanisms leading to epileptiform synchronization in the limbic system *in vitro*', *Prog Neurobiol*, 68(3), pp. 167-207.

3. Bai, D., Zhu, G., Pennefather, P., Jackson, M.F., MacDonald, J.F. and Orser, B.A. (2001) 'Distinct functional and pharmacological properties of tonic and quantal inhibitory postsynaptic currents mediated by gamma-aminobutyric acid(A) receptors in hippocampal neurons', *Mol Pharmacol*, 59(4), pp. 814-24.

4. Barmashenko, G., Hefft, S., Aertsen, A., Kirschstein, T. and Kohling, R. (2011) 'Positive shifts of the GABAA receptor reversal potential due to altered chloride homeostasis is widespread after status epilepticus', *Epilepsia*, 52(9), pp. 1570-8.

5. Bragdon, A.C., Kojima, H. and Wilson, W.A. (1992) 'Suppression of interictal bursting in hippocampus unleashes seizures in entorhinal cortex: a proepileptic effect of lowering [K+]o and raising [Ca2+]o', *Brain Res*, 590(1-2), pp. 128-35.

6. Brooks-Kayal, A.R., Shumate, M.D., Jin, H., Rikhter, T.Y. and Coulter, D.A. (1998) 'Selective changes in single cell GABA(A) receptor subunit expression and function in temporal lobe epilepsy', *Nat Med*, 4(10), pp. 1166-72.

7. Bruckner, C. and Heinemann, U. (2000) 'Effects of standard anticonvulsant drugs on different patterns of epileptiform discharges induced by 4-aminopyridine in combined entorhinal cortex-hippocampal slices', *Brain Res*, 859(1), pp. 15-20.

8. Bruckner, C., Stenkamp, K., Meierkord, H. and Heinemann, U. (1999) 'Epileptiform discharges induced by combined application of bicuculline and 4-aminopyridine are resistant to standard anticonvulsants in slices of rats', *Neurosci Lett*, 268(3), pp. 163-5.

9. Cammarota, M., Losi, G., Chiavegato, A., Zonta, M. and Carmignoto, G. (2013) 'Fast spiking interneuron control of seizure propagation in a cortical slice model of focal epilepsy', *J Physiol*, 591(4), pp. 807-22.

10. Chauviere, L., Doublet, T., Ghestem, A., Siyoucef, S.S., Wendling, F., Huys, R., Jirsa, V., Bartolomei, F. and Bernard, C. (2012) 'Changes in interictal spike features precede the onset of temporal lobe epilepsy', *Ann Neurol*, 71(6), pp. 805-14.

11. Chin, R.F., Neville, B.G., Peckham, C., Wade, A., Bedford, H. and Scott, R.C. (2008) 'Treatment of community-onset, childhood convulsive status epilepticus: a prospective, population-based study', *Lancet Neurol*, 7(8), pp. 696-703.

12. de Curtis, M. and Avanzini, G. (2001) 'Interictal spikes in focal epileptogenesis', *Prog Neurobiol*, 63(5), pp. 541-67.

13. de Curtis, M., Manfridi, A. and Biella, G. (1998) 'Activity-dependent pH shifts and periodic recurrence of spontaneous interictal spikes in a model of focal epileptogenesis', *J Neurosci*, 18(18), pp. 7543-51.

14. Dreier, J.P. and Heinemann, U. (1990) 'Late low magnesium-induced epileptiform activity in rat entorhinal cortex slices becomes insensitive to the anticonvulsant valproic acid', *Neurosci Lett*, 119(1), pp. 68-70.

15. Dreier, J.P., Zhang, C.L. and Heinemann, U. (1998) 'Phenytoin, phenobarbital, and midazolam fail to stop status epilepticus-like activity induced by low magnesium in rat entorhinal slices, but can prevent its development', *Acta Neurol Scand*, 98(3), pp. 154-60.

16. Dzhala, V.I. and Staley, K.J. (2003) 'Transition from interictal to ictal activity in limbic networks *in vitro*', *J Neurosci*, 23(21), pp. 7873-80.

17. Goodkin, H.P., Joshi, S., Mtchedlishvili, Z., Brar, J. and Kapur, J. (2008) 'Subunit-specific trafficking of GABA(A) receptors during status epilepticus', *J Neurosci*, 28(10), pp. 2527-38.

18. Hamann, M., Rossi, D.J. and Attwell, D. (2002) 'Tonic and spillover inhibition of granule cells control information flow through cerebellar cortex', *Neuron*, 33(4), pp. 625-33.

19. Huberfeld, G., Menendez de la Prida, L., Pallud, J., Cohen, I., Le Van Quyen, M., Adam, C., Clemenceau, S., Baulac, M. and Miles, R. (2011) 'Glutamatergic pre-ictal discharges emerge at the transition to seizure in human epilepsy', *Nat Neurosci*, 14(5), pp. 627-34.

20. Isomura, Y., Sugimoto, M., Fujiwara-Tsukamoto, Y., Yamamoto-Muraki, S., Yamada, J. and Fukuda, A. (2003) 'Synaptically activated Cl- accumulation responsible for depolarizing GABAergic responses in mature hippocampal neurons', *J Neurophysiol*, 90(4), pp. 2752-6.

21. Kaila, K., Lamsa, K., Smirnov, S., Taira, T. and Voipio, J. (1997) 'Long-lasting GABA-mediated depolarization evoked by high-frequency stimulation in pyramidal neurons of rat hippocampal slice is attributable to a network-driven, bicarbonate-dependent K+ transient', *J Neurosci*, 17(20), pp. 7662-72.

22. Kapur, J. (2002) 'Prehospital Treatment of Status Epilepticus with Benzodiazepines Is Effective and Safe', *Epilepsy Curr*, 2(4), pp. 121-124.

23. Kapur, J. and Macdonald, R.L. (1997) 'Rapid seizure-induced reduction of benzodiazepine and Zn2+ sensitivity of hippocampal dentate granule cell GABAA receptors', *J Neurosci*, 17(19), pp. 7532-40.

24. Khalilov, I., Holmes, G.L. and Ben-Ari, Y. (2003) '*In vitro* formation of a secondary epileptogenic mirror focus by interhippocampal propagation of seizures', *Nat Neurosci*, 6(10), pp. 1079-85.

25. Librizzi, L. and de Curtis, M. (2003) 'Epileptiform ictal discharges are prevented by periodic interictal spiking in the olfactory cortex', *Ann Neurol*, 53(3), pp. 382-9.

26. Michelson, H.B. and Wong, R.K. (1991) 'Excitatory synaptic responses mediated by GABAA receptors in the hippocampus', *Science*, 253(5026), pp. 1420-3.

27. Naylor, D.E., Liu, H. and Wasterlain, C.G. (2005) 'Trafficking of GABA(A) receptors, loss of inhibition, and a mechanism for pharmacoresistance in status epilepticus', *J Neurosci*, 25(34), pp. 7724-33.

28. Nusser, Z. and Mody, I. (2002) 'Selective modulation of tonic and phasic inhibitions in dentate gyrus granule cells', *J Neurophysiol*, 87(5), pp. 2624-8.

29. Otis, T.S. and Mody, I. (1992) 'Modulation of decay kinetics and frequency of GABAA receptor-mediated spontaneous inhibitory postsynaptic currents in hippocampal neurons', *Neuroscience*, 49(1), pp. 13-32.

30. Peng, Z., Huang, C.S., Stell, B.M., Mody, I. and Houser, C.R. (2004) 'Altered expression of the delta subunit of the GABAA receptor in a mouse model of temporal lobe epilepsy', *J Neurosci*, 24(39), pp. 8629-39.

31. Perreault, P. and Avoli, M. (1992) '4-aminopyridine-induced epileptiform activity and a GABA-mediated long-lasting depolarization in the rat hippocampus', *J Neurosci*, 12(1), pp. 104-15.

32. Pfeiffer, M., Draguhn, A., Meierkord, H. and Heinemann, U. (1996) 'Effects of gamma-aminobutyric acid (GABA) agonists and GABA uptake inhibitors on pharmacosensitive and pharmacoresistant epileptiform activity *in vitro*', *Br J Pharmacol*, 119(3), pp. 569-77.

33. Rogers, C.J., Twyman, R.E. and Macdonald, R.L. (1994) 'Benzodiazepine and beta-carboline regulation of single GABAA receptor channels of mouse spinal neurones in culture', *J Physiol*, 475(1), pp. 69-82.

34. Schousboe, A., Larsson, O.M., Wood, J.D. and Krogsgaard-Larsen, P. (1983) 'Transport and metabolism of gamma-aminobutyric acid in neurons and glia: implications for epilepsy', *Epilepsia*, 24(5), pp. 531-8.

35. Shorvon, S., Baulac, M., Cross, H., Trinka, E., Walker, M. and TaskForce on Status Epilepticus of the, I.C.f.E.A. (2008) 'The drug treatment of status epilepticus in Europe: consensus document from a workshop at the first London Colloquium on Status Epilepticus', *Epilepsia*, 49(7), pp. 1277-85.

36. Silayeva, L., Deeb, T.Z., Hines, R.M., Kelley, M.R., Munoz, M.B., Lee, H.H., Brandon, N.J., Dunlop, J., Maguire, J., Davies, P.A. and Moss, S.J. (2015) 'KCC2 activity is critical in limiting the onset and severity of status epilepticus', *Proc Natl Acad Sci U S A*, 112(11), pp. 3523-8.

37. Staley, K., Hellier, J.L. and Dudek, F.E. (2005) 'Do interictal spikes drive epileptogenesis?', *Neuroscientist*, 11(4), pp. 272-6.

38. Study, R.E. and Barker, J.L. (1981) 'Diazepam and (--)-pentobarbital: fluctuation analysis reveals different mechanisms for potentiation of gamma-aminobutyric acid responses in cultured central neurons', *Proc Natl Acad Sci U S A*, 78(11), pp. 7180-4.

39. Swartzwelder, H.S., Lewis, D.V., Anderson, W.W. and Wilson, W.A. (1987) 'Seizure-like events in brain slices: suppression by interictal activity', *Brain Res*, 410(2), pp. 362-6.

40. Terunuma, M., Xu, J., Vithlani, M., Sieghart, W., Kittler, J., Pangalos, M., Haydon, P.G., Coulter, D.A. and Moss, S.J. (2008) 'Deficits in phosphorylation of GABA(A) receptors by intimately associated protein kinase C activity underlie compromised synaptic inhibition during status epilepticus', *J Neurosci*, 28(2), pp. 376-84.

41. Treiman, D.M., Meyers, P.D., Walton, N.Y., Collins, J.F., Colling, C., Rowan, A.J., Handforth, A., Faught, E., Calabrese, V.P., Uthman, B.M., Ramsay, R.E. and Mamdani, M.B. (1998) 'A comparison of four treatments for generalized convulsive status epilepticus. Veterans Affairs Status Epilepticus Cooperative Study Group', *N Engl J Med*, 339(12), pp. 792-8.

42. Trevelyan, A.J., Sussillo, D., Watson, B.O. and Yuste, R. (2006) 'Modular propagation of epileptiform activity: evidence for an inhibitory veto in neocortex', *J Neurosci*, 26(48), pp. 12447-55.

43. Trevelyan, A.J., Sussillo, D. and Yuste, R. (2007) 'Feedforward inhibition contributes to the control of epileptiform propagation speed', *J Neurosci*, 27(13), pp. 3383-7.

44. Voskuyl, R.A. and Albus, H. (1985) 'Spontaneous epileptiform discharges in hippocampal slices induced by 4-aminopyridine', *Brain Res*, 342(1), pp. 54-66.

45. Walton, N.Y. and Treiman, D.M. (1988) 'Response of status epilepticus induced by lithium and pilocarpine to treatment with diazepam', *Exp Neurol*, 101(2), pp. 267-75.

46. Watts, A.E. and Jefferys, J.G. (1993) 'Effects of carbamazepine and baclofen on 4-aminopyridine-induced epileptic activity in rat hippocampal slices', *Br J Pharmacol*, 108(3), pp. 819-23.

47. White, A., Williams, P.A., Hellier, J.L., Clark, S., Dudek, F.E. and Staley, K.J. (2010) 'EEG spike activity precedes epilepsy after kainate-induced status epilepticus', *Epilepsia*, 51(3), pp. 371-83.

48. Yonekawa, W.D., Kapetanovic, I.M. and Kupferberg, H.J. (1995) 'The effects of anticonvulsant agents on 4-aminopyridine induced epileptiform activity in rat hippocampus *in vitro*', *Epilepsy Res*, 20(2), pp. 137-50.

49. Zhang, C.L., Dreier, J.P. and Heinemann, U. (1995) 'Paroxysmal epileptiform discharges in temporal lobe slices after prolonged exposure to low magnesium are resistant to clinically used anticonvulsants', *Epilepsy Res*, 20(2), pp. 105-11.

Chapter 5 The effects of baclofen on evolving epileptiform activity in the cortical networks

5.1 Introduction

GABA is the major inhibitory neurotransmitter in the brain acting at ionotropic GABA$_A$- and metabotropic GABA$_B$-receptors. Since many years, the role of GABA$_A$-receptors (GABA$_A$Rs) mediated fast inhibition has been extensively investigated in various *in vitro* and *in vivo* models of epilepsy. However, the significant role of GABA$_B$-receptor (GABA$_B$R) mediated slow inhibition in physiological cortical function (Ulrich and Huguenard, 1996; Sanchez-Vives and McCormick, 2000; Perez-Garci *et al.*, 2006; Rigas and Castro-Alamancos, 2007), and pathological states such as epilepsy, has only recently been recognized (Hosford *et al.*, 1992; Empson and Jefferys, 1993; Sanchez-Vives and McCormick, 1997; Prosser *et al.*, 2001).

GABA$_B$Rs are G-protein coupled receptors that occur as heterodimers made up of GABA$_{B1a/b}$ and GABA$_{B2}$ subunits. It is necessary to have both the subunits to form functional GABA$_B$Rs (Galvez *et al.*, 2001; Robbins *et al.*, 2001). GABA$_{B1a}$-GABA$_{B2}$ and GABA$_{B1b}$-GABA$_{B2}$ heterodimers are localised at presynaptic terminals and postsynaptic elements, respectively, at both excitatory and inhibitory synapses (Lopez-Bendito *et al.*, 2002; Lopez-Bendito *et al.*, 2004). At postsynaptic sites, activated GABA$_B$Rs mediate hyperpolarisation by activating G-protein coupled-potassium channels, and/or modulate the generation of dendritic calcium spikes by inhibiting calcium channels (Gahwiler and Brown, 1985; Inoue *et al.*, 1985; Sodickson and Bean, 1996; Perez-Garci *et al.*, 2006). Excess of synaptically released GABA spills over to peri- and extra-synaptic regions to activate GABA$_B$Rs on the postsynaptic membrane. Spill-over GABA also mediates heterosynaptic depression at neighbouring excitatory synapses by activating presynaptic GABA$_B$Rs on excitatory neurons (Isaacson *et al.*, 1993). At inhibitory synapses, GABA reduces the neurotransmitter release by activating presynaptic GABA$_B$ autoreceptors (Davies *et al.*, 1990). A requirement for the activation of GABA$_B$Rs is the accumulation of sufficient amounts of synaptically-released GABA, and such conditions arise during synchronous network activity during network oscillations (Scanziani, 2000).

GABA$_B$Rs modulate the cortical slow network oscillations, comprising UP and Down states. GABA$_B$Rs activation was shown to contribute to the termination of Up-states (Mann *et al.*, 2009). Modulatory actions of GABA$_B$Rs on the slow oscillations can be attributed to their slow kinetics and the mediated longer lasting inhibitory potentials. In thalamocortical–thalamic reticular nuclear (nRt) and nRt-nRt circuits, reciprocal and recurrent inhibition mediated by GABA$_B$Rs underlies the generation of rebound low-threshold calcium spikes in both nRt and thalamocortical (TC) neurons. These bursts of action potentials underlie the physiological thalamocortical rhythm (Ulrich and Huguenard, 1996). GABA$_B$Rs mediated longer-lasting inhibitory postsynaptic potentials in TC neurons are generated by intense activity of perigeniculate and nRt cells triggering pathological rhythmic slow oscillations during generalised absence seizures (Crunelli and Leresche, 1991; Sanchez-Vives and McCormick, 1997).

The causative role of GABA$_B$Rs in inducing absence seizures was demonstrated in lethargic mice, an animal model of absence seizures (Hosford *et al.*, 1992). Likewise, in rats with genetic absence seizures, the epileptic activity was further aggravated by administering GABA$_B$R agonist and suppressed by GABA$_B$R antagonist (Liu *et al.*, 1992; Vergnes *et al.*, 1997). However, unlike in absence seizures, GABA$_B$R antagonists and positive modulators facilitate audiogenic tonic seizures (Vergnes *et al.*, 1997) and suppressed tonic-clonic seizures (Mares, 2012). Moreover, in mice, knocking out GABA$_{B1}$R subunits rendered all the pre- and post-synaptic GABA$_B$Rs non-functional, and although these mice appeared normal at birth, within four post-natal weeks they developed generalised convulsive epilepsy followed by premature death (Prosser *et al.*, 2001).

Research groups have carried out *in vitro* studies in the CA3 subfield of the hippocampus and entorhinal cortex (EC) to evaluate the effects of baclofen, a GABA$_B$R agonist, on epileptiform activity induced by zero-magnesium ACSF (0 Mg^{2+}-ACSF) (Swartzwelder *et al.*, 1987; Jones, 1989). Clinically, baclofen is used as an anti-spastic agent and muscle relaxant. Following wash-out of magnesium ions, tonic-clonic like ictal events (IE) developed in CA3 and EC and the activity later transitioned into recurrent short-duration events that Swartzwelder *et al.,* referred to as interictal-like spikes (Swartzwelder *et al.*, 1987). For the sake of consistency in this thesis, I refer to

these latter events to as late-stage events (LSEs). When the hippocampal slices were superfused with 0 Mg^{2+}-ACSF supplemented with baclofen right from the beginning of the experiment, the hippocampal neuronal network started discharging tonic-clonic like events and this activity continued for the duration of the recordings, and addition of baclofen during the LSEs transformed the activity into tonic-clonic like discharges (Swartzwelder *et al.*, 1987). In neocortex, the rate of LSEs was reduced by brief application of baclofen and this reduction in network activity was due to its hyperpolarising effect (Horne *et al.*, 1986). It was also reported that baclofen abolished the spontaneous and stimulation evoked ictal events in entorhinal cortex (Jones, 1989).

I showed in the earlier chapter (chapter 3) that different regions of the brain show heterogeneous responses to the same pathological insults, that is, hippocampal, entorhinal cortex, and the neocortical networks differ in their sensitivity to pro- and anti-epileptic agents and hence differ in their activity patterns. I now show here that challenging brain slices with zero-magnesium ACSF (0 Mg^{2+}-ACSF) supplemented with baclofen, a GABA$_B$-receptors agonist, induces tonic-clonic like ictal events in neocortex and locks the activity pattern in this stage for the duration of recording, but fails to develop any activity in CA3. Washing out baclofen with 0 Mg^{2+}-ACSF transformed the activity pattern in both the regions. Interestingly, in neocortex, adding baclofen during 0 Mg^{2+}-ACSF induced late-stage events reversibly reverted activity to tonic-clonic like ictal events. In CA3, baclofen suppressed 0 Mg^{2+}-induced spike-wave discharges. These results show protective effects of baclofen that can be translated to control certain types of clinical epilepsies.

5.2 Materials and methods

5.2.1 *Slice preparation and electrophysiology*

For all the experiments described below, combined neocortical-hippocampal horizontal slices were used, that were prepared and stored as described in *slice preparation method 2* (chapter 2, sub-heading 2.4.2). Local field potentials (LFPs) were recorded simultaneously from both the pyramidal cell layer of CA3 subfield of hippocampus and infragranular layers of neocortex (Figure 5.1). The recording setup and the equipment used were as described in chapter 2 (sub-heading 2.5.1).
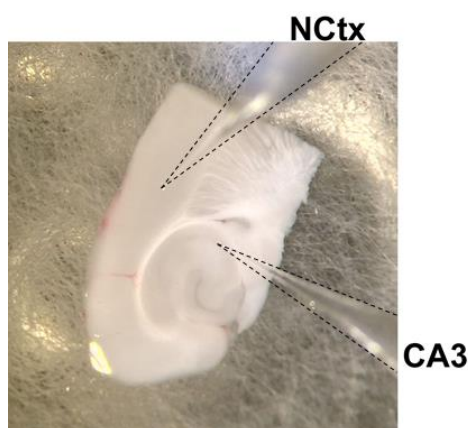
Figure 5.1 Recording setup showing a slice in the interface recording chamber with electrodes placed in the pyramidal cell layer of CA3 (bottom-right) and infragranular layers of neocortex (NCtx, top-right).

5.2.2 *Protocols and drugs*

The effects of $GABA_B$ receptors activation on the evolution of epileptiform activity in neocortex and CA3 subfield of hippocampus was studied using (*RS*)-baclofen and zero-magnesium model (0 Mg^{2+} model). From here on, (*RS*)-baclofen will be mentioned either as 'baclofen' or 'Bac'. The protocol is as follows: brain slices were placed in the interface recording chamber, which were perfused initially with ACSF. Electrodes were placed in the regions of interest and the baseline activity was recorded in ACSF. After 10-15 minutes, the perfusate was switched from ACSF to epileptogenic medium (0Mg^{2+}-ACSF). Measures taken from this set of experiments were considered as controls. For the treatment group, after baseline recordings, the solutions were switched to 0 Mg^{2+}-ACSF containing baclofen (0 Mg^{2+}/Bac-ACSF). To study the effects of baclofen on late-stage events, slices were superfused with 0 Mg^{2+}-ACSF until the

development of late-stage recurrent discharges, and only at this stage was the $0 \, Mg^{2+}$-ACSF supplemented with baclofen. From here on, $0 \, Mg^{2+}$-ACSF with baclofen will be represented as '$0 \, Mg^{2+}$/Bac-ACSF'.

(RS)-Baclofen was purchased from Tocris (U.K). Baclofen stock solution (100 mM) was prepared and stored in -20 $^{\circ}$C. Baclofen at 10μM was effective in producing outward hyperpolarising membrane current (Gahwiler and Brown, 1985). Hence, I chose to use 10 μM of baclofen as final concentration, unless otherwise stated.

5.2.3 *Data analysis*

Data was analysed as described in chapter 2 (sub-heading 2.7). Additionally, estimates of power-spectral density (PSD) for different frequency bandwidths was analysed on hum-removed traces each of 25 seconds length. It was calculated using 'pwelch', a built-in function in Matlab 2015b for frequency ranges of 1-10 Hz, 10-40 Hz, and 60-100 Hz (for details see Chapter 4, section 4.2.4). PSD ratios were calculated for each frequency bandwidth separately, by measuring PSDs for events in baclofen ($0Mg^{2+}$+Bac) and dividing it by PSDs measured for events in control ($0 \, Mg^{2+}$).

5.2.4 *Terminology*

I reserve specific nomenclature for particular type of epileptiform events in these recordings. Baclofen-induced tonic-clonic like ictal event is used to describe the tonic-clonic like ictal events developed in the neocortex after adding baclofen to the perfusate during $0 \, Mg^{2+}$-induced late-stage events.

5.3 Results

5.3.1 *GABA$_B$R activation delays epileptiform evolution in vitro*

In neocortex, GABA$_B$R activation did not alter the pattern early evolution of epileptiform activity in 0 Mg^{2+} model, but significantly slowed this process (Figure 5.2 A, B – black trace; Figure 5.3 A, Table 5.1). In all four experiments, there were repeated tonic-clonic like ictal events (IE) for the entire duration of the recordings. The latency to the first event, and the intervals between all successive events were increased (Figure 5.3 A; Table 5.1). The rate of IEs in 0 Mg^{2+}/Bac-ACSF continued to progressively increase for the duration of the recordings (Figure 5.3 B; first 30 mins, 0.21 ± 0.03 min^{-1}, n = 4; 30-60 mins, 0.37 ± 0.03 min^{-1}, n = 4; 60-90 mins, 0.46 ± 0.07 min^{-1}, n = 3). The duration of these events was shorter, and every event had episodes of sustained rhythmic bursts like the tonic-clonic discharges as observed in zero-magnesium ACSF (Figure 5.3 C, durations of IE: 0 Mg^{2+}, 53.56 ± 17.2 s, n = 5; 0 Mg^{2+}/Bac, 26.57 ± 1.47 s, n = 4; unpaired Student's t-test, p > 0.05). These neocortical tonic-clonic events showed a prominent multi-unit activity, as evidenced by the large deflections in the 300-3000 Hz band-pass filtered signal (Figure 5.2 Cii), whereas, multi-unit activity was not seen in CA3 (Figure 5.2 Dii). In addition to the marked slowing of the evolution of neocortical activity, in none of the experiments did the activity show a second transition into late-stage events (Figure 5.2 B).
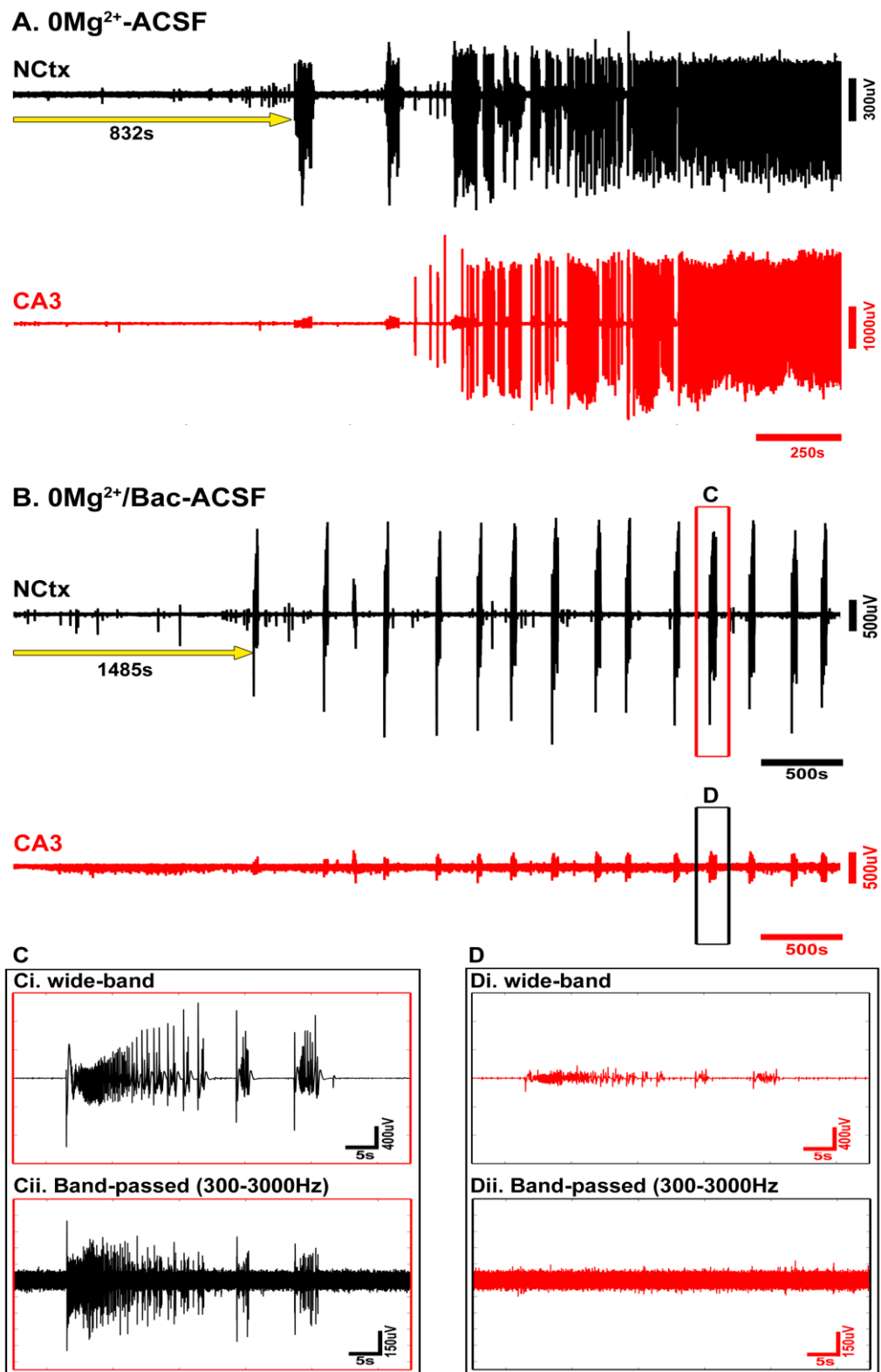
Figure 5.2 Effect of GABA$_B$R activation by baclofen from the start of washing-out Mg^{2+} ions from ACSF. Simultaneous recordings from neocortex and CA3. Washing in 0 Mg^{2+}-ACSF (A), and 0Mg^{2+}/Bac-ACSF (B) at start of the trace. Note the presence of multi-unit activity in the high-pass filtered trace of an ictal event in neocortex (Cii), but the almost complete absence of multi-unit activity in the CA3 recording (Dii). Note: traces in panels A and B were plotted on different time scales
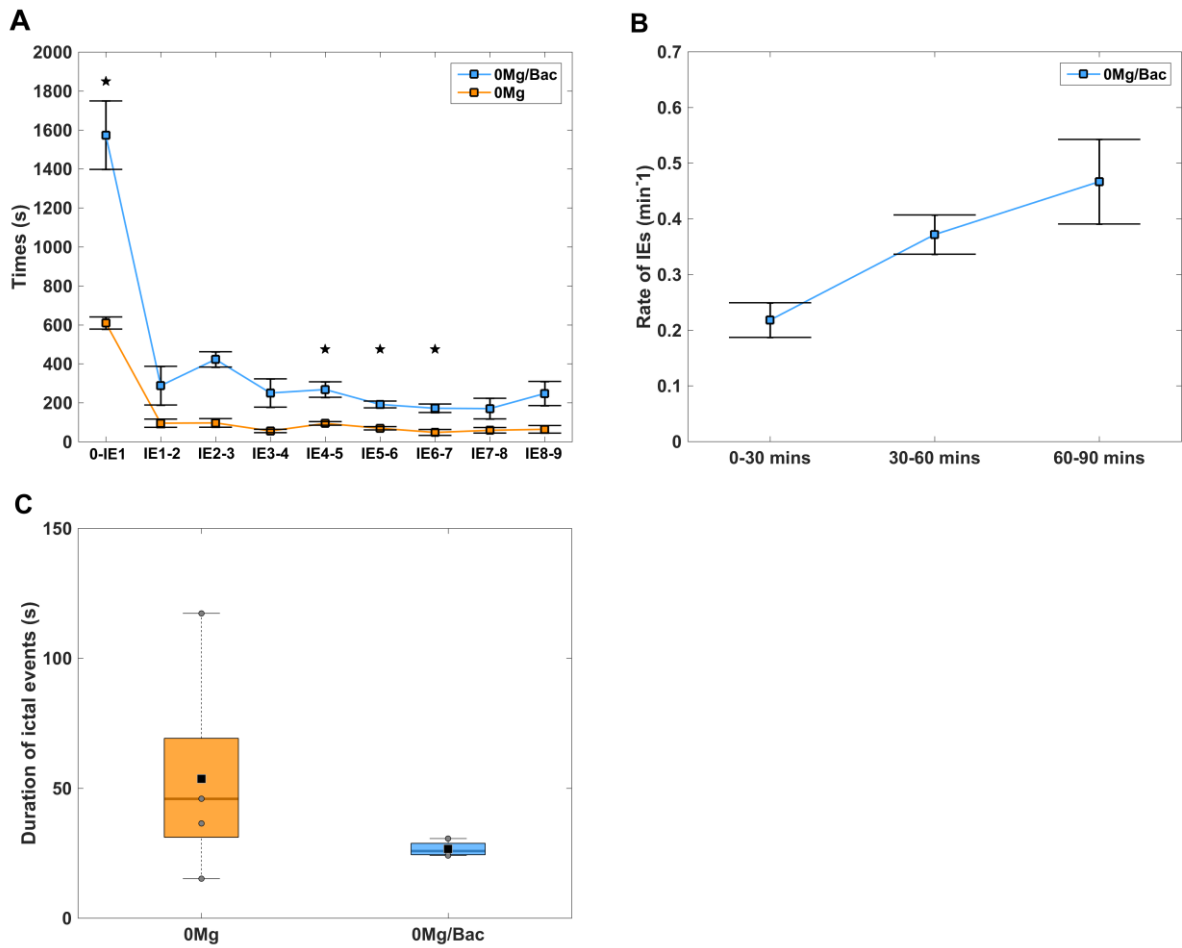
Figure 5.3 A. The early evolution of epileptiform activity had similar features in both 0 Mg^{2+}-ACSF and 0 Mg^{2+}/Bac-ACSF: in both, there was a steep decline in the latency for the occurrence of subsequent ictal events. Unpaired Student's t-test, *p-values less than or equal to Bonferroni corrected critical value (α = 0.005). See table 5.1 for mean ± s.e.m. B. The rate of IE was progressively increasing in 0 Mg^{2+}/Bac-ACSF. C. Duration of IEs was reduced in 0 Mg^{2+}/Bac-ACSF.

| Inter event intervals (s) | Neocortex | | p-values |
	0 Mg^{2+} (n)	0 Mg^{2+}/Bac (n)	^(α = 0.005)
0-IE1	609.24 ± 31.13 (5)	1573.12 ± 175.65 (4)	*0.0005
IE1-IE2	95.04 ± 21.13 (5)	287.78 ± 99.28 (4)	0.07
IE2-IE3	96.57 ± 22.1 (5)	422.53 ± 39.26 (4)	0.06
IE3-IE4	55.13 ± 8.59 (5)	250.03 ± 72.56 (4)	0.01
IE4-IE5	94 ± 9.26 (5)	267.7 ± 39.73 (4)	*0.002
IE5-IE6	69.06 ± 8.48 (4)	191.21 ± 17.41 (4)	*0.0007
IE6-IE7	47.69 ± 15.15 (4)	171.73 ± 21.72 (4)	*0.003
IE7-IE8	58.69 ± 14.2 (4)	170.07 ± 52.92 (4)	0.08
IE8-IE9	63.69 ± 19.54 (4)	247.49 ± 61.95 (4)	0.03

Table 5.1 Times taken for the development of first tonic-clonic like ictal event (IE) and the subsequent inter-event intervals in neocortex in 0 Mg^{2+}-ACSF and 0 Mg^{2+}/Bac-ACSF. *p-values less than or equal to ^Bonferroni corrected critical value (α).

5.3.2 *Different patterns of epileptiform activity in neocortex and CA3 after washing out baclofen*

After washing out baclofen for nearly 30-40 minutes with 0 Mg^{2+}-ACSF, population discharges started to develop in CA3 (Figure 5.4 B). One notable feature of this activity, which distinguished it from previous recordings (no baclofen, chapter 3), was that in CA3 region, along with single large spike-and-wave discharges (SWD, type 1) lasting up to 1.26 ± 0.11 s (n = 3) (Figure 5.5 Bi, Bii), an additional type of synchronous population discharges with polyspike waveforms lasting up to 3.41 ± 0.35

s (n = 3) were observed (type 2; figure 5.6 Bi, Bii). In neocortex, activity showed a transition to late-stage events (Figure 5.4 A) that were occurring regularly and lasted up to 3.29 ± 0.23 s (n = 3). In contrast to the earlier 0 Mg^{2+}/Bac-ACSF induced IEs, late-stage events that developed after washing out baclofen with 0 Mg^{2+}-ACSF occurred with reduced amplitude (Figure 5.4 A, 5.5 A, 5.6 A).
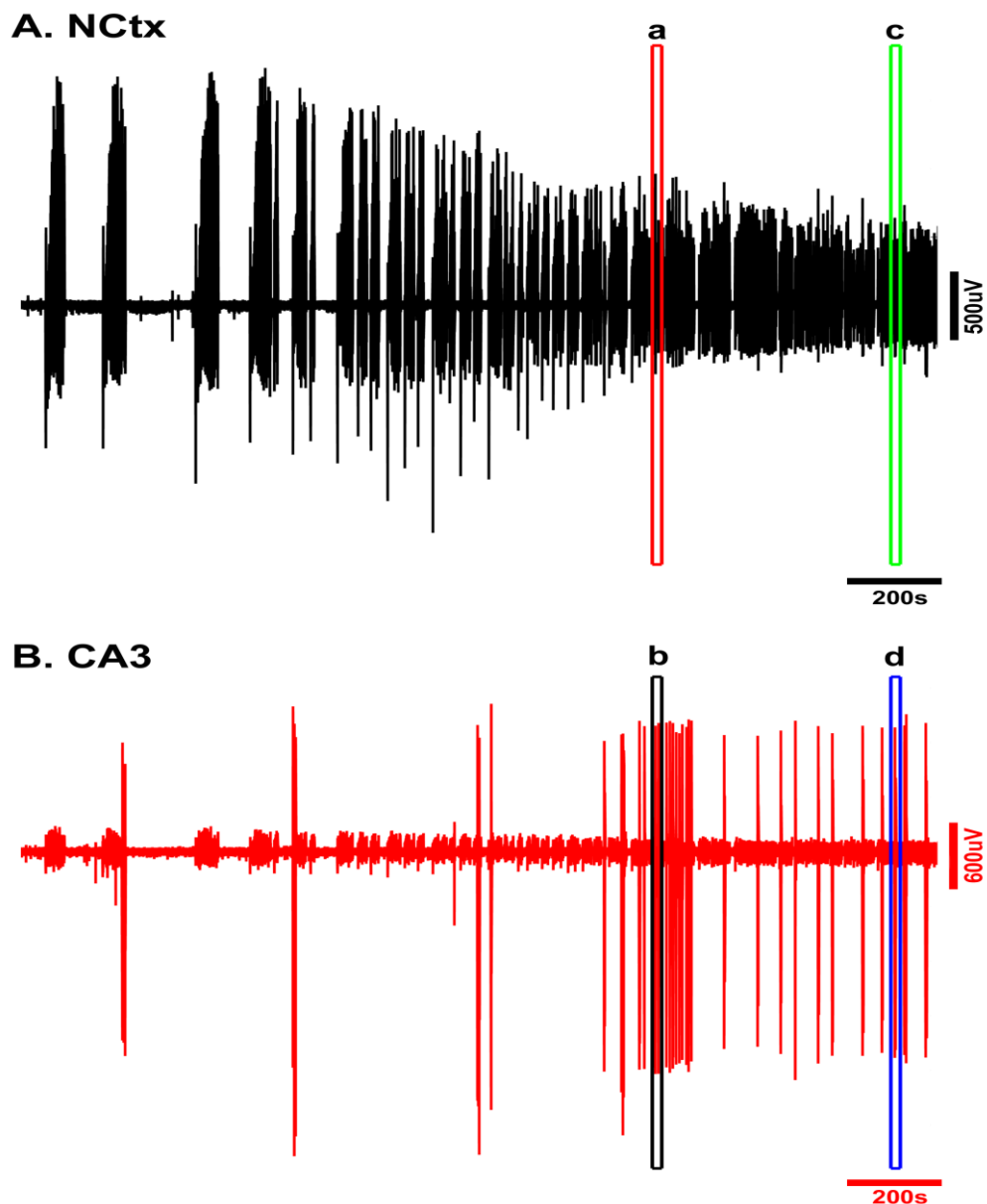
Figure 5.4 Further evolution of epileptiform activity after washout of Baclofen. This figure only shows the recordings after the washout, and for space reasons, do not show the prior 3768 s of recording in 0 Mg^{2+} with baclofen. Two different spiking patterns were noted: spike-wave discharges (black box – expanded in Figure 5.5b) and polyspike discharges (blue box – expanded in Figure 5.5d).
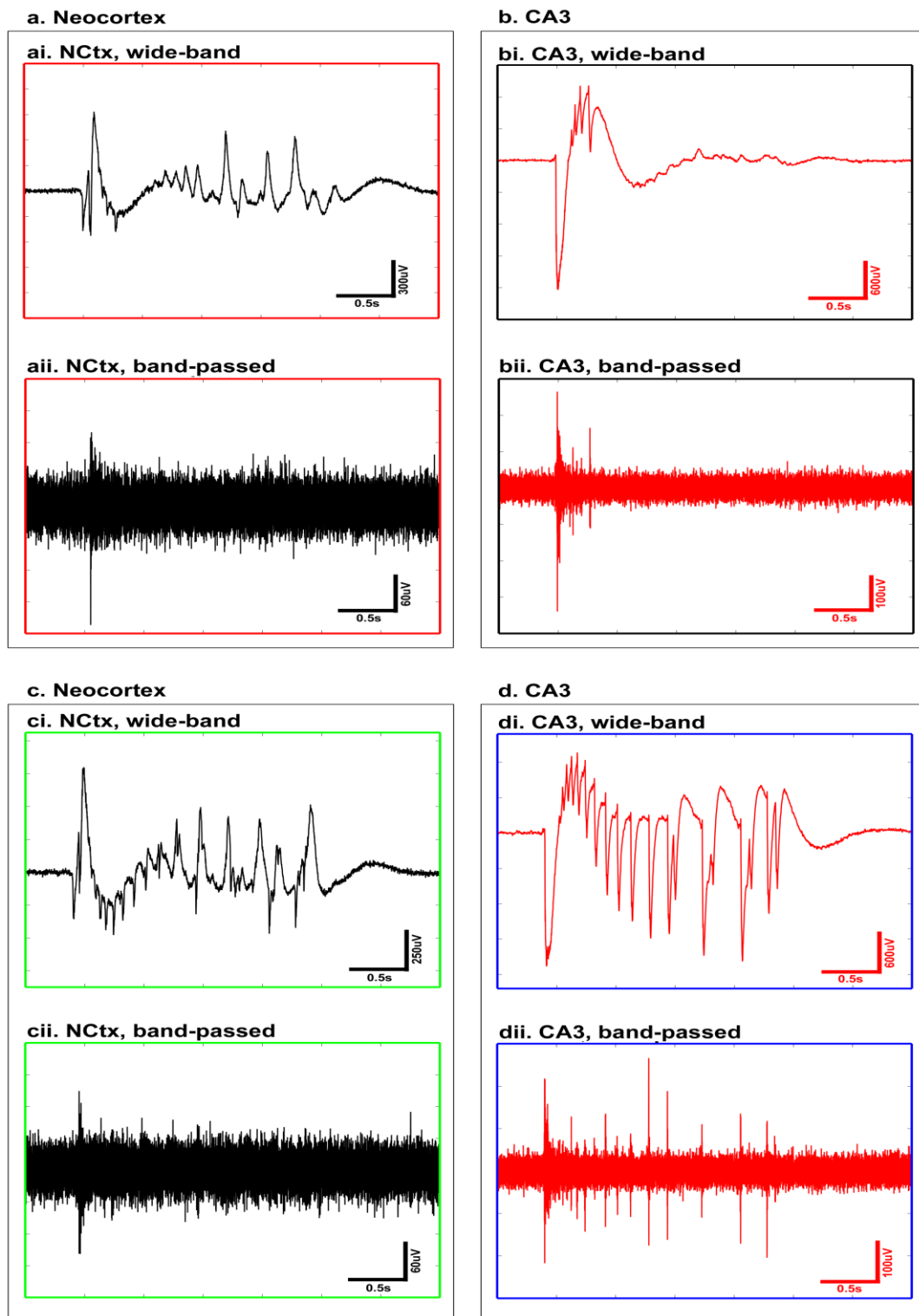
Figure 5.5 Examples of neocortical LSE (panels a, c), type 1 discharge (spike and wave discharge; panel b), and type 2 discharge (polyspike; panel d) that occurred in CA3 after washing out Baclofen with 0 Mg^{2+}-ACSF (expanded from Figure 5.4). Wide-band is raw data, band-passed is filtered for 300-3000 Hz.

5.3.3 *Transformation of late-stage epileptiform activity to tonic-clonic like ictal events in neocortex by baclofen*

In the previous section, I showed that the late-stage activity failed to develop in neocortex if the slices were bathed in baclofen from the start of the perfusion with 0 Mg^{2+}-ACSF. This raised the question of whether the late-stage activity could be reversed by baclofen, after they have already developed (Figure 5.6, aqua bar – far left, box b). Addition of baclofen transformed the late-stage activity pattern in neocortex (Figure 5.6, yellow bar). In all 7 recordings, the late-stage activity reverted to a pattern of intermittent ictal events, tonic-clonic like patterns (Figure 5.6, box c). These baclofen-induced tonic-clonic like ictal events (Bac-IEs), when compared to the early $0Mg^{2+}$-IEs measured in the same slice, were significantly shorter (Figure 5.7 A; 0 Mg^{2+}-IE, 60.51 ± 7.12 s, n = 7; Bac-IE, 29.86 ± 10.8 s, n = 7; normalised percentage change, 47.62 ± 13.07 %, paired Student's t-test, $p < 0.05$), and, had lower and higher power spectral densities for frequencies in 1-15 Hz and 15-40 Hz bandwidths, respectively (Figure 5.7 B; Table 5.2*). After washing out baclofen with 0 Mg^{2+}-ACSF, recurrent late-stage events reappeared (Figure 5.6, aqua bar – far right, box d).
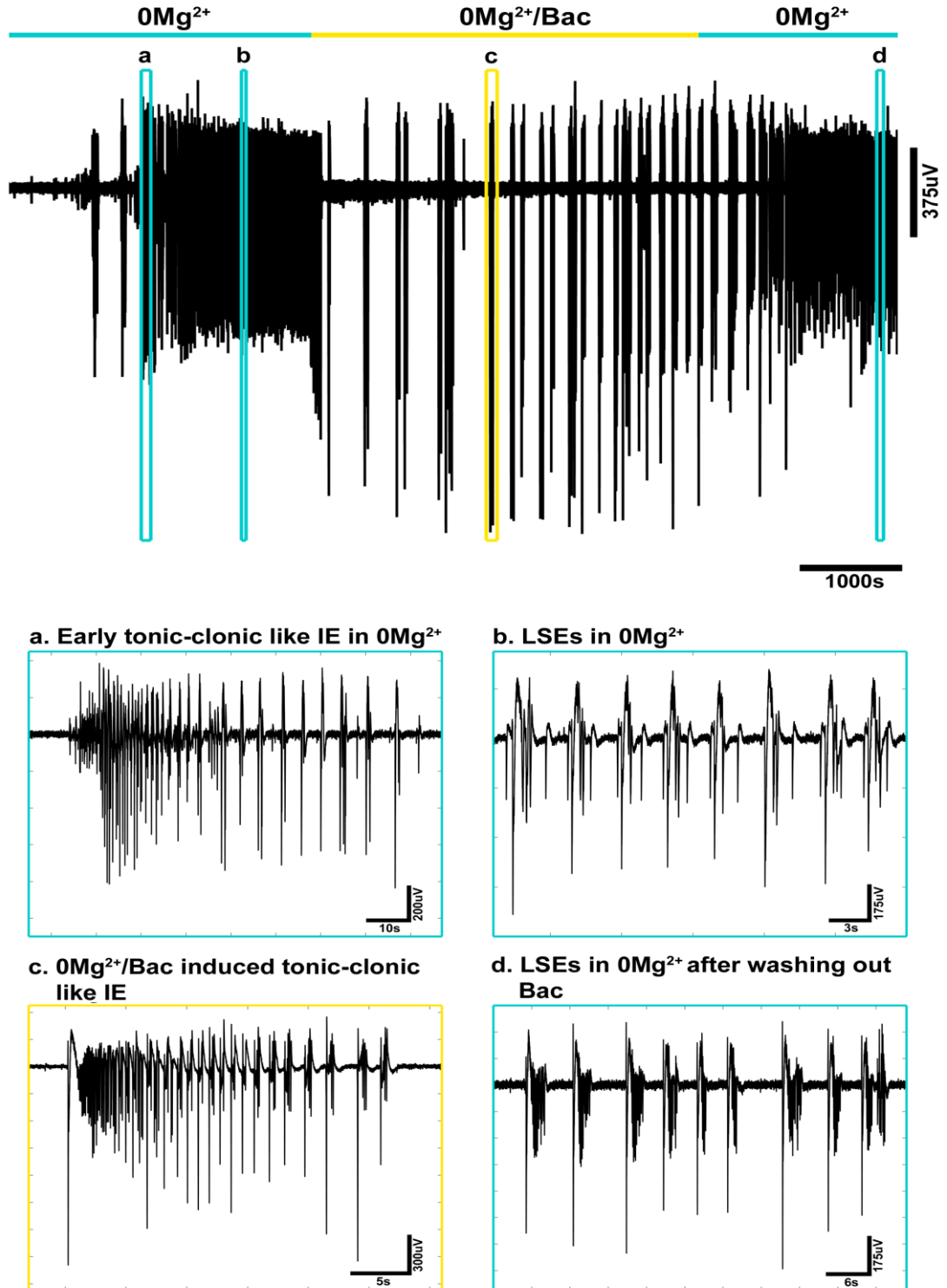
Figure 5.6 Addition of baclofen to 0 Mg^{2+}-ACSF during the late-stage (yellow bar) transformed the activity pattern in the neocortex. Late recurrent discharges in the neocortex (box b) were replaced with 0 Mg^{2+}/Bac-ACSF induced tonic-clonic like ictal events (box c). Late recurrent discharges reappeared after washing-out baclofen (to 0 Mg^{2+}-ACSF – aqua bar, far right; box d).
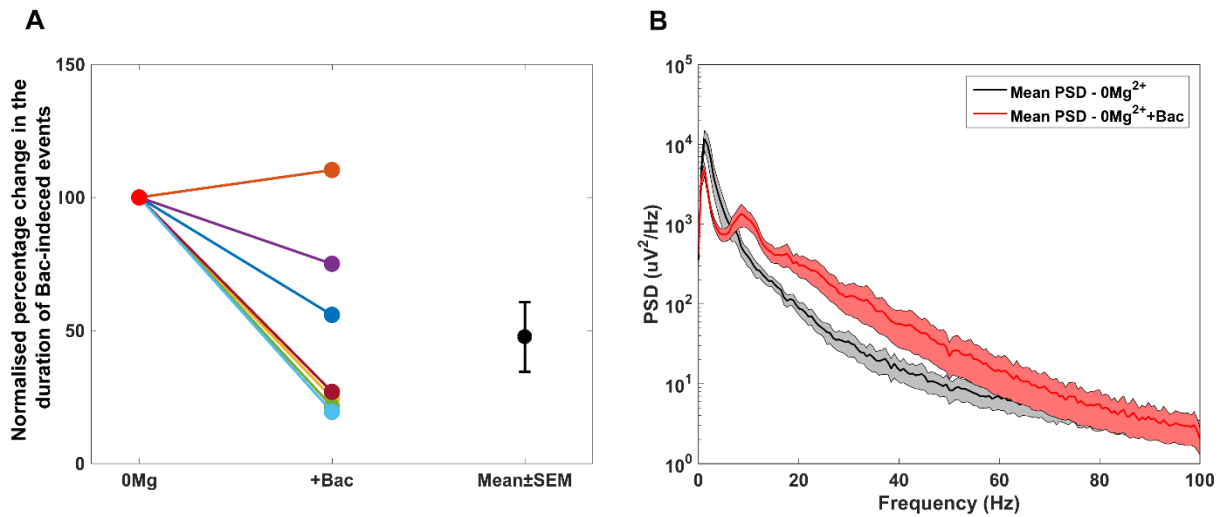
Figure 5.7 A. Baclofen-induced tonic-clonic like ictal events were shorter compared to the ictal events developed prior in $0Mg^{2+}$-ACSF. B. Baclofen-induced tonic-clonic like ictal events had lower and higher PSDs for frequencies in LF and HF bands, respectively (see Table 5.2).

Frequency bandwidths	$0Mg^{2+}$-IE ($\mu V^2/Hz$)	Bac-IE ($\mu V^2/Hz$)	Norm. % change	p=
1-15 Hz	2017.1 ± 691.4	1164.9 ± 200.2	57.8 ± 9.9	0.008
15-40 Hz	55.7 ± 11.0	197.9 ± 66.5	354.7 ± 119.2	0.084

Table 5.2 Power-spectral density measures for early $0 Mg^{2+}$-induced IEs and baclofen-induced IEs (Bac-IE) in same slices (n = 7). p-values were calculated using paired Student's t-test.

5.3.4 *GABA$_B$R activation suppressed SWDs in CA3*

In CA3, baclofen suppressed the on-going $0 Mg^{2+}$-ACSF induced SWDs (figure 5.8, yellow bar). Few discharges appeared in $0 Mg^{2+}$/Bac-ACSF that had different pattern, spike followed by bursts (spike-burst discharges) (figure 5.8, box b). In six slices, the effects of washing out baclofen was examined. Slices showed different responses; there was no activity in two slices, spike-burst discharges appeared in two

slices (Figure 5.8, box c), and tonic-clonic like discharges developed in another two slices (Figure 5.8, box d).
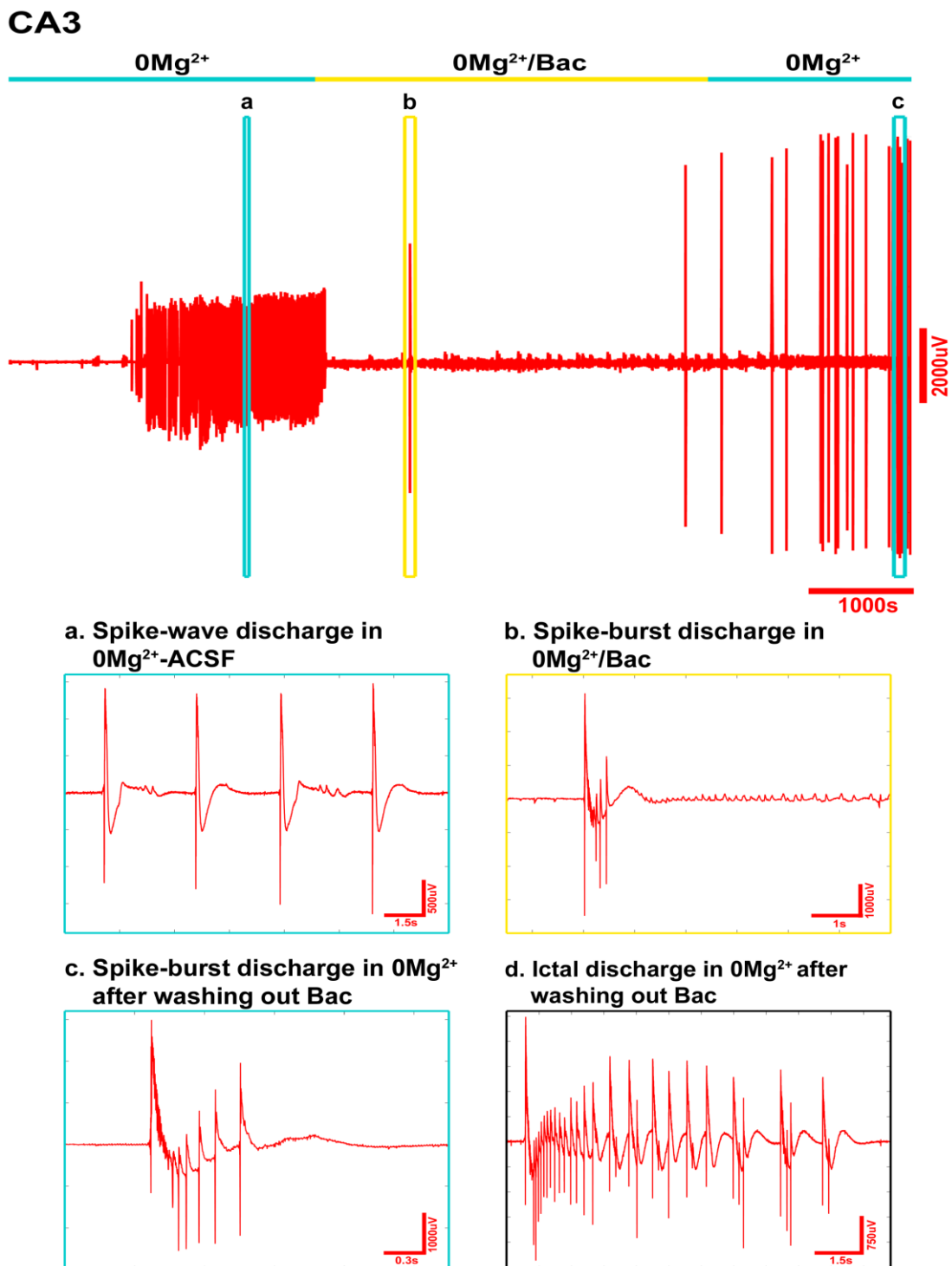
Figure 5.8 Addition of baclofen to 0 Mg^{2+}-ACSF suppressed (yellow bar) 0 Mg^{2+}-ACSF induced SWDs (aqua bar, far left), and there were few spike-bursts like discharges (yellow box, box b) in 0 Mg^{2+}/Bac-ACSF. Activity reappeared after washing-out baclofen with 0 Mg^{2+}-ACSF (aqua bar, far right; box c, d). Note, trace illustrated in box d is taken from a different experiment.

5.3.5 *Baclofen-induced ictal events were insensitive to diazepam*

In earlier sections, I showed that baclofen suppressed 0 Mg^{2+}-ACSF induced SWDs in CA3 and transformed LSEs into tonic-clonic like events (Bac-IEs) in the neocortex. It is not known whether enhancing the activity of $GABA_A$Rs at this stage will have any effect on Bac-IEs in neocortex. In two slices examined, Bac-IEs were neither suppressed nor aggravated by diazepam (Figure 5.9, red, yellow and green bars; Figure 5.10 A, B, C), but all the activity was abolished by a NMDA receptor antagonist, D-AP5 (Figure 5.9, orange bar; Figure 5.10 D).
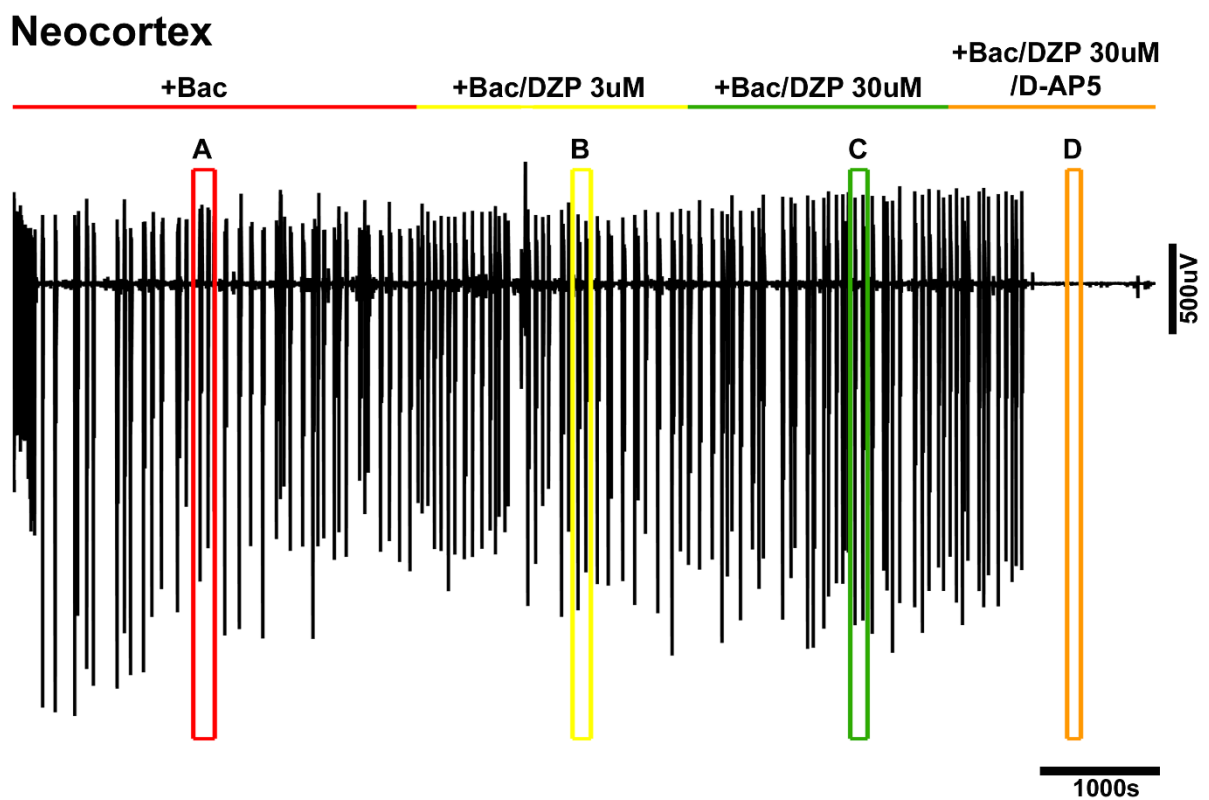
Figure 5.9 Bac-IEs (red bar) were insensitive to DZP at both 3 µM (yellow bar) 30 µM (green bar) concentrations. These events were abolished after blocking NMDARs with D-AP5 (orange bar). The boxed areas are shown expanded in Figure 5.10.

Neocortex

A. +Bac
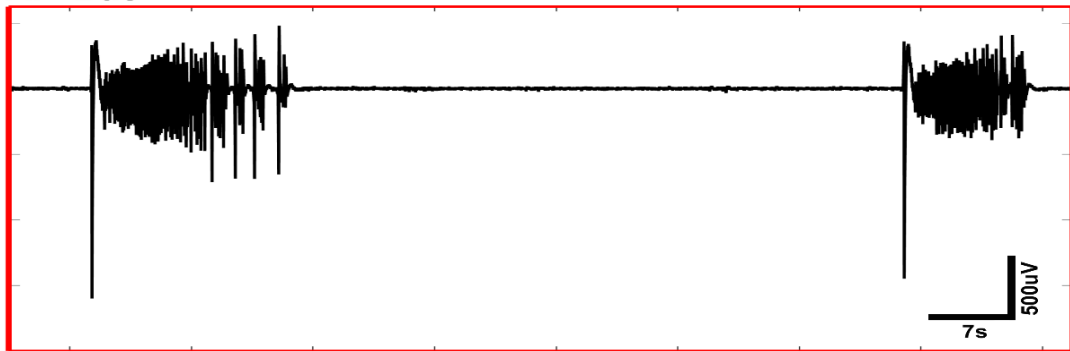
B. +Bac/DZP 3uM
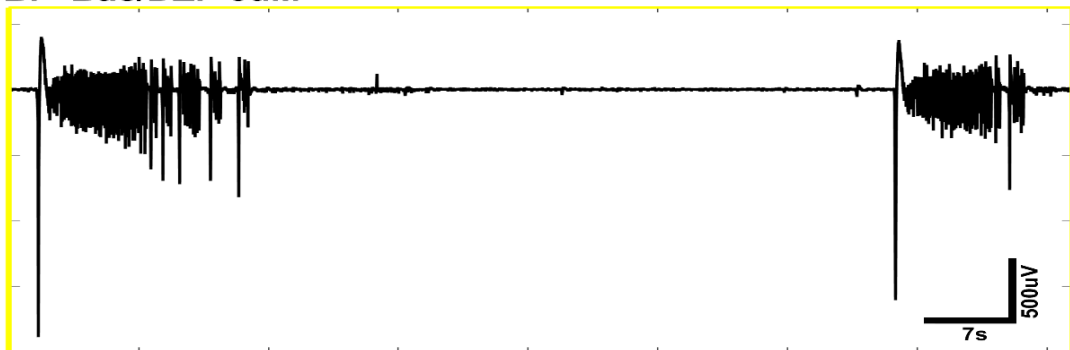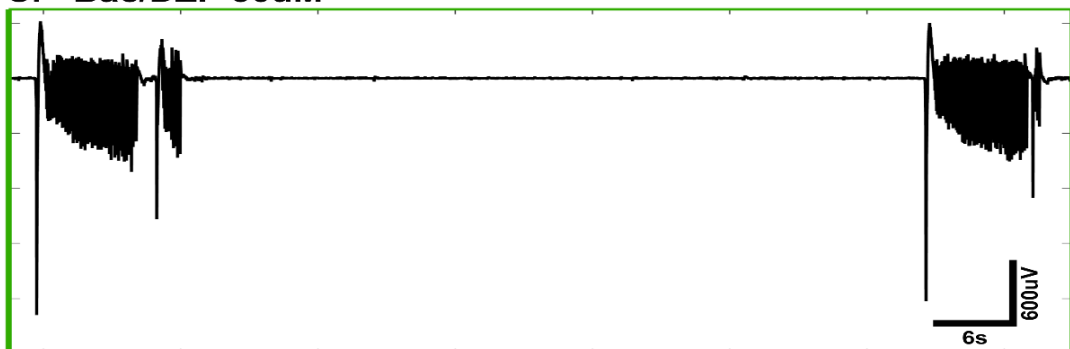
C. +Bac/DZP 30uM

D. +Bac/DZP 30uM/D-AP5
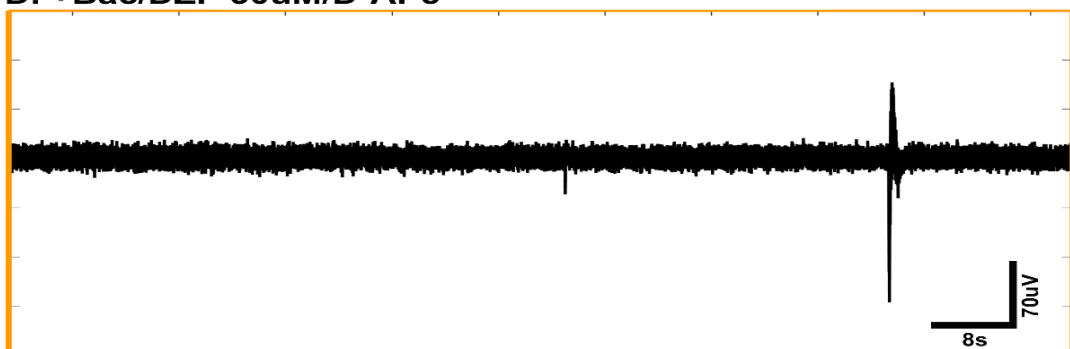
Figure 5.10 Bac-IEs (A) were insensitive to diazepam (B and C), but are abolished by NMDAR antagonist (D). Expanded from Figure 5.10.

110

5.4 Discussion

These results show the differential epileptic responses in hippocampal and neocortical networks to baclofen. Neocortical and hippocampal networks have different cellular connectivity patterns although they are both made up of similar inhibitory and excitatory components.

When naïve tissues were acutely challenged with 0 Mg^{2+}/baclofen-ACSF, the development of the early tonic-clonic like ictal events (IEs) was delayed in the neocortex. Once the IEs were initiated in the neocortex, they continued to appear for the duration of the recordings without showing the second transition to late-stage events. This pattern of activity was earlier reported to occur in CA3, but not in the neocortex (Swartzwelder *et al.*, 1987). In contrast, current results show that the presence of baclofen in 0 Mg^{2+}-ACSF from the beginning of the experiments prevented the development of any type of epileptiform discharges in the hippocampal CA3 region. Furthermore, following the wash-out of baclofen, SWDs of varied patterns and LSEs were developed in CA3 and neocortex, respectively. These results suggest the two cortical networks examined have different mechanisms for the development of epileptiform activity and baclofen interferes these mechanisms preventing and delaying their early development in CA3 and neocortex, respectively. It needs to be further tested whether baclofen can abolish the on-going 0 Mg^{2+}-ACSF induced tonic-clonic like events in the neocortex as in the entorhinal cortex (Jones, 1989). It was reported that elevating extracellular potassium levels in 0 Mg^{2+}/Bac-ACSF after the development of tonic-clonic like ictal events in CA3 reversibly altered the activity pattern to recurrent late-stage like events (Swartzwelder *et al.*, 1987). In our experiments, as mentioned earlier, 0 Mg^{2+}/Bac-ACSF induced no epileptiform activity in CA3 and it was delayed in the neocortex. It needs to be further examined whether this resistance to develop epileptiform activity in 0 Mg^{2+}/Bac-ACSF will be altered by altering extracellular potassium levels.

In CA3, 0 Mg^{2+}-ACSF induced SWDs were suppressed by baclofen, and if there was any epileptiform activity it was of a different pattern having single large spike followed by relatively small amplitude bursts (spike-burst discharges). Furthermore, spike-burst discharges started to occur at a progressively faster rate following wash-out of baclofen and tonic-clonic like ictal events were developed in two of six slices

111

examined. One of the explanations could be that, in CA3, baclofen reduces the neurotransmitters release by acting at presynaptic sites of both inhibitory and excitatory neurons (Scanziani *et al.*, 1992; Thompson and Gahwiler, 1992). The cellular mechanisms might be different at terminals of inhibitory and excitatory neurons though. This effect at the presynaptic sites may prepare the network to fire in synchrony when the inhibitory effects of baclofen wane off and thus developing polyspike, spike-burst, and or tonic-clonic like discharges in CA3.

Application of baclofen for a brief time (~2 mins) only reduced the rate of neocortical late-stage events (LSEs), and it neither changed their amplitudes nor the waveform of the events (Horne *et al.*, 1986). I show here that washing-in baclofen for longer periods has reversibly replaced LSEs with tonic-clonic like ictal events. These events were found to be insensitive to diazepam but were completely abolished by an NMDAR antagonist (D-AP5). The maximal amplitude baclofen-induced tonic-clonic like events was larger than the amplitude of the late-stage events occurring before the addition of baclofen and after its washout. This suggests that, in 0 Mg^{2+}/Bac-ACSF, along with the enhancement of ionic currents, there might have also been an additional recruitment and synchronisation of neuronal activity. Enhancing the activity at $GABA_BRs$ (a) from the beginning of wash-out of magnesium ions has suppressed the development of LSEs, and (b) during LSEs, it has transformed the tonic-clonic like ictal events. In all the experiments, LSEs re-appeared after washing-out baclofen. These observations present the ideas that $GABA_B$-receptors play a key role in maintaining tonic-clonic like activity patterns, and reduced levels of ambient/spill-over GABA and/or failure of $GABA_BR$ activity could be some of many factors involved in the transition of early activity to the recurrent late stage in the neocortex. Reasons for the failure of $GABA_BR$ activity are manifold such as reduced availability of GABA, increased activity of GABA-transporters, increased $GABA_BR$ phosphorylation by protein kinase C, altered expression levels of functional $GABA_BR$ subunits, failure of $GABA_BR$-potassium channel coupling.

In vivo and *in vitro* studies have demonstrated that modulating $GABA_BR$ activity can have either epileptogenic or anti-epileptic actions. This depends primarily on the brain region where its activity is enhanced or reduced, and on the epileptic model used (Horne *et al.*, 1986; Swartzwelder *et al.*, 1987; Jones, 1989; Hosford *et al.*, 1992; Liu

et al., 1992; Watts and Jefferys, 1993; Vergnes *et al.*, 1997; Prosser *et al.*, 2001; Mares, 2012). These different roles of $GABA_B$-Rs in different regions of the brain and in different models of epilepsy stresses their importance and the need to study their role in detail in different stages and types of epilepsies.

In conclusion, the anti-epileptic effect of baclofen appears to be profound in the CA3 networks than in neocortex. These results indicate that, in $0 Mg^{2+}$-model, the mechanisms for the development of SWDs in CA3 and neocortical LSEs are dependent on the nature of activity at $GABA_B$Rs. In the neocortex, baclofen did not suppress the development of the early epileptiform activity, but it locked the network to a pattern of epileptiform activity. It suppressed the transition of early ictal into late-stage activity patterns suggesting a key role of $GABA_B$-receptors in the progression of activity. Future studies are needed to examine at the cellular level using whole-cell patch-clamp technique and network level using calcium imaging technique to understand the role of $GABA_B$Rs in the development of late-stage activity. It is necessary to understand the ionic mechanisms underlying the development of baclofen-induced tonic-clonic like ictal events from late-stage events and to assess the similarities and dissimilarities between these events and early $0 Mg^{2+}$-induced tonic-clonic like ictal events. These results and above mentioned future studies will help us to better understand the mechanisms underlying transition of epileptiform activity pattern from early to late-stage, types of epileptiform activity that are sensitive to baclofen, and enable us to translate the findings into clinics to aid in developing of new combination therapies to treat epilepsy.

5.5 References

1. Crunelli, V. and Leresche, N. (1991) 'A role for GABAB receptors in excitation and inhibition of thalamocortical cells', *Trends Neurosci*, 14(1), pp. 16-21.

2. Davies, C.H., Davies, S.N. and Collingridge, G.L. (1990) 'Paired-pulse depression of monosynaptic GABA-mediated inhibitory postsynaptic responses in rat hippocampus', *J Physiol*, 424, pp. 513-31.

3. Empson, R.M. and Jefferys, J.G. (1993) 'Synaptic inhibition in primary and secondary chronic epileptic foci induced by intrahippocampal tetanus toxin in the rat', *J Physiol*, 465, pp. 595-614.

4. Gahwiler, B.H. and Brown, D.A. (1985) 'GABAB-receptor-activated K+ current in voltage-clamped CA3 pyramidal cells in hippocampal cultures', *Proc Natl Acad Sci U S A*, 82(5), pp. 1558-62.

5. Galvez, T., Duthey, B., Kniazeff, J., Blahos, J., Rovelli, G., Bettler, B., Prezeau, L. and Pin, J.P. (2001) 'Allosteric interactions between GB1 and GB2 subunits are required for optimal GABA(B) receptor function', *EMBO J*, 20(9), pp. 2152-9.

6. Horne, A.L., Harrison, N.L., Turner, J.P. and Simmonds, M.A. (1986) 'Spontaneous paroxysmal activity induced by zero magnesium and bicuculline: suppression by NMDA antagonists and GABA mimetics', *Eur J Pharmacol*, 122(2), pp. 231-8.

7. Hosford, D.A., Clark, S., Cao, Z., Wilson, W.A., Jr., Lin, F.H., Morrisett, R.A. and Huin, A. (1992) 'The role of GABAB receptor activation in absence seizures of lethargic (lh/lh) mice', *Science*, 257(5068), pp. 398-401.

8. Inoue, M., Matsuo, T. and Ogata, N. (1985) 'Baclofen activates voltage-dependent and 4-aminopyridine sensitive K+ conductance in guinea-pig hippocampal pyramidal cells maintained *in vitro*', *Br J Pharmacol*, 84(4), pp. 833-41.

9. Isaacson, J.S., Solis, J.M. and Nicoll, R.A. (1993) 'Local and diffuse synaptic actions of GABA in the hippocampus', *Neuron*, 10(2), pp. 165-75.

10. Jones, R.S. (1989) 'Ictal epileptiform events induced by removal of extracellular magnesium in slices of entorhinal cortex are blocked by baclofen', *Exp Neurol*, 104(2), pp. 155-61.

11. Liu, Z., Vergnes, M., Depaulis, A. and Marescaux, C. (1992) 'Involvement of intrathalamic GABAB neurotransmission in the control of absence seizures in the rat', *Neuroscience*, 48(1), pp. 87-93.

12. Lopez-Bendito, G., Shigemoto, R., Kulik, A., Paulsen, O., Fairen, A. and Lujan, R. (2002) 'Expression and distribution of metabotropic GABA receptor subtypes GABABR1 and GABABR2 during rat neocortical development', *Eur J Neurosci*, 15(11), pp. 1766-78.

13. Lopez-Bendito, G., Shigemoto, R., Kulik, A., Vida, I., Fairen, A. and Lujan, R. (2004) 'Distribution of metabotropic GABA receptor subunits GABAB1a/b and GABAB2 in the rat hippocampus during prenatal and postnatal development', *Hippocampus*, 14(7), pp. 836-48.

14. Mann, E.O., Kohl, M.M. and Paulsen, O. (2009) 'Distinct roles of GABA(A) and GABA(B) receptors in balancing and terminating persistent cortical activity', *J Neurosci*, 29(23), pp. 7513-8.

15. Mares, P. (2012) 'Anticonvulsant action of GABAB receptor positive modulator CGP7930 in immature rats', *Epilepsy Res*, 100(1-2), pp. 49-54.

16. Perez-Garci, E., Gassmann, M., Bettler, B. and Larkum, M.E. (2006) 'The GABAB1b isoform mediates long-lasting inhibition of dendritic Ca2+ spikes in layer 5 somatosensory pyramidal neurons', *Neuron*, 50(4), pp. 603-16.

17. Prosser, H.M., Gill, C.H., Hirst, W.D., Grau, E., Robbins, M., Calver, A., Soffin, E.M., Farmer, C.E., Lanneau, C., Gray, J., Schenck, E., Warmerdam, B.S., Clapham, C., Reavill, C., Rogers, D.C., Stean, T., Upton, N., Humphreys, K., Randall, A., Geppert, M., Davies, C.H. and Pangalos, M.N. (2001) 'Epileptogenesis and enhanced prepulse inhibition in GABA(B1)-deficient mice', *Mol Cell Neurosci*, 17(6), pp. 1059-70.

18. Rigas, P. and Castro-Alamancos, M.A. (2007) 'Thalamocortical Up states: differential effects of intrinsic and extrinsic cortical inputs on persistent activity', *J Neurosci*, 27(16), pp. 4261-72.

19. Robbins, M.J., Calver, A.R., Filippov, A.K., Hirst, W.D., Russell, R.B., Wood, M.D., Nasir, S., Couve, A., Brown, D.A., Moss, S.J. and Pangalos, M.N. (2001) 'GABA(B2) is essential for g-protein coupling of the GABA(B) receptor heterodimer', *J Neurosci*, 21(20), pp. 8043-52.

20. Sanchez-Vives, M.V. and McCormick, D.A. (1997) 'Functional properties of perigeniculate inhibition of dorsal lateral geniculate nucleus thalamocortical neurons *in vitro*', *J Neurosci*, 17(22), pp. 8880-93.

21. Sanchez-Vives, M.V. and McCormick, D.A. (2000) 'Cellular and network mechanisms of rhythmic recurrent activity in neocortex', *Nat Neurosci*, 3(10), pp. 1027-34.

22. Scanziani, M. (2000) 'GABA spillover activates postsynaptic GABA(B) receptors to control rhythmic hippocampal activity', *Neuron*, 25(3), pp. 673-81.

23. Scanziani, M., Capogna, M., Gahwiler, B.H. and Thompson, S.M. (1992) 'Presynaptic inhibition of miniature excitatory synaptic currents by baclofen and adenosine in the hippocampus', *Neuron*, 9(5), pp. 919-27.

24. Sodickson, D.L. and Bean, B.P. (1996) 'GABAB receptor-activated inwardly rectifying potassium current in dissociated hippocampal CA3 neurons', *J Neurosci*, 16(20), pp. 6374-85.

25. Swartzwelder, H.S., Lewis, D.V., Anderson, W.W. and Wilson, W.A. (1987) 'Seizure-like events in brain slices: suppression by interictal activity', *Brain Res*, 410(2), pp. 362-6.

26. Thompson, S.M. and Gahwiler, B.H. (1992) 'Comparison of the actions of baclofen at pre- and postsynaptic receptors in the rat hippocampus *in vitro*', *J Physiol*, 451, pp. 329-45.

27. Ulrich, D. and Huguenard, J.R. (1996) 'Gamma-aminobutyric acid type B receptor-dependent burst-firing in thalamic neurons: a dynamic clamp study', *Proc Natl Acad Sci U S A*, 93(23), pp. 13245-9.

28. Vergnes, M., Boehrer, A., Simler, S., Bernasconi, R. and Marescaux, C. (1997) 'Opposite effects of GABAB receptor antagonists on absences and convulsive seizures', *Eur J Pharmacol*, 332(3), pp. 245-55.

29. Watts, A.E. and Jefferys, J.G. (1993) 'Effects of carbamazepine and baclofen on 4-aminopyridine-induced epileptic activity in rat hippocampal slices', *Br J Pharmacol*, 108(3), pp. 819-23.

Chapter 6 The effects of fluorocitrate, a gliotoxin, on evolving epileptiform activity in the neocortical networks

6.1 Introduction

Astrocytes play a key role in maintaining physiological activity of the cellular networks in the brain. Extracellular levels of potassium and neurotransmitters are rapidly increased following intense neuronal firing activity. Astrocytic uptake of excess potassium from the extracellular space and spatial buffering of potassium ions is through inwardly rectifying potassium channels and gap junctions, respectively (Kofuji and Newman, 2004; Wallraff *et al.*, 2006). Impaired functions of astrocytes increase extracellular concentrations of both potassium and glutamate, and make the network hyperexcitable eventually leading to the development of seizures. The causative link between the reduced ability of astrocytes to clear extracellular potassium and the development of seizures was demonstrated in Kir4.1 knockout mouse model (Chever *et al.*, 2010; Haj-Yasein *et al.*, 2011).

Synaptically released glutamate can trigger calcium elevations in astrocytes (Dani *et al.*, 1992). Activated astrocytes can cause calcium-dependent release of glutamate (gliotransmission) that signals to neighbouring neurons. This signalling leads to glutamate-dependent calcium responses in neurons, and facilitates neuronal synchronisation (Parpura *et al.*, 1994; Fellin *et al.*, 2004). Furthermore, astrocytes regulate the levels of ambient glutamate by their uptake via excitatory amino acid transporters expressed on them. The dynamic interactions between neurons and astrocytes were suggested to have important physiological functions (Halassa *et al.*, 2009; Henneberger *et al.*, 2010). If the interactions are perturbed, then excessive neuronal activity followed by gliotransmission can cause pathological hypersynchrony of neuronal activity (Gomez-Gonzalo *et al.*, 2010).

Astrocytic glutamate transporters are bidirectional, and the direction is dependent on the concentration gradients of ions across the membrane. An increase in extracellular levels of potassium ions reverses the direction of glutamate uptake and mediates glutamate release (Szatkowski *et al.*, 1990). Excessive glutamate accumulation in the synapse leads to deleterious effects on the neuronal network such as excitotoxicity, seizures. Inhibiting glutamate transporters leads to an increase in

ambient glutamate levels and this was reported to lower the threshold for the development of epileptiform activity (Campbell and Hablitz, 2008; Nyitrai *et al.*, 2010). Hence, astrocytic uptake of extracellular glutamate and it metabolism in astrocytes is essential for the maintenance of ambient glutamate levels, and maintaining physiological conditions in the brain.

Astrocytic glutamate is metabolised to glutamine by the enzyme glutamine synthetase, which is localised in astrocytes. Glutamine is then shuttled back to neurons for the synthesis of glutamate and GABA in excitatory neurons and inhibitory neurons, respectively (Tani *et al.*, 2014). Glutamine synthetase expression and function was found to be down regulated in tissue samples resected from patients with temporal lobe epilepsy (Eid *et al.*, 2004; van der Hel *et al.*, 2005). The causative role of down regulation of glutamine synthetase in the pathogenesis of epilepsy was demonstrated by pharmacologically inhibiting glutamine synthetase *in vivo* in the hippocampus of rats (Eid *et al.*, 2008; Wang *et al.*, 2009). Furthermore, inhibiting the activity of glutamine transporters and glutamine synthetase rapidly reduced GABA release from synapses (Liang *et al.*, 2006; Yang and Cox, 2011). In rats, induced-astrocytic gliosis caused down regulation of glutamine synthetase, and a reduction in inhibitory, but not excitatory postsynaptic currents. This reduction of inhibitory postsynaptic currents was rescued by applying exogenous glutamine (Ortinski *et al.*, 2010).

A similar effect on postsynaptic inhibitory currents was reported by treating slices taken from wildtype mice with a gliotoxin, fluorocitrate (FC) (Christian and Huguenard, 2013). Fluorocitrate disrupts astrocytic metabolism by inhibiting aconitase, an enzyme that catalyses the conversion of citrate to isocitrate, a crucial step in tricarboxylic cycle (TCA) (Hassel *et al.*, 1992). FC poisoning of astrocytes leads to build-up of intracellular levels of citrate ions, inhibits mitochondrial citrate carrier, depletes cellular ATP (Hassel *et al.*, 1994), and downstream, FC poisoning also inhibits the formation of glutamine, a key amino acid required for replenishing GABA and glutamate in neurons (Cheng *et al.*, 1972; Kun *et al.*, 1977). Accumulated citrate ions are readily exported to the extracellular space, where they may chelate the available free calcium ions, thus reducing extracellular calcium ion concentration. Lowering extracellular calcium ion concentrations could make the neural network and cause ictal discharges (Jefferys and Haas, 1982; Hornfeldt and Larson, 1990).

It has been shown that injecting FC into cortical regions leads to the development of epileptiform activity (Willoughby *et al.*, 2003; Mirsattari *et al.*, 2008). But various features of the evolution of astrocyte-poisoning induced epileptiform activity has not been investigated. I now show here that poisoning astrocytes in naïve neocortical brain slices with fluorocitrate induces recurrent short-duration discharges that are sensitive to glutamatergic channel blockers. In 4-aminopyridine model, fluorocitrate blocks the development of tonic-clonic like ictal events and instead induces glutamatergic channel blockers-sensitive recurrent short-duration discharges. Furthermore, fluorocitrate also transformed 4-aminopyridine-induced tonic-clonic like activity into recurrent short-duration discharges. These results show that fluorocitrate has a strong effect on slices that overrides 4-aminopyridine effect. Characterisation of various features of this paradigm can provide important insights into the role of astrocytes in epilepsy, and can also produce new targets for drug development to treat epilepsy in clinics.

6.2 Materials and methods

6.2.1 *Slice preparation and electrophysiology*

For all the experiments described below, coronal slices of visual cortex (neocortex, NCtx) were used, that were prepared and stored as described in *slice preparation method 2* (see chapter 2, sub-heading 2.4.2). Slices were then incubated in ACSF containing fluorocitrate (100µM; FC-ACSF) for 2-4 hours before starting the experiments. In all experiments, LFPs were recorded from infragranular layers of neocortex in slices (Figure 6.1). The recording setup and the equipment used were as described in chapter 2 (sub-heading 2.5.1).

Figure 6.1 Recording setup showing a slice in the interface recording chamber with electrode placed infragranular layers of neocortex (NCtx, bottom-right).

6.2.2 *Protocols and drugs*

In all experiments, LFPs were recorded from infragranular layers of neocortex in slices that were pre-incubated in FC-ACSF. Three sets of experiments were performed to characterise the effects of fluorocitrate *in vitro* on naïve neocortical networks and on the evolution of epileptiform activity in 4AP model. First, recordings were performed in pre-incubated slices bathed in FC-ACSF to investigate the effects of fluorocitrate on the neocortical networks. Second, recordings were performed in pre-incubated slices bathed in FC-ACSF supplemented with 4AP (FC/4AP-ACSF) to investigate the effects of FC on the evolution of epileptiform activity. Third, recordings were performed in neocortical slices incubated in ACSF to investigate the ability of FC to alter the on-going 4AP induced epileptiform activity. These slices were perfused initially with ACSF and the baseline activity was recorded in ACSF. After 10-15

minutes, the perfusate was switched from ACSF to epileptogenic medium (4AP-ACSF). After the development of tonic-clonic like ictal discharges, fluorocitrate was added to 4AP-ACSF.

DL-Fluorocitric acid barium salt (FC, fluorocitrate) was purchased from Sigma-Aldrich (USA). FC stock solution (50 mM) was prepared and stored in -20 °C. FC was used at 100 µM concentration for incubations and in all the experiments described below (Hassel *et al.*, 1995). 4AP (100 µM; Sigma-Aldich, USA) was added to ACSF for experiments in 4AP model. NMDA-receptors blocker (D-AP5; 50 µM), and AMPA-receptors blocker (NBQX; 20 µM) were purchased from Tocris (U.K).

6.3 Results

6.3.1 *Fluorocitrate induced recurrent short-duration discharges in neocortical networks*

Fluorocitrate in ACSF induced the development of recurrent population discharges that largely had a waveform of a spike followed by buzz like activity (Figure 6.2 A, Bi). These events were associated with multiunit activity (MUA) suggestive of neuronal participation in these events (Figure 6.2 Bii). FC-induced events were short-duration discharges lasting for a few hundreds of milliseconds (0.83 ± 0.02 s; n = 4) with maximal amplitude of 2.46 ± 0.60 mV (n = 4). They occurred at a rate of 0.05 ± 0.01 Hz (n = 4). This was the only pattern of activity that developed and continued to occur for the duration of the recordings.
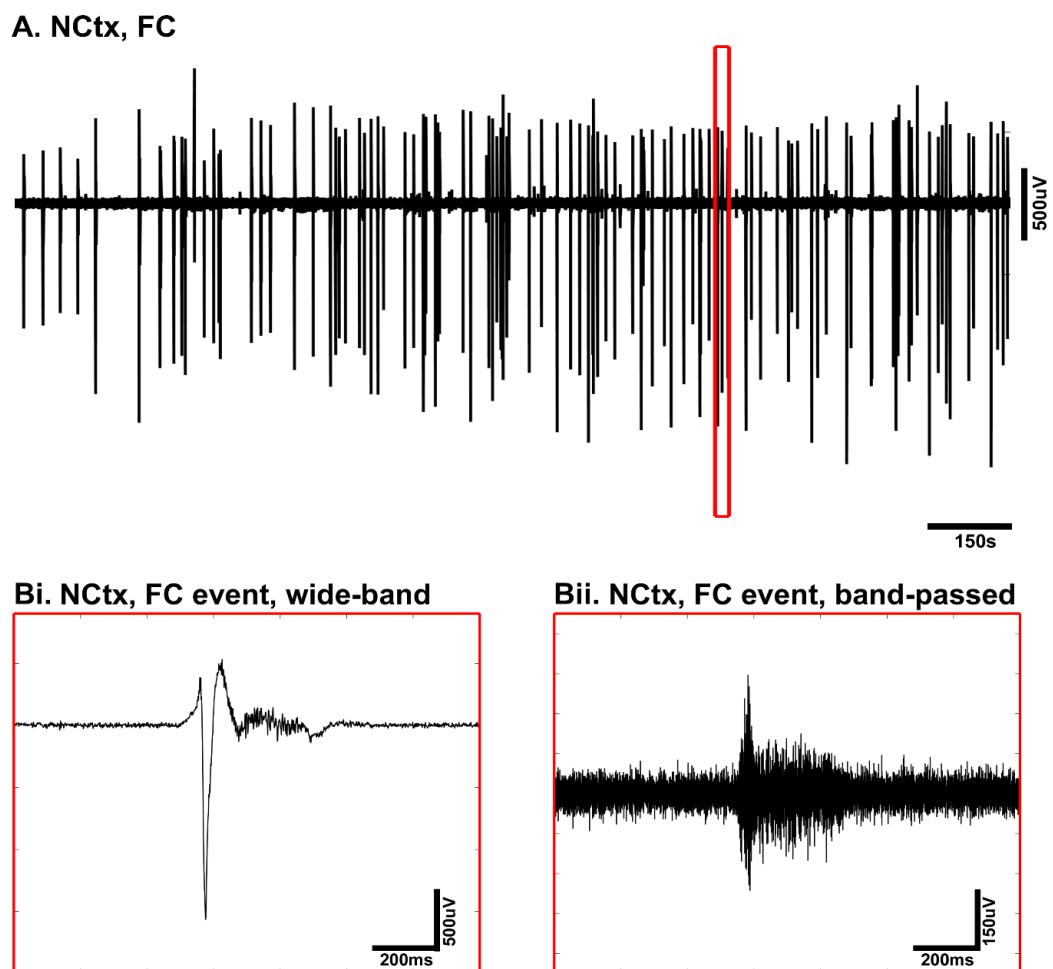
Figure 6.2 Fluorocitrate (FC) induced recurrent population discharges in slices pre-incubated in fluorocitrate-ACSF (A). These events had a spike-and-wave like waveform (Bi) that were associated with neuronal firing activity (Bii, band-pass filtered trace; MUA associated with the event in Bi)

6.3.2 *Recurrent short-duration discharges, but not tonic-clonic like ictal events were developed in fluorocitrate/4AP-ACSF*

In slices incubated in ACSF, 4AP induced the development of epileptiform activity with a characteristic pattern of early tonic-clonic like ictal events that lasted for tens of seconds (Figure 6.3 A). In contrast, in neocortical slices incubated in FC-ACSF, tonic-clonic like ictal events did not develop in response to 4AP in FC-ACSF (FC/4AP-ACSF), but developed population discharges that were similar to the events that developed in FC-ACSF (Figure 6.3 B). FC- and FC/4AP-induced discharges were similar in that they had similar waveforms (Figure 6.2 Bi, 6.3 Di), and were associated with multiunit activity (Figure 6.2 Bii, 6.3 Dii). Both, FC- and FC/4AP-induced events lasted only for a few hundreds of milliseconds (Figure 6.4 A; Table 6.1). However, FC/4AP-induced events occurred at a higher rate and had smaller peak amplitudes (Figure 6.4 B, C; Table 6.1)
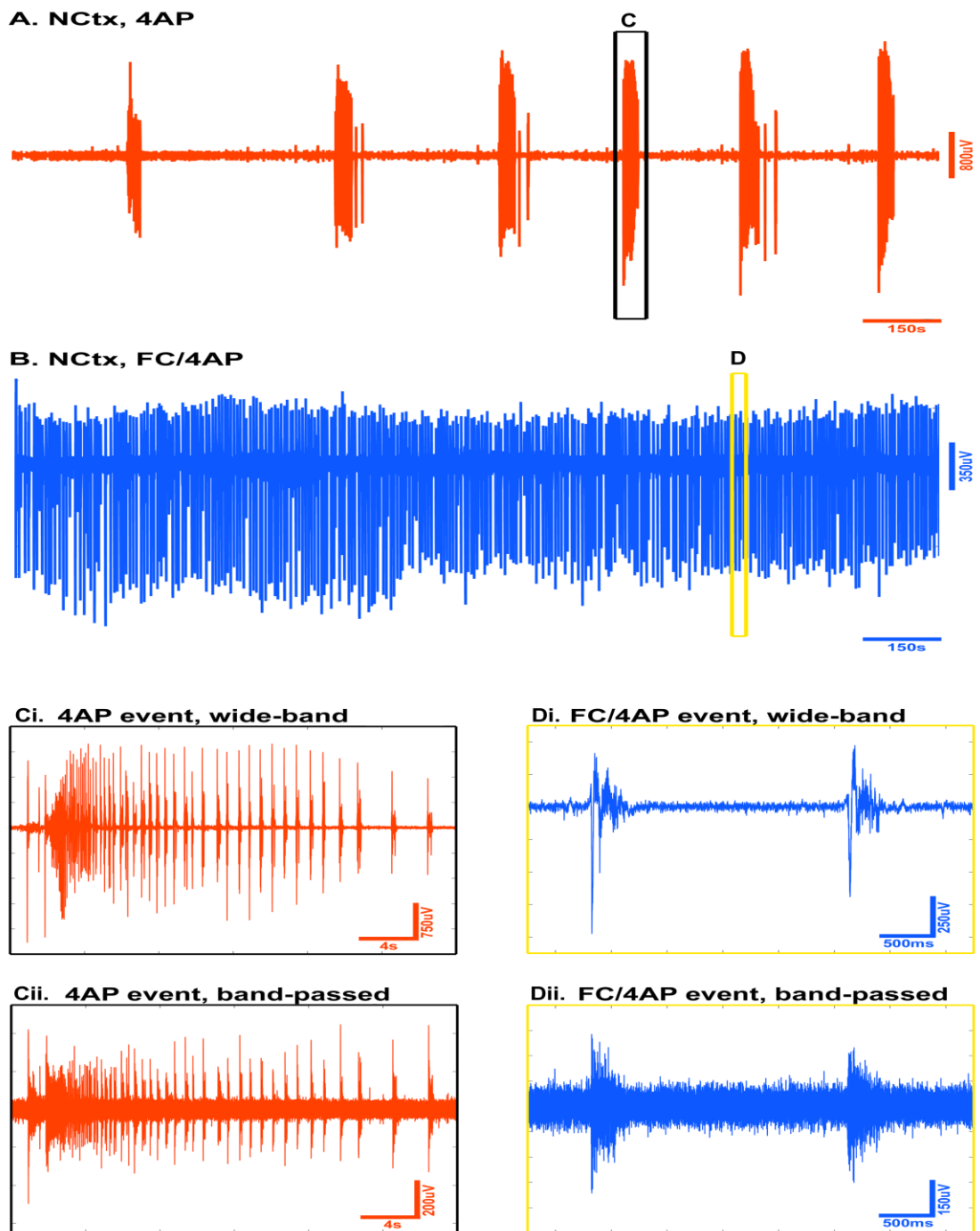
Figure 6.3 Representative traces displaying (A) 4AP-ACSF induced tonic-clonic like IE, and (B) FC/4AP-induced recurrent short-duration events. Traces in panel A, and B are both 1800 s long, displaying activity from 200s after switching solutions to 4AP-ACSF and FC/4AP-ACSF, respectively. C. 4AP-induced tonic-clonic like ictal event (boxed area in panel A), wide-band (Ci) and multiunit activity (300 - 3000 Hz, Cii). D. FC/4AP–induced recurrent discharges (boxed area in panel B), wide-band (Di) and multiunit activity (300 – 3000 Hz, Dii).
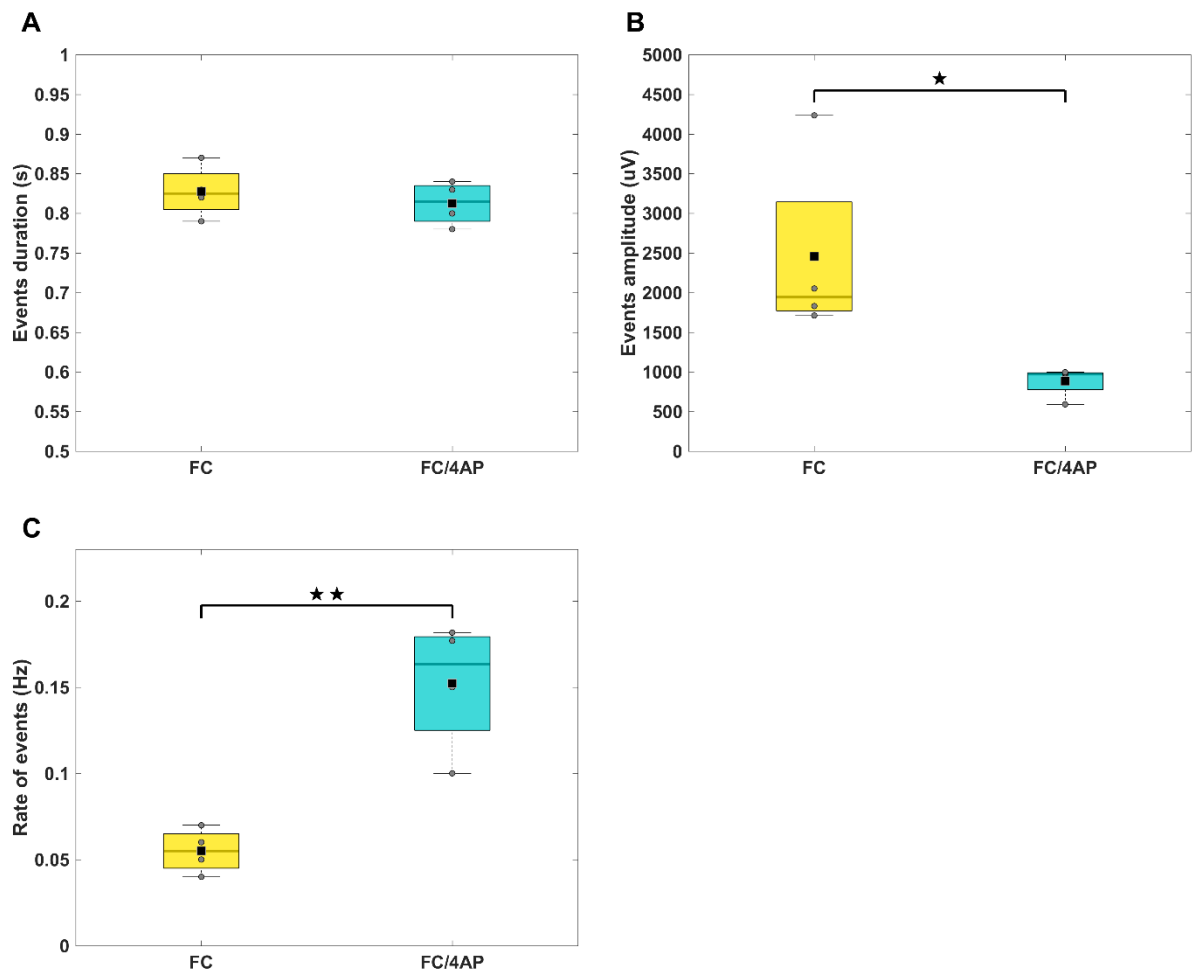
Figure 6.4 FC- and FC/4AP-induced events both lasted for a few hundreds of milliseconds (A), but differed in event amplitudes (B), and rates (C). Unpaired Student's t-test, *p = 0.04, **p = 0.002. For mean ± s.e.m, see Table 6.1.

Neocortex	FC (n)	FC/4AP (n)	p =
Duration (s)	0.83 ± 0.02 (4)	0.81 ± 0.01 (4)	0.51
Max. Amp (mV)	2.46 ± 0.60 (4)	0.88 ± 0.09 (4)	0.04
Rate (Hz)	0.05 ± 0.01 (4)	0.15 ± 0.02 (4)	0.002

Table 6.1 Rate, duration, and maximal amplitude (Max. Amp.) measures of FC- and FC/4AP-induced events. p-values were calculated using unpaired Student's t-test.

6.3.3 *Fluorocitrate-mediated events in ACSF, and 4AP were sensitive to ionotropic glutamate receptors antagonists*

The sensitivity of FC-induced and FC/4AP-induced events to ionotropic glutamate receptors antagonists was examined in preliminary experiments described here. Both, FC- and FC/4AP-induced events were sensitive to D-AP5, a NMDA-receptor antagonist. Blocking NMDA-receptors increased the amplitude of the events in both FC-ACSF and FC/4AP-ACSF groups (Figure 6.5 A, red bar; Figure 6.6 A, red bar). However, it had different effects on the rate of events in both groups. In FC-ACSF, blocking NMDA receptors lowered the rate of events (Figure 6.5 A, red bar), whereas, FC/4AP-induced events occurred at a higher rate (Figure 6.6 A, red bar). Additional blocking of AMPA and kainate receptors by NBQX abolished all the population discharges in both FC-ACSF and FC/4AP-ACSF groups (Figure 6.5 B, blue bar; Figure 6.6 B, blue bar).

A. NCtx
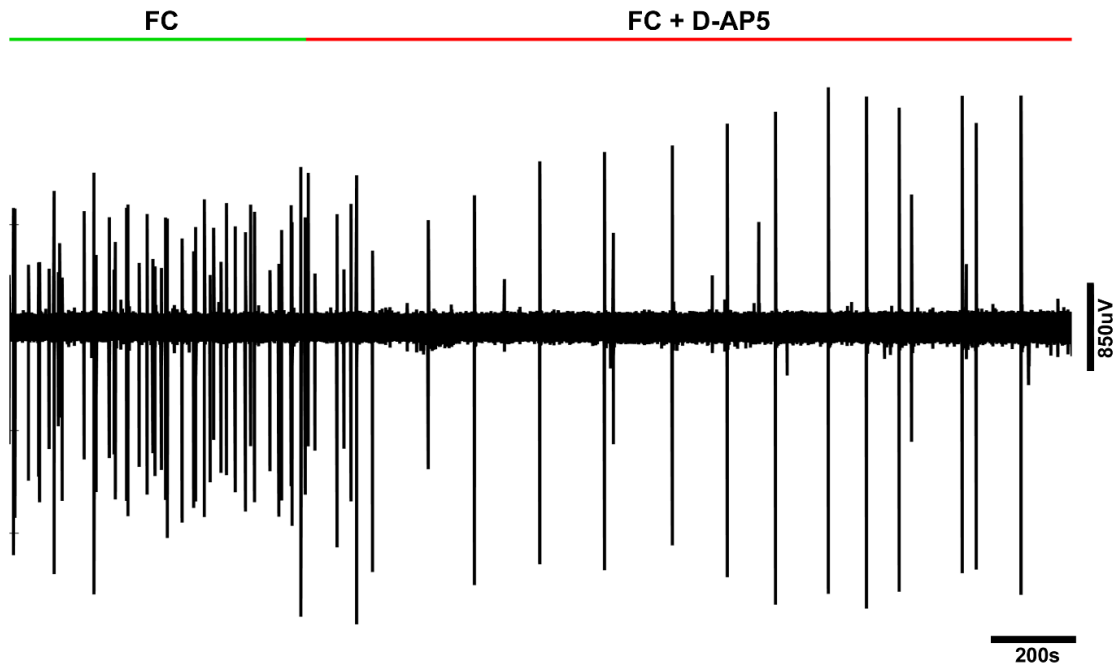
B. NCtx
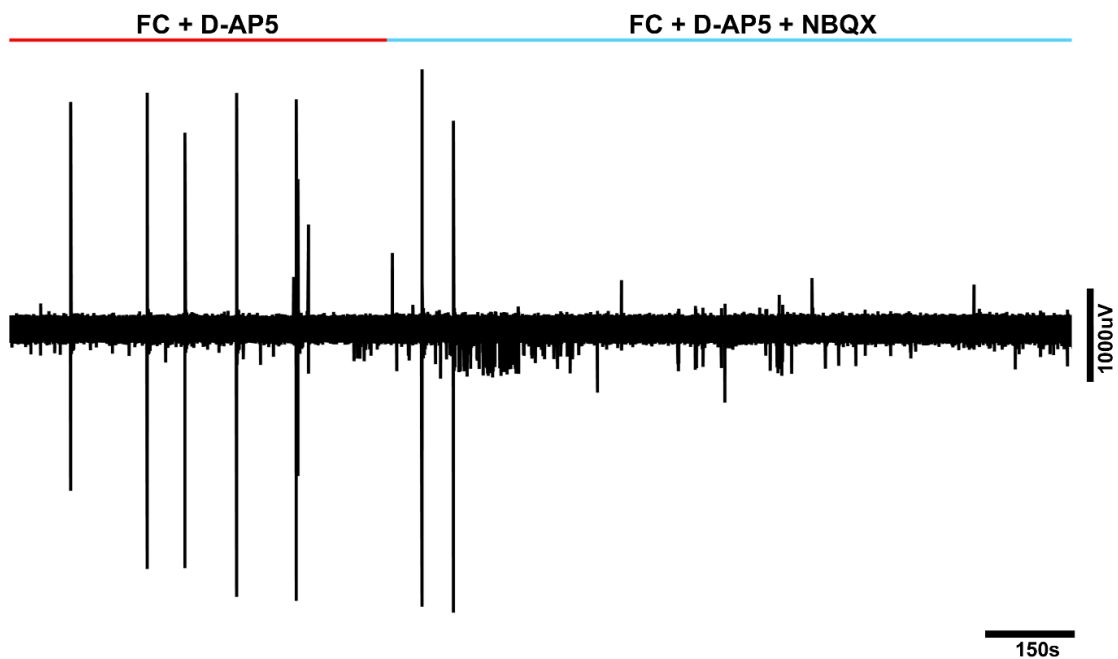
Figure 6.5 Fluorocitrate (FC)-induced events were sensitive to ionotropic glutamate receptor antagonists. Traces in A and B were taken from the same experiment.   A. Blocking NMDA receptors (D-AP5, red bar) had a suppressive effect on FC-induced events (green bar). It reduced the rate of events, but increased the amplitude of the events. B. Additional blockade of AMPA- and kainate-receptors (NBQX, blue bar) abolished all population discharges.

128

A. NCtx

FC/4AP   **FC/4AP + D-AP5**

600uV

80s

B. NCtx

FC/4AP + D-AP5   **FC/4AP + D-AP5 + NBQX**

600uV

125s
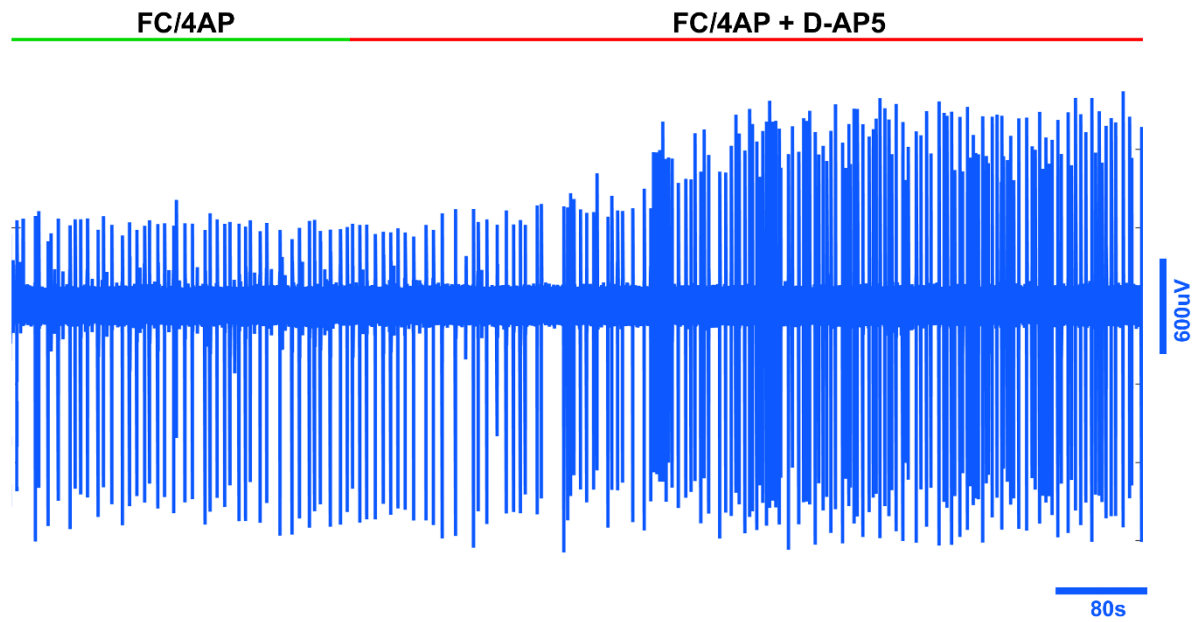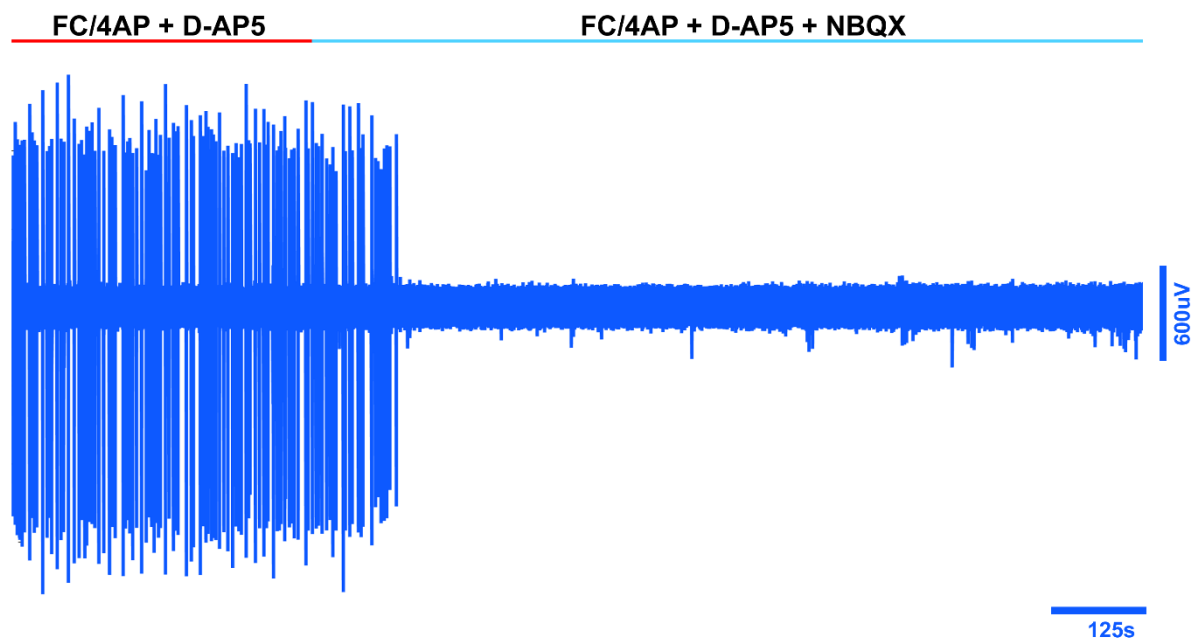
Figure 6.6 Fluorocitrate (FC)/4AP-induced events were sensitive to ionotropic glutamate receptor antagonists. Traces in A and B were taken from the same experiment. A. Blocking NMDA receptors (D-AP5, red bar) enhanced the activity of FC-induced events (green bar). It increased both the rate and amplitudes of FC-induced events. B. Additional blockade of AMPA- and kainate-receptors (NBQX, blue bar) abolished all population discharges.

6.3.4 *Fluorocitrate transformed 4AP-induced tonic-clonic like ictal events to recurrent short-duration events*

In section 6.3.2, I showed that tonic-clonic like activity failed to appear at all if the slices were bathed in FC from the start of the perfusion with 4AP-ACSF. This raised the question whether FC could suppress the 4AP-induced tonic-clonic like ictal events, after they have already developed (Figure 6.7 A, orange bar). Addition of FC transformed the activity pattern of 4AP-induced tonic-clonic like ictal events (Figure 6.7 A, green bar). FC replaced 4AP-induced tonic-clonic like ictal events (Figure 6.7 Bi, Bii) with short-duration recurrent discharges that are associated with multiunit activity (Figure 6.7 Ci, Cii).
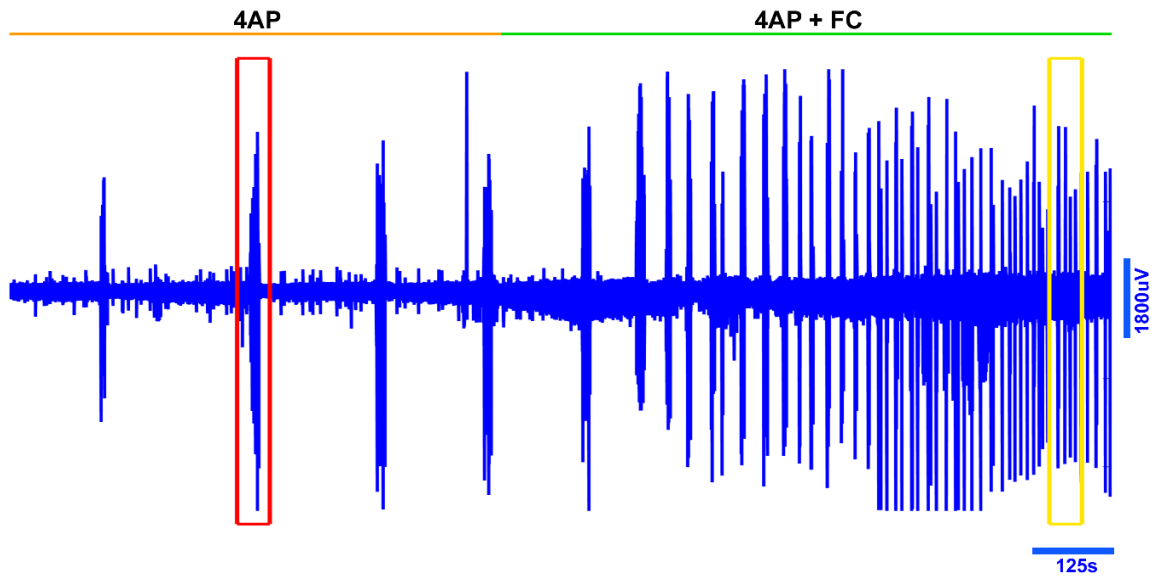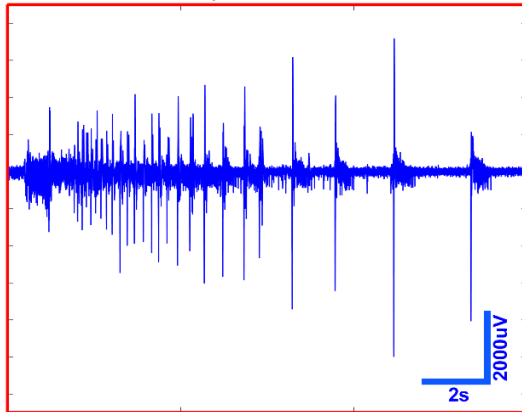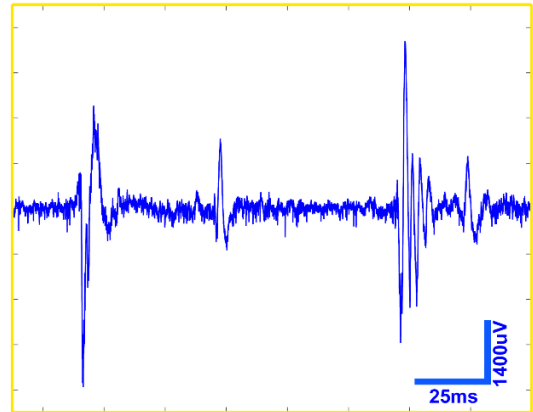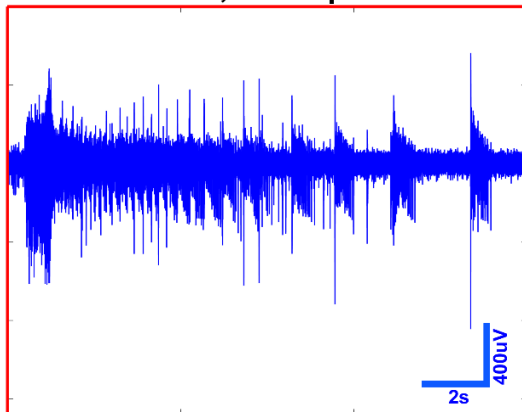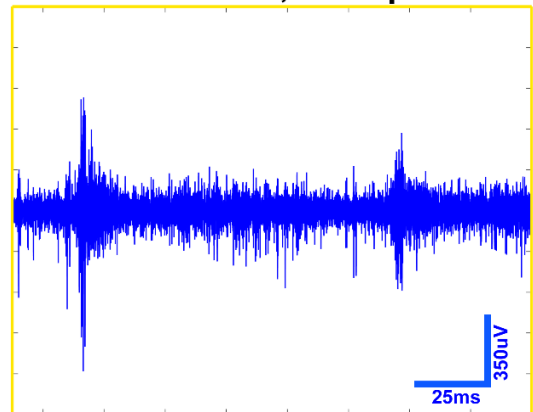
Figure 6.7 Addition of FC to 4AP-ACSF during early tonic-clonic like ictal events transformed the activity pattern in the neocortex. Tonic-clonic like ictal events (A, orange bar, B) were replaced with FC/4AP-induced recurrent short-duration events (A, green bar, C). FC/4AP-induced events (Ci) were associated with multiunit activity (Cii).

6.4 Discussion

These results demonstrate that having dysfunctional astrocytes in neocortical circuits alter the pattern of evolution of epileptiform activity. Inhibiting the functions of astrocytes led to the development of spontaneous recurrent discharges, each lasting for a few hundreds of milliseconds. These events had a spike-and-wave like waveforms, with an intense high-frequency component suggestive of neuronal firing activity, and were sensitive to ionotropic glutamate receptors antagonists. However, it was not clear whether these events were induced due to increased extracellular glutamate resulting from synchronised neuronal activity (Dani *et al.*, 1992; Gomez-Gonzalo *et al.*, 2010) and impaired clearance of glutamate from the synaptic region (Campbell and Hablitz, 2008; Nyitrai *et al.*, 2010), astrocyte-mediated glutamate release (Parpura *et al.*, 1994; Fellin *et al.*, 2004), reduced GABA transmission (disinhibition) due to astrocyte poisoning (Liang *et al.*, 2006; Yang and Cox, 2011), increased extracellular potassium ion concentrations (Largo *et al.*, 1996) or in combination of any of these.

When ACSF was supplemented with both 4AP and FC, neocortical networks developed spike-and-wave like recurrent discharges lasting for a few hundreds of milliseconds that were similar to FC-induced events but failed to develop tonic-clonic like ictal events. Furthermore, the on-going 4AP-induced tonic-clonic like discharges were also transformed by FC, to this same pattern. Gomez-Gonzalo *et al.* (2010) proposed a neuron-astrocyte excitatory loop in an *in vitro* model of focal seizures. In their model, prior to an ictal discharge, neuronal hyperactivity activity initially triggers calcium elevations in astrocytes. These activated astrocytes in turn recruit, via gliotransmission, more neurons and precipitate an ictal discharge. FC treatment reduced the intracellular calcium elevations and calcium-dependent glutamate release from astrocytes (Bonansco *et al.*, 2011), and hence, prevented astrocyte-mediated neuronal recruitment and pathological hypersynchronisation. These may be plausible explanations for the aforementioned results, that is, the inability of the FC/4AP treated network to develop tonic-clonic like discharges. However, previous studies show that FC injected into cortical areas *in vivo* induced convulsions (Willoughby *et al.*, 2003; Mirsattari *et al.*, 2008). It is not clear what mechanisms underlie FC-induced convulsive seizures *in vivo*. Does the same cortical network show different responses to FC in different models/preparations? It will be necessary to further characterise effects of FC

in different models of epilepsy to better understand the role of astrocytes in epileptogenesis.

Blocking GABA$_A$Rs during 4AP-induced tonic-clonic like IEs transformed the activity pattern into recurrent short-discharges that were blocked by NBQX, but enhanced by NMDA receptor antagonist (Bruckner *et al.*, 1999). FC/4AP-induced events also showed similar responses to glutamate receptors antagonists. Blockade of all the activity in FC and FC/4AP-treated slices by NBQX suggests that they depend on glutamatergic transmission. However, it remains unclear whether the FC mediated events were due to neurotransmission or gliotransmission, and if there were any inhibitory currents associated with these events.

Based on the results mentioned in this chapter and literature, I hypothesise that fluorocitrate overrides the effect of 4AP by disinhibiting the network. In future studies, this can be examined by measuring the excitatory and inhibitory currents from a pyramidal neuron while bathing the slice in FC/4AP-ACSF, and assessing the effects of the GABA$_A$-receptors antagonist on this activity. It will also be necessary to examine the effect of fluorocitrate on the concentration of extracellular potassium ions and how it influences the epileptiform activity. This can be examined in a brain slice by using a combination of extracellular field potential recordings and ion-sensitive microelectrode technique. Fluorocitrate can be used as a pharmacological tool to suppress the physiological activity of astrocytes in the network and tease apart various roles played by astrocytes in the evolution of epileptiform activity, and enable us to identify novel drug targets for treating epilepsy.

6.5 References

1. Bonansco, C., Couve, A., Perea, G., Ferradas, C.A., Roncagliolo, M. and Fuenzalida, M. (2011) 'Glutamate released spontaneously from astrocytes sets the threshold for synaptic plasticity', *Eur J Neurosci*, 33(8), pp. 1483-92.

2. Bruckner, C., Stenkamp, K., Meierkord, H. and Heinemann, U. (1999) 'Epileptiform discharges induced by combined application of bicuculline and 4-aminopyridine are resistant to standard anticonvulsants in slices of rats', *Neurosci Lett*, 268(3), pp. 163-5.

3. Campbell, S.L. and Hablitz, J.J. (2008) 'Decreased glutamate transport enhances excitability in a rat model of cortical dysplasia', *Neurobiol Dis*, 32(2), pp. 254-61.

4. Cheng, S.C., Kumar, S. and Casella, G.A. (1972) 'Effects of fluoroacetate and fluorocitrate on the metabolic compartmentation of tricarboxylic acid cycle in rat brain slices', *Brain Res*, 42(1), pp. 117-28.

5. Chever, O., Djukic, B., McCarthy, K.D. and Amzica, F. (2010) 'Implication of Kir4.1 channel in excess potassium clearance: an *in vivo* study on anesthetized glial-conditional Kir4.1 knock-out mice', *J Neurosci*, 30(47), pp. 15769-77.

6. Christian, C.A. and Huguenard, J.R. (2013) 'Astrocytes potentiate GABAergic transmission in the thalamic reticular nucleus via endozepine signaling', *Proc Natl Acad Sci U S A*, 110(50), pp. 20278-83.

7. Dani, J.W., Chernjavsky, A. and Smith, S.J. (1992) 'Neuronal activity triggers calcium waves in hippocampal astrocyte networks', *Neuron*, 8(3), pp. 429-40.

8. Eid, T., Ghosh, A., Wang, Y., Beckstrom, H., Zaveri, H.P., Lee, T.S., Lai, J.C., Malthankar-Phatak, G.H. and de Lanerolle, N.C. (2008) 'Recurrent seizures and brain pathology after inhibition of glutamine synthetase in the hippocampus in rats', *Brain*, 131(Pt 8), pp. 2061-70.

9. Eid, T., Thomas, M.J., Spencer, D.D., Runden-Pran, E., Lai, J.C., Malthankar, G.V., Kim, J.H., Danbolt, N.C., Ottersen, O.P. and de Lanerolle, N.C. (2004) 'Loss of glutamine synthetase in the human epileptogenic hippocampus:

possible mechanism for raised extracellular glutamate in mesial temporal lobe epilepsy', *Lancet*, 363(9402), pp. 28-37.

10. Fellin, T., Pascual, O., Gobbo, S., Pozzan, T., Haydon, P.G. and Carmignoto, G. (2004) 'Neuronal synchrony mediated by astrocytic glutamate through activation of extrasynaptic NMDA receptors', *Neuron*, 43(5), pp. 729-43.

11. Gomez-Gonzalo, M., Losi, G., Chiavegato, A., Zonta, M., Cammarota, M., Brondi, M., Vetri, F., Uva, L., Pozzan, T., de Curtis, M., Ratto, G.M. and Carmignoto, G. (2010) 'An excitatory loop with astrocytes contributes to drive neurons to seizure threshold', *PLoS Biol*, 8(4), p. e1000352.

12. Haj-Yasein, N.N., Jensen, V., Vindedal, G.F., Gundersen, G.A., Klungland, A., Ottersen, O.P., Hvalby, O. and Nagelhus, E.A. (2011) 'Evidence that compromised K+ spatial buffering contributes to the epileptogenic effect of mutations in the human Kir4.1 gene (KCNJ10)', *Glia*, 59(11), pp. 1635-42.

13. Halassa, M.M., Florian, C., Fellin, T., Munoz, J.R., Lee, S.Y., Abel, T., Haydon, P.G. and Frank, M.G. (2009) 'Astrocytic modulation of sleep homeostasis and cognitive consequences of sleep loss', *Neuron*, 61(2), pp. 213-9.

14. Hassel, B., Paulsen, R.E., Johnsen, A. and Fonnum, F. (1992) 'Selective inhibition of glial cell metabolism *in vivo* by fluorocitrate', *Brain Res*, 576(1), pp. 120-4.

15. Hassel, B., Sonnewald, U., Unsgard, G. and Fonnum, F. (1994) 'NMR spectroscopy of cultured astrocytes: effects of glutamine and the gliotoxin fluorocitrate', *J Neurochem*, 62(6), pp. 2187-94.

16. Hassel, B., Westergaard, N., Schousboe, A. and Fonnum, F. (1995) 'Metabolic differences between primary cultures of astrocytes and neurons from cerebellum and cerebral cortex. Effects of fluorocitrate', *Neurochem Res*, 20(4), pp. 413-20.

17. Henneberger, C., Papouin, T., Oliet, S.H. and Rusakov, D.A. (2010) 'Long-term potentiation depends on release of D-serine from astrocytes', *Nature*, 463(7278), pp. 232-6.

18. Hornfeldt, C.S. and Larson, A.A. (1990) 'Seizures induced by fluoroacetic acid and fluorocitric acid may involve chelation of divalent cations in the spinal cord', *Eur J Pharmacol*, 179(3), pp. 307-13.

19. Jefferys, J.G. and Haas, H.L. (1982) 'Synchronized bursting of CA1 hippocampal pyramidal cells in the absence of synaptic transmission', *Nature*, 300(5891), pp. 448-50.

20. Kofuji, P. and Newman, E.A. (2004) 'Potassium buffering in the central nervous system', *Neuroscience*, 129(4), pp. 1045-56.

21. Kun, E., Kirsten, E. and Sharma, M.L. (1977) 'Enzymatic formation of glutathione-citryl thioester by a mitochondrial system and its inhibition by (-)erythrofluorocitrate', *Proc Natl Acad Sci U S A*, 74(11), pp. 4942-6.

22. Largo, C., Cuevas, P., Somjen, G.G., Martin del Rio, R. and Herreras, O. (1996) 'The effect of depressing glial function in rat brain in situ on ion homeostasis, synaptic transmission, and neuron survival', *J Neurosci*, 16(3), pp. 1219-29.

23. Liang, S.L., Carlson, G.C. and Coulter, D.A. (2006) 'Dynamic regulation of synaptic GABA release by the glutamate-glutamine cycle in hippocampal area CA1', *J Neurosci*, 26(33), pp. 8537-48.

24. Mirsattari, S.M., Shen, B., Leung, L.S. and Rajakumar, N. (2008) 'A gliotoxin model of occipital seizures in rats', *Seizure*, 17(6), pp. 483-9.

25. Nyitrai, G., Lasztoczi, B. and Kardos, J. (2010) 'Glutamate uptake shapes low-[Mg2+] induced epileptiform activity in juvenile rat hippocampal slices', *Brain Res*, 1309, pp. 172-8.

26. Ortinski, P.I., Dong, J., Mungenast, A., Yue, C., Takano, H., Watson, D.J., Haydon, P.G. and Coulter, D.A. (2010) 'Selective induction of astrocytic gliosis generates deficits in neuronal inhibition', *Nat Neurosci*, 13(5), pp. 584-91.

27. Parpura, V., Basarsky, T.A., Liu, F., Jeftinija, K., Jeftinija, S. and Haydon, P.G. (1994) 'Glutamate-mediated astrocyte-neuron signalling', *Nature*, 369(6483), pp. 744-7.

28. Szatkowski, M., Barbour, B. and Attwell, D. (1990) 'Non-vesicular release of glutamate from glial cells by reversed electrogenic glutamate uptake', *Nature*, 348(6300), pp. 443-6.

29. Tani, H., Dulla, C.G., Farzampour, Z., Taylor-Weiner, A., Huguenard, J.R. and Reimer, R.J. (2014) 'A local glutamate-glutamine cycle sustains synaptic excitatory transmitter release', *Neuron*, 81(4), pp. 888-900.

30. van der Hel, W.S., Notenboom, R.G., Bos, I.W., van Rijen, P.C., van Veelen, C.W. and de Graan, P.N. (2005) 'Reduced glutamine synthetase in hippocampal areas with neuron loss in temporal lobe epilepsy', *Neurology*, 64(2), pp. 326-33.

31. Wallraff, A., Kohling, R., Heinemann, U., Theis, M., Willecke, K. and Steinhauser, C. (2006) 'The impact of astrocytic gap junctional coupling on potassium buffering in the hippocampus', *J Neurosci*, 26(20), pp. 5438-47.

32. Wang, Y., Zaveri, H.P., Lee, T.S. and Eid, T. (2009) 'The development of recurrent seizures after continuous intrahippocampal infusion of methionine sulfoximine in rats: a video-intracranial electroencephalographic study', *Exp Neurol*, 220(2), pp. 293-302.

33. Willoughby, J.O., Mackenzie, L., Broberg, M., Thoren, A.E., Medvedev, A., Sims, N.R. and Nilsson, M. (2003) 'Fluorocitrate-mediated astroglial dysfunction causes seizures', *J Neurosci Res*, 74(1), pp. 160-6.

34. Yang, S. and Cox, C.L. (2011) 'Attenuation of inhibitory synaptic transmission by glial dysfunction in rat thalamus', *Synapse*, 65(12), pp. 1298-308.

Chapter 7 *In vitro* investigation of seizure susceptibility in transgenic mice

7.1 Introduction

Epilepsy could be the primary syndrome of a gene mutation or secondary presenting feature of gene-related developmental disorders of brain. In the past, epilepsy genetics was more focussed on channelopathies – identifying genes encoding neurotransmitter receptors, and ion channel subunits (Ludwig *et al.*, 2003; Yu *et al.*, 2006). Recent studies are moving epilepsy genetics beyond channelopathies, identifying mutation in new categories of genes. Functional studies in transgenic animals and *in vitro* characterisation of activity patterns in brain tissue from transgenic animals provide insights regarding new mechanisms of ictogenesis and epileptogenesis, compensatory mechanisms for gene mutation-mediated deficits, if any, and even anti-epileptic adaptations in the brain (Poduri and Lowenstein, 2011; Lerche *et al.*, 2013).

To identify novel epileptogenic gene mutations, Neuromouse consortium, a breeding program at MRC (Harwell, U.K), created various genetic strains of mice, and allocated us two of these strains, calsyntenin-3 and neuroplastin-65, to assess the proneness of their neuronal networks to develop epileptiform activity. This chapter is a report on experiments carried out on tissue taken from aforementioned two transgenic mouse lines.

7.1.1 *Calsyntenin-3 (Cst-3)*

Calsyntenins are synapse-organising proteins present primarily in the postsynaptic membrane of both pyramidal cells and interneurons (Hintsch *et al.*, 2002; Pettem *et al.*, 2013; Um *et al.*, 2014). This family of proteins comprise three structurally similar proteins: calsyntenin-1, calsyntenin-2, and calsyntenin-3, encoded by clstn-1, clstn-2 and clstn-3 genes, respectively (Hintsch *et al.*, 2002). Calsyntenin-3 is also known as alcadein-β (Alzheimer-related cadherin-like protein β). It is implicated in the pathophysiology of Alzheimer's disease (Uchida *et al.*, 2011; Uchida *et al.*, 2013).

In mice, calsyntenin-3 is expressed exclusively in the brain, whereas in humans it is expressed in kidneys as well as, at lower levels, in heart, skeletal muscles, liver,

placenta, pancreas, and lungs (Hintsch *et al.*, 2002). It shows a differential expression pattern between distinct neuronal cell types. In neocortex, it is found in cells of all layers, with high immunoreactivity in layer 5 cells. In cerebellum, it is found in few interneurons present in the granule cell layer and in purkinje cells. Pyramidal neurons and interneurons express calsyntenin-3 at lower and higher levels, respectively, throughout the cortex (Hintsch *et al.*, 2002; Pettem *et al.*, 2013; Um *et al.*, 2014)

Calsyntenin-3, but not calsyntenin-2 and calsyntenin -1, has synaptogenic function. It promotes adhesion of postsynaptic cell membrane to axons, and induces differentiation of GABAergic and glutamatergic presynaptic terminals. Calsyntenin-3 interacts with its presynaptic partner – α-neurexin and it is calcium dependent (Pettem *et al.*, 2013; Um *et al.*, 2014). In calsyntenin-3 gene knockout animals (clstn3$^{-/-}$), the density of both asymmetric and symmetric synapses was significantly reduced in stratum radiatum and stratum pyramidale of CA1 region in hippocampus (Pettem *et al.*, 2013). It was reported that miniature currents recorded from CA1 pyramidal neurons in clstn3$^{-/-}$ mice show no change in the amplitude, but a decrease in frequency of the mIPSCs and mEPSCs, compared to wild type (WT) mice. Using paired-pulse field EPSP (fEPSP) recordings, Pettem *et al.* (2013) reported that excitatory neurotransmitter release probabilities were unaltered in clstn3$^{-/-}$ mice.

7.1.2 *Neuroplastin-65 (NP-65)*

Neuroplastins are one of the major cell adhesion molecules (CAM) found in the synaptic membrane encoded by the gene NPTN. They are glycoproteins that belong to Ig-superfamily of CAMs. Neuroplastin-55 (NP-55) and -65 (NP-65) are the two isoforms of neuroplastin. They are expressed widely in the brain tissue and were found in the neuropil of all layers of neocortex (Bernstein *et al.*, 2007). NP-65 is specific to brain tissue whereas NP-55 is present in other tissues of the body as well. In the hippocampus of rat brain, region-specific staining of NP-65 was observed; it is prominently stained in the neuropil of dentate gyrus and CA1 region of hippocampus, and moderately in CA3 region (Bernstein *et al.*, 2007).

NP-65 was shown to have a strong association with the postsynaptic density (PSD) domain of neuron. This association is regulated by the activity of the synapse and is involved in plasticity-dependent restructuring of synapses (Smalla *et al.*, 2000). NP-65 levels were found to be increased in tissue taken from rats with Kainate-induced

generalised tonic-clonic seizures. NP-65 levels in PSD were also found to be higher after tetanisation (Smalla *et al.*, 2000). LTP can be induced, but its maintenance in CA1 is prevented by antibodies against NP-65, demonstrating the role of NP-65 in synaptic plasticity (Smalla *et al.*, 2000). On the other hand, in CA3, Empson *et al.* (2006) showed that both induction and maintenance of LTP are inhibited by homophilic binding of NP-65 protein (Empson *et al.*, 2006).

The neuritogenic effect of NP-65 is mediated through activation of fibroblast growth factor receptor-1 (FGFR1), MAP kinases, and CaMKII. However, this effect of NP-65 is reduced by interfering with established neuroplastin65 homophilic interaction (Owczarek *et al.*, 2011; Owczarek and Berezin, 2012). Another study showed the putative gephyrin-independent $GABA_A$ receptor-anchoring functions of NP-65, at both synaptic and extrasynaptic sites in a receptor subunit-selective fashion. NP-65 was found to co-localise with α1- and α2-subunits, and α5-subunits of $GABA_A$ receptors at postsynaptic and extrasynaptic membrane regions of neurons, respectively. Such an association of NP-65 with $GABA_A$ receptors, intracellular messengers and many other synaptic proteins suggest that perturbation of NP-65 expression may be involved in learning and memory deficits, and pathological conditions such as epilepsy, anxiety, schizophrenia (Sarto-Jackson *et al.*, 2012).

7.2 Materials and methods

7.2.1 *Transgenic mice*

Two strains of transgenic mice, calsyntenin-3 gene knockouts and neuroplastin-65 gene knockouts, were supplied by the Neuromouse Consortium, a breeding program at the MRC at Harwell. From here on, they will be referred to as calsyntenin-3 (Cst-3) and neuroplastin-65 (NP-65).

7.2.1 *Slice preparation and electrophysiology*

Combined neocortical-hippocampal horizontal slices were used in all the experiments described below. *Slice preparation method 1* (chapter 2, sub-heading 2.4.1) was used for preparing brain slices from the tissue taken from calsyntenin-3 and neuroplastin-65. For experiments in brain slices taken from calsyntenin-3 and neuroplastin-65, local field potentials (LFPs) were recorded from infragranular layers of neocortex (Figure 7.1). The recording setup and the equipment used were as described in chapter 2 (sub-heading 2.5.1).
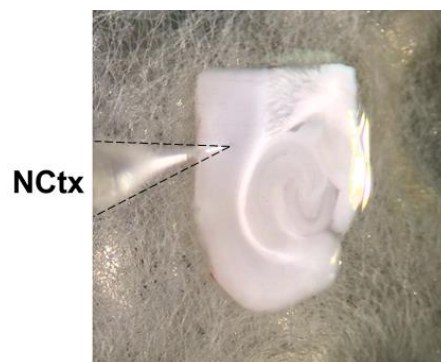
Figure 7.1 Recording setup showing a horizontal slice in the interface recording chamber with an electrode placed in the infragranular layers of neocortex.

7.2.2 *Protocols*

For experiments in brain slices taken from both calsyntenin-3 and neuroplastin-65, slices were placed in the interface recording chamber, which were perfused initially with normal-ACSF. Electrodes were placed in the regions of interest and the baseline activity was recorded in normal-ACSF. After 10-15 minutes, the perfusate was

switched from normal-ACSF to epileptogenic media (0 Mg^{2+}-ACSF or 4AP-ACSF). Experiments in the brain slices taken from wild-type mice were used as controls.

7.3 Results

7.3.1 *Calsyntenin-3: 0 Mg^{2+} model*

Following wash out of magnesium ions from ACSF, early tonic-clonic like ictal events (IE) were developed and later this activity pattern was transformed into late-stage activity. The latency for the development of the first IE was higher in Cst-3 than in the controls (Figure 7.2, Table 7.1). Similar to the controls, there was a steep decline in the time taken for the development of the second IE. However, the inter-ictal events after the second IE were relatively stable and longer than in the controls (Figure 7.3A, Table 7.1). IEs in Cst-3 continued to appear for a long period and eventually transitioned to late-stage events. The latency for this transition was significantly higher in Cst-3 (Figure 7.3B, Table 7.1). These results show that calsyntenin-3 gene knockout delayed the development of tonic-clonic like ictal events, but did not prevent their development.
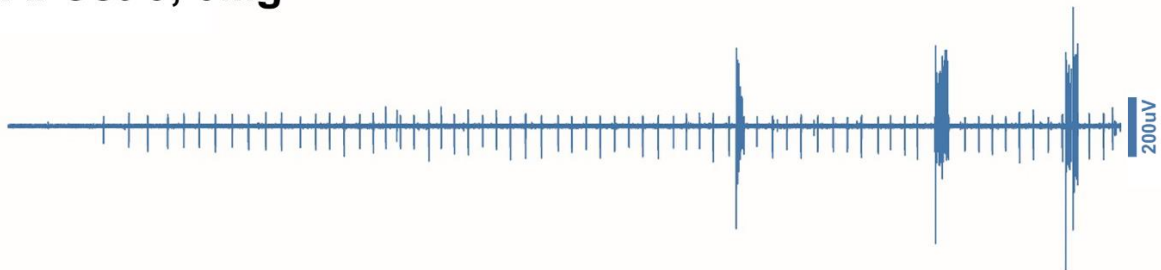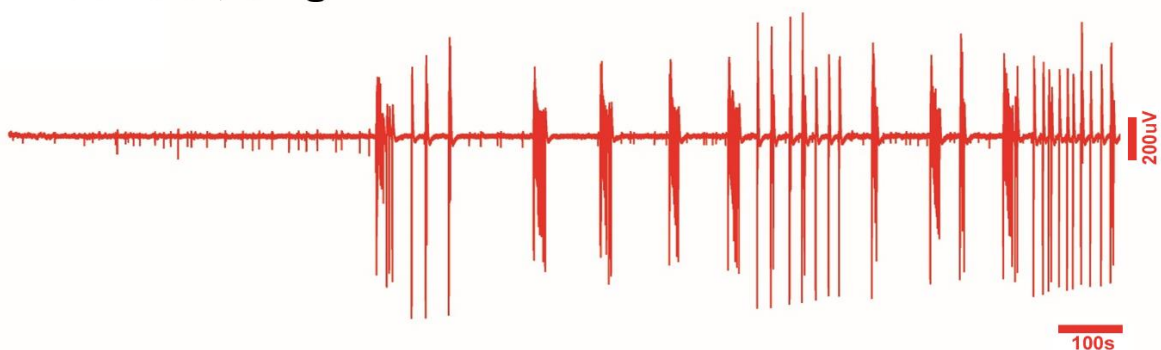
Figure 7.2 Evolution of epileptiform activity following wash out of magnesium ions from ACSF at the start of the recording. These are the raw traces of recordings from Cst-3 (A) and controls (B). Note, the time scale at the bottom of the figure applies to all the traces.
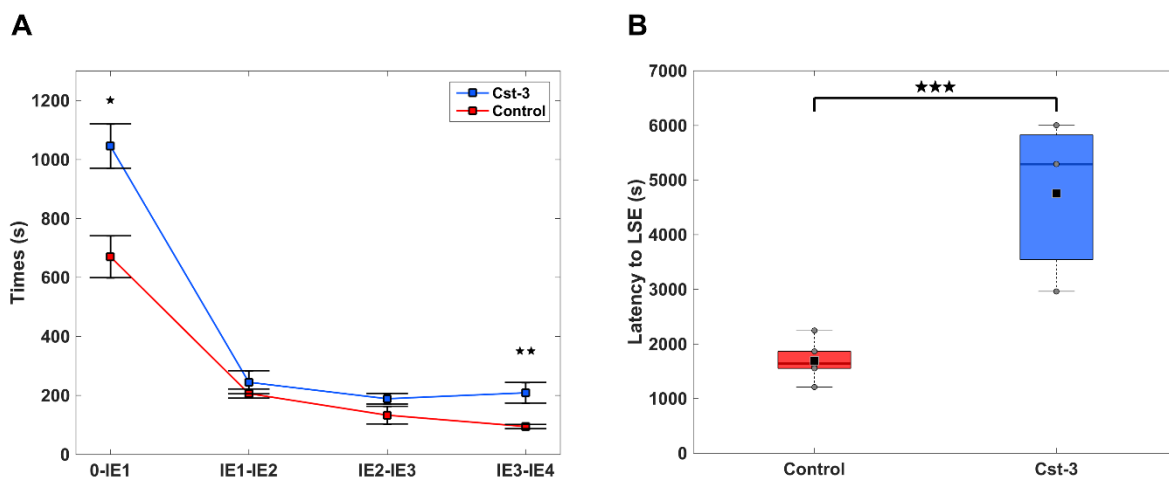
Figure 7.3 A. In Cst-3 slices,   latency for the development of the first IE was longer and after the second IE, the inter-event intervals were relatively stable compared to the controls. B. Latency for the second transition to late-stage events (LSEs) was higher in Cst-3 slices. *,**,***p-values less than or equal to Bonferroni corrected critical value (α = 0.01).

	0 Mg^{2+} model		
Inter-event intervals (s)	**Control (n)**	**Cst-3 (n)**	**p-values ^(α = 0.01)**
0-IE1	670.1 ± 71.1 (6)	1045.4 ± 75.2 (4)	0.008 *
IE1-IE2	206.0 ± 15.2 (6)	244.2 ± 38.9 (4)	0.324
IE2-IE3	132.7 ± 29.9 (6)	188.4 ± 17.9 (4)	0.202
IE3-IE4	94.2 ± 7.2 (6)	208.6 ± 35.1 (4)	0.004 **
Latency to LSE	1689.7 ± 140.7 (6)	4750 ± 918.2 (3)	0.002 ***

Table 7.1 Times taken for the development of first tonic-clonic like ictal event (IE) and the subsequent inter-event intervals, and the latency to LSEs in Cst-3 and controls in

0 Mg2+-ACSF. *, **, ***p-values less than or equal to ^Bonferroni corrected critical value (α). See Figure 7.3.

7.3.2 *Calsyntenin-3: 4AP model*

Activity patterns in 4AP model were different to those observed in 0 Mg^{2+} model (Figure 7.4). However, the activity patterns were not consistent between different slices (Figure 7.4Ai, Aii). Nevertheless, the general trend of activity i.e. longer latency for the first ictal-event and shorter IEIs for successive ictal events was observed in a few slices (figure 7.5A).

In 4AP model, the latency to the first IE in Cst-3 was similar to that measured in controls (Figure 7.5A, Table 7.2). Subsequent IEs were occurring at relatively similar intervals in both the groups (Figure 7.5A). The early activity transitioned to late-stage at similar latencies.
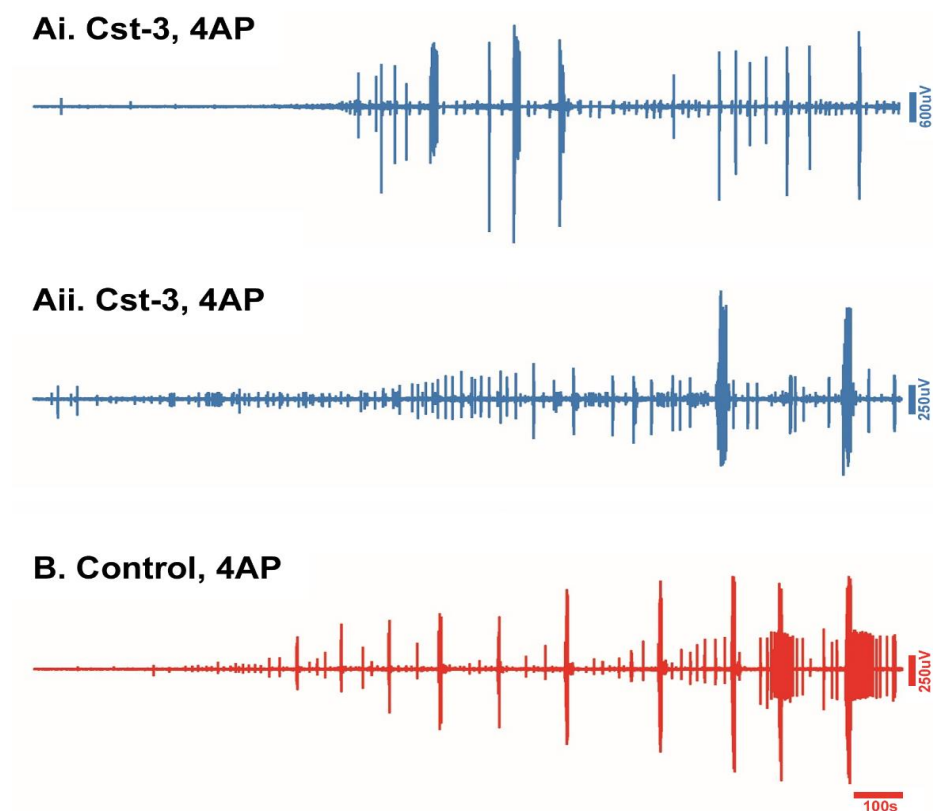
Figure 7.4 Evolution of epileptiform activity in 4AP model. Activity patterns in Cst-3 slices showed some variability. There were IE followed by brief quiescent period, after which activity began to reappear (Ai). In another slice (Aii), the evolution of activity

showed characteristic patterns as in the controls (B). The time scale at the bottom of the figure applies to all the traces.
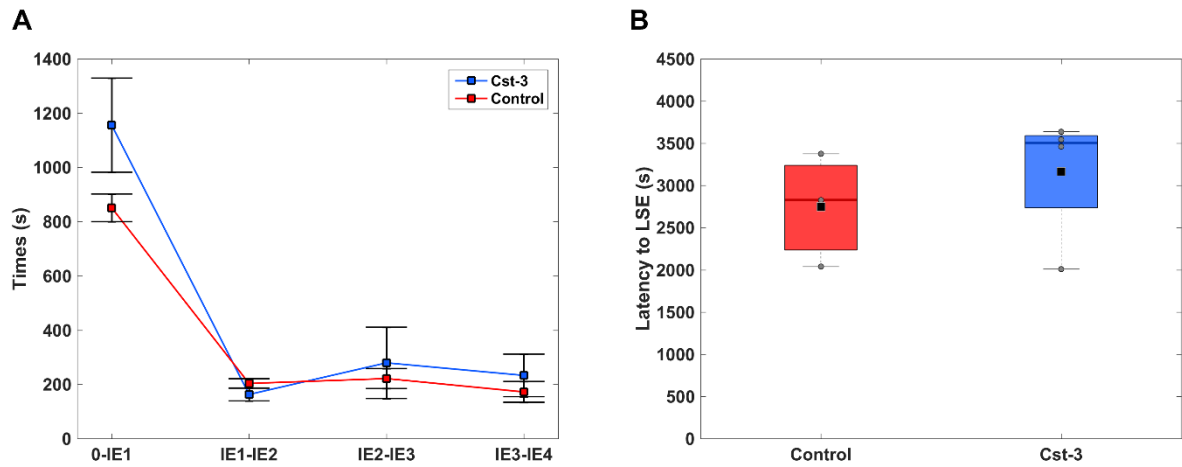
Figure 7.5 In 4AP model, evolution of epileptiform activity pattern in Cst-3 slices was not different from controls. B. Latency for the second transition of activity to late-stage events (LSEs) was similar in both the groups.

4AP model			
Inter-event intervals (s)	*Control (n)*	*Cst-3 (n)*	*p-values* *^(α = 0.01)*
0-IE1	851.2 ± 51.0 (4)	1155.9± 173.5 (6)	0.20
IE1-IE2	203.5 ± 17.7 (4)	162.9 ± 23.8 (6)	0.25
IE2-IE3	221.6 ± 36.9 (4)	279.5 ± 131.4 (6)	0.74
IE3-IE4	172.3 ± 38.4 (4)	233.18 ± 78.4 (6)	0.57
Latency to LSE	2747.4 ± 387.9 (3)	3163.8 ± 386.5 (4)	0.49

Table 7.2 Times taken for the development of first tonic-clonic like ictal event (IE) and the subsequent inter-event intervals, and the latency to LSEs in Cst-3 and controls in 4AP-ACSF. ^Bonferroni corrected critical value (α = 0.01).

7.3.3 *Neuroplastin-65: Inconsistent activity patterns in both 0 Mg^{2+} and 4AP models*

Neuroplastin-65 (NP-65) has shown activity in varying degrees – from no ictal-events being developed to one to two ictal events or development of characteristic ictal-events in both 0 Mg^{2+} and 4AP models (Figure 7.6, 7.7). Slices that did not develop tonic-clonic like ictal events (IE) were not considered for analysis of latencies to first IEs. Latencies to the first IE NP-65 were similar to controls in both the models tested (Figure 7.8; 0 Mg^{2+} model: NP-65, 1394.08 ± 857.1 s, n = 3; control, 985.3 ± 148.6 s, n = 4; unpaired Student's t-test, p = 0.6; 4AP model: NP-65, 1360.7 ± 241.8 s, n = 5; control, 1414.1 ± 158.31 s, n = 4; unpaired Student's t-test, p = 0.86). The high variability in the recorded activity patterns limited our ability to make any conclusions on the seizure susceptibility of the cortical networks tested from tissues taken from NP-65 mice.

NP-65, 0Mg²⁺

A. Animal #1
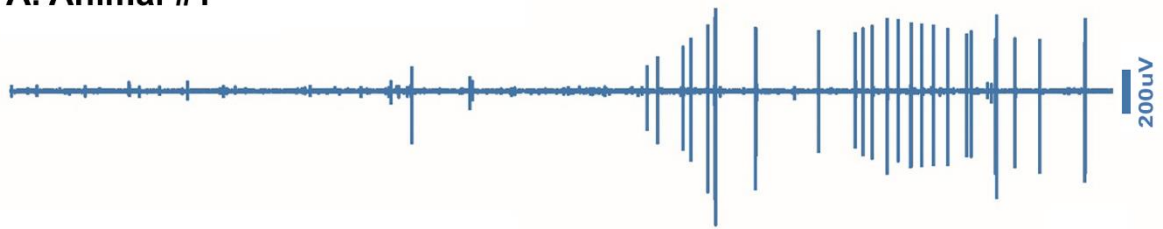
B. Animal #2
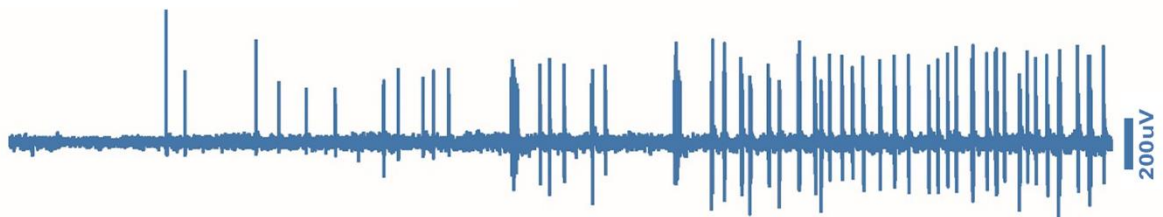
C. Animal #3

Figure 7.6 NP-65 slices have shown varying degrees of responses to 0 Mg²⁺-ACSF. Traces displayed in this figure were recorded from slices prepared from three different NP-65 mice. Ai. Slice was resistant to developing ictal events. B. slice developed only two ictal events, and then progressed to late stage-like events. C. Slice developed full ictal events in a short time. Note, the time scale at the bottom of the figure applies to all the traces.

NP-65, 4AP

A. Animal #1

500uV

B. Animal #2

300uV

C. Animal #3

500uV

100s

Figure 7.7 NP-65 slices have shown varying degrees of responses to 4AP-ACSF. Traces displayed in this figure were recorded from slices prepared from three different NP-65 mice. Note, the time scale at the bottom of the figure applies to all the traces.

A. NP-65, 0Mg^{2+}- model
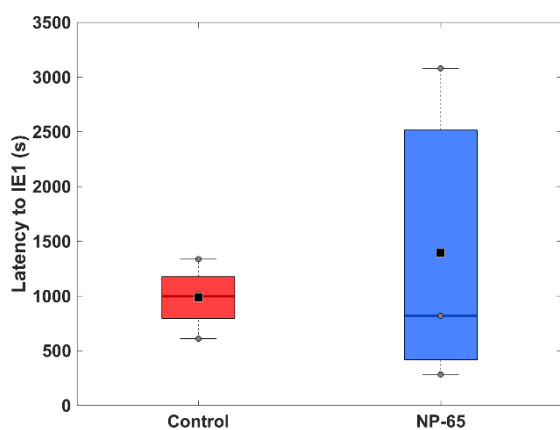
B. NP-65, 4AP model
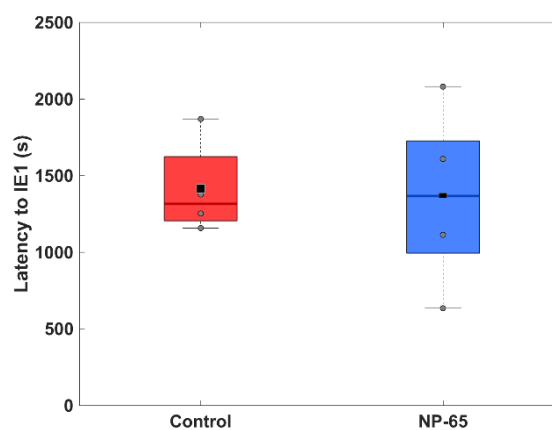
Figure 7.8 Latency to the first tonic-clonic like ictal events in NP-65 slices were not different from controls both in 0 Mg^{2+}-model (A), or 4AP-model (B)

7.4 Discussion

I performed a simple set of *in vitro* experiments and analyses to assess the susceptibility of cortical networks prepared from transgenic mouse lines, calsyntenin-3 and neuroplastin-65, to develop ictal events, and the responses to acute pharmacological manipulations to increase excitability in the network. The results show subtle differences in the responses, but most comparisons with wild-type animals did not reach significance. Based on a limited number of experimental data points, neither calsyntenin-3, nor neuroplastin-65 knockouts, showed marked difference from the wild-type animals.

Post hoc analysis of different measures during the evolution of epileptic activity has been performed on the data sets obtained from these animals. I first looked at the times for the development of ictal events, inter ictal-event intervals, and to late stage events. The results from this analysis would provide with the information of how susceptible the transgenic animals are to develop epilepsy. These results show that in calsyntenin-3 brain slices, different kinds of responses are recorded in 0 Mg^{2+} model and 4AP model. In 0 Mg^{2+} model, Cst-3 take a longer time to develop the first ictal event, and the subsequent IEs occur at relatively constant intervals. This was the only difference that was significant. However, there was great variability in the 4AP model and it was not clear what the relevance of this finding is.

In neuroplastin-65 brain slices, varying responses were seen in both 0 Mg^{2+} and 4AP models. Previous studies have shown neuroplastin-65 to play a role in GluR1 receptor trafficking (Empson *et al.*, 2006), and anchoring protein for GABA$_A$ receptors in a subunit specific manner (Sarto-Jackson *et al.*, 2012). Thus, the anticipation was for NP-65 to develop ictal-events sooner than in wild type. But the results obtained were not in line with predicted activity patterns. Again, the small sample size and high variance in recordings from these animals could be influencing the confidence in the results.

Our ability to find significant differences between experimental groups was limited by the high variance and the small sample size. If we consider these data as preliminary investigations, we can perform power analyses to estimate the appropriate sample size for a proper test of whether these mutations affect network excitability.

150

Table 7.3 shows examples of the calculated power, and an estimate of required total sample size to achieve p≤0.05.

Animals and model	Total sample size (expt.)	Calculated power	Required total sample size to achieve p < 0.05	Stipulated power
Cst-3 vs control; 0 Mg^{2+} model	10	0.87	10	0.8
Cst-3 vs control; 4AP model	10	0.27	36	0.8
NP-65 vs control; 0 Mg^{2+} model	7	0.07	222	0.8
NP-65 vs control; 4AP model	9	0.05	2184	0.8

Table 7.3 Achieved power and required total sample size calculated for times to first IE in different experiments. Here, 'expt.' is an abbreviation of 'experimented'.

These Calsyntenin-3 and neuroplastin-65 were amongst the first to be generated by the Neuromouse Consortium, and available information indicates that they are not thought to have an epilepsy phenotype. Reports from Neuromouse Consortium at Harwell say the animals display some "twitching"; our results suggest that these two mouse strains are, most likely, not epileptic, but may have some cortical pathology.

7.5 References

1. Bernstein, H.G., Smalla, K.H., Bogerts, B., Gordon-Weeks, P.R., Beesley, P.W., Gundelfinger, E.D. and Kreutz, M.R. (2007) 'The immunolocalization of the synaptic glycoprotein neuroplastin differs substantially between the human and the rodent brain', *Brain Res*, 1134(1), pp. 107-12.

2. Empson, R.M., Buckby, L.E., Kraus, M., Bates, K.J., Crompton, M.R., Gundelfinger, E.D. and Beesley, P.W. (2006) 'The cell adhesion molecule neuroplastin-65 inhibits hippocampal long-term potentiation via a mitogen-activated protein kinase p38-dependent reduction in surface expression of GluR1-containing glutamate receptors', *J Neurochem*, 99(3), pp. 850-60.

3. Hintsch, G., Zurlinden, A., Meskenaite, V., Steuble, M., Fink-Widmer, K., Kinter, J. and Sonderegger, P. (2002) 'The calsyntenins--a family of postsynaptic membrane proteins with distinct neuronal expression patterns', *Mol Cell Neurosci*, 21(3), pp. 393-409.

4. Lerche, H., Shah, M., Beck, H., Noebels, J., Johnston, D. and Vincent, A. (2013) 'Ion channels in genetic and acquired forms of epilepsy', *J Physiol*, 591(4), pp. 753-64.

5. Ludwig, A., Budde, T., Stieber, J., Moosmang, S., Wahl, C., Holthoff, K., Langebartels, A., Wotjak, C., Munsch, T., Zong, X., Feil, S., Feil, R., Lancel, M., Chien, K.R., Konnerth, A., Pape, H.C., Biel, M. and Hofmann, F. (2003) 'Absence epilepsy and sinus dysrhythmia in mice lacking the pacemaker channel HCN2', *EMBO J*, 22(2), pp. 216-24.

6. Owczarek, S. and Berezin, V. (2012) 'Neuroplastin: cell adhesion molecule and signaling receptor', *Int J Biochem Cell Biol*, 44(1), pp. 1-5.

7. Owczarek, S., Soroka, V., Kiryushko, D., Larsen, M.H., Yuan, Q., Sandi, C., Berezin, V. and Bock, E. (2011) 'Neuroplastin-65 and a mimetic peptide derived from its homophilic binding site modulate neuritogenesis and neuronal plasticity', *J Neurochem*, 117(6), pp. 984-94.

8. Pettem, K.L., Yokomaku, D., Luo, L., Linhoff, M.W., Prasad, T., Connor, S.A., Siddiqui, T.J., Kawabe, H., Chen, F., Zhang, L., Rudenko, G., Wang, Y.T.,

Brose, N. and Craig, A.M. (2013) 'The specific alpha-neurexin interactor calsyntenin-3 promotes excitatory and inhibitory synapse development', *Neuron*, 80(1), pp. 113-28.

9. Poduri, A. and Lowenstein, D. (2011) 'Epilepsy genetics--past, present, and future', *Curr Opin Genet Dev*, 21(3), pp. 325-32.

10. Sarto-Jackson, I., Milenkovic, I., Smalla, K.H., Gundelfinger, E.D., Kaehne, T., Herrera-Molina, R., Thomas, S., Kiebler, M.A. and Sieghart, W. (2012) 'The cell adhesion molecule neuroplastin-65 is a novel interaction partner of gamma-aminobutyric acid type A receptors', *J Biol Chem*, 287(17), pp. 14201-14.

11. Smalla, K.H., Matthies, H., Langnase, K., Shabir, S., Bockers, T.M., Wyneken, U., Staak, S., Krug, M., Beesley, P.W. and Gundelfinger, E.D. (2000) 'The synaptic glycoprotein neuroplastin is involved in long-term potentiation at hippocampal CA1 synapses', *Proc Natl Acad Sci U S A*, 97(8), pp. 4327-32.

12. Uchida, Y., Gomi, F., Murayama, S. and Takahashi, H. (2013) 'Calsyntenin-3 C-terminal fragment accumulates in dystrophic neurites surrounding abeta plaques in tg2576 mouse and Alzheimer disease brains: its neurotoxic role in mediating dystrophic neurite formation', *Am J Pathol*, 182(5), pp. 1718-26.

13. Uchida, Y., Nakano, S., Gomi, F. and Takahashi, H. (2011) 'Up-regulation of calsyntenin-3 by beta-amyloid increases vulnerability of cortical neurons', *FEBS Lett*, 585(4), pp. 651-6.

14. Um, J.W., Pramanik, G., Ko, J.S., Song, M.Y., Lee, D., Kim, H., Park, K.S., Sudhof, T.C., Tabuchi, K. and Ko, J. (2014) 'Calsyntenins function as synaptogenic adhesion molecules in concert with neurexins', *Cell Rep*, 6(6), pp. 1096-109.

15. Yu, F.H., Mantegazza, M., Westenbroek, R.E., Robbins, C.A., Kalume, F., Burton, K.A., Spain, W.J., McKnight, G.S., Scheuer, T. and Catterall, W.A. (2006) 'Reduced sodium current in GABAergic interneurons in a mouse model of severe myoclonic epilepsy in infancy', *Nat Neurosci*, 9(9), pp. 1142-9.

Chapter 8 Effects of 4-aminopyridine on intrinsic properties of neocortical parvalbumin-positive interneurons

8.1 Introduction

Parvalbumin-positive (PV+) fast-spiking interneurons target the somatic, initial axonic, and proximal dendritic domain of pyramidal neurons and regulate the output of postsynaptic neurons (Cobb *et al.*, 1995; Freund and Buzsaki, 1996; Atallah *et al.*, 2012; Hu *et al.*, 2014). Population of PV+ interneurons are mutually interconnected via chemical synapses and gap-junctions forming a syncytium of PV+ interneurons (Galarreta and Hestrin, 1999; Galarreta and Hestrin, 2002; Hormuzdi *et al.*, 2004). The fast spiking phenotype of PV+ interneurons is attributed to the presence of Kv3.1 and Kv3.2 subtypes of voltage-gated potassium channels (Erisir *et al.*, 1999). During an action potential, Kv3.1-3.2 channels facilitate de-inactivation of voltage-gated sodium channels, and reduce the duration of after-hyperpolarisation (Erisir *et al.*, 1999). This enables PV+ interneurons to fire action potentials at a higher frequency. Another feature of PV+ interneurons is the presence of membrane potential oscillations at depolarised membrane potentials. Injecting steady depolarising current into striatal fast spiking interneurons was reported to evoke bursts of action potentials interspersed with subthreshold membrane potential oscillations (MPO) (Bracci *et al.*, 2003). MPOs were voltage-dependent and were absent at relatively hyperpolarised membrane potentials. At depolarised levels, MPOs triggered and maintained rhythmic bursts of action potentials (Bracci *et al.*, 2003).

In cortical epilepsy, the onset of ictal events was also shown to be associated with synchronised activity of GABAergic networks (Lopantsev and Avoli, 1998; Yekhlef *et al.*, 2015; de Curtis and Avoli, 2016). Synchronised GABAergic activity leads to increased extracellular potassium levels that in turn, cause hyperexcitability of the network and leads to initiation of ictal events (Barolet and Morris, 1991; Yekhlef *et al.*, 2015). Synchronised GABAergic activity mediated increases in extracellular potassium levels could be because of increased firing of GABAergic interneurons, and increased activity of potassium-chloride cotransporters in the postsynaptic neurons (Viitanen *et al.*, 2010; Hamidi and Avoli, 2015; de Curtis and Avoli, 2016). However, PV+ interneurons were also shown to provide a powerful feedforward inhibition ahead of

the ictal wavefront to check or slowdown the spread of ictal activity and recruitment of surrounding territories (Trevelyan *et al.*, 2006; Trevelyan *et al.*, 2007; Cammarota *et al.*, 2013). When this inhibitory restraint fails, the ictal wavefront recruit neurons in the surrounding territories and the activity begins to spread across the tissue. One of the reasons for the collapse of the inhibitory restraint is the failure of the interneurons to fire action potentials after receiving sustained high-frequency depolarising inputs (Cammarota *et al.*, 2013; Losi *et al.*, 2016). To further understand the behaviour of PV+ interneurons in epileptic networks, it is necessary to study how the intrinsic properties of PV+ interneurons are altered in proepileptic media.

In the present study, I show that PV+ interneurons show increased followed by decreased firing activity in response to increasing levels of depolarising current injections in 4-aminopyridine. At higher depolarising current injections, PV+ interneurons in 4-aminopyridine fired lower number of action potentials compared to controls, suggesting the firing potential of PV+ interneurons is reduced in epileptic conditions. I then showed the development and the nature of membrane potential oscillation in PV+ interneurons in presence of 4-aminopyridine that may play a role in synchronisation in epileptic networks. Studying these aspects of PV+ interneurons in different conditions will advance our knowledge of the intrinsic properties of PV+ interneurons, how they are modified and their role in epileptic conditions.

8.2 Materials and methods

8.2.1 *Slice preparation*

Patch-clamp experiments described below were performed in coronal slices containing visual cortex that were prepared and stored as described in *slice preparation method 3* (chapter 2, sub-heading 2.4.3).

8.2.2 *Electrophysiology, protocols, and drugs*

Selective fluorescent labelling of PV+ interneurons was achieved by doing intra-cortical injections of AAV9.hEF1a.lox.mCherry.lox.mTFP1 virus (UPENN Vector Core, USA) in PV-Cre mice (Stock # 008069, The Jackson Laboratory, USA). Details of this procedure was mentioned in Chapter 2, section 2.3. Fluorescently labelled PV+ interneurons in visual cortex (layers 4-6) were targeted for whole-cell recordings. PV+ interneurons were patched in voltage-clamp mode (V_{hold} at -70 mV) and later switched to current clamp (without injecting current) for the rest of the experiments. Patched neurons were confirmed as PV+ interneurons based on the fluorescent tag and on the fast-spiking properties of the neurons. Input resistance was calculated by injecting hyperpolarising current (-100 pA, 100 ms) in current-clamp or by giving a depolarising step (10 mV, 500 ms) in voltage-clamp mode.

All experiments were performed in the presence of ionotropic glutamate receptors antagonists, 50 µM D-AP5 (NMDAR antagonist), 20 µM NBQX (AMPA/kainate receptor antagonist), and GABA receptors antagonists, 10 µM gabazine (GABA$_A$R antagonist) and 5 µM CGP-55845 (GABA$_B$R antagonist). From here on, ACSF with glutamatergic and GABAergic antagonists will be referred to as 'synaptic blockers'.

The firing properties of PV+ interneurons were assessed in 4AP with synaptic blockers (4AP+synaptic blockers) model. Experiments in ACSF+synaptic blockers were considered as controls. The protocol to assess the firing properties was as follows: 10 s sweeps each with 3 seconds hyperpolarisation/depolarisation step (first level: -100 pA, with increments of 100 pA, 8-10 steps) at the beginning of the sweep, and a hyperpolarisation step (-100 pA, 100 ms) towards the end of the sweep. In each

patched neuron, this protocol was first executed in ACSF+synaptic blockers followed by 4AP+synaptic blockers.

To examine the membrane potential oscillations (MPO), PV+ interneurons were patched followed by bathing in 4AP+synaptic blockers, and after MPOs developed, different drugs were added to the perfusate. The following drugs were used in separate experiments in 4AP/blockers ACSF: 50 µM ZD7822 (HCN-channel blocker), 100 µM quinine (gap-junction blocker), and 1 µM tetrodotoxin (TTX; voltage-gated sodium channel blocker). In almost all the patching experiments, KMeSO$_4$-based electrode filling solution was used. To chelate intracellular calcium ions, electrode filling solution was supplemented also with BAPTA, a fast Ca^{2+} chelator.

8.2.3 *Data analysis*

Data was analysed as described in chapter 2 (sub-heading 2.7). Inter-spike interval is the time interval between the peaks of two consecutive action potentials. Firing rate (in Hz) was calculated by using the formula: 1/average (inter-spike interval), that is as the inverse of average inter-spike interval. Frequency (in Hz) of membrane potential oscillations was calculated by the inverse of the time interval between two consecutive peaks (Figure 8.3C, red line).

8.3 Results

8.3.1 *Effect of 4AP on the number of action potentials and firing rate properties of PV+ interneurons*

In presence of 4AP+synaptic blockers, membrane potentials (MP) and input resistance of PV+ interneurons were increased compared with controls (MP: controls, -62.7 ± 2.8 mV, n = 8; 4AP+synaptic blockers, -60.3 ± 3.3 mV, n = 8; paired Student's t-test, p = 0.03; input resistance: control, 120.5 ± 9.9 MΩ, n = 8; 4AP+synaptic blockers, 142.3 ± 9.4 MΩ, n = 8; paired Student's t-test, p < 0.01).

In controls, PV+ interneurons fired action potentials for the entire duration of depolarisation steps at both relatively low (100-400 pA) (Figure 8.1 Ai) and high intensities (400-800 pA) (Figure 8.1 Aii; Table 1). In 4AP+synaptic blockers, at low intensity depolarisation steps, PV+ interneurons fired for the entire durations and with an increased number of action potentials (Figure 8.1 Bi). But with further increases in the intensity, PV+ interneurons failed to sustain the firing activity (Figure 8.1 Bii; 8.2 Ai, Aii; Table 8.1). A similar trend was observed in the average firing rate (Figure 8.2 Bi, Bii; Table 8.2) and maximal firing rate of PV+ interneurons (Figure 8.2 Ci, Cii, Table 8.3).

One notable feature of PV+ interneurons in 4AP+synaptic blockers was the development of membrane potential oscillations (MPO) after depolarisation steps. Immediately after the 3 seconds depolarisation step, the membrane potential undershoots to hyperpolarising potentials, and as the membrane recovers to baseline membrane potentials, brief MPOs were developed in the range of 3-5 Hz (3.90 ± 0.27 Hz; n = 4), and in two cells, they facilitated firing of action potentials (Figure 8.1B).

158

A. PV+ interneuron in ACSF+Synaptic blockers

Ai. I-inj: 300pA
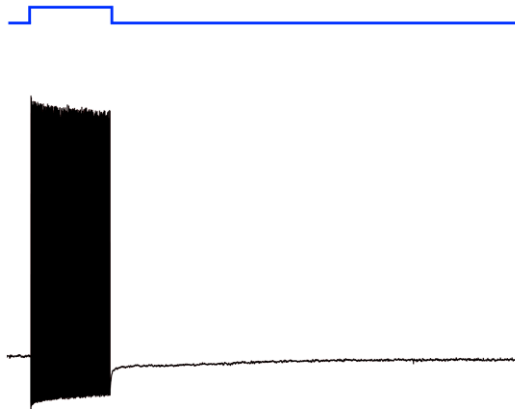
Aii. I-inj: 800pA

B. PV+ interneuron in 4AP+Synaptic blockers
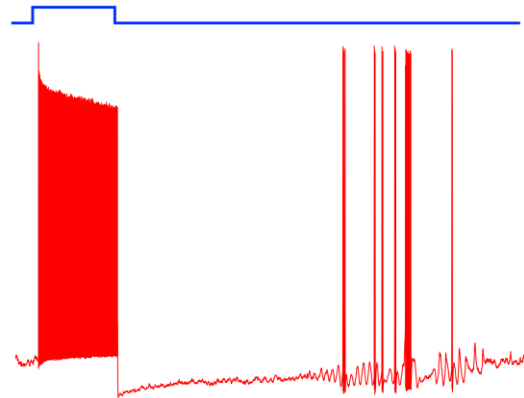
Bi. I-inj: 300pA

Bii. I-inj: 800pA

15mV
2s

15mV
2s
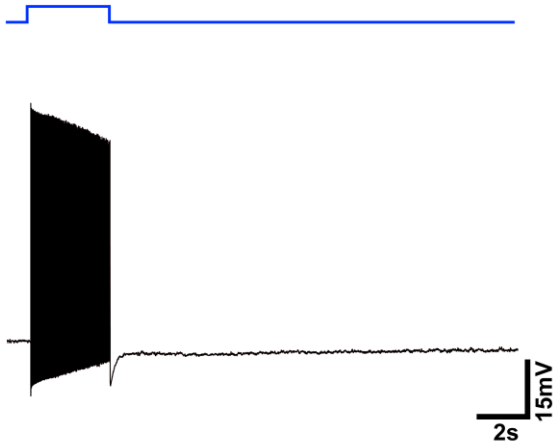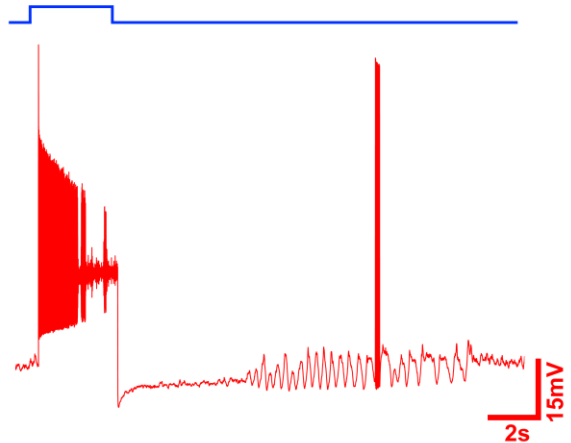
Figure 8.1 Representative traces showing a PV+ interneurons response to depolarising current injections (I-inj) in (A) ACSF+synaptic blockers (control) and (B) 4AP+synaptic blockers. In control conditions, PV+ interneurons successfully fired action potentials throughout the duration of depolarising steps at both lower (Ai, 300 pA) and higher (Aii, 800 pA) intensities. In 4AP+synaptic blockers, the same PV+ interneurons fired action potentials throughout the duration of lower intensity depolarising step (Bi, 300 pA), but failed to sustain the action potentials at higher intensity (Bii, 800 pA). In 4AP+synaptic blockers, at both intensities, MPOs were developed during the membrane potential recovery period after the depolarisation step (Bi, Bii). Note: scale bars at the bottom in panel Aii and Bii are applicable to Ai and Bi, respectively.
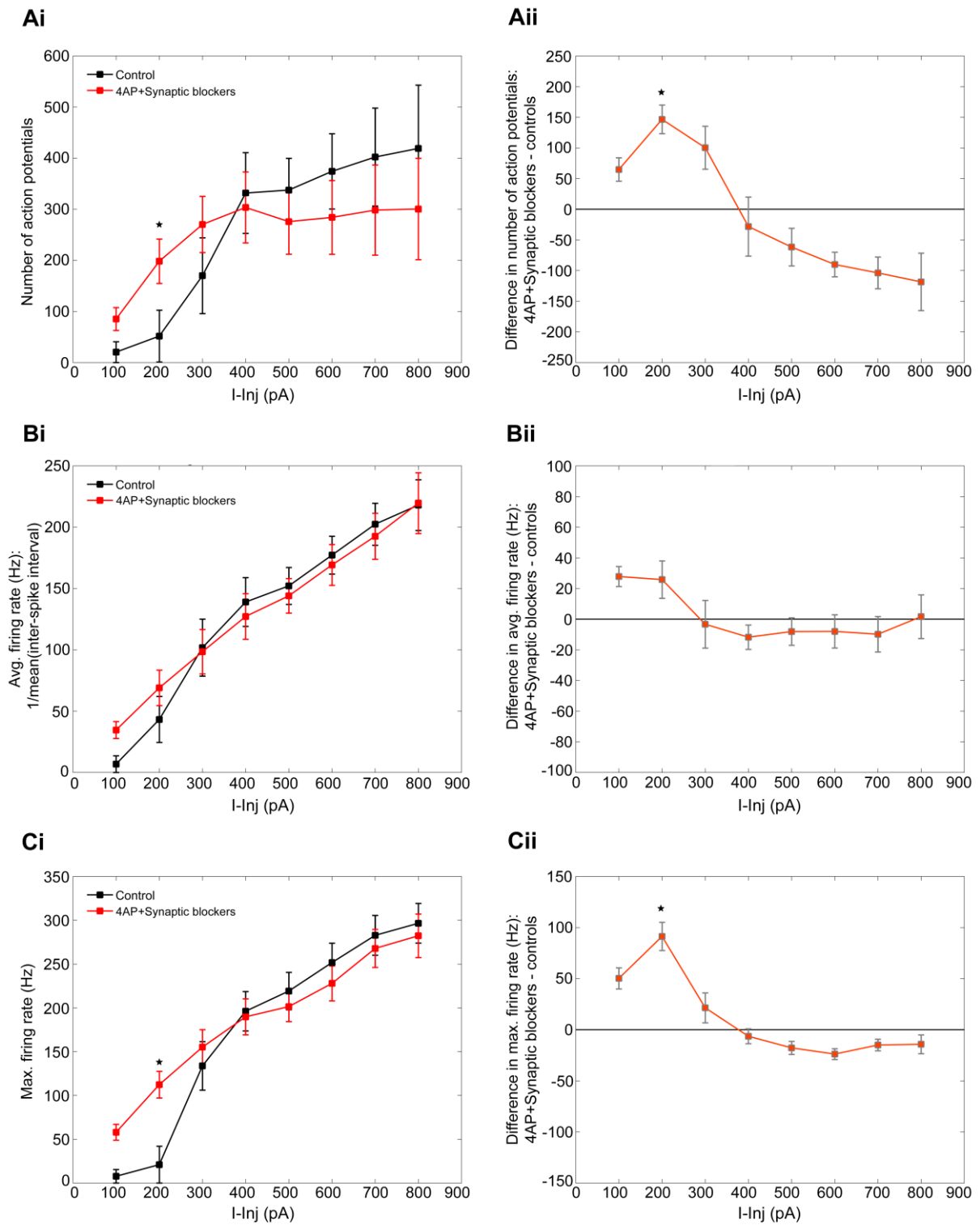
Figure 8.2 Graphs displaying pooled data for the number of action potentials (Ai), average firing rate (Bi), and maximal firing rate (Ci) of the same PV+ interneurons in control and 4AP+synaptic blockers. The difference in number of action potentials, average firing rate, and maximal firing rate between 4AP+synaptic blockers and controls were charted in Aii, Bii, and Cii, respectively. *Paired Student's t-test with p-values less than the Bonferroni corrected critical value (α): 0.006. See Table 8.1, 8.2, and 8.3 for mean ± s.e.m and p-values.

Number of action potentials				
Depolarisation current injection (pA)	Control	4AP+Synaptic blockers	Difference (n)	p-values ^(α = 0.006)
100	20.3 ± 20.3	85.1 ± 22.4	64.8 ± 19.1 (9)	0.009
200	51.7 ± 50.7	198.2 ± 43.5	146.5 ± 23.3 (9)	*0.0002
300	169.9 ± 74.3	270.2 ± 55.0	100.3 ± 35.1 (9)	0.021
400	331.7 ± 78.9	303.4 ± 64.5	-28.2 ± 48.1 (9)	0.57
500	337.5 ± 62.1	275.8 ± 63.7	-61.8 ± 30.7 (8)	0.08
600	374.1 ± 73.5	284.0 ± 72.2	-90.1 ± 19.9 (8)	0.002
700	402.1 ± 95.8	298.3 ± 88.2	-103.9 ± 25.9 (7)	0.007
800	419.0 ± 124.1	300.5 ± 99.1	-118.5 ± 46.8 (6)	0.052

Table 8.1 Number of action potentials fired by PV+ interneurons at different depolarising current injections in control and 4AP+synaptic blockers. *p-values less than the ^Bonferroni corrected critical value (α).

Firing rate (Hz)				
Depolarisation current injection (pA)	**Control**	**4AP+Synaptic blockers**	**Difference (n)**	**p-values** **^(α = 0.006)**
100	6.8 ± 6.8	34.6 ± 6.9	27.8 ± 6.5 (9)	0.016
200	43.2 ± 18.7	68.9 ± 14.4	25.8 ± 12.2 (9)	0.536
300	101.8 ± 23.2	98.4 ± 18.1	-3.3 ± 15.6 (9)	0.836
400	138.9 ± 19.9	127.2 ± 18.6	-11.8 ± 7.9 (9)	0.176
500	152.1 ± 15.1	143.9 ± 14.1	-8.1 ± 8.9 (8)	0.395
600	177.2 ±15.4	169.2 ± 16.7	-8.0 ± 10.8 (8)	0.482
700	202.4 ± 17.1	192.6 ± 18.8	-9.9 ± 11.5 (7)	0.426
800	217.9 ± 20.7	219.6 ± 24.8	1.6 ± 14.2 (6)	0.913

Table 8.2 Firing rate of action potentials by PV+ interneurons at different depolarising current injections in control and 4AP+synaptic blockers. *p-values less than the **^**Bonferroni corrected critical value (α).

Maximal firing rate (Hz)				
Depolarisation current injection (pA)	Control	4AP+Synaptic blockers	Difference (n)	p-values ^(α = 0.006)
100	7.7 ± 7.7	57.9 ± 9.1	50.3 ± 10.3 (9)	0.008
200	20.9 ± 20.9	112.3 ± 15.2	91.3 ± 13.8 (9)	*0.001
300	133.7 ± 27.7	155.2 ± 19.9	21.4 ± 14.6 (9)	0.180
400	196.1 ± 22.5	189.7 ± 20.5	-6.4 ± 7.28 (9)	0.405
500	219.2 ± 21.3	201.4 ± 17.1	-17.7 ± 6.4 (8)	0.216
600	251.7 ± 22.1	227.9 ± 19.9	-23.8 ± 5.2 (8)	0.001
700	282.8 ± 22.7	267.8 ± 21.7	-14.9 ± 5.7 (7)	0.304
800	296.5 ± 22.7	282.3 ± 24.8	-14.3 ± 9.2 (6)	0.181

Table 8.3 Maximal firing rate of action potentials by PV+ interneurons at different depolarising current injections in control and 4AP+synaptic blockers. *p-values less than the ^Bonferroni corrected critical value (α).

8.3.2 *4AP induced sustained firing activity and MPOs in PV+ interneurons*

In the absence of glutamatergic and GABAergic transmission, washing in 4AP+synaptic blockers induced the development of recurrent bursts of action potentials in PV+ interneurons (Figure 8.3 A). Following burst of action potentials, spontaneous MPOs developed that were occurring at a frequency of 5.17 ± 0.10 Hz (n = 5) at membrane potentials of -60.90 ± 2.12 mV (n=5) (Figure 8.3 B, C). In four of five experiments, MPOs appeared to sustain and facilitate the firing of action potential (Figure 8.3 B), whereas in other recordings membrane potential oscillations dissipated.

A. PV+ interneuron in 4AP+Synaptic blockers

MP: -77.8mV

10mV

30s
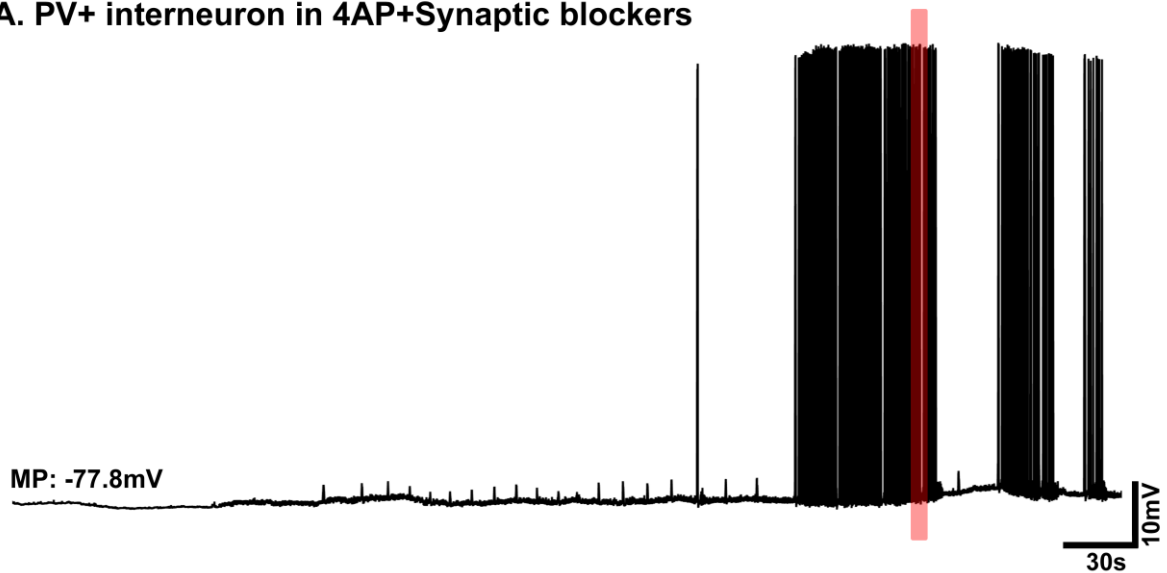
B. Action potentials and MPOs

10mV

2s

C. MPOs

1.5mV
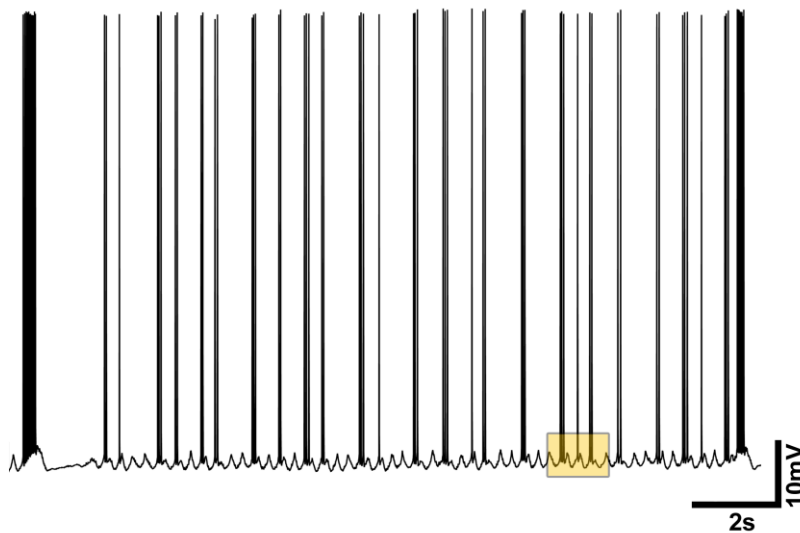
400ms
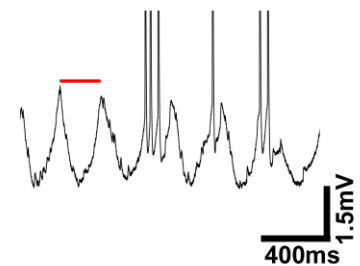
Figure 8.3 A. In 4AP+synaptic blockers, PV+ interneurons developed rhythmic bursts of action potentials and membrane potential oscillations (MPOs). B. Bursts of action potentials interspersed with MPOs. Enlarged view of the highlighted area (red) in panel A. C. Membrane potential oscillations developed at nearly -77.8 mV membrane potential in 4AP+synaptic blockers. Red line – peak to peak time used for calculating frequencies of MPOs. Enlarged view of the highlighted area (yellow) in panel B.

8.3.3 *Intracellular calcium ions were not necessary for the development of 4AP-induced MPOs in PV+ interneurons*

To examine if intracellular calcium ions and calcium-activated potassium currents were required for the generation of 4AP-induced MPOs, PV+ interneurons were patched with KMeSO$_4$/BAPTA-based EFS. BAPTA was used in the EFS to chelate the intracellular calcium ions. In all three experiments, washing in 4AP+synaptic blockers induced firing of action potentials and the development of MPOs (Figure 8.4). However, MPOs occurred at a higher rate in calcium ions-chelated PV+ interneurons than in the non-chelated PV+ interneurons (MPOs: non-chelated PV+ interneurons, 5.17 ± 0.10 Hz, n = 5; calcium-chelated PV+ interneurons, 6.59 ± 0.42 Hz, n = 3; unpaired Student's t-test, p = 0.017). This suggested neither intracellular calcium ions nor calcium-activated potassium currents were required for the generation of MPOs in PV+ interneurons but they may have a modulatory role.
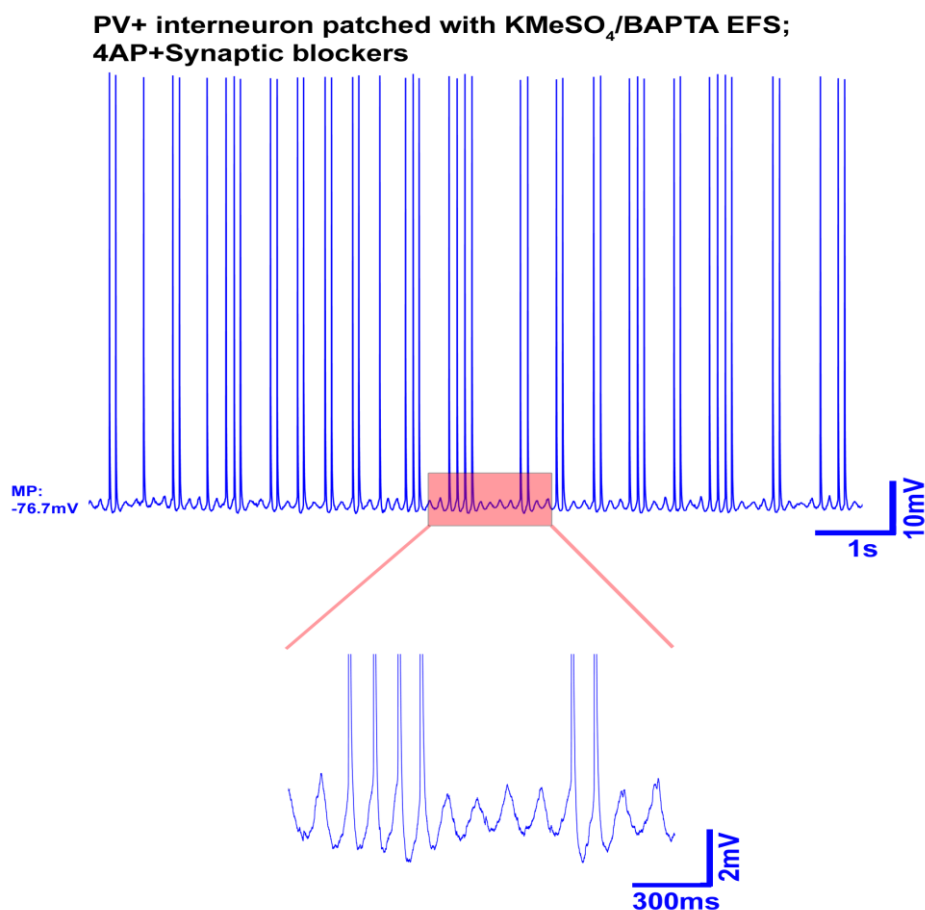
Figure 8.4 PV+ interneurons patched with KMeSO$_4$/BAPTA-based EFS, to chelate intracellular calcium ions, developed action potentials and MPOs in 4AP+synaptic blockers.

8.3.4 *Inhibition of HCN-channels altered 4AP-induced firing pattern and abolished MPOs in PV+ interneurons*

In 4AP+synaptic blockers, inhibiting HCN-channels transformed the firing pattern of PV+ interneurons from rhythmic bursts of action potentials (Figure 8.5 A) to the development of large membrane depolarisations superimposed with action potentials (Figure 8.5 B). Furthermore, spontaneously occurring 4AP+synaptic blockers-induced MPOs were completely abolished (Figure 8.5 B). Tonic excitatory drive mediated by HCN channels shaped the firing pattern of PV+ interneurons, and was necessary for maintenance and generation of MPOs.

A. PV+ interneuron in 4AP+Synaptic blockers

MP: -53.8mV　　　　　　　　10mV　　2s

B. PV+ interneuron in 4AP+Synaptic blockers + ZD7822

MP: -52.0mV　　　　　　　　10mV　　2s
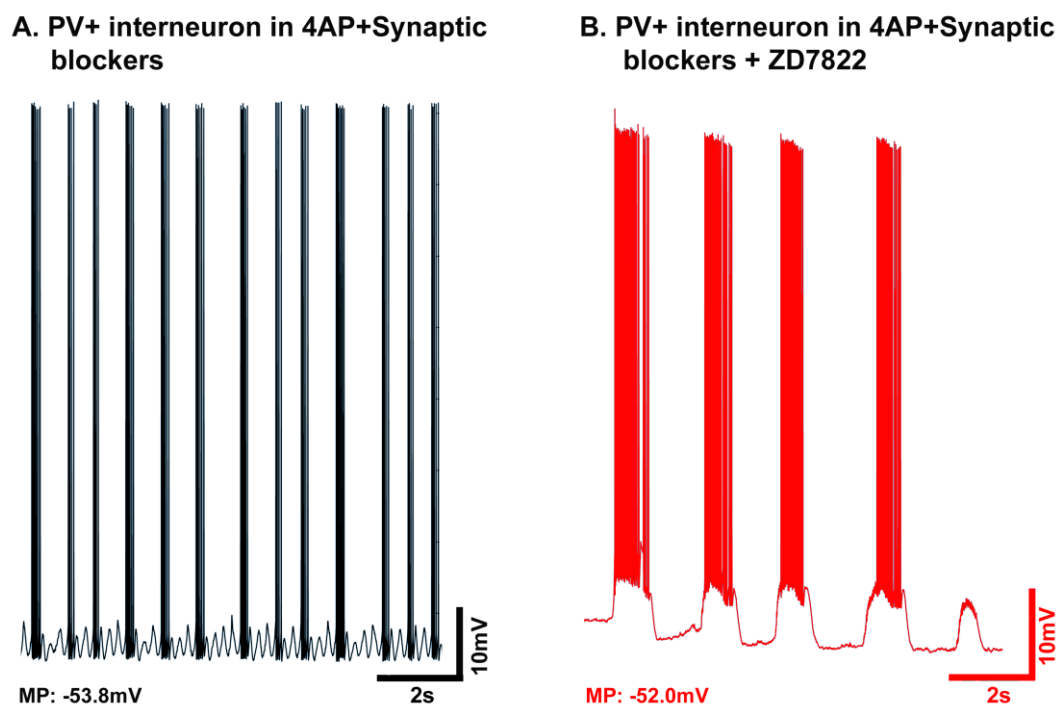
Figure 8.5 Blocking HCN channels modified the pattern of action potentials firing and suppressed MPOs in PV+ interneurons that were already developed in 4AP+synaptic blockers.

8.3.5 *Quinine reduced 4AP-induced bursts of action potentials and modulated MPOs*

PV+ interneurons communicate with other PV+ interneurons via chemical synapses and electrical synapses (gap-junctions). In these experiments, I used quinine, a gap-junction blocker, to examine the role of gap-junctions in sustaining

MPOs (Srinivas *et al.*, 2001). Quinine was added to the perfusate after the development of 4AP+synaptic blockers-induced MPOs. Quinine reduced the number of bursts of action potentials, but generally did not abolish MPOs (Figure 8.6). In three of four experiments, the frequencies of MPOs were significantly reduced (without quinine, 3.87 ± 0.13 Hz; with quinine, 2.21 ± 0.28 Hz; paired Student's t-test, p = 0.008; n = 3), and in one other experiment, action potentials and MPOs were completely abolished.
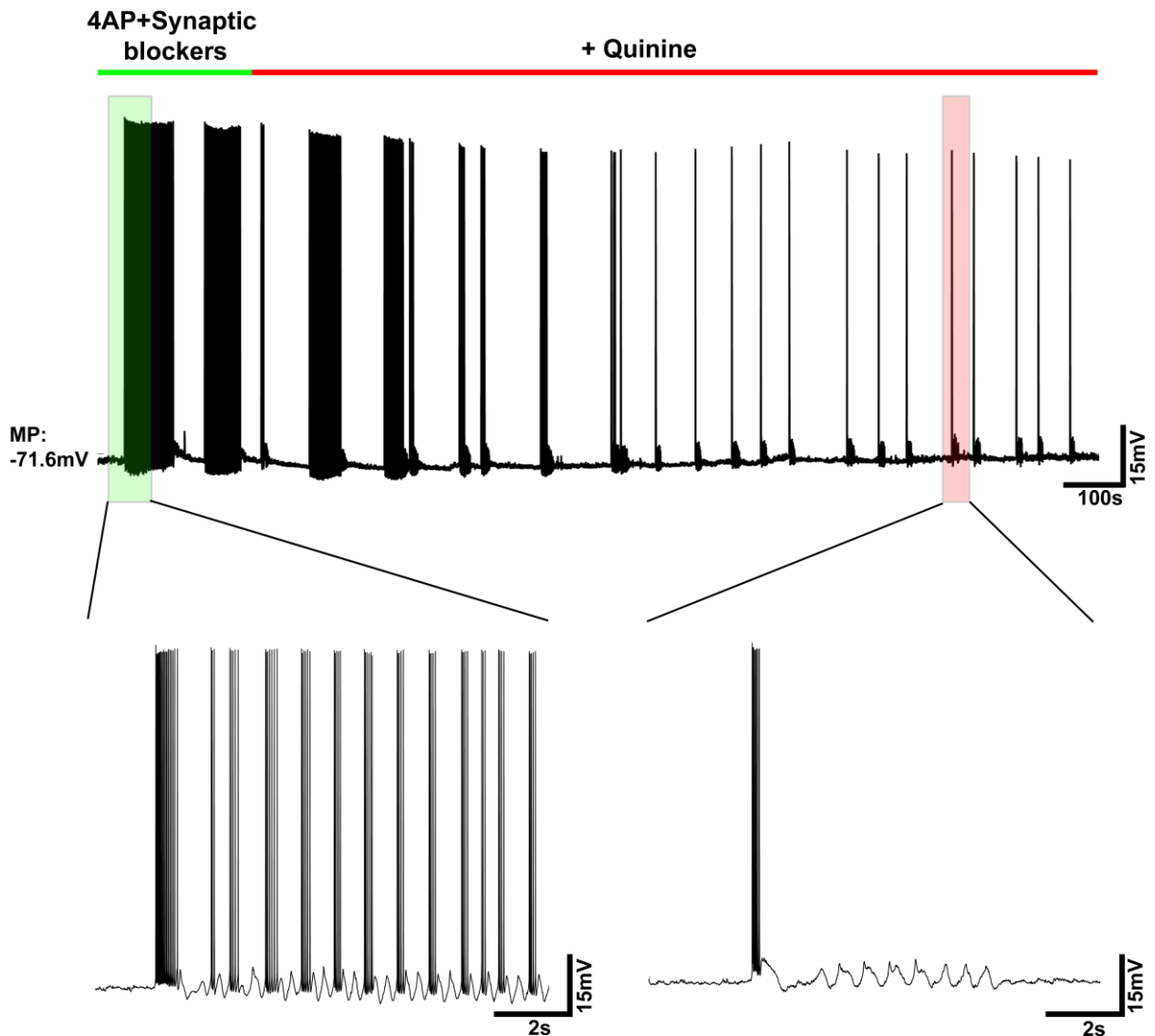
Figure 8.6 Quinine reduced the number of action potentials bursts and the frequency of MPOs in PV+ interneuron bathed in 4AP+synaptic blockers. Top trace: green bar, 4AP+synaptic blockers; red bar, quinine in 4AP+synaptic blockers. Bottom left, 4AP+synaptic blockers induced activity (enlarged view of the green highlighted area in top trace). Bottom right, activity recorded in 4AP+synaptic blockers+quinine (enlarged view of the red highlighted area in top trace).

8.3.6 *Tetrodotoxin blocked both 4AP-induced action potentials and MPOs*

Addition of voltage-gated sodium channels (VGSC) blocker, tetrodotoxin, to the perfusate suppressed the already developed 4AP+synaptic blockers-induced bursts of action potentials and MPOs in PV+ interneurons, suggesting a strong dependency of MPOs on VGSCs (Figure 8.7).
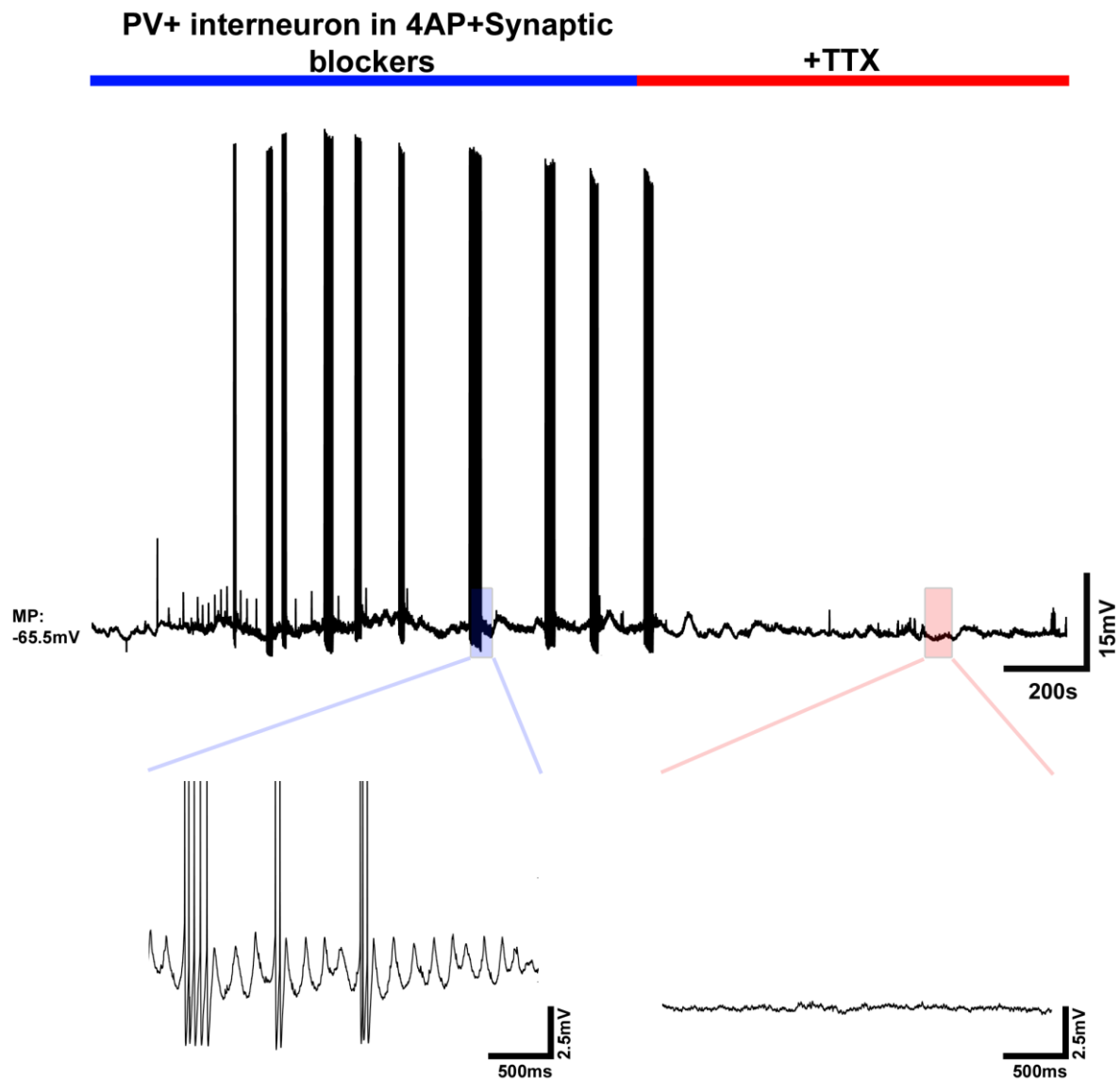
Figure 8.7 Inhibiting voltage-gated sodium channels with tetrodotoxin (TTX) abolished both 4AP+synaptic blockers induced action potential bursts and MPOs. Top trace: blue bar, 4AP+synaptic blockers; red bar, TTX in 4AP+synaptic blockers. Bottom left, 4AP+synaptic blockers induced activity (enlarged view of the blue highlighted area in top trace). Bottom right, PV+ interneurons responses recorded in 4AP+synaptic blockers+TTX (enlarged view of the red highlighted area in top trace).

8.4 Discussion

These results show that the firing capability of PV+ interneurons was altered by 4AP. In both, 4AP+synaptic blockers and control conditions, the number of action potentials fired by PV+ interneurons steeply increased with increasing intensity of depolarising current injections (I-inj) until 400 pA. At lower intensities of current injections (I-inj < 400 pA), the excitability of PV+ interneurons was enhanced in 4AP+synaptic blockers compared with control conditions; that is, they fired at a higher mean rate and also had a greater maximal firing rate. This pattern in 4AP+synaptic blockers was flipped with further increasing I-inj. In 4AP+synaptic blockers, for I-inj > 400 pA, the number of action potentials fired plateaued, whereas, in controls, PV+ interneurons continued to fire increasing number of action potentials. This plateauing effect observed in 4AP+synaptic blockers could have been due to the depolarisation block of the neurons (Losi *et al.*, 2016). Although there was no further increase in the number of action potentials in 4AP+synaptic blockers, the firing rate continued to rise with increasing current injection. The average firing rate was similar in both the conditions, but PV+ interneurons in controls had greater maximal firing rates.

Membrane potential oscillations (MPO) have previously been reported in striatal fast-spiking interneurons (Bracci *et al.*, 2003), stellate cells in the entorhinal cortex (Alonso and Llinas, 1989), and regular spiking neurons in the somatosensory cortex (Amitai, 1994). MPOs were shown to develop in ACSF at depolarised potentials after somatic current injections. In this study, I showed that in the absence of transmitter mediated currents, 4AP induced action potentials and MPOs, and these MPOs developed spontaneously relatively hyperpolarised membrane potentials (-60.90 ± 2.12 mV; n = 5). 4AP+synaptic blockers-induced MPOs were abolished in the presence of either HCN-channels blocker (ZD7822) or voltage-gated sodium ion channels blocker (TTX), suggesting these two channels were required for the development of MPOs. This was similar to the MPOs described in different cell types (Alonso and Llinas, 1989; Amitai, 1994; Bracci et al., 2003). Dickson et al. (2000) reported MPOs at depolarised membrane potentials in stellate cells of the entorhinal cortex, and proposed an interplay between persistent sodium currents and HCN mediated currents as a requirement for the generation of MPOs at depolarised levels (Dickson *et al.*, 2000). Adding to it, my results indicate a role of 4AP-sensitive voltage-gated potassium channels in setting the threshold of the membrane potential oscillations.

169

In earlier studies, it was demonstrated that the membrane oscillations triggered the first action potential firing after a quiescent period at depolarised potentials (Bracci *et al.*, 2003). In the current study though, at relatively hyperpolarised membrane potentials, MPOs developed following a burst of action potentials and were then sustained for a period by an intrinsic mechanism (see Figure 8.6, lower left trace). However, action potentials triggered by MPOs were also observed, but during the recovery of the membrane potential from hyperpolarisation potentials after the depolarisation step (see Figure 8.1 B). Furthermore, chelating intracellular calcium ions increased the frequency of 4AP+synaptic blockers-induced MPOs. It needs to be tested whether this effect was because of blockade of the calcium-activated potassium currents.

Cortical PV+ interneurons are highly interconnected via chemical synapses and gap-junctions (electrical synapses) forming a syncytium of PV+ interneurons (Galarreta and Hestrin, 1999; Galarreta and Hestrin, 2002; Hormuzdi *et al.*, 2004). Gap-junctions enable PV+ interneurons to synchronise and enhance their spiking activity and coordinate the activity of the network (Galarreta and Hestrin, 1999; Deans *et al.*, 2001; Hjorth *et al.*, 2009). Blocking gap-junctions with quinine modulated the firing pattern and MPOs recorded in PV+ interneurons in 4AP+synaptic blockers. Both, the number of bursts of action potentials and frequency of MPOs were reduced after blocking gap-junctions. Along with blocking gap-junctions, quinine also has other effects; it reduces the firing of neurons in a voltage-dependent manner and thereby reducing the accumulation of extracellular potassium ion concentrations (Bikson *et al.*, 2002). Kinetics of certain voltage-dependent potassium channels was also reported to be altered by quinine (Kotani *et al.*, 2001). Hence, it is important to confirm the role of gap-junctions on membrane potential oscillations in PV+ interneuron with a more specific gap-junction blocker.

PV+ interneurons were shown to be involved in maintaining epileptiform activity by firing during synchronous after-discharges (Ellender *et al.*, 2014). Membrane potential oscillations in PV+ interneurons could be involved in maintaining this pattern of activity during an ictal event and enhance their firing synchronicity via gap-junctions. These can be examined by recording simultaneously from synaptically coupled PV+ interneuron and pyramidal neurons, and gap-junction coupled PV+ interneurons,

respectively, in brain slices acutely challenged with pro-epileptic media. Results described in this chapter and aforementioned future studies will help us to better understand the role of membrane potential oscillations in regulating the activity of interconnected PV+ interneurons and their involvement in epileptic network activity.

8.5 References

1. Alonso, A. and Llinas, R.R. (1989) 'Subthreshold Na+-dependent theta-like rhythmicity in stellate cells of entorhinal cortex layer II', *Nature*, 342(6246), pp. 175-7.

2. Amitai, Y. (1994) 'Membrane potential oscillations underlying firing patterns in neocortical neurons', *Neuroscience*, 63(1), pp. 151-61.

3. Atallah, B.V., Bruns, W., Carandini, M. and Scanziani, M. (2012) 'Parvalbumin-expressing interneurons linearly transform cortical responses to visual stimuli', *Neuron*, 73(1), pp. 159-70.

4. Barolet, A.W. and Morris, M.E. (1991) 'Changes in extracellular K+ evoked by GABA, THIP and baclofen in the guinea-pig hippocampal slice', *Exp Brain Res*, 84(3), pp. 591-8.

5. Bikson, M., Id Bihi, R., Vreugdenhil, M., Kohling, R., Fox, J.E. and Jefferys, J.G. (2002) 'Quinine suppresses extracellular potassium transients and ictal epileptiform activity without decreasing neuronal excitability *in vitro*', *Neuroscience*, 115(1), pp. 251-61.

6. Bracci, E., Centonze, D., Bernardi, G. and Calabresi, P. (2003) 'Voltage-dependent membrane potential oscillations of rat striatal fast-spiking interneurons', *J Physiol*, 549(Pt 1), pp. 121-30.

7. Cammarota, M., Losi, G., Chiavegato, A., Zonta, M. and Carmignoto, G. (2013) 'Fast spiking interneuron control of seizure propagation in a cortical slice model of focal epilepsy', *J Physiol*, 591(4), pp. 807-22.

8. Cobb, S.R., Buhl, E.H., Halasy, K., Paulsen, O. and Somogyi, P. (1995) 'Synchronization of neuronal activity in hippocampus by individual GABAergic interneurons', *Nature*, 378(6552), pp. 75-8.

9. de Curtis, M. and Avoli, M. (2016) 'GABAergic networks jump-start focal seizures', *Epilepsia*, 57(5), pp. 679-87.

10. Deans, M.R., Gibson, J.R., Sellitto, C., Connors, B.W. and Paul, D.L. (2001) 'Synchronous activity of inhibitory networks in neocortex requires electrical synapses containing connexin36', *Neuron*, 31(3), pp. 477-85.

11. Dickson, C.T., Magistretti, J., Shalinsky, M.H., Fransen, E., Hasselmo, M.E. and Alonso, A. (2000) 'Properties and role of I(h) in the pacing of subthreshold oscillations in entorhinal cortex layer II neurons', *J Neurophysiol*, 83(5), pp. 2562-79.

12. Ellender, T.J., Raimondo, J.V., Irkle, A., Lamsa, K.P. and Akerman, C.J. (2014) 'Excitatory effects of parvalbumin-expressing interneurons maintain hippocampal epileptiform activity via synchronous afterdischarges', *J Neurosci*, 34(46), pp. 15208-22.

13. Erisir, A., Lau, D., Rudy, B. and Leonard, C.S. (1999) 'Function of specific K(+) channels in sustained high-frequency firing of fast-spiking neocortical interneurons', *J Neurophysiol*, 82(5), pp. 2476-89.

14. Freund, T.F. and Buzsaki, G. (1996) 'Interneurons of the hippocampus', *Hippocampus*, 6(4), pp. 347-470.

15. Galarreta, M. and Hestrin, S. (1999) 'A network of fast-spiking cells in the neocortex connected by electrical synapses', *Nature*, 402(6757), pp. 72-5.

16. Galarreta, M. and Hestrin, S. (2002) 'Electrical and chemical synapses among parvalbumin fast-spiking GABAergic interneurons in adult mouse neocortex', *Proc Natl Acad Sci U S A*, 99(19), pp. 12438-43.

17. Hamidi, S. and Avoli, M. (2015) 'KCC2 function modulates *in vitro* ictogenesis', *Neurobiol Dis*, 79, pp. 51-8.

18. Hjorth, J., Blackwell, K.T. and Kotaleski, J.H. (2009) 'Gap junctions between striatal fast-spiking interneurons regulate spiking activity and synchronization as a function of cortical activity', *J Neurosci*, 29(16), pp. 5276-86.

19. Hormuzdi, S.G., Filippov, M.A., Mitropoulou, G., Monyer, H. and Bruzzone, R. (2004) 'Electrical synapses: a dynamic signaling system that shapes the activity of neuronal networks', *Biochim Biophys Acta*, 1662(1-2), pp. 113-37.

20. Hu, H., Gan, J. and Jonas, P. (2014) 'Interneurons. Fast-spiking, parvalbumin(+) GABAergic interneurons: from cellular design to microcircuit function', *Science*, 345(6196), p. 1255263.

21. Kotani, S., Hasegawa, J., Meng, H., Suzuki, T., Sato, K., Sakakibara, M., Takiguchi, M. and Tokimasa, T. (2001) 'Hyperpolarizing shift by quinine in the steady-state inactivation curve of delayed rectifier-type potassium current in bullfrog sympathetic neurons', *Neurosci Lett*, 300(2), pp. 87-90.

22. Lopantsev, V. and Avoli, M. (1998) 'Participation of GABAA-mediated inhibition in ictallike discharges in the rat entorhinal cortex', *J Neurophysiol*, 79(1), pp. 352-60.

23. Losi, G., Marcon, I., Mariotti, L., Sessolo, M., Chiavegato, A. and Carmignoto, G. (2016) 'A brain slice experimental model to study the generation and the propagation of focally-induced epileptiform activity', *J Neurosci Methods*, 260, pp. 125-31.

24. Srinivas, M., Hopperstad, M.G. and Spray, D.C. (2001) 'Quinine blocks specific gap junction channel subtypes', *Proc Natl Acad Sci U S A*, 98(19), pp. 10942-7.

25. Trevelyan, A.J., Sussillo, D., Watson, B.O. and Yuste, R. (2006) 'Modular propagation of epileptiform activity: evidence for an inhibitory veto in neocortex', *J Neurosci*, 26(48), pp. 12447-55.

26. Trevelyan, A.J., Sussillo, D. and Yuste, R. (2007) 'Feedforward inhibition contributes to the control of epileptiform propagation speed', *J Neurosci*, 27(13), pp. 3383-7.

27. Viitanen, T., Ruusuvuori, E., Kaila, K. and Voipio, J. (2010) 'The K+-Cl cotransporter KCC2 promotes GABAergic excitation in the mature rat hippocampus', *J Physiol*, 588(Pt 9), pp. 1527-40.

28. Yekhlef, L., Breschi, G.L., Lagostena, L., Russo, G. and Taverna, S. (2015) 'Selective activation of parvalbumin- or somatostatin-expressing interneurons triggers epileptic seizurelike activity in mouse medial entorhinal cortex', *J Neurophysiol*, 113(5), pp. 1616-30.

Chapter 9 Discussion

Epilepsy is a complex neurological disorder that is characterised by recurrent seizures and psychological consequences of seizures. For a better understanding of the pathology of seizures, it is important to consider not just what triggers a seizure, but also how the normal-functioning neuronal circuits react to potential seizure threats. In this thesis, these issues were investigated using *in vitro* models.

Brain slices (*in vitro* models) have been widely used to study epileptic activity, but still we lack a full understanding of how the pathological activity arises in these models, and whether the activity is equivalent in each, and if not, how the models differ. While the literature covering these different models is large, many studies involve only field recordings, which can be difficult to interpret if not put in the context of other types of recording. Moreover, typically only one pharmacological model has been studied and there has been virtually no systematic attempt to compare and contrast the different models. This is made worse by a poverty of terminology, where frequently the same terms are used for what is likely to be rather different patterns of discharge. This is best exemplified by the term "interictal event", referring to short events, lasting a few hundred milliseconds, but which has been used to describe what are clearly very different types of discharge, occurring in different parts of the brain and provoked by different triggers (for example (Voskuyl and Albus, 1985; Dreier and Heinemann, 1991; Avoli *et al.*, 1993; Chauviere *et al.*, 2012)). This lumping of different activity patterns under the same term is very problematic for the field. It is reasonable to suggest that a clearer understanding of these differences will eventually provide insights into the fundamental pathophysiology of spontaneously occurring seizures *in vivo*, leading to better facilities for preventing the pathological discharges without compromising normal brain function. This was the motivation for the work described in this thesis, although there remains much more to discover.

In these studies, I showed that there are, in fact, striking differences between the models: in the way activity evolves, which cortical territories are acting as the source of the discharges, and how epileptiform activity spreads. I will first collate the key findings for the different models, and then attempt to draw some conclusions about

how these relate to the clinical condition of epilepsy, and how this work might inform future studies.

9.1 Characteristics of activity patterns induced by 0 Mg^{2+} ACSF in brain slices

In the 0 Mg^{2+} model, epileptiform activity developed initially in neocortex and entorhinal cortex, and only later, in hippocampal CA. The neocortical activity showed two distinct stages; the early activity is characterised by intermittent, transient (<1s), "interictal" events, interspersed with tonic-clonic-like ictal events. After a period of this pattern of activity, lasting between 10 minutes to sometimes well over an hour, there was a marked transition in the neocortical activity, into the second stage, a pattern of regular discharges, each lasting several hundred milliseconds, and repeating every few seconds. This second stage, we termed "late-stage activity". One of our main insights was that the transition from the early to the late stages coincided with the development of discharges in the hippocampal CA territories.

Our second novel finding regarding the 0 Mg^{2+} model is that these late-stage discharges appeared to have a hippocampal pacemaker, which entrained also the neocortical discharges. Furthermore, this entrainment could propagate via a non-canonical pathway, which persisted even after the potential axonal connections through entorhinal cortex had been severed (although, of course, activity may still spread also through any intact synaptic paths – see discussion in Chapter 3, section 3.4). These distinctive electrographic features are broadly consistent with earlier descriptions of this model (Mody *et al.*, 1987; Dreier and Heinemann, 1991), although these earlier studies did not appear to make the explicit connection between the late-stage neocortical transition and the onset of hippocampal activity, nor recognise the non-canonical propagation patterns. These researchers did, however, note that the early activity was sensitive to several, commonly used anti-epileptic medications (phenytoin, carbamazepine, phenobarbital, and midazolam), and whereas the late stage activity was not (Heinemann *et al.*, 1994; Zhang *et al.*, 1995).

Another important feature of 0 Mg^{2+} model is that the early tonic-clonic like ictal events in neocortex propagate across the network in a modular fashion (Trevelyan *et al.*, 2006). The delays in propagation are influenced by powerful feed-forward inhibitory barrages, manifested as pre-ictal discharges, ahead of the propagating ictal wavefront, and which are suggested to be protective against the spread of epileptic activity. When

the inhibitory restraint is intact, early ictal events spread at low velocities (~0.1mm/second) (Wong and Prince, 1990; Trevelyan *et al.*, 2007).

The inhibitory restraint is largely provided by parvalbumin-positive fast-spiking interneuron (Cammarota *et al.*, 2013). When the inhibitory restraint collapses, pre-ictal discharges transition into ictal events and the ictal wavefront begins to spread (Trevelyan *et al.*, 2006; Trevelyan *et al.*, 2007; Cammarota *et al.*, 2013). This fast collapse of inhibitory restraint could be of many reasons such as depolarisation block of interneurons (Cammarota *et al.*, 2013), increase in postsynaptic chloride concentration due to intense GABAergic activation, thereby shifting E_{GABA} to depolarising potentials (Thompson and Gahwiler, 1989; Thompson and Gahwiler, 1992; Staley *et al.*, 1995; Cohen *et al.*, 2002; Fujiwara-Tsukamoto *et al.*, 2010; Ellender *et al.*, 2014; Pallud *et al.*, 2014; Alfonsa *et al.*, 2015). The chloride loading effect may further be amplified by a rise in extracellular potassium ion levels due to intense neuronal firing, and can also, in turn, contribute to the K^+ rise (Viitanen *et al.*, 2010). Intracellular chloride is cleared by potassium gradient driven potassium-chloride cotransporter (KCC2). Therefore, any substantial increase extracellular potassium levels may hinder chloride clearance from the postsynaptic neuron, thus maintaining depolarised E_{GABA} (Lillis *et al.*, 2012)

Later tonic-clonic-like events tend to be preceded by far fewer, or even no pre-ictal discharges (progressive loss of inhibitory restraint) (Trevelyan *et al.*, 2007). These late events propagate across the tissue almost instantly without any delay at relatively higher velocities (~10 mm/second) (Trevelyan *et al.*, 2007), suggesting an inverse correlation between the number of pre-ictal discharges and propagation of events. This progressive deterioration in inhibition has been attributed to various mechanisms including chloride loading (Dzhala *et al.*, 2010), and also a partial de-phosphorylation of GABA$_A$-receptors secondary to reduced intracellular Mg^{2+} (Whittington *et al.*, 1995).

9.2 Characteristics of activity patterns induced by 4-aminopyridine in brain slices

In this model, in contrast to zero-magnesium model, I showed that epileptiform activity developed early in hippocampal CA and later in the neocortex. In the

hippocampus, 4AP led to the generation of transient spike-wave synchronous field discharges that each last for 1.5-3 seconds, while tonic-clonic like ictal discharges are rarely observed. Note, though, that tonic-clonic like discharges have been observed in hippocampal slices prepared from younger mice (2-3 weeks old) (Chesnut and Swann, 1988; Avoli, 1990). Neocortical activity showed early tonic-clonic like ictal events, each lasting for tens of seconds, that later transitioned to a pattern of transient recurrent discharges (lasting hundred milliseconds to few seconds), referred to as late-stage events.

Previous studies demonstrated the sensitivity of ictal events to anti-epileptic drugs (phenytoin, carbamazepine, valproic acid, and phenobarbital), but the inter-ictal discharges continued to occur, and different types of inter-ictal events were identified in 4AP model that had different pharmaco-sensitivities to carbamazepine (Fueta and Avoli, 1992; Watts and Jefferys, 1993; Bruckner and Heinemann, 2000). This pattern of evolution of activity in the neocortex is electrographically similar to that observed in the zero-magnesium model. However, the key difference is that the transition of early to late stage activity in neocortex was not associated with the development of discharges in the hippocampus. Furthermore, there are stark differences in responses to pharmacological manipulations that I will discuss later in the discussion; see section 9.4). GABA$_A$-receptors signalling is involved in 4AP induced inter-ictal events as they persisted even in the presence of glutamatergic antagonists and were abolished by application of GABA$_A$-receptor blockers (Perreault and Avoli, 1992). A notable difference in the nature of interictal events in 4AP and 0Mg^{2+} models is illustrated in Figure 9.1 (unpublished data, Andrew Trevelyan), showing that in 4AP, interictal events appears to lack any significant pyramidal cell activity, but the pyramidal neurons experience pronounced GABAergic signalling (Figure 9.1 B). In contrast, in 0 Mg^{2+} model, during interictal events, pyramidal neurons show both GABAergic as well as excitatory currents (Figure 9.1 A).
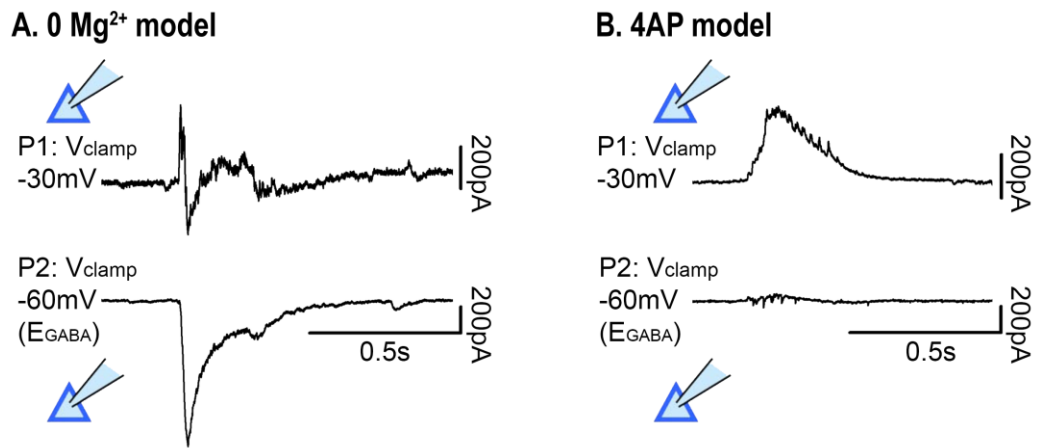
Figure 9.1 Paired pyramidal whole cell recordings of interictal events developed in (A) 0Mg^{2+} and (B) 4AP models. Pyramidal neurons are voltage clamped at -30mV (P1; halfway between glutamatergic and GABAergic reversal potentials), and at -60mV (P2; near GABAergic reversal potential). A. Interictal event in 0 Mg^{2+} model involves, both GABAergic (upper trace, upward deflection) and glutamatergic currents (upper trace, downward deflection). B. Interictal event in 4AP model involves largely GABAergic (upper trace, upward deflection) and almost no glutamatergic signalling (upper and lower traces, lack of downward deflections).

In the 4AP model, the functional implication of enhanced and synchronous GABAergic signalling prior to ictal events has been interpreted as pro-ictogenic (Ives and Jefferys, 1990; Gnatkovsky *et al.*, 2008; de Curtis and Gnatkovsky, 2009; Avoli and de Curtis, 2011; Sessolo *et al.*, 2015; de Curtis and Avoli, 2016; Librizzi *et al.*, 2017). In line with this interpretation, optogenetic stimulation of interneurons was shown to trigger epileptiform discharges (Sessolo *et al.*, 2015; Shiri *et al.*, 2015; Yekhlef *et al.*, 2015; Shiri *et al.*, 2016), and drugs that interfere with GABAergic signalling suppressed 4AP-induced ictal events (Avoli *et al.*, 1993; Avoli *et al.*, 1996; Lopantsev and Avoli, 1998; Benini *et al.*, 2003; Sudbury and Avoli, 2007). It is hypothesised that the increase in extracellular potassium levels due to an excessive or intense activity of inhibitory interneurons, largely PV+ interneurons, underlies the onset of ictal events (Barolet and Morris, 1991; de Curtis and Avoli, 2016). However, in both, 4AP and 0 Mg^{2+} models, activity subsequently evolves to develop ictal events which involve both pyramidal and interneuronal cell activity (Galvan *et al.*, 1982; Avoli *et al.*, 2002; Trevelyan *et al.*, 2006; Trevelyan *et al.*, 2007).

Another interesting feature of the 4AP model (Chapter 8), spontaneous subthreshold membrane potential oscillations developed in PV+ interneurons at

relatively hyperpolarised membrane potentials in presence of synaptic blockers (glutamatergic and GABAergic channel blockers). Previous studies demonstrated such membrane potential oscillations in striatal fast-spiking interneurons, stellate cells, and regular spiking neurons, but at depolarised membrane potentials (Bracci *et al.*, 2003; Alonso and Llinas, 1989; Amitai, 1994). Furthermore, the oscillations observed in 4AP-synaptic blockers appeared to facilitate and sustain rhythmic bursts of action potential firing. Coordination and spike timing of PV+ interneurons in a network are, in part, synchronised by gap-junction coupling (Galarreta and Hestrin, 1999; Deans *et al.*, 2001; Hjorth *et al.*, 2009). Propagation of membrane potential oscillations through gap-junction coupled PV+ interneurons may be involved in enhancing synchronous firing activity of the cells. PV+ interneurons appear to underlie the clonic structure (after-discharges) of tonic-clonic like ictal events (Ellender *et al.*, 2014). The network mechanisms underlying these after-discharges may involve such synchronous firing of PV+ interneurons. These hypotheses remain to be tested in future studies using similar protocols as mentioned in this thesis and paired whole-cell patch clamp recording from gap-junction coupled PV+ interneurons.

9.3 Characteristics of activity patterns induced by blockade of fast GABAergic transmission in brain slices

Blocking $GABA_A$-receptors produced short-lasting synchronised epileptiform discharges that appeared electrographically similar to interictal events or prolonged events with after-discharges after high-frequency stimulation (Gutnick *et al.*, 1982; Miles and Wong, 1983; de Curtis and Avanzini, 2001; Librizzi and de Curtis, 2003). In some cases, repetitive stimulation induced tonic-clonic like ictal events (Matsumoto and Marsan, 1964; Prince, 1968; Ayala *et al.*, 1973). In an intact whole brain *in vitro* preparation, tonic-clonic like ictal events involving different limbic structures developed following the application of bicuculline (Uva *et al.*, 2005; Gnatkovsky *et al.*, 2008). Intracellularly, short-lasting discharges are associated with large depolarisations with sustained firing activity (Avoli and Olivier, 1989; McCormick, 1989; Hwa *et al.*, 1991; Tasker *et al.*, 1992). The synchronous discharges induced by $GABA_A$-receptor antagonists show differential sensitivity to anti-epileptic drugs ((Schneiderman and

Schwartzkroin, 1982; Piredda *et al.*, 1986; Kohr and Heinemann, 1990; Armand *et al.*, 1998).

In this model, for discharges to propagate, disinhibition requires to be above a certain threshold and, above which, the discharges propagate with high velocities (20-80 mm/s) (Chervin *et al.*, 1988; Wadman and Gutnick, 1993; Pinto *et al.*, 2005). This contrasts with the propagation velocities of early ictal wavefront observed in 0 Mg^{2+} model which is nearly two orders of magnitude slower, but similar with that of after-discharges and fast events observed in 0 Mg^{2+} model (Wong and Prince, 1990; Trevelyan *et al.*, 2007).

In disinhibited tissue, the behaviour of the network can be influenced by the activity on a single neuron. Miles and Wong (1983) showed that in a network that is sort of primed to have epileptic discharges, then it can be entrained by the action of a single neuron (Miles and Wong, 1983). This observation serves as an important precedent to our novel finding – the entrainment phenomenon (Chapter 3, section 3.3.2) – in that this was another demonstration of how epileptiform discharges may be entrained by very weak electrophysiological triggers: either by the stimulation of a single pyramidal cell (Miles and Wong, 1983), or by a weak extracellular field effect (Chapter 3). We demonstrated that the epileptiform events occurring in a hyperexcitable neocortical network (primed tissue) can be entrained by the effects of hippocampal discharges.

9.4 Model-dependent effects of further pharmacological manipulations

The diversity of activity patterns in these *in vitro* models is further illustrated by the effects of other drugs on the epileptiform activity. There is much potential for future work on this topic, for drug development and validation, and I will come to this in section 9.6. My studies were limited to an exploration of three drugs which target different parts of the network: diazepam, baclofen and fluorocitrate.

9.4.1 *Diazepam*

Diazepam, a benzodiazepine, is used as one of the first-line drugs for controlling status epilepticus (Chin *et al.*, 2008). Diazepam is a positive allosteric modulator at $GABA_A$-receptors that increases the frequency of $GABA_A$-channel opening (Study and Barker, 1981; Otis and Mody, 1992; Rogers *et al.*, 1994). Here, I will discuss the key findings of the effects of diazepam on epileptiform activity induced by two models, 0 Mg^{2+} and 4-aminopyridine (4AP).

Diazepam showed distinctive effects on 0 Mg^{2+} and 4AP induced early epileptiform activity. In the neocortex, diazepam enhanced the development of 0 Mg^{2+} induced pre-ictal events and delayed the onset of tonic-clonic like ictal events, but had no such effects on 4AP induced epileptiform activity. Diazepam was also shown to be ineffective in *in vivo* for suppressing 4AP-induced seizures (Yamaguchi and Rogawski, 1992). In both *in vitro* models ($0Mg^{2+}$ and 4AP), diazepam neither suppressed nor delayed the transition of early tonic-clonic like ictal events into late-stage events. Furthermore, if activity was allowed to progress to the late-stage events before the application of diazepam, it did not suppress or show any significant effects on these on-going discharges. This was consistent with previous studies, which showed that benzodiazepine (midazolam) did not suppress the on-going late-stage events (Zhang *et al.*, 1995; Richter *et al.*, 2010), although my studies have extended these findings, by examining differences in the effects on early activity in the two different pharmacological models. In summary, my studies suggest that the model dependent effects of diazepam rests, at least in part, on the mechanisms underlying the epileptiform activity, and highlights the importance of identifying these underlying mechanisms for effective treatment.

9.4.2 *Baclofen*

Baclofen, a $GABA_B$-receptor agonist, is commonly used in clinics to treat muscle spasms. It has also been used, in conjunction with other medicines, to treat epilepsy (Terrence *et al.*, 1983; Kofler *et al.*, 1994; Becker *et al.*, 1997). However, baclofen has been shown to have pro-epileptic and well as anti-epileptic effects, and this may depend on factors such as the type of epilepsy and other associated neurological

conditions, as well as the brain region (Terrence *et al.*, 1983; Rush and Gibberd, 1990; Kofler *et al.*, 1994; Vergnes *et al.*, 1997; Buonaguro *et al.*, 2005; Mares, 2012). To get a better understanding of how baclofen affects epileptiform activity, I examined its effects on 0 Mg^{2+}-ACSF induced epileptiform activity.

Previous studies showed that baclofen abolished spontaneous and stimulus-evoked ictal events in the entorhinal cortex, and suggested that it interfered with the ictogenesis (Jones, 1989). In my studies, baclofen delayed the onset of tonic-clonic-like ictal events in the neocortex, and also prevented the transition to late-stage activity. Interestingly, baclofen also prevented the development of any type of epileptiform activity in hippocampal CA3. Furthermore, when baclofen was applied only after the development late-stage activity, it completely suppressed the hippocampal activity, and reversed the neocortical late-stage transition, allowing the reappearance of tonic-clonic like ictal events. These baclofen experiments thus provide strong further support for the link between hippocampal epileptiform discharges and the late-stage transition in neocortex.

9.4.3 *Fluorocitrate*

Astrocytes play an important role in maintaining a physiological environment in the brain. They are essential in recycling neurotransmitters, and buffering extracellular potassium ions (Kofuji and Newman, 2004; Wallraff *et al.*, 2006; Tani *et al.*, 2014). Hence, it is not surprising to see that dysfunctional astrocytes are implicated in various neurological conditions such as multiple sclerosis, Alzheimer's disease, epilepsy (Seifert *et al.*, 2006; John Lin and Deneen, 2013; Scuderi *et al.*, 2013). Previous research suggested that astrocytes along with neuronal populations are involved in generating and sustaining ictal discharges (Gomez-Gonzalo *et al.*, 2010). I used fluorocitrate, a gliotoxin, to study how having dysfunctional astrocytes in neocortical networks influence the network activity and characterise its effects on the evolution of epileptiform activity induced by 4-aminopyridine (4AP).

Fluorocitrate, in the absence of proepileptic media, caused the development of glutamate-dependent spontaneous recurring transient events that appear electrographically similar to late-stage events. When used in tandem with 4AP,

fluorocitrate prevented the occurrence of tonic-clonic-like events in neocortical tissue, but instead, activity appeared to progress directly to the late stage pattern, with transient recurrent discharges. Furthermore, fluorocitrate transformed 4AP induced ictal events to recurrent short duration discharges. The exact mechanism of how fluorocitrate is interfering with the network mechanisms to generate and maintain ictal events is not known. Fluorocitrate was shown to reduce inhibitory post-synaptic currents (Ortinski *et al.*, 2010), suggesting that one plausible mechanism is that fluorocitrate creates a disinhibited network (see descriptions earlier in this chapter). Bruckner *et al.* (1999) reported similar changes in activity patterns when $GABA_A$ signalling was blocked in 4AP treated slices (Bruckner *et al.*, 1999). Altered astrocytic clearance of potassium ions and glutamate from extracellular space could also be involved in fluorocitrate-mediated changes in activity patterns. These findings demonstrate that the development and maintenance of 4-aminopyridine induced ictal events are dependent on functional astrocytes.

There are many more features of fluorocitrate-mediated events that need to be characterised, such as measuring extracellular potassium ion levels, post-synaptic glutamatergic and GABAergic currents, both in the presence, and absence, of different pro-epileptic agents, in different cortical areas. I suggest that these studies will help refine our understanding of the role of astrocytes in inducing and maintaining epileptiform activity, and possibly provide new targets for developing drugs to treat epilepsy.

9.5 The utility of *in vitro* models

In vitro models have been a mainstay of epileptic research for many years. They have been used to understand cellular (Traub *et al.*, 1987; Traub *et al.*, 1989; von Krosigk *et al.*, 1993), and network activity patterns (Traub *et al.*, 1999), including the pattern of propagation (Wadman and Gutnick, 1993; Telfeian and Connors, 1999; Pinto *et al.*, 2005; Trevelyan *et al.*, 2006; Trevelyan *et al.*, 2007). They have also been used to explore the effects of anti-epileptic drugs on different patterns of epileptiform discharges that led to the identification of 2 categories of epileptiform discharges: pharmaco-sensitive and pharmaco-resistant (Zhang *et al.*, 1995; Dreier *et al.*, 1998). Validation of some features of epileptiform activity has only recently been provided

from recordings of spontaneous seizures *in vivo* in the human brain (Schevon *et al.*, 2012). That study demonstrated in humans the presence of characteristic features of seizures; the hyper-synchronous discharges which was termed the "ictal core", and the effects on the surrounding tissue, which was termed the "ictal penumbra", relating these findings to what had been described previously in experimental *in vitro* models (Trevelyan *et al.*, 2006; Trevelyan *et al.*, 2007).

Of course, *in vitro* models cannot capture all features of the *in vivo* state; many long-range connections are severed *in vitro*, and it is likely that the extracellular ionic concentrations, which can change dramatically during seizures (Somjen, 2004), may be subtly different *in vitro* because of the way the tissue is perfused. It is pertinent, therefore, to ask why and how are *in vitro* models helpful? *In vitro* models should be viewed as a platform to tease apart various aspects of the epilepsy pathology and ultimately translate the findings towards improved treatment options for human patients. The biggest benefit of *in vitro* preparations is that they allow hugely better access to the tissue and control over the experimental conditions, and so facilitate the study of the pathological processes. Other benefits are that they are simple to use, cost-effective, and importantly, animals suffering is minimised prior to being sacrificed. There are certain key points the experimenter needs to consider, such as the effects of the brain slice preparation method and the potential for introducing unnecessary experimental variability.

In this thesis, the susceptibility of different cortical areas to develop epileptiform activity was investigated in brain slices using two *in vitro* models; zero-magnesium ($0Mg^{2+}$), and 4-aminopyridine (4AP) models. The cortical areas examined showed differences in their susceptibility to develop epileptiform activity. Activity developing in the hippocampal CA regions and neocortex had distinctive electrographic features that are broadly consistent with earlier findings (Mody *et al.*, 1987; Dreier and Heinemann, 1991). One surprising finding was that in the $0Mg^{2+}$ model, the first epileptiform discharge associated with multiunit activity in CA only developed much later compared with the neocortex. This appears at odds with the general view that hippocampal circuits are the most epileptogenic, arising perhaps from the relatively high incidence of temporal lobe epilepsy (Falconer *et al.*, 1964; Wiebe, 2000; Curia *et al.*, 2014) and also from the large body of literature focussed on hippocampal changes in certain

widely used animal models (Cronin and Dudek, 1988; Cavalheiro *et al.*, 1991; Ben-Ari and Cossart, 2000; Bortel *et al.*, 2010; White *et al.*, 2010; Suarez *et al.*, 2012).

Interestingly, in 4AP model, it was the other way around; that is, CA subfields of the hippocampus developed epileptiform activity much earlier than the neocortex. The reasons for these model-dependent differences in regional susceptibility remain to be established. In hippocampal CA regions, the form of the individual discharges was similar in both 4AP- and $0Mg^{2+}$-models, that is, recurrent short duration discharges with a characteristic large spike followed by a wave (SWD). An important issue here regards how we interpret these recordings: when electrographic recordings look the same, are they indeed arising by the same mechanisms?

9.5.1 *Benefits of in vitro preparations: experimental access*

One of the great strengths of *in vitro* preparations is that the pathophysiological mechanisms can be studied in great detail. Furthermore, they facilitate many valuable recording formulations that are not feasible for *in vivo* preparations. These include, but are not limited to: paired patch recordings of synaptically connected cells (Markram *et al.*, 1997), gap-junction coupled cells (Galarreta and Hestrin, 1999; Galarreta and Hestrin, 2002), combined whole-cell electrophysiological recording with calcium imaging of network activity (Tian *et al.*, 2005; Trevelyan *et al.*, 2006; Trevelyan *et al.*, 2007; Cammarota *et al.*, 2013); simultaneous measurements of local field potentials and extracellular ion concentrations (Jefferys and Haas, 1982; Dreier and Heinemann, 1991); and recordings of cells and/or local field potentials while manipulating the local environment with bath applied drugs – that remain at best difficult, and often impossible to do *in vivo*. Furthermore, the ethical considerations mean that these types of recordings will almost certainly never be done in humans even if the technical considerations could be overcome.

Within this thesis, the versatility of *in vitro* preparations enabled the rapid switching of solutions while maintaining patch clamp recordings of parvalbumin-positive fast-spiking interneurons (PVIN). The development of membrane potential oscillations (MPO) in PVINs in response to 4AP, and the underlying ionic mechanisms were examined, for example, changing perfusate to one containing tetrodotoxin

abolished MPOs in PVINs indicating that voltage-gated sodium channels were necessary for the development of MPOs.

LFP recordings also allowed the study of the contribution of astrocytes to the development of epileptiform activity in brain slices. Bath application of a gliotoxin, and later glutamate receptor blockers induced rapid changes in the pattern of 4AP-induced epileptiform activity. This demonstrated that the development and maintenance of ictal events in the 4AP model were dependent on functional astrocytes.

Combining different techniques is a powerful approach to studying various aspects of the epileptiform activity. For example, Miles and Wong (1983) made simultaneous *in vitro* patch-clamp recordings from single neurons in combination with LFPs. They consequently showed that in a disinhibited network, a single cell may trigger epileptiform bursts (Miles and Wong, 1983). Another powerful combination is the pairing of patch-clamp technique with imaging of network activity achieved by loading neurons and/or astrocytes with calcium-sensitive dyes. For example, *in vitro* studies have identified astrocytic involvement in the initiation of ictal discharges (Tian *et al.*, 2005; Gomez-Gonzalo *et al.*, 2010), and the pattern of seizure propagation (Trevelyan *et al.*, 2006; Trevelyan *et al.*, 2007; Cammarota *et al.*, 2013).

Acute brain slices are only viable for approximately 6 hours post-slicing, making them unsuitable for studying chronic changes due to epileptiform activity. Organotypic brain slices are an alternative type of *in vitro* preparation that can be maintained for days to weeks, whilst preserving much of the connectivity as observed in acute brain slices (Gahwiler *et al.*, 1997). A key difference is that organotypic slices can develop spontaneous epileptiform activity (Malouf *et al.*, 1990; Dyhrfjeld-Johnsen *et al.*, 2010). These features coupled with the ease of electrophysiological recordings in organotypic brain slices, make them suitable for studying epileptogenesis (Dyhrfjeld-Johnsen *et al.*, 2010; Koyama, 2013), chronic spontaneous epileptiform activity (McBain *et al.*, 1989), epileptiform activity induced plasticity (Abegg *et al.*, 2004), mossy fibre sprouting (Routbort *et al.*, 1999), and neuronal degeneration (Thompson *et al.*, 1996). Furthermore, organotypic brain slices preparations provide easy access to drugs and other treatments (Albus *et al.*, 2008).

9.5.2 *Benefits of in vitro preparations: experimental control*

A further advantage of *in vitro* preparations is the level of control that they offer. For instance, in horizontal hippocampal-neocortical brain slices, the occurrence of non-synaptic interactions between hippocampal regions (CA1/CA3) and neocortex was demonstrated by progressive sectioning of all potential synaptic connections. Briefly, late-stage epileptiform activity was found to develop in both territories, and during this stage, hippocampal activity entrained patterns of activity in the neocortex. This entrainment persisted even after the entorhinal cortex was dissected out, thereby removing all potential synaptic pathways between the two regions. Furthermore, physical isolation of the hippocampal region and neocortex abolished the entrainment phenomenon. This indicated that the synaptic connectivity between the two territories was not an essential criterion for the entrainment phenomenon and that it could arise from field effects due to focal discharges that occurred elsewhere in the tissue (Jefferys, 1995; Frohlich and McCormick, 2010; Anastassiou *et al.*, 2011).

9.6 The use of *in vitro* models for future work

There are many cellular interactions that we still have little understanding about, and while this remains so, there will be a continued utility for *in vitro* preparations to understand various facets of epilepsy, identifying new drug targets, screening of AEDs, and for epileptic transgenic mouse lines. *In vitro* preparations are simple assays that can be used effectively and efficiently, but it is essential to optimise various aspects of *in vitro* the prior to starting the experiments.

9.6.1 *Optimising in vitro preparations*

Mouse strain:

The first thing to consider is which mouse strain will be used for the experiments. One should not pool data collected from 'wild-types' of different strains, for example, data acquired from experiments performed on brain slices collected from C57BL/6J mouse line should not be pooled with that collected from '129/SV' mouse line.

Slice preparation method:

The output of experiments mainly depends on the quality of slices prepared. For different experiments, different brain slice preparation methods were used.

Method 1 (see section 2.4.1, chapter 2): this method was used for reducing the excitotoxicity induced damage caused during slicing of the brain tissue and transportation of slices to from one location to another. In this method, kynurenic acid, a wide spectrum blocker of excitatory amino acid receptors, and ascorbic acid in were used in calcium ion-free slicing medium. Good quality local field potentials (LFP) recorded from these slices proved the quality of slices.

Method 2 (see section 2.4.2, chapter 2): Ice-cold calcium ion-free slicing medium was used for preparing brain slices. These slices were then used in the same room where they were prepared. Based on LFP recordings, the quality of slices was proved to be good.

Method 3 (see section 2.4.3, chapter 2): in this method, transcardial perfusion was performed on anaesthetised mice. In the solution used for transcardial perfusion and slicing, sodium chloride ions were replaced with sucrose to reduce the inflammatory responses and overall activity in the brain. Slices prepared by this method were used for targeted cell-patching experiments. In this thesis, fluorescently labelled PV+ interneurons were targeted for patching. PV+ interneurons in slices prepared by this method were observed to be easier to patch, compared with slices prepared using method 2.

Setting up an interface recording chamber:

There are multiple types of interface recording chambers and the settings vary for the individual type. Haas type interface recording chamber was used for all local field potential recordings described in this thesis. There are 4 key settings that will affect the recordings: the rate of perfusion, the temperature of perfusate and the chamber, oxygenation within the chamber, and solution levels in the chamber. The rate of perfusion should be maintained constant for all the experiments to minimise variability, for example, different perfusion rates may vary the latency to the first ictal event in neocortex. The temperature of both perfusate and the interface recording

chamber should be maintained at the physiological range. If only one of the two is heated, then the tissue will experience different temperatures leading to variable activity patterns. In the type of interface chamber, I used, oxygenation inside the chamber was necessary to prevent slice from dying and keep alive. Finally, regarding solution levels, too much solution in the chamber is more likely to make the slice unstable and drift away.

9.6.2 *Assessing drug effects on epileptiform activity in different brain regions*

Trevelyan *et al.* demonstrated that the features of the inhibitory restraint – the numbers of pre-ictal bursts prior to transition to PDS bursts; recruitment of pyramidal cells in a spatially clustered population; modular propagation (Trevelyan *et al.*, 2006; Cammarota *et al.*, 2013); and the concomitant increase in ictal propagation speed – become progressively weaker with each full ictal event (Trevelyan *et al.*, 2007). There is thus a highly characteristic evolution in the brain slice preparations, from an early pattern, characterised by periods of interictal events interspersed with more intense full ictal events lasting for tens of seconds, to a late-stage pattern, which is characterised by repeated large amplitude, but relatively short lasting (<5s) events. This late stage has been likened to the clinical condition, status epilepticus (Zhang *et al.*, 1995).

Clinically, benzodiazepines (BDZ) are used as first-line drugs in therapies for status epilepticus, (Chin *et al.*, 2008). However, not all patients respond to BDZs. There may be a number factors influencing the patients' response to BDZs; mechanism underlying the epileptic seizures is an important factor. My results show that diazepam (DZP), a benzodiazepine, has differential effects on epileptiform activity in neocortex induced by $0Mg^{2+}$, and 4AP. DZP enhanced the preictal activity and delayed the development of the first tonic-clonic like ictal event in the neocortex in $0Mg^{2+}$ model, but not in 4AP. This model-dependent difference in the effects of diazepam suggests that even though the presenting feature is electrographically similar in both the models, its anti-epileptic actions depend, to a certain extent, on the underlying mechanism. This underscores the importance of knowing the mechanism of seizures for choosing an AED. Furthermore, DZP did not suppress the ongoing $0Mg^{2+}$-induced ictal events. This result is in contradiction with the earlier study in rat brain slices (Dreier *et al.*, 1998).

This could potentially be explained by two key differences in the design of the two studies: the animal species and the drug used. Dreier *et al.* used rat brain slices and midazolam as a benzodiazepine. However, if the discrepancy between their and our results arises from inter-species variability, this would need to be addressed in the screening of AEDs. In the 4AP model, DZP was effective in delaying the onset of activity in CA3, but had no effect on the neocortex, as mentioned earlier. Further investigations are necessary to characterise its effect on hippocampal regions in the $0Mg^{2+}$ model.

9.6.3 *Screening of transgenic mouse lines*

Along with the aforementioned applications, another important utility of *in vitro* models is to assess the seizure susceptibility of the cortical networks and other features of the epileptiform activity in brain slices taken from transgenic mouse lines. The starting point for studying transgenic animals is often just two things: (1) the knowledge of a very specific molecular deficit, and (2) a vaguely formulated recognition that the animal has a reduced susceptibility to induced seizures, or may even suffer spontaneous seizures. There then remains a large absence of understanding regarding how that molecular deficit gives rise to the clinical phenotype, through the altered cellular and network interactions, or even which part of the brain is the critical location of these pathophysiological changes. These simple *in vitro* experiments provide a rapid way to screen transgenic mouse lines, to find other molecular associations (e.g. mouse strain differences), how the mutation affects the network excitability, various facets of epileptiform activity evolution, and the mechanisms of epileptogenesis. It will also provide insights into the functional role of the protein encoded by the gene in the network under physiological conditions.

9.7 The limitations of *in vitro* models

Despite their many advantages, acute *in vitro* models have several limitations. They are not suitable for investigating mechanisms involved in chronic epileptogenesis (although note my comments regarding organotypic cultures for more chronic studies), long-range axonal connections are severed, they lack the behavioural components of

in vivo seizures, and are uninformative about comorbidities. A further consideration is that an intermediate step for translating *in vitro* observations into clinically significant findings is generally required.

There are many other aspects of biology that are lost in *in vitro* preparations, such as inflammatory responses, functions of the blood-brain barrier, and vascular behaviour. Epilepsy is associated with inflammatory reactions, and emerging evidence indicates that inflammation might be both a cause and consequence of epilepsy (Vezzani and Granata, 2005). Recent advances in the field showed that modulation of inflammatory responses can be an effective epilepsy therapy (Yu *et al.*, 2013). Studying such inflammatory responses in epilepsy, and seizure-induced changes in the synthesis and expression of proteins such as BDNF, neuropeptide Y is not possible in acute *in vitro* preparations (Vezzani *et al.*, 1999a; Vezzani *et al.*, 1999b)

As a final example, changes in the function of the blood-brain barrier (BBB) during epilepsy are not possible to study using *in vitro* preparations. The permeability of BBB has been shown to be increased during chronic spontaneous seizures in different *in vivo* models of epilepsy (van Vliet *et al.*, 2015). However, it is not established whether BBB dysfunction is a cause or an effect of seizures. This increased permeability leads to accumulation of albumin, a serum protein, in the brain. Albumin is taken up by astrocytes resulting in down-regulation of inward-rectifying potassium channels, leading to impaired buffering of potassium and causing neuronal hyperexcitability (Ivens *et al.*, 2007). In summary, some biological processes involved in epilepsy can only be studied *in vivo.*

9.8 The relevance of the *in vitro* epileptiform patterns for clinical work

Over past few decades, different types of acute *in vitro* models, techniques, and preparations that included brain slices of isolated or interconnected areas were developed to replicate and study the epileptiform activity resembling that observed in epileptic patients. The *in vitro* preparations, of course, do not capture the behavioural aspects or the effects of long-range connections but are helpful in that they have reasonably intact inhibitory and excitatory components that can be provoked to develop the epileptiform activity to study various facets of its initiation, propagation,

and termination. It is ethically impossible to use patch-clamp recordings or calcium imaging techniques to understand epileptiform activity in patients with epilepsy, and possibilities are limited to recording electroencephalography (EEG) and/or electrocorticography signals. Moreover, the quality of these signals is poor, and the probability of recording a seizure event is low.

Previous studies have examined inhibitory restraint, a key feature of the normal functioning cortex, and its nature in the epileptic cortex in *in vitro* preparations. These studies suggested the co-existence of dysfunctional GABAergic inhibition at the core of epileptiform activity and functional GABAergic inhibition in the surrounding areas of the cortex, and this inhibition is, in large part, mediated by PV+ interneurons (Cammarota *et al.*, 2013; Trevelyan *et al.*, 2013). Similar observations were made in *in vitro* and *in vivo* animal models, and also in epileptic patients (Prince and Wilder, 1967; Dichter and Spencer, 1969; Schwartz and Bonhoeffer, 2001; Timofeev *et al.*, 2002; Trevelyan *et al.*, 2006; Schevon *et al.*, 2012). This approach can be used for mapping of epileptic activity in the brain and will be valuable in clinics, particularly during tissue resection, to distinguish the pathological core from the surrounding tissue.

In another *in vitro* model, acute pharmacological manipulation with bicuculline led to the development of ictal events, that showed, at their onset, either, hypersynchronous activity or fast activity (Uva *et al.*, 2005; Gnatkovsky *et al.*, 2008; Boido *et al.*, 2014; de Curtis *et al.*, 2016). Similar, patterns of seizures were also reported to occur in *in vivo* rat models and patients with temporal lobe epilepsy (Bragin *et al.*, 1999; Velasco *et al.*, 2000; Bartolomei *et al.*, 2001; Wendling *et al.*, 2003; Ogren *et al.*, 2009).

9.9 Conclusions

With the current state of technology and our advancement in the understanding of epilepsy, one may argue that experiments using *in vivo* models are appropriate and more feasible. But, the problem is that we do not have a clear and detailed understanding of structure and functions of the network activity or all the properties of the different type of cells forming the network. Furthermore, there are many new findings coming out of the work on *in vitro* models; to give two examples from this thesis, the entrainment phenomenon and non-synaptic propagation of activity. There is much more to understand and explore at the cellular and small network level itself, for which *in vitro* preparations are ideal on many fronts.

In vitro slice preparations should be viewed as reduced models of normal functioning *in vivo* state. In these models, different pharmacological manipulations acutely challenge normal-functioning brain slices to evoke surges of activity. Analysing propagation of the evoked ictal events and many other aspects can provide insights into cellular mechanisms and network interactions underlying its evolution and the restraint mechanisms engaged by normal tissue. There are thus, many possible measures that can be taken during this evolution of epileptic activity in these *in vitro* models, which can potentially be used to examine the effect of drugs on epileptiform activity, and differences between different genetic strains with different epilepsy susceptibilities.

In vitro models of epilepsy remain valuable tools for advancing our knowledge about epilepsy, and still offer great utility for epilepsy research going forward. They can be used for studying physiology and pathophysiology at both cellular and networks level. A wealth of information can be extracted from simple experiments using *in vitro* models. However, key tasks will be examining, analysing, understanding, and interpreting this information, and extrapolating it to the clinical issues. This will provide insights into the pathophysiology of epilepsy, and physiology of the brain.

9.10 References

1. Abegg, M.H., Savic, N., Ehrengruber, M.U., McKinney, R.A. and Gahwiler, B.H. (2004) 'Epileptiform activity in rat hippocampus strengthens excitatory synapses', *J Physiol*, 554(Pt 2), pp. 439-48.

2. Albus, K., Wahab, A. and Heinemann, U. (2008) 'Standard antiepileptic drugs fail to block epileptiform activity in rat organotypic hippocampal slice cultures', *Br J Pharmacol*, 154(3), pp. 709-24.

3. Alfonsa, H., Merricks, E.M., Codadu, N.K., Cunningham, M.O., Deisseroth, K., Racca, C. and Trevelyan, A.J. (2015) 'The contribution of raised intraneuronal chloride to epileptic network activity', *J Neurosci*, 35(20), pp. 7715-26.

4. Anastassiou, C.A., Perin, R., Markram, H. and Koch, C. (2011) 'Ephaptic coupling of cortical neurons', *Nat Neurosci*, 14(2), pp. 217-23.

5. Armand, V., Louvel, J., Pumain, R. and Heinemann, U. (1998) 'Effects of new valproate derivatives on epileptiform discharges induced by pentylenetetrazole or low Mg2+ in rat entorhinal cortex-hippocampus slices', *Epilepsy Res*, 32(3), pp. 345-55.

6. Avoli, M. (1990) 'Epileptiform discharges and a synchronous GABAergic potential induced by 4-aminopyridine in the rat immature hippocampus', *Neurosci Lett*, 117(1-2), pp. 93-8.

7. Avoli, M., Barbarosie, M., Lucke, A., Nagao, T., Lopantsev, V. and Kohling, R. (1996) 'Synchronous GABA-mediated potentials and epileptiform discharges in the rat limbic system *in vitro*', *J Neurosci*, 16(12), pp. 3912-24.

8. Avoli, M., D'Antuono, M., Louvel, J., Kohling, R., Biagini, G., Pumain, R., D'Arcangelo, G. and Tancredi, V. (2002) 'Network and pharmacological mechanisms leading to epileptiform synchronization in the limbic system *in vitro*', *Prog Neurobiol*, 68(3), pp. 167-207.

9. Avoli, M. and de Curtis, M. (2011) 'GABAergic synchronization in the limbic system and its role in the generation of epileptiform activity', *Prog Neurobiol*, 95(2), pp. 104-32.

10. Avoli, M. and Olivier, A. (1989) 'Electrophysiological properties and synaptic responses in the deep layers of the human epileptogenic neocortex *in vitro*', *J Neurophysiol*, 61(3), pp. 589-606.

11. Avoli, M., Psarropoulou, C., Tancredi, V. and Fueta, Y. (1993) 'On the synchronous activity induced by 4-aminopyridine in the CA3 subfield of juvenile rat hippocampus', *J Neurophysiol*, 70(3), pp. 1018-29.

12. Ayala, G.F., Dichter, M., Gumnit, R.J., Matsumoto, H. and Spencer, W.A. (1973) 'Genesis of epileptic interictal spikes. New knowledge of cortical feedback systems suggests a neurophysiological explanation of brief paroxysms', *Brain Res*, 52, pp. 1-17.

13. Barolet, A.W. and Morris, M.E. (1991) 'Changes in extracellular K+ evoked by GABA, THIP and baclofen in the guinea-pig hippocampal slice', *Exp Brain Res*, 84(3), pp. 591-8.

14. Bartolomei, F., Wendling, F., Bellanger, J.J., Regis, J. and Chauvel, P. (2001) 'Neural networks involving the medial temporal structures in temporal lobe epilepsy', *Clin Neurophysiol*, 112(9), pp. 1746-60.

15. Becker, R., Alberti, O. and Bauer, B.L. (1997) 'Continuous intrathecal baclofen infusion in severe spasticity after traumatic or hypoxic brain injury', *J Neurol*, 244(3), pp. 160-6.

16. Ben-Ari, Y. and Cossart, R. (2000) 'Kainate, a double agent that generates seizures: two decades of progress', *Trends Neurosci*, 23(11), pp. 580-7.

17. Benini, R., D'Antuono, M., Pralong, E. and Avoli, M. (2003) 'Involvement of amygdala networks in epileptiform synchronization *in vitro*', *Neuroscience*, 120(1), pp. 75-84.

18. Boido, D., Jesuthasan, N., de Curtis, M. and Uva, L. (2014) 'Network dynamics during the progression of seizure-like events in the hippocampal-parahippocampal regions', *Cereb Cortex*, 24(1), pp. 163-73.

19. Bortel, A., Levesque, M., Biagini, G., Gotman, J. and Avoli, M. (2010) 'Convulsive status epilepticus duration as determinant for epileptogenesis and

interictal discharge generation in the rat limbic system', *Neurobiol Dis*, 40(2), pp. 478-89.

20. Bragin, A., Engel, J., Jr., Wilson, C.L., Fried, I. and Mathern, G.W. (1999) 'Hippocampal and entorhinal cortex high-frequency oscillations (100--500 Hz) in human epileptic brain and in kainic acid--treated rats with chronic seizures', *Epilepsia*, 40(2), pp. 127-37.

21. Bruckner, C. and Heinemann, U. (2000) 'Effects of standard anticonvulsant drugs on different patterns of epileptiform discharges induced by 4-aminopyridine in combined entorhinal cortex-hippocampal slices', *Brain Res*, 859(1), pp. 15-20.

22. Bruckner, C., Stenkamp, K., Meierkord, H. and Heinemann, U. (1999) 'Epileptiform discharges induced by combined application of bicuculline and 4-aminopyridine are resistant to standard anticonvulsants in slices of rats', *Neurosci Lett*, 268(3), pp. 163-5.

23. Buonaguro, V., Scelsa, B., Curci, D., Monforte, S., Iuorno, T. and Motta, F. (2005) 'Epilepsy and intrathecal baclofen therapy in children with cerebral palsy', *Pediatr Neurol*, 33(2), pp. 110-3.

24. Cammarota, M., Losi, G., Chiavegato, A., Zonta, M. and Carmignoto, G. (2013) 'Fast spiking interneuron control of seizure propagation in a cortical slice model of focal epilepsy', *J Physiol*, 591(4), pp. 807-22.

25. Cavalheiro, E.A., Leite, J.P., Bortolotto, Z.A., Turski, W.A., Ikonomidou, C. and Turski, L. (1991) 'Long-term effects of pilocarpine in rats: structural damage of the brain triggers kindling and spontaneous recurrent seizures', *Epilepsia*, 32(6), pp. 778-82.

26. Chauviere, L., Doublet, T., Ghestem, A., Siyoucef, S.S., Wendling, F., Huys, R., Jirsa, V., Bartolomei, F. and Bernard, C. (2012) 'Changes in interictal spike features precede the onset of temporal lobe epilepsy', *Ann Neurol*, 71(6), pp. 805-14.

27. Chervin, R.D., Pierce, P.A. and Connors, B.W. (1988) 'Periodicity and directionality in the propagation of epileptiform discharges across neocortex', *J Neurophysiol*, 60(5), pp. 1695-713.

28. Chesnut, T.J. and Swann, J.W. (1988) 'Epileptiform activity induced by 4-aminopyridine in immature hippocampus', *Epilepsy Res*, 2(3), pp. 187-95.

29. Chin, R.F., Neville, B.G., Peckham, C., Wade, A., Bedford, H. and Scott, R.C. (2008) 'Treatment of community-onset, childhood convulsive status epilepticus: a prospective, population-based study', *Lancet Neurol*, 7(8), pp. 696-703.

30. Cohen, I., Navarro, V., Clemenceau, S., Baulac, M. and Miles, R. (2002) 'On the origin of interictal activity in human temporal lobe epilepsy *in vitro*', *Science*, 298(5597), pp. 1418-21.

31. Cronin, J. and Dudek, F.E. (1988) 'Chronic seizures and collateral sprouting of dentate mossy fibers after kainic acid treatment in rats', *Brain Res*, 474(1), pp. 181-4.

32. Curia, G., Lucchi, C., Vinet, J., Gualtieri, F., Marinelli, C., Torsello, A., Costantino, L. and Biagini, G. (2014) 'Pathophysiogenesis of mesial temporal lobe epilepsy: is prevention of damage antiepileptogenic?', *Curr Med Chem*, 21(6), pp. 663-88.

33. de Curtis, M. and Avanzini, G. (2001) 'Interictal spikes in focal epileptogenesis', *Prog Neurobiol*, 63(5), pp. 541-67.

34. de Curtis, M. and Avoli, M. (2016) 'GABAergic networks jump-start focal seizures', *Epilepsia*, 57(5), pp. 679-87.

35. de Curtis, M. and Gnatkovsky, V. (2009) 'Reevaluating the mechanisms of focal ictogenesis: The role of low-voltage fast activity', *Epilepsia*, 50(12), pp. 2514-25.

36. de Curtis, M., Librizzi, L. and Uva, L. (2016) 'The *in vitro* isolated whole guinea pig brain as a model to study epileptiform activity patterns', *J Neurosci Methods*, 260, pp. 83-90.

37. Deans, M.R., Gibson, J.R., Sellitto, C., Connors, B.W. and Paul, D.L. (2001) 'Synchronous activity of inhibitory networks in neocortex requires electrical synapses containing connexin36', *Neuron*, 31(3), pp. 477-85.

38. Dichter, M. and Spencer, W.A. (1969) 'Penicillin-induced interictal discharges from the cat hippocampus. II. Mechanisms underlying origin and restriction', *J Neurophysiol*, 32(5), pp. 663-87.

39. Dreier, J.P. and Heinemann, U. (1991) 'Regional and time dependent variations of low Mg2+ induced epileptiform activity in rat temporal cortex slices', *Exp Brain Res*, 87(3), pp. 581-96.

40. Dreier, J.P., Zhang, C.L. and Heinemann, U. (1998) 'Phenytoin, phenobarbital, and midazolam fail to stop status epilepticus-like activity induced by low magnesium in rat entorhinal slices, but can prevent its development', *Acta Neurol Scand*, 98(3), pp. 154-60.

41. Dyhrfjeld-Johnsen, J., Berdichevsky, Y., Swiercz, W., Sabolek, H. and Staley, K.J. (2010) 'Interictal spikes precede ictal discharges in an organotypic hippocampal slice culture model of epileptogenesis', *J Clin Neurophysiol*, 27(6), pp. 418-24.

42. Dzhala, V.I., Kuchibhotla, K.V., Glykys, J.C., Kahle, K.T., Swiercz, W.B., Feng, G., Kuner, T., Augustine, G.J., Bacskai, B.J. and Staley, K.J. (2010) 'Progressive NKCC1-dependent neuronal chloride accumulation during neonatal seizures', *J Neurosci*, 30(35), pp. 11745-61.

43. Ellender, T.J., Raimondo, J.V., Irkle, A., Lamsa, K.P. and Akerman, C.J. (2014) 'Excitatory effects of parvalbumin-expressing interneurons maintain hippocampal epileptiform activity via synchronous afterdischarges', *J Neurosci*, 34(46), pp. 15208-22.

44. Falconer, M.A., Serafetinides, E.A. and Corsellis, J.A. (1964) 'Etiology and Pathogenesis of Temporal Lobe Epilepsy', *Arch Neurol*, 10, pp. 233-48.

45. Frohlich, F. and McCormick, D.A. (2010) 'Endogenous electric fields may guide neocortical network activity', *Neuron*, 67(1), pp. 129-43.

46. Fueta, Y. and Avoli, M. (1992) 'Effects of antiepileptic drugs on 4-aminopyridine-induced epileptiform activity in young and adult rat hippocampus', *Epilepsy Res*, 12(3), pp. 207-15.

47. Fujiwara-Tsukamoto, Y., Isomura, Y., Imanishi, M., Ninomiya, T., Tsukada, M., Yanagawa, Y., Fukai, T. and Takada, M. (2010) 'Prototypic seizure activity driven by mature hippocampal fast-spiking interneurons', *J Neurosci*, 30(41), pp. 13679-89.

48. Gahwiler, B.H., Capogna, M., Debanne, D., McKinney, R.A. and Thompson, S.M. (1997) 'Organotypic slice cultures: a technique has come of age', *Trends Neurosci*, 20(10), pp. 471-7.

49. Galarreta, M. and Hestrin, S. (1999) 'A network of fast-spiking cells in the neocortex connected by electrical synapses', *Nature*, 402(6757), pp. 72-5.

50. Galarreta, M. and Hestrin, S. (2002) 'Electrical and chemical synapses among parvalbumin fast-spiking GABAergic interneurons in adult mouse neocortex', *Proc Natl Acad Sci U S A*, 99(19), pp. 12438-43.

51. Galvan, M., Grafe, P. and ten Bruggencate, G. (1982) 'Convulsant actions of 4-aminopyridine on the guinea-pig olfactory cortex slice', *Brain Res*, 241(1), pp. 75-86.

52. Gnatkovsky, V., Librizzi, L., Trombin, F. and de Curtis, M. (2008) 'Fast activity at seizure onset is mediated by inhibitory circuits in the entorhinal cortex *in vitro*', *Ann Neurol*, 64(6), pp. 674-86.

53. Gomez-Gonzalo, M., Losi, G., Chiavegato, A., Zonta, M., Cammarota, M., Brondi, M., Vetri, F., Uva, L., Pozzan, T., de Curtis, M., Ratto, G.M. and Carmignoto, G. (2010) 'An excitatory loop with astrocytes contributes to drive neurons to seizure threshold', *PLoS Biol*, 8(4), p. e1000352.

54. Gutnick, M.J., Connors, B.W. and Prince, D.A. (1982) 'Mechanisms of neocortical epileptogenesis *in vitro*', *J Neurophysiol*, 48(6), pp. 1321-35.

55. Heinemann, U., Draguhn, A., Ficker, E., Stabel, J. and Zhang, C.L. (1994) 'Strategies for the development of drugs for pharmacoresistant epilepsies', *Epilepsia*, 35 Suppl 5, pp. S10-21.

56. Hjorth, J., Blackwell, K.T. and Kotaleski, J.H. (2009) 'Gap junctions between striatal fast-spiking interneurons regulate spiking activity and synchronization as a function of cortical activity', *J Neurosci*, 29(16), pp. 5276-86.

57. Hwa, G.G., Avoli, M., Oliver, A. and Villemure, J.G. (1991) 'Bicuculline-induced epileptogenesis in the human neocortex maintained *in vitro*', *Exp Brain Res*, 83(2), pp. 329-39.

58. Ivens, S., Kaufer, D., Flores, L.P., Bechmann, I., Zumsteg, D., Tomkins, O., Seiffert, E., Heinemann, U. and Friedman, A. (2007) 'TGF-beta receptor-mediated albumin uptake into astrocytes is involved in neocortical epileptogenesis', *Brain*, 130(Pt 2), pp. 535-47.

59. Ives, A.E. and Jefferys, J.G. (1990) 'Synchronization of epileptiform bursts induced by 4-aminopyridine in the *in vitro* hippocampal slice preparation', *Neurosci Lett*, 112(2-3), pp. 239-45.

60. Jefferys, J.G. (1995) 'Nonsynaptic modulation of neuronal activity in the brain: electric currents and extracellular ions', *Physiol Rev*, 75(4), pp. 689-723.

61. Jefferys, J.G. and Haas, H.L. (1982) 'Synchronized bursting of CA1 hippocampal pyramidal cells in the absence of synaptic transmission', *Nature*, 300(5891), pp. 448-50.

62. John Lin, C.C. and Deneen, B. (2013) 'Astrocytes: the missing link in neurologic disease?', *Semin Pediatr Neurol*, 20(4), pp. 236-41.

63. Jones, R.S. (1989) 'Ictal epileptiform events induced by removal of extracellular magnesium in slices of entorhinal cortex are blocked by baclofen', *Exp Neurol*, 104(2), pp. 155-61.

64. Kofler, M., Kronenberg, M.F., Rifici, C., Saltuari, L. and Bauer, G. (1994) 'Epileptic seizures associated with intrathecal baclofen application', *Neurology*, 44(1), pp. 25-7.

65. Kofuji, P. and Newman, E.A. (2004) 'Potassium buffering in the central nervous system', *Neuroscience*, 129(4), pp. 1045-56.

66. Kohr, G. and Heinemann, U. (1990) 'Anticonvulsant effects of tetronic acid derivatives on picrotoxin induced epileptiform activity in rat hippocampal slices', *Neurosci Lett*, 112(1), pp. 43-7.

67. Koyama, R. (2013) 'The use of organotypic slice cultures for the study of epileptogenesis', *Neuropathology*, 33(4), pp. 475-9.

68. Librizzi, L. and de Curtis, M. (2003) 'Epileptiform ictal discharges are prevented by periodic interictal spiking in the olfactory cortex', *Ann Neurol*, 53(3), pp. 382-9.

69. Librizzi, L., Losi, G., Marcon, I., Sessolo, M., Scalmani, P., Carmignoto, G. and de Curtis, M. (2017) 'Interneuronal Network Activity at the Onset of Seizure-Like Events in Entorhinal Cortex Slices', *J Neurosci*, 37(43), pp. 10398-10407.

70. Lillis, K.P., Kramer, M.A., Mertz, J., Staley, K.J. and White, J.A. (2012) 'Pyramidal cells accumulate chloride at seizure onset', *Neurobiol Dis*, 47(3), pp. 358-66.

71. Lopantsev, V. and Avoli, M. (1998) 'Participation of GABAA-mediated inhibition in ictallike discharges in the rat entorhinal cortex', *J Neurophysiol*, 79(1), pp. 352-60.

72. Malouf, A.T., Robbins, C.A. and Schwartzkroin, P.A. (1990) 'Epileptiform activity in hippocampal slice cultures with normal inhibitory synaptic drive', *Neurosci Lett*, 108(1-2), pp. 76-80.

73. Mares, P. (2012) 'Anticonvulsant action of GABAB receptor positive modulator CGP7930 in immature rats', *Epilepsy Res*, 100(1-2), pp. 49-54.

74. Markram, H., Lubke, J., Frotscher, M., Roth, A. and Sakmann, B. (1997) 'Physiology and anatomy of synaptic connections between thick tufted pyramidal neurones in the developing rat neocortex', *J Physiol*, 500 (Pt 2), pp. 409-40.

75. Matsumoto, H. and Marsan, C.A. (1964) 'Cortical Cellular Phenomena in Experimental Epilepsy: Ictal Manifestations', *Exp Neurol*, 9, pp. 305-26.

76. McBain, C.J., Boden, P. and Hill, R.G. (1989) 'Rat hippocampal slices '*in vitro*' display spontaneous epileptiform activity following long-term organotypic culture', *J Neurosci Methods*, 27(1), pp. 35-49.

77. McCormick, D.A. (1989) 'GABA as an inhibitory neurotransmitter in human cerebral cortex', *J Neurophysiol*, 62(5), pp. 1018-27.

78. Miles, R. and Wong, R.K. (1983) 'Single neurones can initiate synchronized population discharge in the hippocampus', *Nature*, 306(5941), pp. 371-3.

79. Mody, I., Lambert, J.D. and Heinemann, U. (1987) 'Low extracellular magnesium induces epileptiform activity and spreading depression in rat hippocampal slices', *J Neurophysiol*, 57(3), pp. 869-88.

80. Ogren, J.A., Bragin, A., Wilson, C.L., Hoftman, G.D., Lin, J.J., Dutton, R.A., Fields, T.A., Toga, A.W., Thompson, P.M., Engel, J., Jr. and Staba, R.J. (2009) 'Three-dimensional hippocampal atrophy maps distinguish two common temporal lobe seizure-onset patterns', *Epilepsia*, 50(6), pp. 1361-70.

81. Ortinski, P.I., Dong, J., Mungenast, A., Yue, C., Takano, H., Watson, D.J., Haydon, P.G. and Coulter, D.A. (2010) 'Selective induction of astrocytic gliosis generates deficits in neuronal inhibition', *Nat Neurosci*, 13(5), pp. 584-91.

82. Otis, T.S. and Mody, I. (1992) 'Modulation of decay kinetics and frequency of GABAA receptor-mediated spontaneous inhibitory postsynaptic currents in hippocampal neurons', *Neuroscience*, 49(1), pp. 13-32.

83. Pallud, J., Le Van Quyen, M., Bielle, F., Pellegrino, C., Varlet, P., Cresto, N., Baulac, M., Duyckaerts, C., Kourdougli, N., Chazal, G., Devaux, B., Rivera, C., Miles, R., Capelle, L. and Huberfeld, G. (2014) 'Cortical GABAergic excitation contributes to epileptic activities around human glioma', *Sci Transl Med*, 6(244), p. 244ra89.

84. Perreault, P. and Avoli, M. (1992) '4-aminopyridine-induced epileptiform activity and a GABA-mediated long-lasting depolarization in the rat hippocampus', *J Neurosci*, 12(1), pp. 104-15.

85. Pinto, D.J., Patrick, S.L., Huang, W.C. and Connors, B.W. (2005) 'Initiation, propagation, and termination of epileptiform activity in rodent neocortex *in vitro* involve distinct mechanisms', *J Neurosci*, 25(36), pp. 8131-40.

86. Piredda, S., Yonekawa, W., Whittingham, T.S. and Kupferberg, H.J. (1986) 'Effects of antiepileptic drugs on pentylenetetrazole-induced epileptiform activity in the *in vitro* hippocampus', *Epilepsia*, 27(4), pp. 341-6.

87. Prince, D.A. (1968) 'The depolarization shift in "epileptic" neurons', *Exp Neurol*, 21(4), pp. 467-85.

88. Prince, D.A. and Wilder, B.J. (1967) 'Control mechanisms in cortical epileptogenic foci. "Surround" inhibition', *Arch Neurol*, 16(2), pp. 194-202.

89. Richter, D., Luhmann, H.J. and Kilb, W. (2010) 'Intrinsic activation of GABA(A) receptors suppresses epileptiform activity in the cerebral cortex of immature mice', *Epilepsia*, 51(8), pp. 1483-92.

90. Rogers, C.J., Twyman, R.E. and Macdonald, R.L. (1994) 'Benzodiazepine and beta-carboline regulation of single GABAA receptor channels of mouse spinal neurones in culture', *J Physiol*, 475(1), pp. 69-82.

91. Routbort, M.J., Bausch, S.B. and McNamara, J.O. (1999) 'Seizures, cell death, and mossy fiber sprouting in kainic acid-treated organotypic hippocampal cultures', *Neuroscience*, 94(3), pp. 755-65.

92. Rush, J.M. and Gibberd, F.B. (1990) 'Baclofen-induced epilepsy', *J R Soc Med*, 83(2), pp. 115-6.

93. Schevon, C.A., Weiss, S.A., McKhann, G., Jr., Goodman, R.R., Yuste, R., Emerson, R.G. and Trevelyan, A.J. (2012) 'Evidence of an inhibitory restraint of seizure activity in humans', *Nat Commun*, 3, p. 1060.

94. Schneiderman, J.H. and Schwartzkroin, P.A. (1982) 'Effects of phenytoin on normal activity and on penicillin-induced bursting in the guinea pig hippocampal slice', *Neurology*, 32(7), pp. 730-8.

95. Schwartz, T.H. and Bonhoeffer, T. (2001) '*In vivo* optical mapping of epileptic foci and surround inhibition in ferret cerebral cortex', *Nat Med*, 7(9), pp. 1063-7.

96. Scuderi, C., Stecca, C., Iacomino, A. and Steardo, L. (2013) 'Role of astrocytes in major neurological disorders: the evidence and implications', *IUBMB Life*, 65(12), pp. 957-61.

97. Seifert, G., Schilling, K. and Steinhauser, C. (2006) 'Astrocyte dysfunction in neurological disorders: a molecular perspective', *Nat Rev Neurosci*, 7(3), pp. 194-206.

98. Sessolo, M., Marcon, I., Bovetti, S., Losi, G., Cammarota, M., Ratto, G.M., Fellin, T. and Carmignoto, G. (2015) 'Parvalbumin-Positive Inhibitory Interneurons Oppose Propagation But Favor Generation of Focal Epileptiform Activity', *J Neurosci*, 35(26), pp. 9544-57.

99. Shiri, Z., Manseau, F., Levesque, M., Williams, S. and Avoli, M. (2015) 'Interneuron activity leads to initiation of low-voltage fast-onset seizures', *Ann Neurol*, 77(3), pp. 541-6.

100. Shiri, Z., Manseau, F., Levesque, M., Williams, S. and Avoli, M. (2016) 'Activation of specific neuronal networks leads to different seizure onset types', *Ann Neurol*, 79(3), pp. 354-65.

101. Somjen, G.G. (2004) 'Ions and seizures', in *Ions in the brain*. Oxford University Press, pp. 201 - 216.

102. Staley, K.J., Soldo, B.L. and Proctor, W.R. (1995) 'Ionic mechanisms of neuronal excitation by inhibitory GABAA receptors', *Science*, 269(5226), pp. 977-81.

103. Study, R.E. and Barker, J.L. (1981) 'Diazepam and (--)-pentobarbital: fluctuation analysis reveals different mechanisms for potentiation of gamma-

aminobutyric acid responses in cultured central neurons', *Proc Natl Acad Sci U S A*, 78(11), pp. 7180-4.

104.   Suarez, L.M., Cid, E., Gal, B., Inostroza, M., Brotons-Mas, J.R., Gomez-Dominguez, D., de la Prida, L.M. and Solis, J.M. (2012) 'Systemic injection of kainic acid differently affects LTP magnitude depending on its epileptogenic efficiency', *PLoS One*, 7(10), p. e48128.

105.   Sudbury, J.R. and Avoli, M. (2007) 'Epileptiform synchronization in the rat insular and perirhinal cortices *in vitro*', *Eur J Neurosci*, 26(12), pp. 3571-82.

106.   Tani, H., Dulla, C.G., Farzampour, Z., Taylor-Weiner, A., Huguenard, J.R. and Reimer, R.J. (2014) 'A local glutamate-glutamine cycle sustains synaptic excitatory transmitter release', *Neuron*, 81(4), pp. 888-900.

107.   Tasker, J.G., Peacock, W.J. and Dudek, F.E. (1992) 'Local synaptic circuits and epileptiform activity in slices of neocortex from children with intractable epilepsy', *J Neurophysiol*, 67(3), pp. 496-507.

108.   Telfeian, A.E. and Connors, B.W. (1999) 'Epileptiform propagation patterns mediated by NMDA and non-NMDA receptors in rat neocortex', *Epilepsia*, 40(11), pp. 1499-506.

109.   Terrence, C.F., Fromm, G.H. and Roussan, M.S. (1983) 'Baclofen. Its effect on seizure frequency', *Arch Neurol*, 40(1), pp. 28-9.

110.   Thompson, S.M., Fortunato, C., McKinney, R.A., Muller, M. and Gahwiler, B.H. (1996) 'Mechanisms underlying the neuropathological consequences of epileptic activity in the rat hippocampus *in vitro*', *J Comp Neurol*, 372(4), pp. 515-28.

111.   Thompson, S.M. and Gahwiler, B.H. (1989) 'Activity-dependent disinhibition. II. Effects of extracellular potassium, furosemide, and membrane potential on ECl- in hippocampal CA3 neurons', *J Neurophysiol*, 61(3), pp. 512-23.

112.   Thompson, S.M. and Gahwiler, B.H. (1992) 'Comparison of the actions of baclofen at pre- and postsynaptic receptors in the rat hippocampus *in vitro*', *J Physiol*, 451, pp. 329-45.

113.   Tian, G.F., Azmi, H., Takano, T., Xu, Q., Peng, W., Lin, J., Oberheim, N., Lou, N., Wang, X., Zielke, H.R., Kang, J. and Nedergaard, M. (2005) 'An astrocytic basis of epilepsy', *Nat Med*, 11(9), pp. 973-81.

114.   Timofeev, I., Grenier, F. and Steriade, M. (2002) 'The role of chloride-dependent inhibition and the activity of fast-spiking neurons during cortical spike-wave electrographic seizures', *Neuroscience*, 114(4), pp. 1115-32.

115.   Traub, R.D., Jefferys, J.G. and Whittington, M.A. (1999) 'Functionally relevant and functionally disruptive (epileptic) synchronized oscillations in brain slices', *Adv Neurol*, 79, pp. 709-24.

116.   Traub, R.D., Miles, R. and Wong, R.K. (1989) 'Model of the origin of rhythmic population oscillations in the hippocampal slice', *Science*, 243(4896), pp. 1319-25.

117.   Traub, R.D., Wong, R.K. and Miles, R. (1987) '*In vitro* Models of Epilepsy', in *Neurotransmitters and Epilepsy*. Humana Press, pp. 161 - 190.

118.   Trevelyan, A.J., Bruns, W., Mann, E.O., Crepel, V. and Scanziani, M. (2013) 'The information content of physiological and epileptic brain activity', *J Physiol*, 591(4), pp. 799-805.

119.   Trevelyan, A.J., Sussillo, D., Watson, B.O. and Yuste, R. (2006) 'Modular propagation of epileptiform activity: evidence for an inhibitory veto in neocortex', *J Neurosci*, 26(48), pp. 12447-55.

120.   Trevelyan, A.J., Sussillo, D. and Yuste, R. (2007) 'Feedforward inhibition contributes to the control of epileptiform propagation speed', *J Neurosci*, 27(13), pp. 3383-7.

121.   Uva, L., Librizzi, L., Wendling, F. and de Curtis, M. (2005) 'Propagation dynamics of epileptiform activity acutely induced by bicuculline in the

hippocampal-parahippocampal region of the isolated Guinea pig brain', *Epilepsia*, 46(12), pp. 1914-25.

122.   van Vliet, E.A., Aronica, E. and Gorter, J.A. (2015) 'Blood-brain barrier dysfunction, seizures and epilepsy', *Semin Cell Dev Biol*, 38, pp. 26-34.

123.   Velasco, A.L., Wilson, C.L., Babb, T.L. and Engel, J., Jr. (2000) 'Functional and anatomic correlates of two frequently observed temporal lobe seizure-onset patterns', *Neural Plast*, 7(1-2), pp. 49-63.

124.   Vergnes, M., Boehrer, A., Simler, S., Bernasconi, R. and Marescaux, C. (1997) 'Opposite effects of GABAB receptor antagonists on absences and convulsive seizures', *Eur J Pharmacol*, 332(3), pp. 245-55.

125.   Vezzani, A. and Granata, T. (2005) 'Brain inflammation in epilepsy: experimental and clinical evidence', *Epilepsia*, 46(11), pp. 1724-43.

126.   Vezzani, A., Ravizza, T., Moneta, D., Conti, M., Borroni, A., Rizzi, M., Samanin, R. and Maj, R. (1999a) 'Brain-derived neurotrophic factor immunoreactivity in the limbic system of rats after acute seizures and during spontaneous convulsions: temporal evolution of changes as compared to neuropeptide Y', *Neuroscience*, 90(4), pp. 1445-61.

127.   Vezzani, A., Sperk, G. and Colmers, W.F. (1999b) 'Neuropeptide Y: emerging evidence for a functional role in seizure modulation', *Trends Neurosci*, 22(1), pp. 25-30.

128.   Viitanen, T., Ruusuvuori, E., Kaila, K. and Voipio, J. (2010) 'The K+-Cl cotransporter KCC2 promotes GABAergic excitation in the mature rat hippocampus', *J Physiol*, 588(Pt 9), pp. 1527-40.

129.   von Krosigk, M., Bal, T. and McCormick, D.A. (1993) 'Cellular mechanisms of a synchronized oscillation in the thalamus', *Science*, 261(5119), pp. 361-4.

130.   Voskuyl, R.A. and Albus, H. (1985) 'Spontaneous epileptiform discharges in hippocampal slices induced by 4-aminopyridine', *Brain Res*, 342(1), pp. 54-66.

131.   Wadman, W.J. and Gutnick, M.J. (1993) 'Non-uniform propagation of epileptiform discharge in brain slices of rat neocortex', *Neuroscience*, 52(2), pp. 255-62.

132.   Wallraff, A., Kohling, R., Heinemann, U., Theis, M., Willecke, K. and Steinhauser, C. (2006) 'The impact of astrocytic gap junctional coupling on potassium buffering in the hippocampus', *J Neurosci*, 26(20), pp. 5438-47.

133.   Watts, A.E. and Jefferys, J.G. (1993) 'Effects of carbamazepine and baclofen on 4-aminopyridine-induced epileptic activity in rat hippocampal slices', *Br J Pharmacol*, 108(3), pp. 819-23.

134.   Wendling, F., Bartolomei, F., Bellanger, J.J., Bourien, J. and Chauvel, P. (2003) 'Epileptic fast intracerebral EEG activity: evidence for spatial decorrelation at seizure onset', *Brain*, 126(Pt 6), pp. 1449-59.

135.   White, A., Williams, P.A., Hellier, J.L., Clark, S., Dudek, F.E. and Staley, K.J. (2010) 'EEG spike activity precedes epilepsy after kainate-induced status epilepticus', *Epilepsia*, 51(3), pp. 371-83.

136.   Whittington, M.A., Traub, R.D. and Jefferys, J.G. (1995) 'Erosion of inhibition contributes to the progression of low magnesium bursts in rat hippocampal slices', *J Physiol*, 486 (Pt 3), pp. 723-34.

137.   Wiebe, S. (2000) 'Epidemiology of temporal lobe epilepsy', *Can J Neurol Sci*, 27 Suppl 1, pp. S6-10; discussion S20-1.

138.   Wong, B.Y. and Prince, D.A. (1990) 'The lateral spread of ictal discharges in neocortical brain slices', *Epilepsy Res*, 7(1), pp. 29-39.

139.   Yekhlef, L., Breschi, G.L., Lagostena, L., Russo, G. and Taverna, S. (2015) 'Selective activation of parvalbumin- or somatostatin-expressing interneurons triggers epileptic seizurelike activity in mouse medial entorhinal cortex', *J Neurophysiol*, 113(5), pp. 1616-30.

140.   Yu, N., Liu, H. and Di, Q. (2013) 'Modulation of Immunity and the Inflammatory Response: A New Target for Treating Drug-resistant Epilepsy', *Curr Neuropharmacol*, 11(1), pp. 114-27.

141.   Zhang, C.L., Dreier, J.P. and Heinemann, U. (1995) 'Paroxysmal epileptiform discharges in temporal lobe slices after prolonged exposure to low magnesium are resistant to clinically used anticonvulsants', *Epilepsy Res*, 20(2), pp. 105-11.